

**EARLY TRANSITION METAL COMPLEXES SUPPORTED BY  
AMIDOPHOSPHINE AND AMIDOCARBENE LIGANDS**

by

LIAM PATRICK SPENCER

B.Sc. (Hons.), The University of Victoria, 2000  
M.Sc. The University of Windsor, 2002

A THESIS SUBMITTED IN PARTIAL FULFILLMENT  
OF THE REQUIREMENTS FOR THE DEGREE OF

DOCTOR OF PHILOSOPHY

in

THE FACULTY OF GRADUATE STUDIES

(CHEMISTRY)

THE UNIVERSITY OF BRITISH COLUMBIA

September 2006

© Liam Patrick Spencer, 2006

## ABSTRACT

The reactivity of the tantalum dinitrogen complex  $([\text{NPN}]\text{Ta})_2(\mu\text{-H})_2(\mu\text{-}\eta^1:\eta^2\text{-N}_2)$  (where  $[\text{NPN}] = [(\text{PhNSiMe}_2\text{CH}_2)_2\text{PPh}]^{2-}$ ) with several zirconium hydride reagents is explored. The addition of  $[\text{Cp}_2\text{Zr}(\text{Cl})\text{H}]_x$  leads to the unanticipated reduction of the N-N bond without Zr-H addition. The coordinated  $\text{N}_2$  ligand is cleaved to form a triply bridging nitride and a phosphinimide functional group that bridges between Ta and Zr centres. A series of experiments to determine the mechanism of this reaction reveals that a "Cp<sub>2</sub>Zr" species promotes reduction of the N-N unit. This type of dinitrogen reduction is extended to include the insertion of a "Cp<sub>2</sub>Ti" fragment into the N-N bond.

The synthesis of early transition metal complexes employing a tridentate diamido N-heterocyclic carbene (NHC) ligand set (denoted  $[\text{NCN}]$ ) is also investigated. Aminolysis reactions with diamino-NHC precursors and  $\text{M}(\text{NMe}_2)_4$  ( $\text{M} = \text{Ti}, \text{Zr}, \text{Hf}$ ) provide bis(amido)-NHC-metal complexes that can be further converted to chloro and alkyl derivatives. Alkyl elimination reactions with the diamino-NHC ligands and  $\text{Zr}(\text{CH}_2\text{R})_4$  ( $\text{R} = \text{Ph}, \text{SiMe}_3$ ) yield dialkyl-NHC-zirconium complexes. The central position of the NHC donor in this tridentate architecture renders the carbene stable to dissociation from the metal centre in strongly coordinating solvents. The hafnium dialkyl complexes are thermally stable with the exception of the dialkyl complex,  $^{\text{Mes}}[\text{NCN}]\text{Hf}(\text{CH}_2\text{CH}_3)_2$ , (where  $^{\text{Mes}}[\text{NCN}] = (2,4,6\text{-Me}_3\text{-C}_6\text{H}_2\text{NHCH}_2\text{CH}_2)_2\text{N}_2\text{C}_3\text{H}_2$ ) which undergoes  $\beta$ -hydrogen transfer and subsequent C-H bond activation with an *ortho*-methyl substituent on the mesityl group.

Activation of  $^{\text{Mes}}[\text{NCN}]\text{M}(\text{CH}_3)_2$  ( $\text{M} = \text{Zr}, \text{Hf}$ ) with  $[\text{Ph}_3\text{C}][\text{B}(\text{C}_6\text{F}_5)_4]$  yields  $\{^{\text{Mes}}[\text{NCN}]\text{MCH}_3\}\{\text{B}(\text{C}_6\text{F}_5)_4\}$ , which is a moderately active ethylene polymerization catalyst. The hafnium dialkyl complexes also insert carbon monoxide, substituted isocyanides, and substituted cumulenes into a hafnium-sp<sup>3</sup>-carbon bond to yield expected insertion products. In some circumstances, further C-C bond coupling occurs to yield enediolate and enamidolate metallacycles. Attempts to reduce  $^{\text{Mes}}[\text{NCN}]\text{ZrCl}_2$  in the presence of dinitrogen lead to mixtures of products. In one case, an ether cleavage product is isolated, which is a result of C-O bond activation of the solvent used in the reaction.

Aminolysis and alkyl elimination reactions with the diamino-NHC ligand and tantalum(V) reagents provide complexes with an amide-amine donor configuration. Attempts to promote coordination of the remaining pendant amine donor have been unsuccessful. Metathesis reactions with the lithiated diamido-NHC ligand ( $\text{Li}_2^{\text{Ar}}[\text{NCN}]$ ) and  $\text{Cl}_x\text{Ta}(\text{NR}_2)_{5-x}$  derivatives provide a successful method to coordinate both amide donors, yielding the desired  $^{\text{Ar}}[\text{NCN}]\text{TaCl}_x(\text{NR}_2)_{3-x}$  complexes. Attempts to prepare trialkyl tantalum complexes by this methodology resulted in the formation of a metallaaziridine derivative. DFT calculations on model complexes suggest the lowest energy pathway involves a tantalum alkylidene intermediate, which undergoes amido C-H bond activation to form the metallaaziridine moiety. This mechanism was confirmed by examining the distribution of deuterium atoms in an experiment between  $^{\text{Mes}}[\text{NCN}]\text{Li}_2$  and  $\text{Cl}_2\text{Ta}(\text{CD}_2\text{Ph})_3$ .

The preparation of chiral [NCN] group 4 complexes is achieved by aminolysis and alkyl elimination reactions with a chiral diamino-NHC ligand and suitable group 4 reagents. The titanium and zirconium derivatives are investigated in the asymmetric intramolecular hydroamination of an aminoalkene in an attempt to promote selectivity in the N-heterocycle synthesized. While the titanium [NCN] complex shows no activity, the zirconium [NCN] complex is an efficient catalyst for the intramolecular formation of a substituted pyrrolidine. Examination of the stereoselectivity in the N-heterocyclic product formed reveals very low enantioselective excess.



2.3.	Reduction and Functionalization of <b>2.5</b> with Cp <sub>2</sub> Ti(II) .....	43
2.4.	Conclusions.....	44
2.5.	Experimental	45
	<b>2.5.1.</b> General Considerations.....	45
	<b>2.5.2.</b> Materials and Reagents.....	45
	<b>2.5.3.</b> Synthesis and Characterization of <b>2.10</b> and <b>2.13</b> .....	46
2.6.	References.....	49

**Chapter Three      *Synthesis of Group 4 Bis(amido)-N-Heterocyclic Carbene Complexes***

3.1.	Introduction.....	51
3.2.	Synthesis of Ar[NCN]H <sub>2</sub> and Lithium Derivatives.....	54
3.3.	Attempted Syntheses of an Ar[NCN] Ligand with an Aryl Backbone.....	59
3.4.	Synthesis of Group 4 [NCN] Aamido, Chloride, and Alkyl Complexes.....	62
3.5.	Conclusions.....	75
3.6.	Experimental.....	77
	<b>3.6.1.</b> General Considerations.....	77
	<b>3.6.2.</b> Materials and Reagents.....	77
	<b>3.6.3.</b> Synthesis and Characterization of Complexes <b>3.1 - 3.40</b> .....	77
3.7.	References.....	94

**Chapter Four      *Synthesis of Group 4 Bis(amido)-N-Heterocyclic Carbene Complexes***

4.1.	Introduction.....	97
4.2.	Hf and Zr Cation Formation and Polymerization Studies.....	98
4.3.	Formation of [NCN] Hafnium η <sup>2</sup> -Iminoacyls and an Eneamidolate Metallacycle.....	100
4.4.	Formation of a Hafnium Vinyl-enolate and Enediolate Metallacycle.....	108
4.5.	Formation of Amidate and Amidinate Metallacycles.....	115
4.6.	Attempted Synthesis of Group 4 [NCN] Dinitrogen Complexes.....	120
4.7.	Synthesis of Hydrazido(1-) Hafnium [NCN] Complexes.....	125

4.8.	Conclusions.....	130
4.9.	Experimental.....	132
	4.9.1. General Considerations.....	132
	4.9.2. Materials and Reagents.....	132
	4.9.3. Synthesis and Characterization of Complexes 4.4 - 4.18, 4.24 - 4.26.....	132
4.10.	References.....	143

**Chapter Five**                    *Synthesis and DFT Studies of Tantalum [NCN] Transition Metal Complexes*

5.1.	Introduction.....	148
5.2.	Synthesis of Amine-Amide [NCNH] Tantalum Derivatives.....	150
5.3.	Successful Synthesis of Ta[NCN] Amide Complexes.....	154
5.4.	Isolation of Cyclometallated [NCCN]Ta Dialkyl Derivatives.....	157
5.5.	Mechanistic Insight Into the Formation of 5.7-5.9.....	160
5.6.	Determination of Mechanism by DFT Calculations.....	161
5.7.	Verification of the Mechanism Proposed by DFT Calculations.....	165
5.8.	Conclusions.....	168
5.9.	Experimental.....	170
	5.9.1. General Considerations.....	170
	5.9.2. Materials and Reagents.....	170
	5.9.3. Synthesis and Characterization of Complexes 5.1 - 5.10.....	170
5.10.	References.....	177

**Chapter Six**                    *Thesis Extensions: Chiral Group 4 [NCN] Complexes*

6.1.	Introduction.....	180
6.2.	Synthesis of Group 4 [NCN] Complexes.....	184
6.3.	Asymmetric Intramolecular Hydroamination Studies.....	191
6.4.	Conclusions and Future Work.....	193
6.5.	Experimental.....	197
	6.5.1. General Considerations.....	197

6.5.2.	Materials and Reagents.....	197
6.5.3.	Synthesis and Characterization of Complexes <b>6.8 - 6.13,</b> <b>6.14 - 6.15</b> .....	197
6.7.	References.....	203
<i>Chapter Seven</i>	<i>Thesis Summary and Future Work</i> .....	206
<i>Appendix A</i>	<i>X-ray Crystal Structure Data</i>	
A.1.	General Considerations.....	208
A.2.	References.....	210
A.3.	Tables of Crystallographic Data.....	211
<i>Appendix B</i>	<i>Evaluating the Formation of a Tantalum Metallaziridine Complex by DFT Calculations</i>	
B.1.	Evaluation of a $\sigma$ -Bond Metathesis Mechanism.....	219
B.2.	Investigation of an Alkylidene Intermediate Followed by C-H Bond Activation.....	221
B.3.	Thermodynamic Considerations for the Formation of Metallated Ta [NCCN] Derivatives.....	224
B.4.	General Considerations.....	232
B.5.	References.....	233

## LIST OF TABLES

*Chapter Two                      Promoting Dinitrogen Cleavage and Functionalization with  
Zr(II) and Ti(II) reagents*

<u>Table</u>	<u>Title</u>	<u>Page</u>
<b>Table 2.1.</b>	Selected bond distances (Å) and angles (deg) for ([NP(N)N]Ta(μ-H) <sub>2</sub> (μ-N)(Ta[NPN])(ZrCp <sub>2</sub> ) (2.10) .....	41

*Chapter Three                      Synthesis of Group 4 Bis(amido)-N-Heterocyclic Carbene  
Complexes*

<u>Table</u>	<u>Title</u>	<u>Page</u>
<b>Table 3.1.</b>	Selected Bond Distances (Å) and Bond Angles (°) for <sup>Mes</sup> [NCN]H <sub>2</sub> ·Cl (3.5) and <sup>Mes</sup> [NCN]H <sub>2</sub> , (3.8). .....	57
<b>Table 3.2.</b>	Selected Bond Distances (Å) and Bond Angles (°) for <sup>tol</sup> [NCN]Zr(NEt <sub>2</sub> ) <sub>2</sub> , (3.17). .....	64
<b>Table 3.3.</b>	Selected Bond Distances (Å) and Bond Angles (°) for <sup>Mes</sup> [NCNH]Ti(NMe <sub>2</sub> ) <sub>3</sub> , (3.22). .....	66
<b>Table 3.4.</b>	Selected Bond Distances (Å) and Bond Angles (°) for <sup>tol</sup> [NCN]ZrCl <sub>2</sub> (py), (3.30). .....	68
<b>Table 3.5.</b>	Selected Bond Distances (Å) and Bond Angles (°) for <sup>tol</sup> [NCN]Zr(CH <sub>2</sub> SiMe <sub>3</sub> ) <sub>2</sub> , (3.31). .....	71
<b>Table 3.6.</b>	Selected Bond Distances (Å) and Bond Angles (°) for <sup>Mes</sup> [NCN]Hf <sup>t</sup> Bu <sub>2</sub> , (3.38). .....	73

*Chapter Four                      Synthesis of Group 4 Bis(amido)-N-Heterocyclic Carbene  
Complexes*

<u>Table</u>	<u>Title</u>	<u>Page</u>
<b>Table 4.1.</b>	Selected Bond Distances (Å) and Bond Angles (°) for <sup>Mes</sup> [NCN]Hf(η <sup>2</sup> -XyNCCH <sub>3</sub> )(CH <sub>3</sub> ), (4.7). .....	103
<b>Table 4.2.</b>	Selected Bond Distances (Å) and Bond Angles (°) for	

	$^{\text{Mes}}[\text{NCN}]\text{Hf}(\eta^2\text{-XyNCCH}_3)_2$ , (4.8). . . . .	105
<b>Table 4.3.</b>	Selected Bond Distances (Å) and Bond Angles (°) for $^{\text{Mes}}[\text{NCN}]\text{Hf}(\text{OC}(\text{CH}_3)=\text{C}(\text{CH}_3)\text{NXy})$ , (4.11). . . . .	108
<b>Table 4.4.</b>	Selected Bond Distances (Å) and Bond Angles (°) for $(^{\text{Mes}}[\text{NCN}]\text{Hf})_2(\mu\text{-OC}(\text{}^i\text{Bu})=\text{C}(\text{}^i\text{Bu})\text{O})_2$ , (4.16). . . . .	112
<b>Table 4.5.</b>	Selected Bond Distances (Å) and Bond Angles (°) for $^{\text{Mes}}[\text{NCN}]\text{Hf}(\text{Me})(\eta^3\text{-}^i\text{BuNC}(\text{Me})\text{O})$ , (4.17). . . . .	117
<b>Table 4.6.</b>	Selected Bond Distances (Å) and Bond Angles (°) for $^{\text{Mes}}[\text{NCN}]\text{Hf}(\text{Me})(\eta^3\text{-}^i\text{PrNC}(\text{Me})\text{N}^i\text{Pr})$ , (4.18). . . . .	119
<b>Table 4.7.</b>	Selected Bond Distances (Å) and Bond Angles (°) for $^{\text{Mes}}[\text{NCN}]\text{Zr}(\text{Cl})(\text{OCH}_2\text{CH}_2\text{CH}_2\text{CH}_3)$ , (4.24). . . . .	124
<b>Table 4.8.</b>	Selected Bond Distances (Å) and Bond Angles (°) for $^{\text{Mes}}[\text{NCN}]\text{Hf}(\text{Me})(\eta^2\text{-NHNMe}_2)$ , (4.25). . . . .	129

*Chapter Five                      Synthesis and DFT Studies of Tantalum [NCN] Transition Metal Complexes*

<u>Table</u>	<u>Title</u>	<u>Page</u>
<b>Table 5.1.</b>	Selected bond distances (Å) and angles (°) for $^{\text{tol}}[\text{NCNH}]\text{Ta}(\text{NMe}_2)_4$ , 5.1. . . . .	152
<b>Table 5.2.</b>	Selected bond distances (Å) and angles (°) for $^{\text{Mes}}[\text{NCNH}]\text{Ta}(\text{CHPh})(\text{CH}_2\text{Ph})_2$ (5.2). . . . .	154
<b>Table 5.3.</b>	Selected bond distances (Å) and angles (°) for $^{\text{tol}}[\text{NCN}]\text{Ta}(\text{NMe}_2)_3$ (5.3). . . . .	156
<b>Table 5.4.</b>	Selected bond distances (Å) and angles (°) for $^{\text{Mes}}[\text{NCCN}]\text{Ta}(\text{CH}_2^i\text{Bu})_2$ (5.7). . . . .	159
<b>Table 5.5.</b>	Selected bond distances (Å) and angles (°) for $^{\text{Mes}}[\text{NCCN}]\text{Ta}(\text{Cl})(\text{CH}_2^i\text{Bu})$ (5.10). . . . .	167

*Chapter Six Thesis Summary and Extensions: Chiral Group 4 [NCN] Complexes*

<u>Table</u>	<u>Title</u>	<u>Page</u>
<b>Table 6.1.</b>	Selected Bond Distances (Å) and Bond Angles (°) for (-)-(1 <i>R</i> ,2' <i>S</i> ,4 <i>R</i> )-2-(1,7,7-trimethylbicyclo[2.2.1]hept-2-ylamino)ethyl ammonium chloride, (6.8). .....	186

*Appendix A X-ray Crystal Structure Data*

<u>Table</u>	<u>Title</u>	<u>Page</u>
<b>Table A.1.</b>	Crystallographic and structure refinement for [NP(N)N]Ta(μ-H) <sub>2</sub> (μ-N)(Ta[NPN])(ZrCp <sub>2</sub> ) (2.10), <sup>Mes</sup> (NCHN)H <sub>2</sub> -Cl (3.5), and <sup>Mes</sup> (NCN)H <sub>2</sub> (3.8). .....	211
<b>Table A.2.</b>	Crystallographic and structure refinement for <sup>tol</sup> [NCN]Zr(NEt <sub>2</sub> ) <sub>2</sub> (3.17), <sup>Mes</sup> [NCNH]Ti(NMe <sub>2</sub> ) <sub>3</sub> (3.22), and <sup>tol</sup> [NCN]ZrCl <sub>2</sub> (py) (3.30)..	212
<b>Table A.3.</b>	Crystallographic and structure refinement for <sup>tol</sup> [NCN]Zr(CH <sub>2</sub> SiMe <sub>3</sub> ) <sub>2</sub> (3.30), <sup>Mes</sup> [NCN]Hf <sup>t</sup> Bu <sub>2</sub> (3.38), and <sup>Mes</sup> [NCN]Hf(η <sup>2</sup> -XyNCCH <sub>3</sub> )(CH <sub>3</sub> ) (4.7). .....	213
<b>Table A.4.</b>	Crystallographic and structure refinement for <sup>Mes</sup> [NCN]Hf(η <sup>2</sup> -XyNCCH <sub>3</sub> ) <sub>2</sub> (4.8), <sup>Mes</sup> [NCN]Hf(OC(CH <sub>3</sub> )=C(CH <sub>3</sub> )NXy) (4.11), and <sup>Mes</sup> [NCN]Hf <sub>2</sub> (μ-OC( <sup>t</sup> Bu)=C( <sup>t</sup> Bu)O) <sub>2</sub> (4.16). .....	214
<b>Table A.5.</b>	Crystallographic and structure refinement for <sup>Mes</sup> [NCN]Hf(Me)(η <sup>3</sup> - <sup>t</sup> BuNC(Me)O) (4.17), <sup>Mes</sup> [NCN]Hf(Me)(η <sup>3</sup> - <sup>i</sup> PrNC(Me)N <sup>i</sup> Pr) (4.18), and <sup>Mes</sup> [NCN]Zr(Cl)(OBu) (4.22). .....	215
<b>Table A.6.</b>	Crystallographic and structure refinement for <sup>Mes</sup> [NCN]Hf(Me)(η <sup>2</sup> -NNMe <sub>2</sub> ) (4.23), <sup>tol</sup> [NCNH]Ta(NMe <sub>2</sub> ) <sub>4</sub> (5.1), and <sup>Mes</sup> [NCNH]Ta(CHPh)(CH <sub>2</sub> Ph) <sub>2</sub> (5.2). .....	216
<b>Table A.7.</b>	Crystallographic and structure refinement for <sup>tol</sup> [NCN]Ta(NMe <sub>2</sub> ) <sub>3</sub> (5.3), <sup>Mes</sup> [NCCN]Ta(CH <sub>2</sub> <sup>t</sup> Bu) <sub>2</sub> (5.7), and <sup>Mes</sup> [NCCN]Ta(Cl)(CH <sub>2</sub> <sup>t</sup> Bu) (5.10). .....	217

<b>Table A.8.</b>	Crystallographic and structure refinement for (-)-(1 <i>R</i> ,2' <i>S</i> ,4 <i>R</i> )-2-(1,7,7-trimethylbicyclo[2.2.1]hept-2-ylamino)ethyl ammonium chloride ( <b>6.8</b> ). .....	218
-------------------	---	-----

*Appendix B                      Evaluating the Formation of a Tantalum Metallaaziridine Complex by DFT Calculations*

<u>Table</u>	<u>Title</u>	<u>Page</u>
<b>Table B.1.</b>	Gas-phase relative energies (kcal/mol) of the intermediates and transition states in a $\sigma$ -bond metathesis mechanism. ....	221
<b>Table B.2.</b>	Gas-phase relative energies (kcal/mol) of the intermediates and transition states in a mechanism involving $\alpha$ -H abstraction followed by alkylidene mediated C-H bond activation. ....	223
<b>Table B.3.</b>	NBO Occupancies of bonding and anti-bonding orbitals in the trimethyl complex <b>A</b> and the metallaaziridine complex <b>D</b> .....	227
<b>Table B.4.</b>	Important second order perturbation theory analysis NBO donor-acceptor interactions $\Delta E_{ij}$ (kcal/mol) that contribute to shorter Ta-carbene and Ta-Me bonds in the metallaaziridine product <b>D</b> relative to the trimethyl complex <b>A</b> . ....	228

## LIST OF FIGURES

<u>Figure</u>	<u>Title</u>	<u>Page</u>
<i>Chapter One                      Dinitrogen Chemistry and Ligand Design</i>		
<b>Figure 1.1.</b>	Interpretation of the coordination sphere of $\text{CoCl}_2 \cdot 6 \text{NH}_3$ by (a) Blömstrand/Jorgensen and (b) Werner. ....	2
<b>Figure 1.2.</b>	Catalytic formation of N-containing compounds from $\text{N}_2$ .....	4
<b>Figure 1.3.</b>	The first reported transition metal dinitrogen complex ( $\text{X}^- = \text{Br}^-$ , $\text{I}^-$ , $\text{BF}_4^-$ , $\text{PF}_6^-$ ).....	5
<b>Figure 1.4.</b>	Examples of zirconocene-based dinitrogen complexes. ....	6
<b>Figure 1.5.</b>	Successful catalyst for the synthesis of $\text{NH}_3$ from $\text{N}_2$ .....	10
<b>Figure 1.6.</b>	Design of a diamido-N-heterocyclic carbene [NCN] ligand.....	14
<b>Figure 1.7.</b>	Possible electronic configurations of carbenes. ....	15
<b>Figure 1.8.</b>	Attempted synthesis of an NHC by chloroform elimination.....	20
<b>Figure 1.9.</b>	Reported methodology for the synthesis of NHCs.....	20
<b>Figure 1.10.</b>	a) $\pi$ -Stabilization and b) inductive effects of NHCs.....	21
<b>Figure 1.11.</b>	(a) An example and (b) schematic representation of donor-acceptor bonding in Fischer-carbene complexes.....	22
<b>Figure 1.12.</b>	(a) An example and (b) schematic representation of covalent bonding in Schrock-alkylidene complexes.....	22
<b>Figure 1.13.</b>	Metal-NHC complexes reported by Wanzlick and Öfele.....	23
<b>Figure 1.14.</b>	Modification to a Ru catalyst with an NHC ligand.....	25
<b>Figure 1.15.</b>	Examples of a) phosphine and b) pyridine NHC metal complexes for Heck catalysis. ....	25
 <i>Chapter Two                      Promoting Dinitrogen Cleavage and Functionalization with Zr(II) and Ti(II) reagents</i>		
<u>Figure</u>	<u>Title</u>	<u>Page</u>
<b>Figure 2.1.</b>	ORTEP view of $([\text{NP}(\text{N})\text{N}]\text{Ta}(\mu\text{-H})_2(\mu\text{-N})(\text{Ta}[\text{NPN}])(\text{ZrCp}_2))$ (2.10) depicted with 50% ellipsoids; all hydrogen atoms, silyl methyl and phenyl ring carbon atoms except <i>ipso</i> carbons have	

been omitted for clarity..... 40

**Chapter Three      *Synthesis of Group 4 Bis(amido)-N-Heterocyclic Carbene Complexes***

<b><u>Figure</u></b>	<b><u>Title</u></b>	<b><u>Page</u></b>
<b>Figure 3.1.</b>	ORTEP view of <sup>Mes</sup> [NCHN]H <sub>2</sub> ·Cl ( <b>3.5</b> ) depicted with 50% thermal ellipsoids; all hydrogen atoms have been omitted for clarity.....	56
<b>Figure 3.2.</b>	ORTEP view of <sup>Mes</sup> [NCN]H <sub>2</sub> , ( <b>3.8</b> ) depicted with 50% thermal ellipsoids; all hydrogen atoms have been omitted for clarity.....	58
<b>Figure 3.3.</b>	Imidazolium ( <b>3.12</b> ) and imidazolinium ( <b>3.13</b> ) candidates with an aryl backbone. ....	59
<b>Figure 3.4.</b>	ORTEP view of <sup>tol</sup> [NCN]Zr(NEt <sub>2</sub> ) <sub>2</sub> ( <b>3.17</b> ) depicted with 50% thermal ellipsoids; all hydrogen atoms have been omitted for clarity. ....	64
<b>Figure 3.5.</b>	ORTEP view of <sup>Mes</sup> [NCNH]Ti(NMe <sub>2</sub> ) <sub>3</sub> ( <b>3.22</b> ) depicted with 50% thermal ellipsoids; all hydrogen atoms have been omitted for clarity. ....	65
<b>Figure 3.6.</b>	ORTEP view of <sup>tol</sup> [NCN]ZrCl <sub>2</sub> (py) ( <b>3.30</b> ) depicted with 50% thermal ellipsoids; all hydrogen atoms have been omitted for clarity. ....	68
<b>Figure 3.7.</b>	ORTEP view of <sup>tol</sup> [NCN]Zr(CH <sub>2</sub> SiMe <sub>3</sub> ) <sub>2</sub> ( <b>3.31</b> ) depicted with 50% thermal ellipsoids; all hydrogen atoms have been omitted for clarity. ....	71
<b>Figure 3.8.</b>	ORTEP view of <sup>Mes</sup> [NCN]Hf <sup>t</sup> Bu <sub>2</sub> ( <b>3.39</b> ) depicted with 50% thermal ellipsoids; all hydrogen atoms have been omitted for clarity. ....	73

**Chapter Four      *Synthesis of Group 4 Bis(amido)-N-Heterocyclic Carbene Complexes***

<b><u>Figure</u></b>	<b><u>Title</u></b>	<b><u>Page</u></b>
<b>Figure 4.1.</b>	Examples of Group 4 olefin polymerization catalysts.....	98

<b>Figure 4.2.</b>	ORTEP view of $^{\text{Mes}}[\text{NCN}]\text{Hf}(\eta^2\text{-XyNCCH}_3)(\text{CH}_3)$ ( <b>4.7</b> ) (THF omitted), depicted with 50% ellipsoids; all hydrogen atoms have been omitted for clarity. ....	103
<b>Figure 4.3.</b>	ORTEP view of $^{\text{Mes}}[\text{NCN}]\text{Hf}(\eta^2\text{-XyNCCH}_3)_2$ ( <b>4.8</b> ) ( $\text{CH}_2\text{Cl}_2$ omitted), depicted with 50% ellipsoids; all hydrogen atoms and mesityl groups have been omitted for clarity. ....	104
<b>Figure 4.4.</b>	ORTEP view of $^{\text{Mes}}[\text{NCN}]\text{Hf}(\text{OC}(\text{CH}_3)=\text{C}(\text{CH}_3)\text{NXy})$ , ( <b>4.11</b> ) (1/2 $\text{Et}_2\text{O}$ omitted), depicted with 50% ellipsoids; all hydrogen atoms and mesityl groups have been omitted for clarity.....	108
<b>Figure 4.5.</b>	ORTEP view of $^{\text{Mes}}[\text{NCN}]\text{Hf}_2(\mu\text{-OC}(\text{iBu})=\text{C}(\text{iBu})\text{O})_2$ , ( <b>4.16</b> ) (4 $\text{C}_6\text{H}_6$ omitted), depicted with 50% ellipsoids; all hydrogen atoms and mesityl groups have been omitted for clarity.....	112
<b>Figure 4.6.</b>	ORTEP view of $^{\text{Mes}}[\text{NCN}]\text{Hf}(\text{Me})(\eta^3\text{-tBuNC}(\text{Me})\text{O})$ ( <b>4.17</b> ) depicted with 50% ellipsoids; all hydrogen atoms have been omitted for clarity. ....	117
<b>Figure 4.7.</b>	ORTEP view of $^{\text{Mes}}[\text{NCN}]\text{Hf}(\text{Me})(\eta^3\text{-iPrNC}(\text{Me})\text{N}^{\text{iPr}})$ ( <b>4.18</b> ) depicted with 50% ellipsoids; all hydrogen atoms have been omitted for clarity. ....	119
<b>Figure 4.8.</b>	ORTEP view of $^{\text{Mes}}[\text{NCN}]\text{Zr}(\text{Cl})(\text{OCH}_2\text{CH}_2\text{CH}_2\text{CH}_3)$ ( <b>4.24</b> ) depicted with 50% ellipsoids; all hydrogen atoms have been omitted for clarity. ....	124
<b>Figure 4.9.</b>	Coordination modes of hydrazido ligands. ....	126
<b>Figure 4.10.</b>	Examples of hydrazido(1-) and hydrazido(2-) titanium complexes..	127
<b>Figure 4.11.</b>	ORTEP view of $^{\text{Mes}}[\text{NCN}]\text{Hf}(\text{Me})(\eta^2\text{-NHNMe}_2)$ ( <b>4.25</b> ) depicted with 50% ellipsoids; with the exception of H100, all hydrogen atoms have been omitted for clarity. ....	128

**Chapter Five**                      *Synthesis and DFT Studies of Tantalum [NCN] Transition Metal Complexes*

<u>Figure</u>	<u>Title</u>	<u>Page</u>
<b>Figure 5.1.</b>	ORTEP view of $^{\text{tol}}[\text{NCNH}]\text{Ta}(\text{NMe}_2)_4$ ( <b>5.1</b> ) ( $\text{CH}_3\text{C}_6\text{H}_5$ omitted)	

	depicted with 50% thermal ellipsoids; all hydrogen atoms have been omitted for clarity. ....	152
<b>Figure 5.2.</b>	ORTEP view of <sup>Mes</sup> [NCNH]Ta(CHPh)(CH <sub>2</sub> Ph) <sub>2</sub> ( <b>5.2</b> ), depicted with 50% thermal ellipsoids; all hydrogen atoms have been omitted for clarity with the exception of H101. ....	154
<b>Figure 5.3.</b>	ORTEP view of <sup>tol</sup> [NCN]Ta(NMe <sub>2</sub> ) <sub>3</sub> ( <b>5.3</b> ), depicted with 50% thermal ellipsoids; all hydrogen atoms have been omitted for clarity. ....	156
<b>Figure 5.4.</b>	ORTEP view of <sup>Mes</sup> [NCCN]Ta(CH <sub>2</sub> <sup>t</sup> Bu) <sub>2</sub> ( <b>5.7</b> ), depicted with 50% thermal ellipsoids; all hydrogen atoms have been omitted for clarity.....	159
<b>Figure 5.5.</b>	Potential pathways for ligand β-H abstraction. ....	161
<b>Figure 5.6.</b>	Computational model of the trimethyl tantalum starting complex...	162
<b>Figure 5.7.</b>	Relative energies of the intermediates and transition states in a potential σ-bond metathesis mechanism. ....	163
<b>Figure 5.8.</b>	JIMP Pictures of the one-step σ-bond metathesis pathway.....	163
<b>Figure 5.9.</b>	Relative energies of the intermediates and transition states in a potential two-step α-H abstraction/alkylidene mediated C-H activation mechanism. ....	164
<b>Figure 5.10.</b>	JIMP Pictures of alkylidene mediated C-H activation of the ligand backbone. ....	165
<b>Figure 5.11.</b>	ORTEP view of <sup>Mes</sup> [NCCN]Ta(Cl)(CH <sub>2</sub> <sup>t</sup> Bu) ( <b>5.10</b> ), depicted with 50% thermal ellipsoids; all hydrogen atoms have been omitted for clarity. ....	167

*Chapter Six                      Thesis Summary and Extensions: Chiral Group 4 [NCN] Complexes*

<u>Figure</u>	<u>Title</u>	<u>Page</u>
<b>Figure 6.1.</b>	<sup>1</sup> H NMR spectrum of (1 <i>R</i> ,2' <i>S</i> ,4 <i>R</i> )-2-(1,7,7-trimethylbicyclo[2.2.1]hept-2-ylamino)ethyl ammonium chloride ( <b>6.8</b> ) in CDCl <sub>3</sub> . (* denotes ½ equivalent of CH <sub>3</sub> C(O)CH <sub>3</sub> ). ....	185



<b>Figure B.6.</b>	JIMP view of <b>D</b> . Selected bond distances (Å) and angles (deg): Ta1-C1 2.248, Ta1-C2 2.219, Ta1-C3 2.173, Ta1-C4 2.257, Ta1-N1 2.065, Ta1-N2 1.982, C1-Ta1-C2 130.5, C1-Ta1-C3 122.7, C2-Ta1-C3 106.1, C4-Ta1-N2 38.2. ....	226
<b>Figure B.7.</b>	Gaussview representations of selected NBO bonding and antibonding orbitals in the trimethyl complex <b>A</b> .....	229
<b>Figure B.8.</b>	Gaussview representations of selected NBO bonding and antibonding orbitals in the trimethyl complex <b>D</b> .....	230
<b>Figure B.9.</b>	JIMP Pictures of <b>A'</b> and <b>D'</b> .....	231

## GLOSSARY OF TERMS

The following abbreviations, most of which are commonly found in the literature, are used in this thesis.

Å	Angström
a, b, c	unit cell dimensions, lengths (Å)
$\alpha, \beta, \gamma$	unit cell dimensions, angles ( $^{\circ}$ )
Anal.	analysis
atm	atmosphere
Ar	aryl
$B_{eq}$	equivalent isotropic parameter
BBI	broad band inverse
Bn	benzyl, $-\text{CH}_2\text{C}_6\text{H}_5$
br	broad
<i>n</i> -Bu	<i>n</i> -butyl group, $-\text{CH}_2\text{CH}_2\text{CH}_2\text{CH}_3$
$^{13}\text{C}$	carbon-13
$C_1, C_2, C_{2v}$	Schoenflies symmetry designations
cal	calories
Calcd	calculated
CCD	charge coupled device
cm	centimetres
Cp	cyclopentadienyl, $\text{C}_5\text{H}_5$
Cp*	pentamethylcyclopentadienyl, $\text{C}_5\text{Me}_5$
cryst	crystal
Cy	cyclohexyl, $-\text{C}_6\text{H}_{11}$
d	doublet
dd	doublet of doublets
dq	doublet of quartets
dt	doublet of triplets
deg (or $^{\circ}$ )	degrees
diox	1,4-dioxane

°C	degrees Celsius
DFT	density functional theory
DME	1,2-dimethoxyethane
$d^n$	numbers of <i>d</i> -electrons
$d_n$	n-deuterated
$\Delta E_0$	zero point corrected electronic energy
$\Delta E_c$	electronic energy
EI-MS	electron ionization/mass spectrometry
Et	ethyl group, -CH <sub>2</sub> CH <sub>3</sub>
ETM	early transition metal
$\Delta G^\circ$	free energy
g	grams
gof	goodness of fit
GC-MS	gas chromatography/mass spectrometry
$\Delta H^\circ$	enthalpy
<sup>1</sup> H	proton
{ <sup>1</sup> H}	proton decoupled
h	hour
HIPT	hexaisopropylterphenyl, -(3,5-(2,4,6- <sup>i</sup> Pr <sub>3</sub> -C <sub>6</sub> H <sub>2</sub> ) <sub>2</sub> C <sub>6</sub> H <sub>3</sub> )
HMDSO	hexamethyldisiloxane
HOMO	highest occupied molecular orbital
Hz	Hertz, seconds <sup>-1</sup>
IR	infrared
<sup>n</sup> J <sub>AB</sub>	n-bond scalar coupling constant between nuclei A and B
K	Kelvin
kcal	kilocalories
kJ	kiloJoules
<sup>6</sup> Li	lithium-6
L	neutral two-electron donor
LTM	late transition metal
LUMO	lowest unoccupied molecular orbital

M	central metal atom (or molar, when referring to concentration)
M <sup>+</sup>	parent ion
<i>m</i>	meta
m	multiplet (NMR spectroscopy)
mm	millimetres
mM	millimolar
Me	methyl group
Mes	mesityl group, -2,4,6-Me <sub>3</sub> C <sub>6</sub> H <sub>2</sub>
mg	milligram(s)
MHz	megaHertz
MgADP	adenosine diphosphate, magnesium salt
MgATP	adenosine triphosphate, magnesium salt
mL	millilitre
mmol	millimole
MO	molecular orbital
mol	mole
MS	mass spectrometry
no.	number
<sup>15</sup> N	nitrogen-15
NHC	N-heterocyclic carbene
NMR	nuclear magnetic resonance
Np	Neopentyl group, -CH <sub>2</sub> C(CH <sub>3</sub> ) <sub>3</sub>
[NPN]	diamidophosphine ligand, -(PhNSiMe <sub>2</sub> CH <sub>2</sub> ) <sub>2</sub> PPh
<i>o</i>	ortho
ORTEP	Oakridge Thermal Ellipsoid Program
<i>p</i>	para
p	pentet
P <sub>i</sub>	inorganic phosphate, PO <sub>4</sub> <sup>3-</sup>
<sup>31</sup> P	phosphorus-31
{ <sup>31</sup> P}	phosphorus-31 decoupled
Ph	phenyl group, -C <sub>6</sub> H <sub>5</sub>

PhH	benzene
PhMe	toluene
<sup>R</sup> [PNP]	amidodiphosphine ligand, $-(R_2PCH_2SiMe_2)_2N$
[P <sub>2</sub> N <sub>2</sub> ]	diamidodiphosphine ligand, $-PhP(CH_2SiMe_2NSiMe_2CH_2)_2PPh$
ppm	parts per million
<sup>i</sup> Pr	isopropyl group, $-CH(CH_3)_2$
py	pyridine
q	quartet
R, R'	hydrocarbon substituents
R, R <sub>w</sub>	residual errors, (X-ray crystallography)
R <sup>2</sup>	coefficient of determination for a linear regression
reflns	reflections (X-ray crystallography)
rt	room temperature
s	singlet
sept	septet
syst	system
t	triplet
T	temperature in Kelvin or °C
THF	tetrahydrofuran
TMS	trimethylsilyl group, $-Si(CH_3)_3$
U(eq)	equivalent isotropic displacement parameter
V	unit cell volume
VT	variable temperature
X	halide substituent
XHYDEX	hydride location program
Z	asymmetric units per unit cell
<b>x</b> -d <sub>n</sub>	Complex <b>x</b> has n number of <sup>1</sup> H atoms replaced by <sup>2</sup> H atoms
<b>x</b> - <sup>15</sup> N <sub>2</sub>	Complex <b>x</b> has a <sup>15</sup> N <sub>2</sub> labeled dinitrogen moiety
η <sup>n</sup>	n-hapto
μ	bridging or absorption coefficient (X-ray crystallography)
ρ	density

$\rho_{\text{calc}}$	calculated density
$\lambda$	wavelength
$\delta$	chemical shift in ppm
$\sigma, \pi, \delta$	notations for bonding symmetries

---

## ACKNOWLEDGEMENTS

I wish to acknowledge first and foremost, Dr. Michael D. Fryzuk. My studies at UBC under his supervision have been memorable and truly a learning experience. During this time, I have learned an immense amount of chemistry and have been challenged on a daily basis to thoroughly investigate not only chemistry that pertains to me, but research that exists outside my expertise. Despite his busy schedule, he has always found the time to listen to my ideas (and problems), and offered words of encouragement and guidance when needed.

I would also like to thank those post-docs, graduate and undergraduate students who I have worked with in the Fryzuk in the past and present. I especially wish to thank: Erin MacLachlan for all her help and enthusiasm in the lab and always going for a coffee run whenever one was needed.

Howard Jong for his assistance with crystallographic questions and his expertise in restaurants.

Fiona Hess for all her assistance with editing and critical comments on this thesis.

Kevin Noonan for his help with polarimetry and other thought provoking discussions, and also golf.

Bryan Shaw for his golfing prowess and the introduction to a "turbo".

The department of chemistry at UBC has also been an immense help in making my research here easy and enjoyable. I would especially like to thank Howie Jong and Dr. Brian Patrick for their expertise in X-ray crystallography. I would also like to thank Dr. Nick Burlinson and the NMR personnel for their assistance with any questions and concerns I had with running the NMR spectrometers. I am also grateful to Brian Ditchburn for his timely help in glassblowing the many broken J. Young tubes I brought to him. I also must acknowledge the personnel in the mechanical and electronics shops with the timely help they provided during the many crisis periods encountered with the glovebox.

## DEDICATION

This work is dedicated to the two important women in my life. To my mother, Carolyn Norris, you have always been there for me and I greatly appreciate all that you have given me (especially my sense of humour (“Illegitimus Non Carborundum”)). If it wasn't for you, I hesitate to think where I would be. To my soon to be wife, Dr. Pauline Vykruta, your approach to life is truly inspirational. You have challenged me in many ways, and I look forward to spending the rest of my life with you, milačku.

## STATEMENT OF AUTHORSHIP

Chapters two, three, four, five and six were conducted in collaboration with Professor Michael D. Fryzuk, the research supervisor for this thesis, who assisted with identification and design of the research presented.

Chapter two features some initial research performed by a previous graduate student, Dr. Bruce MacKay, under the supervision of Professor Michael D. Fryzuk.

Chapter three and appendix B presents DFT calculations that were performed by Dr. Chad L. Beddie at the Texas A&M University under the supervision of Professor Michael Hall.

All experimental research, data analysis, and manuscript preparation were performed by the thesis author.

## **Chapter One**

# **Dinitrogen Chemistry and Ligand Design**

### ***1.1. Origins of Coordination and Organometallic Chemistry***

Our modern view of coordination chemistry began at the end of the 19<sup>th</sup> century at a time when the understanding of valence bonding and geometry in transition metal complexes was in a state of confusion. Prior to this period, the configuration and composition of many inorganic compounds were written in accordance with a theory described by the Swedish chemist, Jöns Jacob Berzelius.<sup>1</sup> Berzelius ardently attempted to sort all chemical compounds using a paired system which he called “the two-component theory”. The Swedish chemists, Christian Wilhelm Blömstrand and Sophus Mads Jørgensen,<sup>2,3</sup> applied this theory to describe the bonding and geometry of hexaammine cobalt(II) complexes. Blömstrand and Jørgensen postulated that in a material with the composition  $\text{CoCl}_2 \cdot 6 \text{NH}_3$ , the divalent  $\text{Co}^{2+}$  metal centre could only form two bonds to the ammonia molecules. As a result, the binding of the ammonia residues to the metal centre must occur in a linking fashion that would form chains (Figure 1.1).<sup>3</sup>

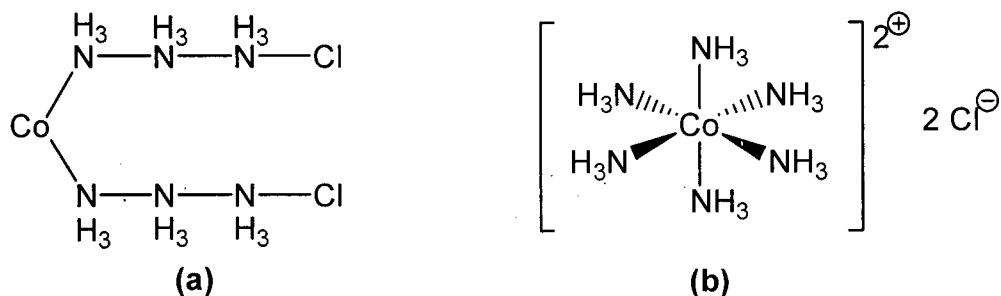


**Figure 1.1.** Interpretation of the coordination sphere of  $\text{CoCl}_2 \cdot 6 \text{NH}_3$  by (a) Blömstrand/Jørgensen and (b) Werner.

Upon examination of Blömstrand and Jørgensen's research, Alfred Werner noted several anomalies that did not corroborate physical and chemical experimentation.<sup>4,5</sup> This evidence led Werner to postulate that "single atoms or ions act as central positions, where a certain number of other compounds, atoms, ions, or other molecules are ordered in simple geometrical patterns" (Figure 1.1).<sup>6,7</sup> Werner found that this hypothesis could successfully explain experimental discrepancies that were observed in the structures of the complexes proposed by Blömstrand and Jørgensen. Werner also introduced the term coordination number, which describes the number of atoms that are grouped around a central nucleus. For his seminal work in this area, Alfred Werner was awarded the Nobel Prize in Chemistry in 1913 "in recognition of his work on the linkage of atoms in molecules".<sup>3</sup> Werner's contributions led to conception of the term ligand, which refers to atoms or groups attached to a central atom in the formation of a coordination compound.<sup>8</sup>

The progress in coordination chemistry stimulated interest in the coordination of other ligands and one mature area of chemistry which has emerged is the study of organometallic complexes. Organometallic chemistry is defined as the study of compounds containing a metal-carbon bond.<sup>7,9</sup> Despite the prior isolation of organometallic compounds like  $\text{Zn}(\text{CH}_2\text{CH}_3)_2$  and  $\text{Ni}(\text{CO})_4$ ,<sup>9</sup> the origins of modern organometallic chemistry are believed to have begun with the discovery of ferrocene, reported separately by both Wilkinson and Fischer.<sup>10-12</sup> The importance of this finding in the field of chemistry was embodied in the awarding of the Nobel Prize in Chemistry in 1973 to both scientists. The field of organometallic chemistry has grown since this discovery to include transition metal complexes with ligands such as CO,  $\text{CN}^-$ , and benzene.<sup>9</sup> Bonding in these complexes is usually described by molecular orbital theory

and the reactivity dictated by the effective atomic number (EAN) or “18-electron rule”.<sup>9,13</sup> Organometallic complexes are of interest from both an academic perspective in terms of their synthesis and bonding implications, and from an industrial perspective regarding their potential to mediate catalytic reactions. Indeed, two recent Nobel Prizes in Chemistry were awarded in 2001 to Knowles, Noyori, and Sharpless<sup>14</sup> and in 2005 to Chauvin, Grubbs, and Schrock<sup>15</sup> for research involving the use of organometallic catalysts in organic synthesis.

The emergence of organometallic chemistry and the continued relevance of coordination chemistry has also been driven in part by its application and relevance in other areas of science. In particular, research in the biological field has relied on fundamental research in both organometallic and inorganic chemistry. Evidence of this comes from the ubiquitous role metal complexes play in living organisms. For example, iron plays a fundamental role in the daily function of human life forms.<sup>16</sup> Other metals, such as copper, are also known to serve an integral part in enzymatic processes and vitamin synthesis.<sup>17</sup> One important progression in the borderline field of inorganic chemistry and biology is the area of dinitrogen fixation,<sup>18</sup> which is the topic of discussion in the next section.

## **1.2. Reactivity of Dinitrogen**

The utilization of molecular nitrogen, or dinitrogen, to form organic nitrogen-containing products is one of the substantial challenges in organometallic chemistry.<sup>19-27</sup> Nitrogen appears in all biological systems and is vital for the synthesis of amino acids, nucleotides, enzymes, and other biologically important compounds.<sup>28</sup> One could envision the synthesis of these organic nitrogen-containing compounds from the catalytic reaction of dinitrogen with simple organic reagents (Figure 1.2). A formidable hurdle for the successful implementation of this catalytic cycle is the inertness of molecular nitrogen. Dinitrogen possesses a strong triple bond that must be completely cleaved and functionalized to form organic compounds. Furthermore, the robust dinitrogen molecule features a large dissociation energy (941 kJ mol<sup>-1</sup>), the absence of a dipole, and possesses a large HOMO-LUMO gap, which makes oxidation and reduction difficult.

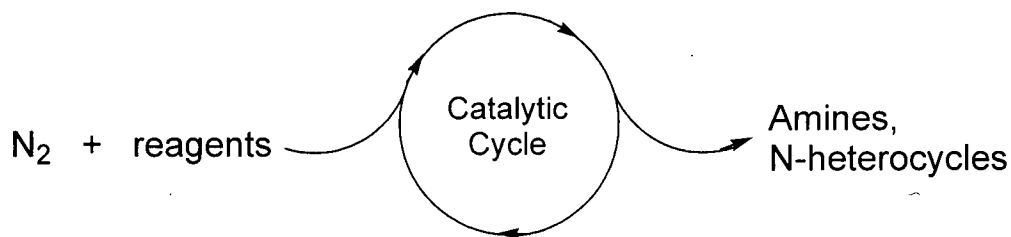
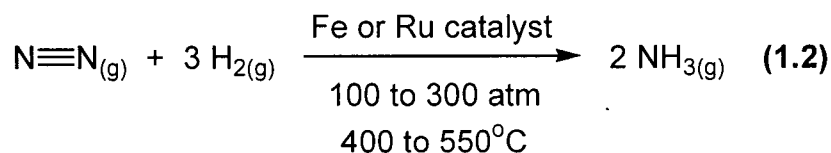


**Figure 1.2.** Catalytic formation of N-containing compounds from  $N_2$ .

Notwithstanding its poor reactivity, dinitrogen can be converted to ammonia by several well-known pathways. Several biological systems are known to activate and functionalize dinitrogen to form ammonia.<sup>29,30</sup> For example, the enzyme nitrogenase is able to bind to  $N_2$  and other substrates, reducing these bound molecules using electrons provided by metal clusters. This facilitates the protonation of the reduced nitrogen atoms and produces  $H_2$  as a byproduct of the reaction. As a result of this protonation, the bound nitrogen atoms become “fixed” and are released as ammonia (Equation 1.1). It is important to note that the reduction of  $N_2$  in this process is energy intensive, requiring 16 equivalents of MgATP. While the mechanistic details of this transformation remain unclear, the catalytic process has been scrutinized in detail.<sup>31</sup>



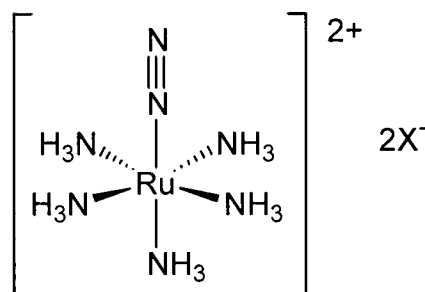
The most significant example in which dinitrogen is converted to ammonia is the Haber-Bosch process.<sup>32,33</sup> Both  $N_2$  and  $H_2$  are reacted at high temperature (400-450°C) and pressure (270 atm) in the presence of a Fe or Ru catalyst to yield ammonia (Equation 1.2). In this process,  $H_2$  is both a reducing agent and substrate for the production of ammonia. The impact of this discovery to the field of chemistry was monumental as both Haber and Bosch each received the Nobel Prize in Chemistry in 1918 and 1931, respectively,<sup>34,35</sup> for their discovery and refinement of the technique.



One feature consistent with the known examples of dinitrogen fixation is the incidence of transition metals at the active site during catalysis. This fact has shifted research efforts towards the development of other transition-metal-assisted dinitrogen reduction systems with an aim to achieve a homogeneous version of the Haber-Bosch process. To this end, the coordination of dinitrogen to transition metals has been investigated and will be discussed further.

### 1.3. Coordinated Dinitrogen Complexes

The necessity of a transition metal catalyst in the Haber-Bosch process suggests that the activation of  $N_2$  can be induced by a transition metal. This assumption has stimulated interest in the potential coordination of  $N_2$  to transition metals. In 1965, Allen and Senoff serendipitously discovered the first metal dinitrogen complex by the reaction of  $RuCl_3$  with hydrazine hydrate.<sup>36,37</sup> This result was revolutionary, as it became apparent that  $N_2$  could act as a ligand in a coordination complex. In these complexes, dinitrogen is typically “activated” when coordinated to the transition metal. This activation can decrease the bond order of the  $N\equiv N$  bond to varying degrees. In general, late transition metal (LTM) complexes feature an  $N_2$  ligand that is weakly activated. An examination of the N-N bond lengths by X-ray crystallography in **1.1** and many other LTM dinitrogen complexes<sup>19</sup> reveals distances that are close to free  $N_2$  (1.0975 Å).<sup>38,39</sup>



**1.1**

**Figure 1.3.** The first reported transition metal dinitrogen complex ( $X^- = Br^-, I^-, BF_4^-, PF_6^-$ ).

Early transition metals (ETMs) have also been extensively studied for the coordination and activation of dinitrogen. In general, stronger activation of the dinitrogen ligand is observed compared to LTM complexes. One series of ETM complexes that have been examined for their potential to activate molecular dinitrogen are substituted zirconium metallocenes. The reduction of  $(\eta^5\text{-C}_5\text{Me}_5)_2\text{ZrCl}_2$  with Na/Hg amalgam under nitrogen produces  $[(\eta^5\text{-C}_5\text{Me}_5)_2\text{Zr}(\eta^1\text{-N}_2)]_2(\mu\text{-}\eta^1\text{:}\eta^1\text{-N}_2)$  with three bound  $\text{N}_2$  ligands (Figure 1.4).<sup>40</sup> A slight modification in the cyclopentadienyl ancillary ligand reveals a different bonding mode for  $\text{N}_2$  and higher degree of activation.<sup>41</sup> The reduction of  $(\eta^5\text{-C}_5\text{Me}_4\text{H})_2\text{ZrCl}_2$  with Na/Hg amalgam under  $\text{N}_2$  yields  $((\eta^5\text{-C}_5\text{Me}_4\text{H})_2\text{Zr})_2(\mu\text{-}\eta^2\text{:}\eta^2\text{-N}_2)$  (**1.3**), a side-on bound dinitrogen complex with a N-N bond length of 1.377(3) Å, which is significantly lengthened from free  $\text{N}_2$  (1.0976 Å).<sup>38,39</sup>

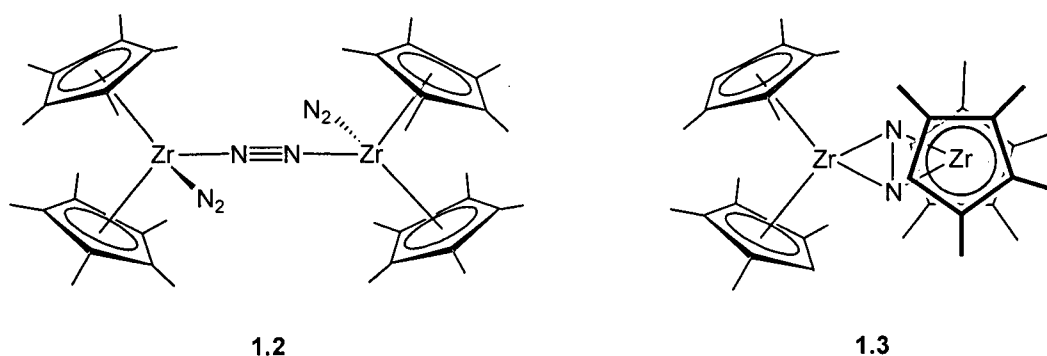
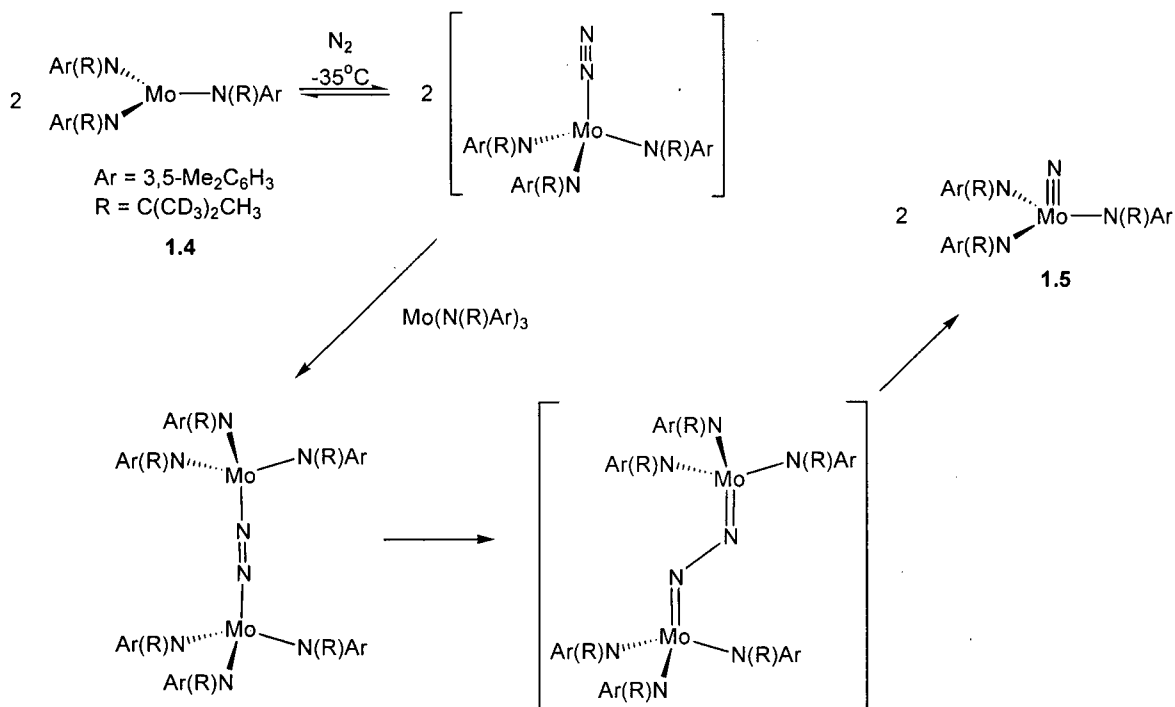


**Figure 1.4.** Examples of zirconocene-based dinitrogen complexes.

Although dinitrogen complexes of almost all the transition metals have been reported, including the actinides and lanthanides, the transformation of the dinitrogen ligand in these complexes has proven to be difficult. One goal of dinitrogen activation via transition metal complexes is the complete cleavage of the  $\text{N}\equiv\text{N}$  bond. This objective is quite challenging since dinitrogen possesses characteristics that make  $\text{N}_2$  an unreactive ligand. Attempts to cleave the “activated”  $\text{N}\equiv\text{N}$  bond with chemical reagents reveal the inert  $\text{N}_2$  ligand is susceptible to displacement by more reactive ligands such as  $\text{H}_2$ ,<sup>42-47</sup>  $\text{CO}$ ,<sup>44-49</sup> and olefins.<sup>42,44,48,50,51</sup>

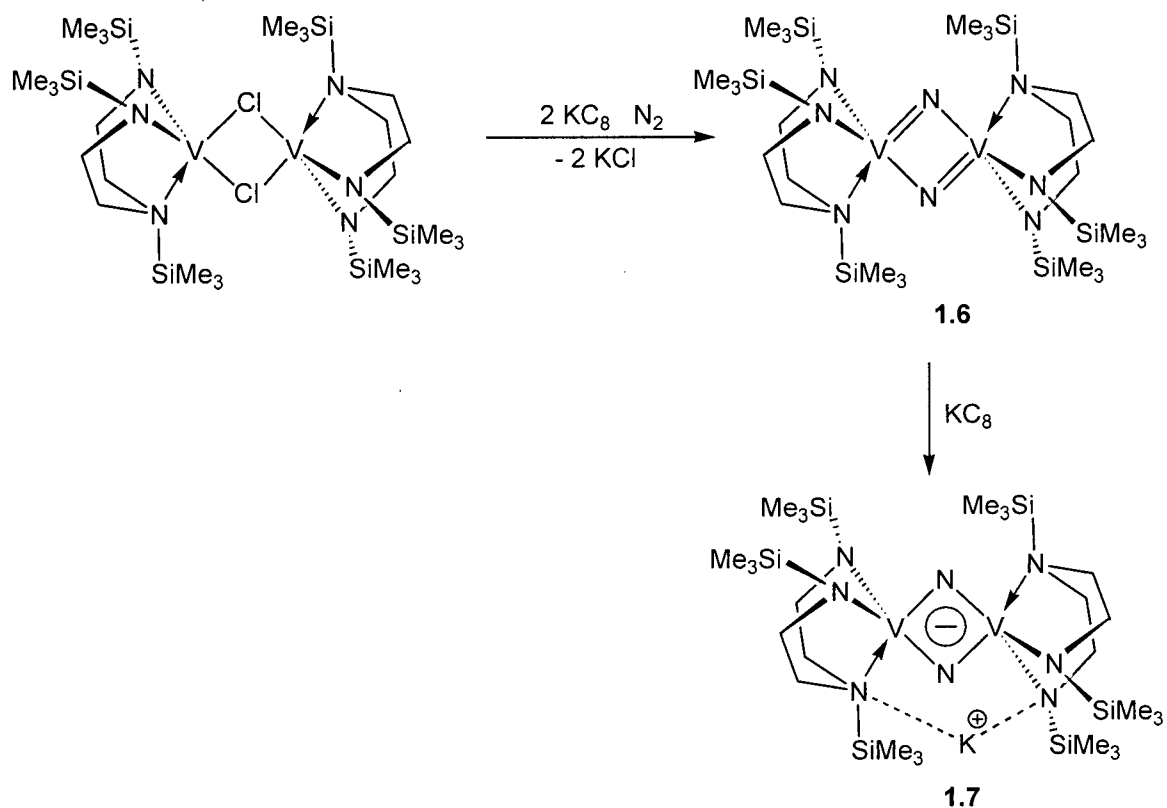
## 1.4. Dinitrogen Cleavage

The synthesis of ammonia from  $N_2$  by biological methods and the Haber-Bosch process requires the cleavage of the  $N\equiv N$  bond. Several assays have focused on promoting the cleavage of molecular nitrogen with ETMs. Perhaps the most recognized example of dinitrogen cleavage involves molybdenum amide complexes reported by Cummins.<sup>52,53</sup> A three-coordinate  $Mo[NR(Ar)]_3$  stabilized by bulky *N-tert*-butyl anilide ligands (**1.4**) is able to bind to  $N_2$  to yield a dinuclear end-on bound dinitrogen complex at  $-35^\circ C$  (Scheme 1.1). Warming solutions of this product to room temperature results in the cleavage of the  $N\equiv N$  bond to form the terminal nitride complex  $N\equiv Mo[NR(Ar)]_3$  (**1.5**). Density functional theory calculations on this transformation suggest that bond cleavage proceeds through a zig-zag dinuclear molybdenum dinitrogen transition state.<sup>54</sup> This process is remarkable as the reduction of the  $N_2$  ligand occurs under mild conditions and requires no added reagents. In this example, the reducing power required for N-N bond scission originates from the two molybdenum metal centres from which six reducing equivalents reductively cleave the  $N\equiv N$  triple bond. While ammonia synthesis from this nitride species has not been reported, a niobium analog of **1.5** has recently been used in a nitrogen atom transfer reaction with acid chlorides to generate new organic nitrile products.<sup>55</sup> Unfortunately, the formation of these organic nitrogen containing compounds is still stoichiometric in nature and this process has yet to be developed into a catalytic system.



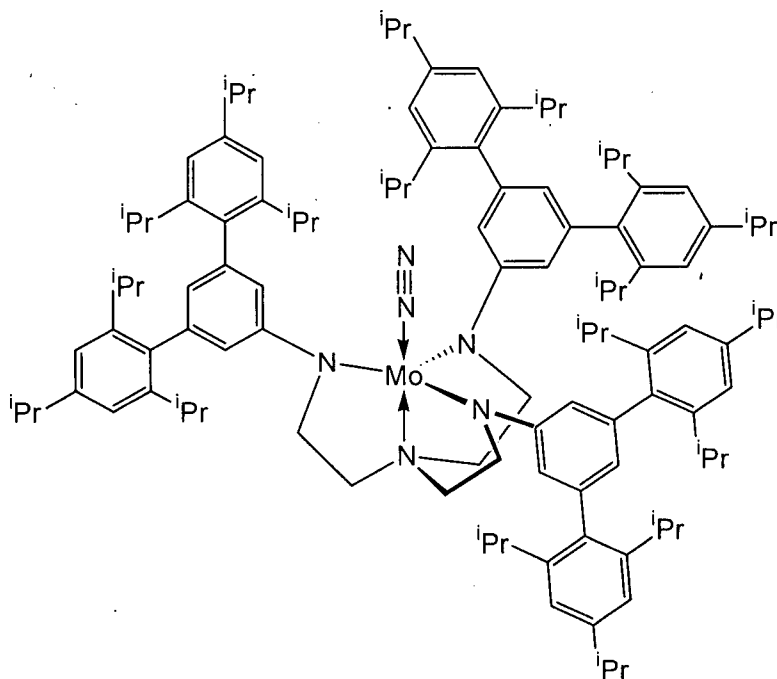
Scheme 1.1.

Vanadium complexes are also known to effect  $\text{N}\equiv\text{N}$  bond cleavage. For example, the reduction of the diamidoamine vanadium complex  $(\text{Me}_3\text{Si}(\text{CH}_2\text{CH}_2\text{NSiMe}_3)_2\text{V})_2(\mu\text{-Cl})_2$  with potassium graphite ( $\text{KC}_8$ ) in the presence of  $\text{N}_2$  results in the coordination and cleavage of dinitrogen to form the dimeric vanadium bis(nitride) complex  $(\text{Me}_3\text{Si}(\text{CH}_2\text{CH}_2\text{NSiMe}_3)_2\text{V})_2(\mu\text{-N})_2$  (**1.6**) (Scheme 1.2).<sup>56</sup> The vanadium-nitrogen bond from the cleaved dinitrogen unit can be further reduced with potassium graphite to generate **1.7**.



Scheme 1.2.

The cleavage of molecular dinitrogen can also be achieved by the sterically encumbered molybdenum triamidoamine complex  $\text{HIPT}(\text{N}_3\text{N})\text{MoCl}$  (where  $\text{HIPT}(\text{N}_3\text{N}) = [[(3,5-(2,4,6\text{-}i\text{Pr}_3\text{C}_6\text{H}_2)_2\text{C}_6\text{H}_3)\text{NCH}_2\text{CH}_2]_3\text{N}]^{3-}$ ).<sup>57,58</sup> The dinitrogen complex **1.8** (Figure 1.5) can be synthesized by the stepwise reduction and oxidation of  $\text{HIPT}(\text{N}_3\text{N})\text{MoCl}$ . While no discrete molybdenum nitride species has been isolated as a result of cleavage of the  $\text{N}_2$  ligand in **1.8**, experiments with a compatible proton source and reducing agent reveal that **1.8** is capable of catalytically transforming dinitrogen into ammonia (four turnovers are reported before the catalyst loses function). This result and subsequent modeling studies of the intermediates formed during this reaction demonstrate that cleavage of  $\text{N}_2$  is possible under certain conditions.



1.8

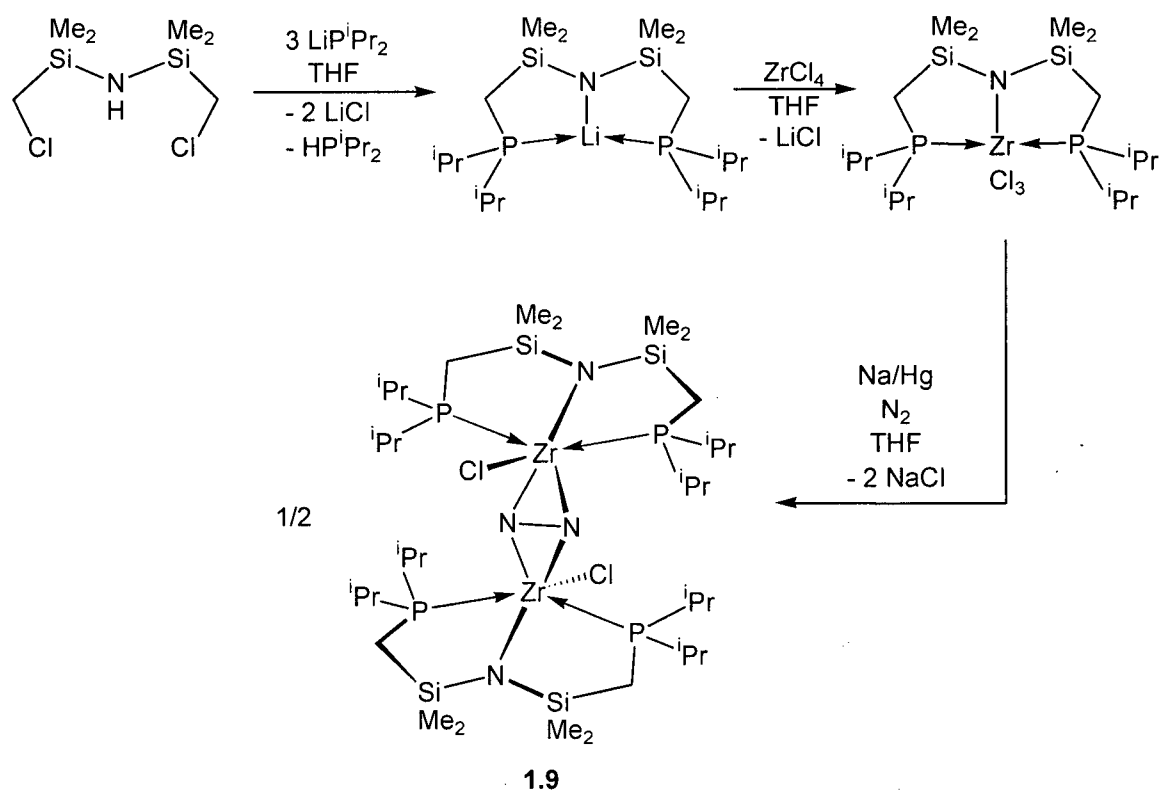
**Figure 1.5.** Successful catalyst for the synthesis of  $\text{NH}_3$  from  $\text{N}_2$

The activation and cleavage of molecular nitrogen by transition metal complexes can be largely influenced by the ligands encompassing a metal centre. It has been demonstrated that this chemistry can be regulated by slight modifications of the ligand architecture. One aspect of research in the Fryzuk group has been the design and synthesis of ancillary ligands effective for stabilizing transition metal dinitrogen complexes. For the most part, ancillary ligands involving mixed phosphine and amide donors have been investigated.

### 1.5. *Amidophosphine Ligands for $\text{N}_2$ Activation*

The combination of both phosphine and amido donors into a chelating ligand framework was anticipated to be suitable for the stabilization of different types of transition metals across the transition series in various oxidation states. Phosphine donors are well known to coordinate to LTM centres, while anionic amido donors have been used extensively in many ETM complexes. The first ligand that was investigated employing these donor groups was the [PNP] design, utilizing a centrally positioned

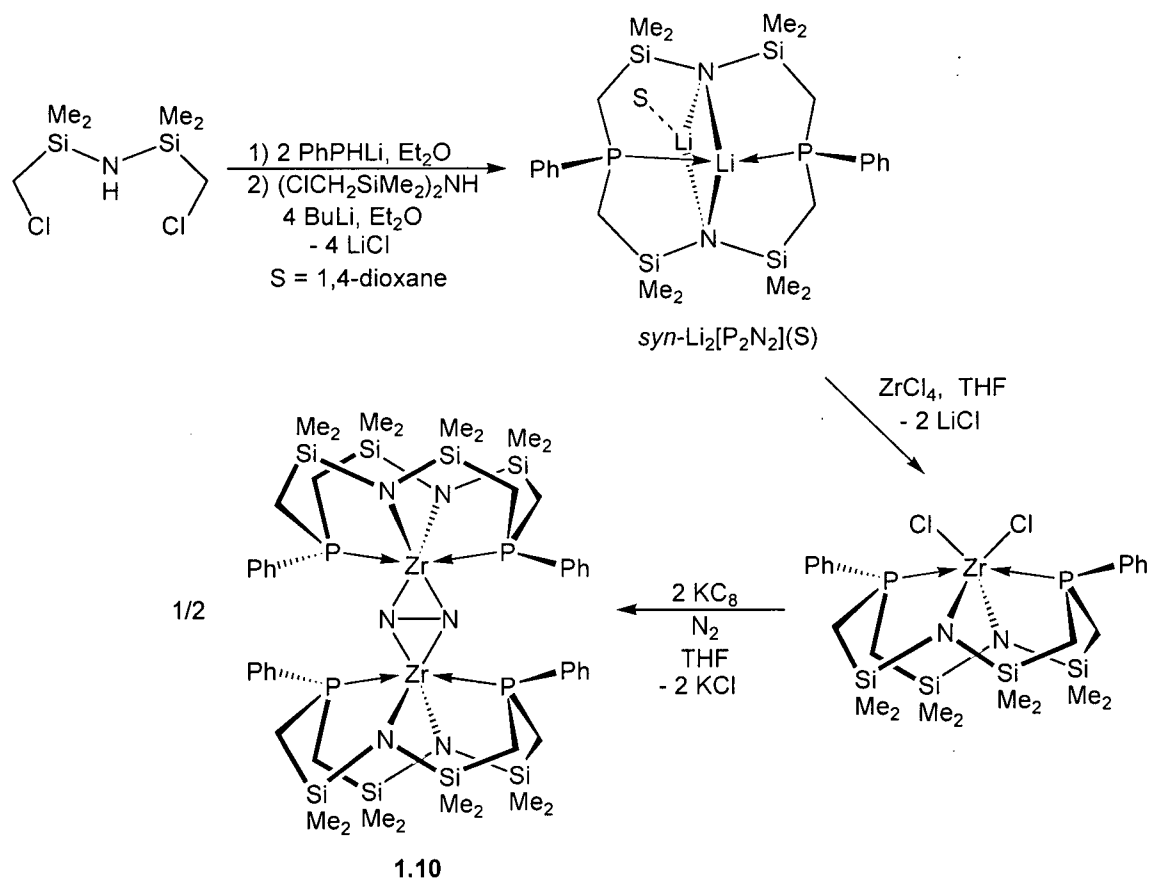
amido donor and two flanking phosphine groups.<sup>59</sup> The preparation of this ligand is shown in Scheme 1.5, and involves the addition of three equivalents of  $\text{LiP}^i\text{Pr}_2$  to commercially available  $\text{HN}(\text{SiMe}_2\text{CH}_2\text{Cl})_2$  to generate the lithiated [PNP] ligand. Both early and LTM complexes have been stabilized using this ligand and, in some cases, activated dinitrogen complexes (ie. **1.9**) have been isolated.<sup>59-64</sup> Despite these successful outcomes, one drawback of the [PNP] design in ETM chemistry is the potential for the phosphine groups to dissociate from the metal centre.<sup>62,65,66</sup> Given this possibility, further modifications involving phosphine and amide donors have been investigated.



Scheme 1.5.

A macrocyclic  $[\text{P}_2\text{N}_2]$  ligand was investigated that employs two neutral phosphine and two anionic amido donor groups. The preparation of this ligand follows a similar synthetic methodology to the [PNP] ligand. A diphosphinoamine precursor is synthesized by the addition of  $\text{PhPHLi}$  to  $\text{HN}(\text{SiMe}_2\text{CH}_2\text{Cl})_2$ . This reagent is deprotonated and reacted with a second equivalent of  $\text{HN}(\text{SiMe}_2\text{CH}_2\text{Cl})_2$  to generate the lithiated  $[\text{P}_2\text{N}_2]$  ligand (Scheme 1.6).<sup>67</sup> The arrangement of the phosphine atoms offers

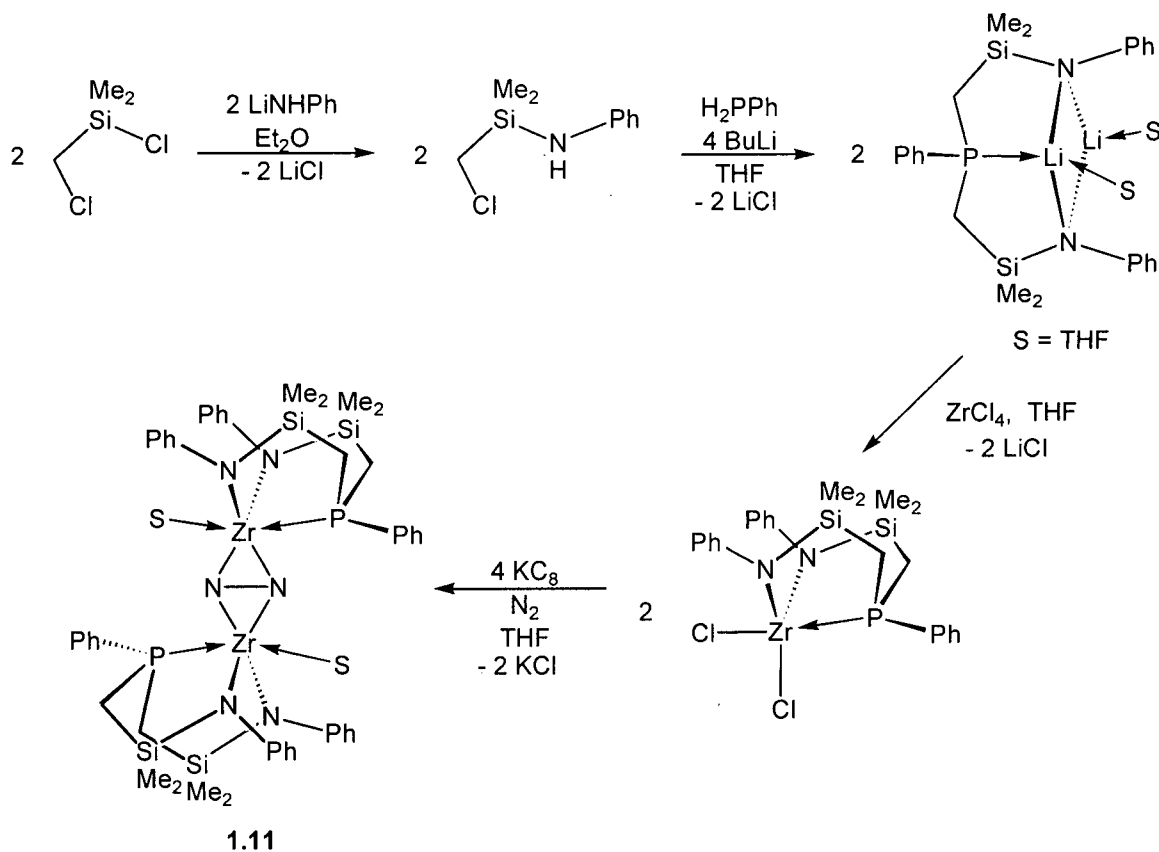
the potential for the synthesis of two isomeric forms of the ligand; the *syn* isomer can be selectively synthesized by controlling the experimental conditions of the reaction. The  $[P_2N_2]$  macrocycle has been effectively used as a supporting ligand for the isolation of several ETM dinitrogen complexes (ie. **1.10**).<sup>68-70</sup> One drawback that has been found of certain  $[P_2N_2]$  complexes of tantalum has been their lack of reactivity. The additional donor in the ligand, as compared to [PNP], has resulted in several coordinatively and electronically saturated  $[P_2N_2]$  systems that possess diminished reactivity.<sup>71</sup>



Scheme 1.6.

Another variant of the amidophosphine ligand involves the [NPN] design that utilizes one phosphine donor and two anionic amido groups. This design reconciles the problems encountered with the reactivity of  $[P_2N_2]$  complexes and still maintains a dianionic bonding nature. The synthesis of the Li<sub>2</sub>[NPN] ligand involves the addition of four equivalents of *n*-BuLi to a mixture of one equivalent of PhPH<sub>2</sub> and two equivalents

of  $\text{PhNSiMe}_2\text{CH}_2\text{Cl}$  (Scheme 1.7). Metathesis reactions with metal chloride reagents and the  $\text{Li}_2[\text{NPN}]$  ligand were used successfully to synthesize  $[\text{NPN}]\text{MCl}_2$  complexes. For example, the reaction between  $\text{Li}_2[\text{NPN}]$  and  $\text{ZrCl}_4$  proceeds to give  $[\text{NPN}]\text{ZrCl}_2$ . This complex can be reduced in the presence of nitrogen to form the dinitrogen complex **1.11**.<sup>72</sup>



Scheme 1.7.

Modifications to the  $[\text{NPN}]$  ligand design have generally focused on the replacement of the reactive N-Si bond.<sup>73,74</sup> Not only is this bond sensitive to water and air, it can rupture during the reduction process forming products which result from deleterious modification of the  $[\text{NPN}]$  ligand.<sup>74-76</sup> One aspect that remains relatively unexplored is the substitution of the phosphine group for another neutral donor. N-Heterocyclic carbenes (NHCs) have come to be regarded as phosphine equivalents and have been extensively studied as essential ligands in homogeneous catalysis and small

molecule activation processes.<sup>77</sup> Given this parity with phosphines, the substitution of an NHC in place of the phosphine donor in the [NPN] architecture can be examined, which could generate a [NCN] ancillary ligand (Figure 1.6). The following sections of this chapter will describe the discovery of NHCs and their emergence as ligands in selected areas of organometallic catalysis.

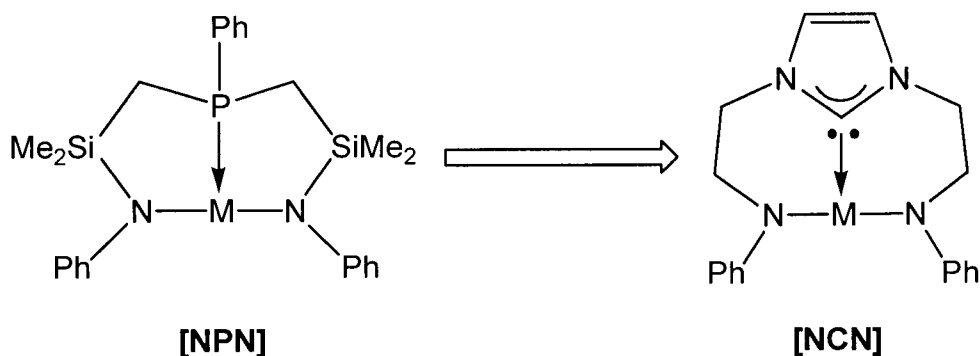


**Figure 1.6.** Design of a diamido-N-heterocyclic carbene [NCN] ligand.

### 1.6. Introduction to Carbenes

Our understanding of carbene chemistry has progressed in the past 20 years as a result of greater insight into the electronic structure and stability of carbenes.<sup>78,79</sup> Carbenes are neutral species that contain a divalent carbon atom with only six electrons.<sup>80</sup> Two nonbonding electrons can be found in two different frontier orbitals, commonly referred to as the  $\sigma$  and  $p_\pi$  orbitals. The existence of these valence electrons in these orbitals presents the possibility of two unique electronic configurations (Figure 1.7). The singlet state involves the pairing of these electrons in the same  $\sigma$  orbital. In the parallel triplet state, the two electrons can occupy unique  $\sigma$  and  $p_\pi$  orbitals.

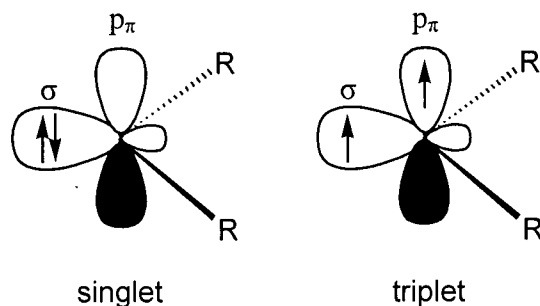


**Figure 1.7.** Possible electronic configurations of carbenes.

The nature of this electronic configuration directly influences the reactivity of the carbene molecule.<sup>81</sup> Singlet carbenes possess a filled and a vacant orbital and thus exhibit an ambiphilic nature. As a result, singlet carbenes are very reactive species and difficult to isolate. Attempts to isolate singlet carbenes often result in rearrangement reactions such as 1,2-migration,<sup>82</sup> dimerization,<sup>83,84</sup> [1+2]-cycloadditions to C=C bonds,<sup>85,86</sup> and insertion into C-H bonds.<sup>87</sup> Conversely, triplet carbenes display a diradical nature owing to two singly occupied orbitals. As a result, these species have been reported to perform carbene dimerization,<sup>88-90</sup> [1+2]-cycloadditions to C=C bonds,<sup>91</sup> and insertion reactions<sup>89</sup> that are similar to their singlet carbene counterparts but proceed by a different mechanism.

The spin multiplicity of a carbene is dictated by the energetic difference between the  $\sigma$  and  $p_\pi$  orbitals.<sup>92-99</sup> A large  $\sigma$ - $p_\pi$  energy separation favors a singlet ground configuration, whereas a small energy difference can induce the triplet spin state. The  $\sigma$ - $p_\pi$  energy gap can be increased by the presence of  $\sigma$ -electron withdrawing substituents adjacent to the divalent carbon atom. These groups inductively stabilize the  $\sigma$ -nonbonding orbital by increasing its  $s$  character, while leaving the  $p_\pi$  orbital unchanged. This gap can also be increased with adjacent  $\pi$ -donating atoms, which quenches the electron deficient nature of the carbene and results in a polarized four electron three-centered  $\pi$  system.

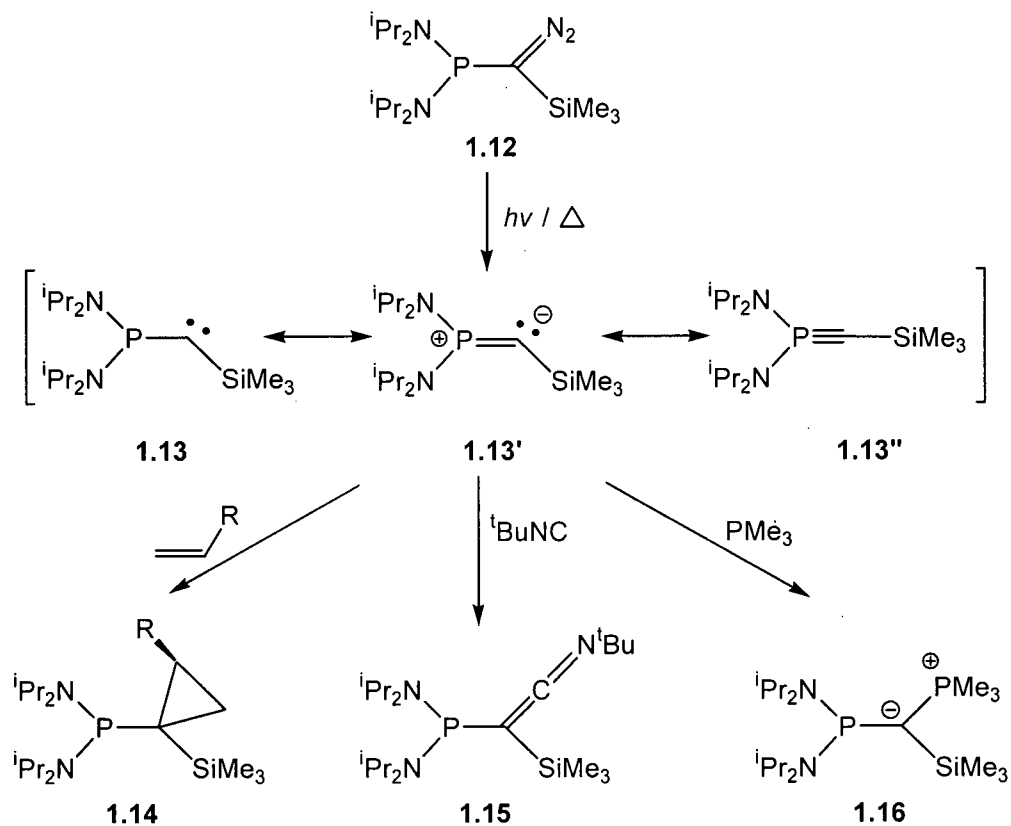
Steric effects also influence the ground state multiplicity of a carbene.<sup>100-102</sup> Bulky substituents on the carbene can dictate the multiplicity in the absence of electronic effects. For example, dimethylcarbene has a bent singlet ground state with a bond angle of  $111^\circ$  at the central carbon atom.<sup>100,101</sup> Conversely, carbenes with two bulky

substituents, such as di(*tert*-butyl)carbene, exist in the triplet state and exhibit larger bond angles (ie.  $143^\circ$  for di(*tert*-butyl)carbene).<sup>102</sup>

## 1.7. Isolation of Stable Carbenes

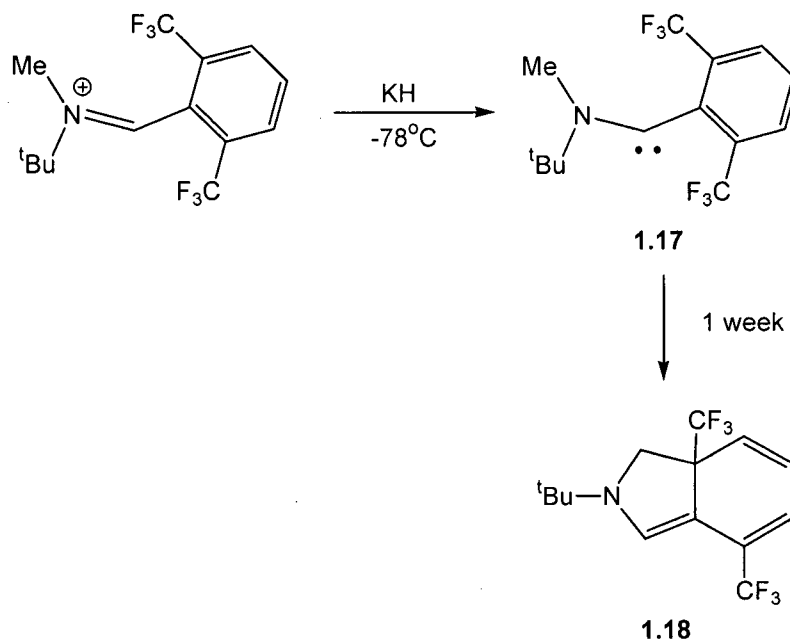
### 1.7.1. Acyclic Carbenes

The first discovery of a stable isolable carbene was reported by Bertrand in 1988 (Scheme 1.8).<sup>79,103,104</sup> Phosphanyl(silyl) carbenes can be prepared by the thermolysis or photolysis of a diazo precursor (**1.12**). The carbene **1.13** is remarkably stable for weeks at room temperature and can be purified by distillation under vacuum at  $75^\circ\text{C}$ - $80^\circ\text{C}$ . At the time, the notion that this species was a carbene was met with skepticism as **1.13** does not exhibit reactivity typical of singlet carbenes. For example, **1.13** does not react with simple alkenes but can add to polar C=C bonds to give cyclopropane products (ie. **1.14**)<sup>104,105</sup> Nucleophilic reactions were also reported with **1.13** and isonitriles<sup>106-108</sup> and phosphines<sup>109</sup> to give **1.15** and **1.16**, respectively. Despite this skepticism, the existence of a carbene was confirmed by both computational methods<sup>110</sup> and an X-ray crystallographic study on an analog of **1.13**.<sup>111</sup> A P-C-Si bond angle of  $152.6^\circ$  was noted, in addition to short C-P and C-Si bond lengths, which suggests the ylide resonance form **1.13'** contributes to the overall structure of the acyclic carbene.



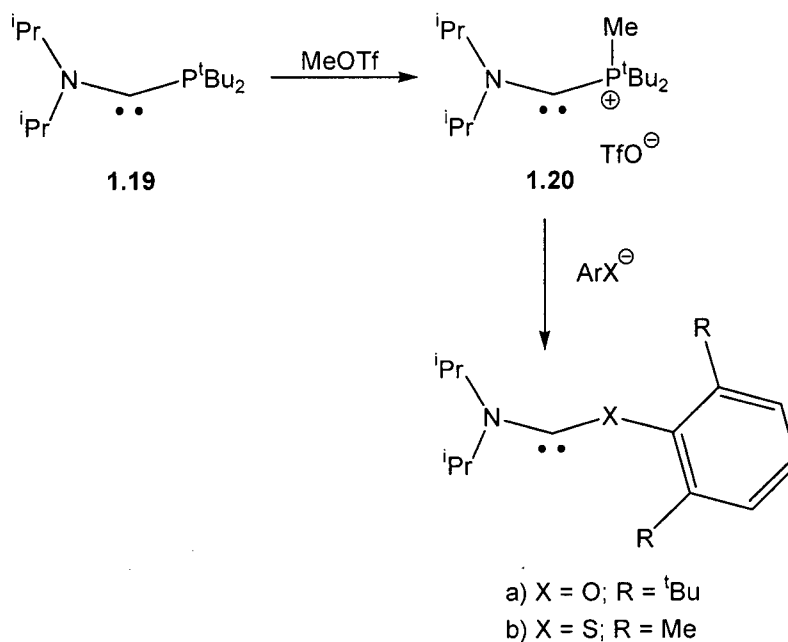
Scheme 1.8.

Following these results, the isolation of other stable aminocarbenes were pursued. For example, an amino(aryl)carbene is accessible by deprotonation of the iminium salt **1.17** (Scheme 1.9).<sup>112,113</sup> Although **1.17** could be isolated, its instability represents a common characteristic consistent of many acyclic carbenes. Compound **1.17** slowly decomposes over a period of 1 week to give **1.18**, which is a product of an intramolecular cyclization reaction.<sup>112</sup>



**Scheme 1.9.**

The combination of phosphanyl and amino groups on a divalent carbon centre has also been investigated, for example **1.19** in Scheme 1.10.<sup>114</sup> This class of carbenes exhibits thermal sensitivity and decomposes at temperatures above  $-20^{\circ}\text{C}$ . The stability of phosphanyl(amino) carbenes can be enhanced by the alkylation of **1.19** to afford the phosphonium salt **1.20**. This phosphonium salt is indefinitely stable in the solid state at room temperature,<sup>115</sup> but susceptible to displacement by nucleophiles like *tert*-butoxide. This substitution of functional groups on the carbene allows for the formation of other amino heteroatom carbenes.



Scheme 1.10.

### 1.7.2. N-Heterocyclic Carbenes

In the early 1960's, Wanzlick proposed that the incorporation of a carbene unit in a cyclic structure between two amino substituents would enhance the stability and lead to the isolation of this reactive species.<sup>83,84,116</sup> It was envisioned that the elimination of chloroform from **1.21** could yield the corresponding carbene product (Figure 1.8). Although the dimeric species **1.22** was the only product isolated from this reaction, recent findings suggest an equilibrium exists between the carbene and **1.22**.<sup>117</sup> While these results did not lead to the isolation of a stable carbene molecule, this idea did stimulate interest into the incorporation of a carbene unit in an N-heterocyclic manifold.

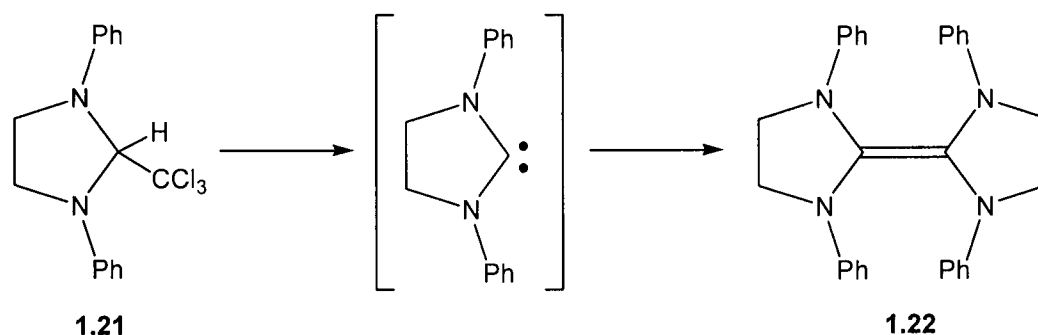


**Figure 1.8.** Attempted synthesis of an NHC by chloroform elimination.

The first stable NHC was isolated by Arduengo in 1991.<sup>118</sup> Deprotonation of bis(1-adamantyl)imidazolium chloride with NaH provides the first stable crystalline NHC compound, which melts at 240-241°C without decomposition. Since this discovery, other methods for the syntheses of NHCs have been reported, which includes the desulfurization of imidazole-2(3H)-thiones<sup>119</sup> and methanol elimination by thermolysis of 5-methoxy-1,3,4-triphenyl-4,5-dihydro-1H-1,2,4-triazoles (Figure 1.9).<sup>120</sup>

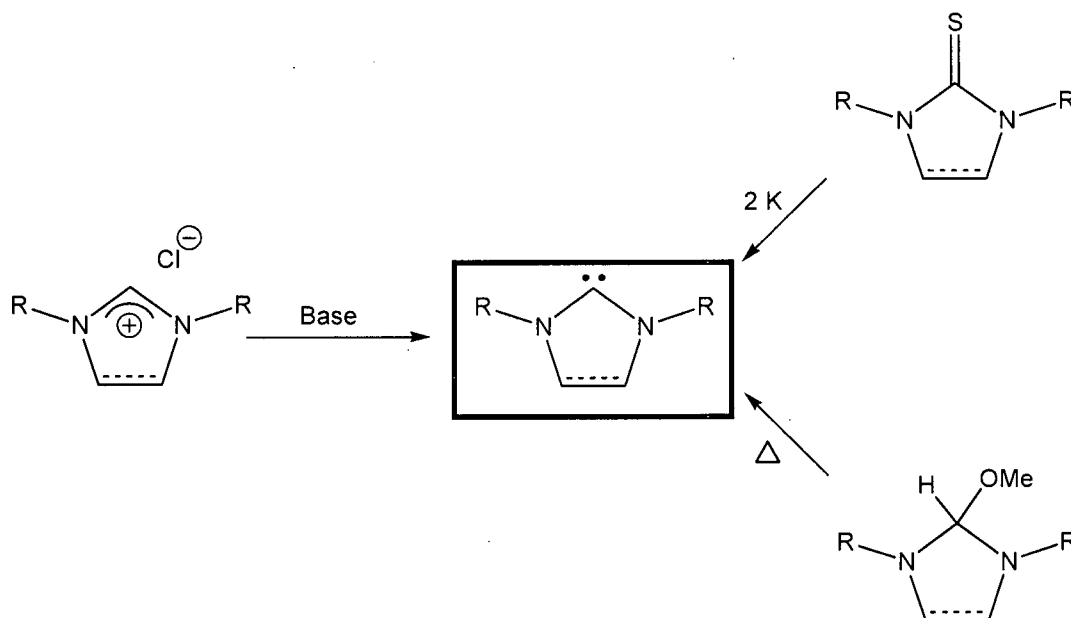


**Figure 1.9.** Reported methodology for the synthesis of NHCs.

The stability of NHCs originates mainly from electronic factors, but steric factors also play a role. The presence of two adjacent nitrogen donors asserts a mesomeric effect

on the divalent carbon carbene atom. The electron deficient nature of the carbene atom is reduced by the delocalization of the two nitrogen lone pairs into a vacant  $p$  orbital on the carbon atom and results in a four electron three-centered  $\pi$  system. Furthermore, the carbene lone pair is stabilized inductively by the electronegative nitrogen atoms (Figure 1.10). As a result, a large  $\sigma$ - $p_{\pi}$  energy separation is present, which allows NHCs to exist in the singlet ground state configuration.

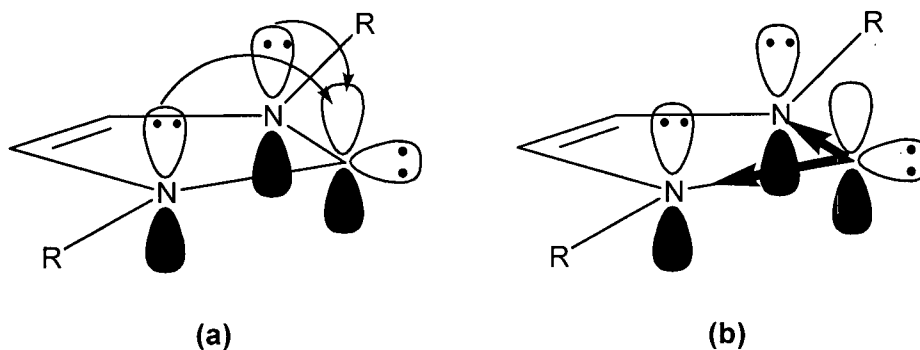


**Figure 1.10.** a)  $\pi$ -Stabilization and b) inductive effects of NHCs.

## 1.8. Transition Metal Complexes With Carbene Ligands

### 1.8.1. Transition Metal Acyclic Carbene Complexes

The first transition metal-carbene complex was discovered by Fischer in 1964.<sup>121</sup> These complexes, historically referred to as Fischer-carbene complexes, feature a low-valent transition metal fragment and a carbene bearing at least one  $\pi$ -donating substituent (Figure 1.11). As a result, the carbene atom has an electrophilic nature. The metal-carbon bond is best described as a donor-acceptor interaction resulting from the superposition of carbene to metal  $\sigma$ -donation and metal to carbene  $\pi$ -back donation.<sup>122</sup>

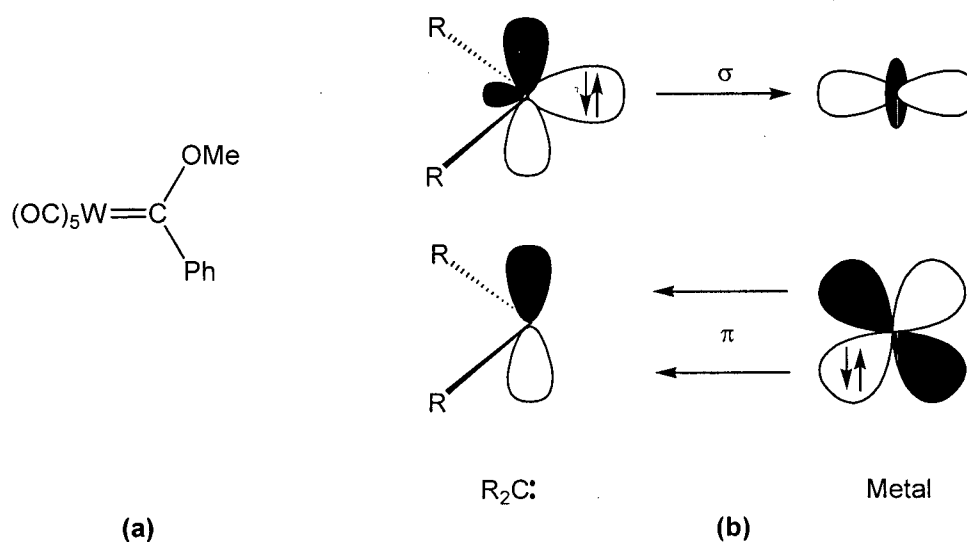


**Figure 1.11.** (a) An example and (b) schematic representation of donor-acceptor bonding in Fischer-carbene complexes.

A second class of transition metal-carbene complexes was identified by Schrock in the 1970's.<sup>123</sup> These Schrock-carbene or alkylidene complexes feature a high oxidation state metal and a carbene bearing two alkyl substituents (Figure 1.12). The carbene possesses a nucleophilic nature and forms a covalent bond with the metal. The metal-carbene bond can be regarded as an interaction between a carbene fragment in the triplet state with two spin parallel electrons on the metal centre.<sup>122</sup>

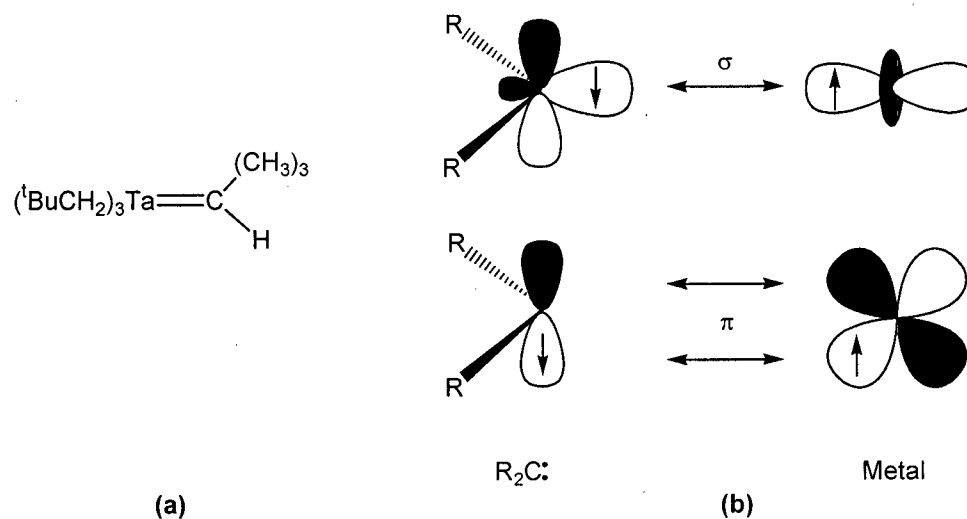


**Figure 1.12.** (a) An example and (b) schematic representation of covalent bonding in Schrock-alkylidene complexes.

Transition metal complexes of the acyclic carbenes described in chapter 1.7.1 are also known. The coordination of aryl(phosphoranyl),<sup>124</sup> amino(silyl),<sup>125</sup> amino(alkyl),<sup>126</sup> and aryl(amino)<sup>127</sup> carbene ligands to rhodium were found to yield thermally stable metal complexes, which melt at temperatures above 150°C. In one case, a thermally sensitive aryl(phosphoranyl) carbene complex was observed to isomerize to an  $\eta^1$ -phosphaalkene complex at -10°C.<sup>124</sup> While the coordination of these carbenes has been investigated, their application in transition-metal-mediated catalysis has yet to be reported.

### 1.8.2. Transition Metal NHC Complexes

In 1968, the first metal-NHC complexes were reported independently by Wanzlick and Öfele (Figure 1.13).<sup>128,129</sup> Since this discovery, NHC complexes of almost all the transition metals have been reported. NHCs are strong  $\sigma$  donors and very weak  $\pi$ -acceptors, despite having an empty  $p_\pi$  orbital. Unlike the Fischer- and Schrock-carbene complexes, NHC ligands have been reported to stabilize transition metals in both low and high oxidation states.<sup>80</sup> Given their  $\sigma$ -donating ability, NHCs have been compared to other strong  $\sigma$ -donors such as phosphines. Probably the aspect that has propelled the use of NHCs to prominent levels has been their ability to replace phosphine ligands to generate catalytic precursors more robust and versatile than their phosphine counterparts.<sup>77,78,130-132</sup> These attractive features have stimulated the use of NHCs as essential ligands for LTM complexes in homogeneous catalysis and small molecule activation processes.

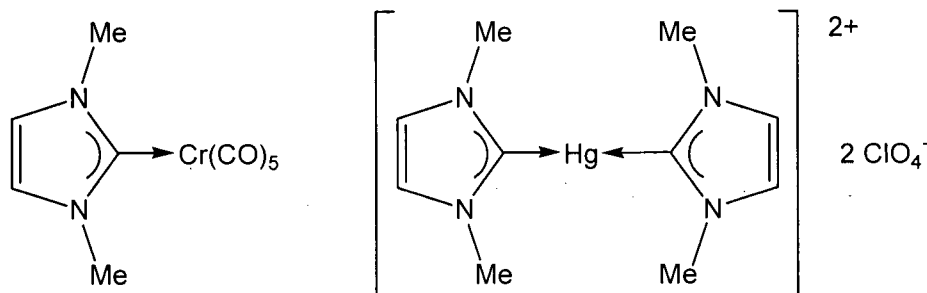
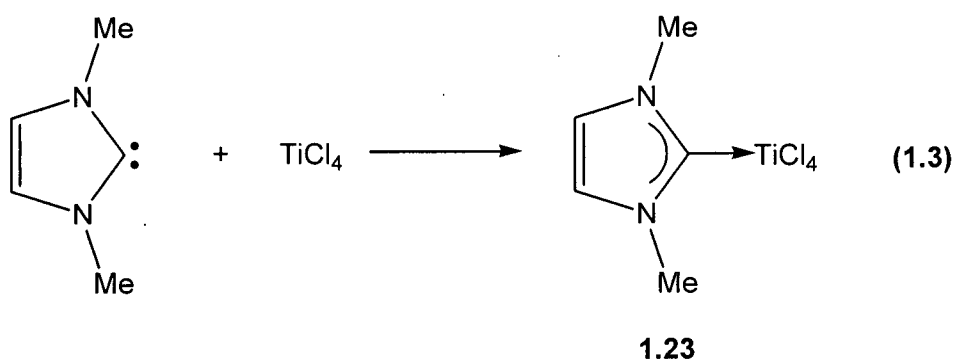


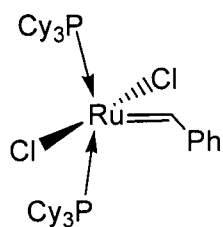
**Figure 1.13.** Metal-NHC complexes reported by Wanzlick and Öfele.

ETM complexes utilizing NHC ligands have generally been regarded as chemical curiosities, with reports focused on the routine coordination of an NHC ligand to an ETM.<sup>133-136</sup> For example, the addition of  $\text{TiCl}_4$  to a 1,3-dialkyl substituted NHC gives the NHC titanium complex **1.23** (Equation 1.3).<sup>137</sup> X-ray diffraction studies performed on this and other ETM NHC complexes show a pure  $\sigma$ -donor character of the NHC-metal bond. Furthermore, the C-N bond distances in these metal complexes feature bond lengths that are intermediate between free carbenes and imidazolium salts, which suggests a  $\pi$ -delocalization in the NHC five membered ring.

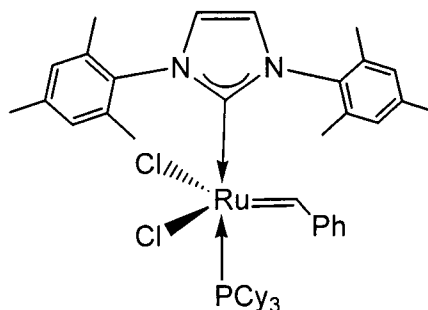


### 1.9. Late Transition Metal NHC Complexes in Homogeneous Catalysis

NHC complexes of LTMs have found applications in many different catalytic processes, some of which have been traditionally carried out using phosphine-based systems. Due to their remarkable stability, NHC complexes have shown promise as catalysts in C-Si, C-C, C-N, and C-H bond activation processes.<sup>80,138-142</sup> One example where NHCs have matched phosphine analogs in generating an active and robust catalyst involves the Ru-mediated ring closing metathesis of olefins.<sup>142</sup> The replacement of one tertiary phosphine in complex **1.24** with an NHC ligand yields **1.25** (Figure 1.14). While both **1.24** and **1.25** exhibit similar catalytic activities for the ring closing metathesis of diethyldiallylmalonate, the NHC complex **1.25** shows remarkable stability in air and to prolonged heating. This observation is in marked contrast to **1.24**, which decomposes after a short period of heating.



1.24



1.25

**Figure 1.14.** Modification to a Ru catalyst with an NHC ligand.

NHC donors have also been effectively incorporated into a chelating ligand to yield catalysts that can be electronically and sterically attenuated. For example, pincer ligands containing NHC donors have been reported to be effective auxiliary ligands in several palladium catalyzed cross coupling reactions.<sup>143-145</sup> Both bidentate and tridentate NHC ligands with phosphine and pyridine donors have been used with good success in the Heck reaction. Examples of these catalysts are given in Figure 1.15.

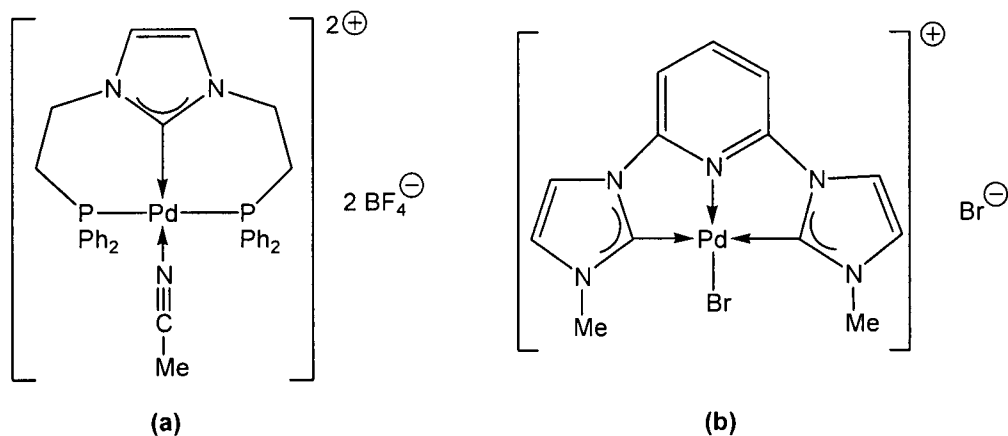


**Figure 1.15.** Examples of a) phosphine and b) pyridine NHC metal complexes for Heck catalysis.

### 1.10. Scope of This Thesis

This introduction has highlighted the origins of coordination and organometallic chemistry, and the potential for organometallic complexes and biological systems to

promote dinitrogen activation and cleavage. This daunting task has been shown to be influenced by the ligands surrounding the metal centre. ETM complexes with amidophosphine ligands have been used extensively in the Fryzuk group for the activation and cleavage of N<sub>2</sub>. Recent work has focused on the effects that changing the electronic nature of the donating group in the ligand and the modification of the ligand backbone would have on dinitrogen activation. The focus of this thesis is to both explore the cleavage of an N<sub>2</sub> ligand and to prepare a dinitrogen complex with a coordinated NHC ligand.

In chapter 2 the reactivity of the tantalum dinitrogen complex ([NPN]Ta)<sub>2</sub>(μ-H)<sub>2</sub>(μ-η<sup>1</sup>:η<sup>2</sup>-N<sub>2</sub>) with several zirconium hydride reagents is explored. Activation of the dinitrogen unit occurs and is followed by unique functionalization of one of the cleaved nitrogen atoms. The mechanism of this process is investigated and new methods to cleave a coordinated N<sub>2</sub> ligand are suggested.

The synthesis of group 4 metal complexes stabilized by the [NCN] ligand is the focus of chapter 3. Several [NCN] precursors are synthesized and used to prepare group 4-amido, -halide, and -alkyl complexes. The stability of the metal-NHC bond towards dissociation from the metal centre is probed, as is the thermal stability of several hafnium dialkyl compounds.

Chapter 4 examines the reactivity and application of [NCN] complexes synthesized in chapter 3. The migratory insertion reactivity of the hafnium dialkyl derivatives with carbon monoxide, substituted isocyanides, and several cumulenes is investigated. A cationic zirconium-methyl complex is also evaluated for its potential to polymerize α-olefins. This chapter also explores the attempted synthesis of a group 4 dinitrogen complex in addition to other N-N containing complexes.

Chapter 5 explores the synthesis of Ta(V) [NCN] complexes using both synthetic and theoretical methods. The attempted synthesis of a tantalum [NCN] trialkyl complex results in the formation of products that result from C-H bond activation of the [NCN] ligand. The mechanism of this reaction is probed by DFT calculations and isotopic labeling experiments.

The final chapter briefly details the synthesis of chiral group 4 [NCN] complexes and evaluates their potential as catalysts in asymmetric intramolecular hydroamination.

### 1.11. References

- (1) Kauffman, G. B. *Chem. Ind. (London)* **1998**, 1027.
- (2) Jorgensen, S. M. *J. Prakt. Chem.* **1886**.
- (3) Kauffman, G. B. *Educ. Chem.* **1967**, 4, 11.
- (4) Hantzsch, A.; Werner, A. *Ber. Dtsch. Chem. Ges.* **1890**, 23, 11.
- (5) Werner, A. *Z. Anorg. Chem.* **1897**, 15, 1.
- (6) Huheey, J. E. *Inorganic Chemistry. 3rd Ed*, 1983.
- (7) Douglas, B.; McDaniel, D.; Alexander, J. *Concepts and Models of Inorganic Chemistry. 2nd Ed*, 1983.
- (8) Kauffman, G. B.; Brock, W. H.; Jensen, K. A.; Klixbuell Joergensen, C. *J. Chem. Ed.* **1983**, 60, 509.
- (9) Collman, J. P.; Hegedus, L. *Principles and Applications of Organotransition Metal Chemistry*, 1980.
- (10) Wilkinson, G.; Rosenblum, M.; Whiting, M. C.; Woodward, R. B. *J. Am. Chem. Soc.* **1952**, 74, 2125.
- (11) Kealy, T. J.; Paulson, P. L. *Nature* **1951**, 168, 1039.
- (12) Miller, S. A.; Tebboth, J. A.; Tremaine, J. F. *J. Chem. Soc.* **1952**, 632.
- (13) Tolman, C. A. *Chem. Soc. Rev.* **1972**, 1, 337.
- (14) Ault, A. *J. Chem. Ed.* **2002**, 79, 572.
- (15) Casey, C. P. *J. Chem. Ed.* **2006**, 83, 192.
- (16) Katz, J. H. *J. Clin. Invest.* **1961**, 40, 2143.
- (17) Uauy, R.; Olivares, M.; Gonzalez, M. *Am. J. Clin. Nutr.* **1998**, 67, 952S.
- (18) MacKay, B. A.; Fryzuk, M. D. *Chem. Rev.* **2004**, 104, 385.
- (19) Fryzuk, M. D.; Johnson, S. A. *Coord. Chem. Rev.* **2000**, 200-202, 379.
- (20) Hidai, M.; Mizobe, Y. *Pure Appl. Chem.* **2001**, 73, 261.
- (21) Hidai, M.; Mizobe, Y. *Met. Ions Biol. Syst.* **2002**, 39, 121.
- (22) Hidai, M. *Coord. Chem. Rev.* **1999**, 185-186, 99.
- (23) Pickett, C. J. *J. Biol. Inorg. Chem.* **1996**, 1, 601.
- (24) Chatt, J.; Dilworth, J. R.; Richards, R. L. *Chem. Rev.* **1978**, 78, 589.
- (25) Bazhenova, T. A.; Shilov, A. E. *Coord. Chem. Rev.* **1995**, 144, 69.

- (26) Hidai, M.; Mizobe, Y. *Chem. Rev.* **1995**, *95*, 1115.
- (27) Gambarotta, S. *J. Organomet. Chem.* **1995**, *500*, 117.
- (28) Lehninger, A. L.; Nelson, D. L.; Cox, M. M. *Principles of Biochemistry, Pt. 2. 2nd Ed*, 1993.
- (29) Howard, J. B.; Rees, D. C. *Chem. Rev.* **1996**, *96*, 2965.
- (30) Burgess, B. K.; Lowe, D. J. *Chem. Rev.* **1996**, *96*, 2983.
- (31) Kastner, J.; Hemmen, S.; Blochl, P. E. *J. Chem. Phys.* **2005**, *123*, 074306/1.
- (32) Postgate, J. *Modern Coordination Chemistry* **2002**, 233.
- (33) Appl, M. *Ammonia: Principles and Industrial Practice*, 1999.
- (34) Haber, F. *Nobel Lectures, Including Presentation Speeches and Laureates' Biographies*; Elsevier Pub. Co. for the Nobel Foundation: Amsterdam, 1918.
- (35) Bosch, C. *Nobel Lectures, Including Presentation Speeches and Laureates' Biographies*; Elsevier Pub. Co. for the Nobel Foundation: Amsterdam, 1931.
- (36) Allen, A. D.; Senoff, C. W. *Chem. Commun.* **1965**, 621.
- (37) Allen, A. D.; Bottomley, F.; Harris, R. O.; Reinsalu, V. P.; Senoff, C. V. *J. Am. Chem. Soc.* **1967**, *89*, 5595.
- (38) Sutton, L. E.; Editor *Tables of Interatomic Distances and Configuration in Molecules and Ions: Supplement 1956-1959 (Chemical Society (London) Special Publication No. 18)*, 1965.
- (39) Stoicheff, B. P. *Can. J. Phys.* **1954**, *32*, 630.
- (40) Manriquez, J. M.; Bercaw, J. E. *J. Am. Chem. Soc.* **1974**, *96*, 6229.
- (41) Pool, J. A.; Lobkovsky, E.; Chirik, P. J. *Nature* **2004**, *427*, 527.
- (42) Yamamoto, A.; Pu, L. S.; Kitazume, S.; Ikeda, S. *J. Am. Chem. Soc.* **1967**, *89*, 3071.
- (43) Archer, L. J.; George, T. A. *Inorg. Chem.* **1979**, *18*, 2079.
- (44) Perthuisot, C.; Jones, W. D. *New J. Chem.* **1994**, *18*, 621.
- (45) Oliván, M.; Caulton, K. G. *Inorg. Chem.* **1999**, *38*, 566.
- (46) Amoroso, D.; Yap, G. P. A.; Fogg, D. E. *Can. J. Chem.* **2001**, *79*, 958.
- (47) Ernst, M. F.; Roddick, D. M. *Organometallics* **1990**, *9*, 1586.
- (48) Bianchini, C.; Peruzzini, M.; Zanolini, F. *Organometallics* **1991**, *10*, 3415.

- (49) George, T. A.; Rose, D. J.; Chang, Y.; Chen, Q.; Zubieta, J. *Inorg. Chem.* **1995**, *34*, 1295.
- (50) Fryzuk, M. D.; Kozak, C. M.; Bowdridge, M. R.; Patrick, B. O.; Rettig, S. J. *J. Am. Chem. Soc.* **2002**, *124*, 8389.
- (51) Papenfuhs, B.; Dirnberger, T.; Werner, H. *Can. J. Chem.* **2006**, *84*, 205.
- (52) Cummins, C. C. *Chem. Commun.* **1998**, 1777.
- (53) Laplaza, C. E.; Cummins, C. C. *Science* **1995**, *268*, 861.
- (54) Cui, Q.; Musaev, D. G.; Svensson, M.; Sieber, S.; Morokuma, K. *J. Am. Chem. Soc.* **1995**, *117*, 12366.
- (55) Mendiratta, A.; Cummins, C. C.; Kryatova, O. P.; Rybak-Akimova, E. V.; McDonough, J. E.; Hoff, C. D. *J. Am. Chem. Soc.* **2006**, *128*, 4881.
- (56) Clentsmith, G. K. B.; Bates, V. M. E.; Hitchcock, P. B.; Cloke, F. G. N. *J. Am. Chem. Soc.* **1999**, *121*, 10444.
- (57) Yandulov, D. V.; Schrock, R. R. *J. Am. Chem. Soc.* **2002**, *124*, 6252.
- (58) Yandulov, D. V.; Schrock, R. R. *Science* **2003**, *301*, 76.
- (59) Fryzuk, M. D.; Haddad, T. S.; Mylvaganam, M.; McConville, D. H.; Rettig, S. J. *J. Am. Chem. Soc.* **1993**, *115*, 2782.
- (60) Fryzuk, M. D.; Haddad, T. S.; Rettig, S. J. *J. Am. Chem. Soc.* **1990**, *112*, 8185.
- (61) Walstrom, A.; Pink, M.; Tsvetkov, N. P.; Fan, H.; Ingleson, M.; Caulton, K. G. *J. Am. Chem. Soc.* **2005**, *127*, 16780.
- (62) Cohen, J. D.; Fryzuk, M. D.; Loehr, T. M.; Mylvaganam, M.; Rettig, S. J. *Inorg. Chem.* **1998**, *37*, 112.
- (63) Fryzuk, M. D.; Mylvaganam, M.; Zaworotko, M. J.; MacGillivray, L. R. *Polyhedron* **1996**, *15*, 689.
- (64) Cohen, J. D.; Mylvaganam, M.; Fryzuk, M. D.; Loehr, T. M. *J. Am. Chem. Soc.* **1994**, *116*, 9529.
- (65) Fryzuk, M. D.; Williams, H. D.; Rettig, S. J. *Inorg. Chem.* **1983**, *22*, 863.
- (66) Fryzuk, M. D.; Williams, H. D. *Organometallics* **1983**, *2*, 162.
- (67) Fryzuk, M. D.; Love, J. B.; Rettig, S. J. *Chem. Commun.* **1996**, 2783.
- (68) Fryzuk, M. D.; Corkin, J. R.; Patrick, B. O. *Can. J. Chem.* **2003**, *81*, 1376.
- (69) Fryzuk, M. D.; Love, J. B.; Rettig, S. J.; Young, V. G. *Science* **1997**, *275*, 1445.

- (70) Fryzuk, M. D.; Kozak, C. M.; Patrick, B. O. *Inorg. Chim. Acta* **2003**, *345*, 53.
- (71) Johnson, S. A., Ph. D. thesis, University of British Columbia, 2000.
- (72) Morello, L.; Yu, P.; Carmichael, C. D.; Patrick, B. O.; Fryzuk, M. D. *J. Am. Chem. Soc.* **2005**, *127*, 12796.
- (73) MacLachlan, E. A.; Fryzuk, M. D. *Organometallics* **2005**, *24*, 1112.
- (74) Fryzuk, M. D.; MacKay, B. A.; Johnson, S. A.; Patrick, B. O. *Angew. Chem. Int. Ed.* **2002**, *41*, 3709.
- (75) MacKay, B. A.; Johnson, S. A.; Patrick, B. O.; Fryzuk, M. D. *Can. J. Chem.* **2005**, *83*, 315.
- (76) MacKay, B. A.; Patrick, B. O.; Fryzuk, M. D. *Organometallics* **2005**, *24*, 3836.
- (77) Herrmann, W. A.; Kocher, C. *Angew. Chem., Int. Ed. Engl.* **1997**, *36*, 2162.
- (78) Regitz, M. *Angew. Chem., Int. Ed. Engl.* **1996**, *35*, 725.
- (79) Igau, A.; Grutzmacher, H.; Baceiredo, A.; Bertrand, G. *J. Am. Chem. Soc.* **1988**, *110*, 6463.
- (80) Bourissou, D.; Guerret, O.; Gabbaie, F. P.; Bertrand, G. *Chem. Rev.* **2000**, *100*, 39.
- (81) Schuster, G. B. *Adv. Phys. Org. Chem.* **1986**, *22*, 311.
- (82) Sander, W.; Bucher, G.; Wierlacher, S. *Chem. Rev.* **1993**, *93*, 1583.
- (83) Wanzlick, H. W.; Kleiner, H. J. *Angew. Chem., Int. Ed.* **1961**, *73*, 493.
- (84) Wanzlick, H. W.; Esser, F.; Kleiner, H. J. *Ber.* **1963**, *96*, 1208.
- (85) Moss, R. A. *Acc. Chem. Res.* **1980**, *13*, 58.
- (86) Moss, R. A. *Acc. Chem. Res.* **1989**, *22*, 15.
- (87) Bethell, D. *Adv. Phys. Org. Chem.* **1969**, *7*, 153.
- (88) Zimmerman, H. E.; Paskovich, D. H. *J. Am. Chem. Soc.* **1964**, *86*, 2149.
- (89) Tomioka, H.; Hirai, K.; Fujii, C. *Acta Chem. Scand.* **1992**, *46*, 680.
- (90) Terazima, M.; Tomioka, H.; Hirai, K.; Tanimoto, Y.; Fujiwara, Y.; Akimoto, Y. *J. Chem. Soc., Faraday Trans.* **1996**, *92*, 2361.
- (91) Tomioka, H.; Nakajima, J.; Mizuno, H.; Sone, T.; Hirai, K. *J. Am. Chem. Soc.* **1995**, *117*, 11355.
- (92) Harrison, J. F.; Liedtke, R. C.; Liebman, J. F. *J. Am. Chem. Soc.* **1979**, *101*, 7162.
- (93) Harrison, J. F. *J. Am. Chem. Soc.* **1971**, *93*, 4112.

- (94) Bauschlicher, C. W., Jr.; Schaefer, H. F., III; Bagus, P. S. *J. Am. Chem. Soc.* **1977**, *99*, 7106.
- (95) Feller, D.; Borden, W. T.; Davidson, E. R. *Chem. Phys. Lett.* **1980**, *71*, 22.
- (96) Schoeller, W. W. *Tetrahedron Lett.* **1980**, *21*, 1505.
- (97) Schoeller, W. W. *Tetrahedron Lett.* **1980**, *21*, 1509.
- (98) Schoeller, W. W. *J. Chem. Soc., Chem. Commun.* **1980**, 124.
- (99) Pauling, L. *J. Chem. Soc., Chem. Commun.* **1980**, 688.
- (100) Modarelli, D. A.; Morgan, S.; Platz, M. S. *J. Am. Chem. Soc.* **1992**, *114*, 7034.
- (101) Richards, C. A., Jr.; Kim, S.-J.; Yamaguchi, Y.; Schaefer, H. F., III *J. Am. Chem. Soc.* **1995**, *117*, 10104.
- (102) Myers, D. R.; Senthilnathan, V. P.; Platz, M. S.; Jones, M., Jr. *J. Am. Chem. Soc.* **1986**, *108*, 4232.
- (103) Baceiredo, A.; Bertrand, G.; Sicard, G. *J. Am. Chem. Soc.* **1985**, *107*, 4781.
- (104) Igau, A.; Baceiredo, A.; Trinquier, G.; Bertrand, G. *Angew. Chem., Int. Ed.* **1989**, *101*, 617.
- (105) Goumri-Magnet, S.; Kato, T.; Gornitzka, H.; Baceiredo, A.; Bertrand, G. *J. Am. Chem. Soc.* **2000**, *122*, 4464.
- (106) Illa, O.; Gornitzka, H.; Branchadell, V.; Baceiredo, A.; Bertrand, G.; Ortuno, R. *M. Eur. J. Org. Chem.* **2003**, 3147.
- (107) Illa, O.; Gornitzka, H.; Baceiredo, A.; Bertrand, G.; Branchadell, V.; Ortuno, R. *M. J. Org. Chem.* **2003**, *68*, 7707.
- (108) Gillette, G. R.; Igau, A.; Baceiredo, A.; Bertrand, G. *New J. Chem.* **1991**, *15*, 393.
- (109) Goumri-Magnet, S.; Polishchuk, O.; Gornitzka, H.; Marsden, C. J.; Baceiredo, A.; Bertrand, G. *Angew. Chem. Int. Ed.* **1999**, *38*, s3727.
- (110) Dixon, D. A.; Dobbs, K. D.; Arduengo, A. J., III; Bertrand, G. *J. Am. Chem. Soc.* **1991**, *113*, 8782.
- (111) Kato, T.; Gornitzka, H.; Baceiredo, A.; Savin, A.; Bertrand, G. *J. Am. Chem. Soc.* **2000**, *122*, 998.
- (112) Cattoen, X.; Sole, S.; Pradel, C.; Gornitzka, H.; Miqueu, K.; Bourissou, D.; Bertrand, G. *J. Org. Chem.* **2003**, *68*, 911.

- (113) Solet, S.; Gornitzka, H.; Schoeller, W. W.; Bourissou, D.; Bertrand, G. *Science* **2001**, *292*, 1901.
- (114) Merceron, N.; Miqueu, K.; Baceiredo, A.; Bertrand, G. *J. Am. Chem. Soc.* **2002**, *124*, 6806.
- (115) Merceron-Saffon, N.; Baceiredo, A.; Gornitzka, H.; Bertrand, G. *Science* **2003**, *301*, 1223.
- (116) Wanzlick, H. W.; Schikora, E. *Angew. Chem.* **1960**, *72*, 494.
- (117) Denk, M. K.; Hatano, K.; Ma, M. *Tetrahedron Lett.* **1999**, *40*, 2057.
- (118) Arduengo, A. J., III; Harlow, R. L.; Kline, M. *J. Am. Chem. Soc.* **1991**, *113*, 361.
- (119) Kuhn, N.; Kratz, T. *Synthesis* **1993**, 561.
- (120) Enders, D.; Breuer, K.; Raabe, G.; Runsink, J.; Teles, J. H.; Melder, J.-P.; Ebel, K.; Brode, S. *Angew. Chem., Int. Ed. Engl.* **1995**, *34*, 1021.
- (121) Fischer, E. O.; Maasboel, A. *Angew. Chem.* **1964**, *76*, 645.
- (122) Taylor, T. E.; Hall, M. B. *J. Am. Chem. Soc.* **1984**, *106*, 1576.
- (123) Schrock, R. R. *J. Am. Chem. Soc.* **1974**, *96*, 6796.
- (124) Despagnet, E.; Miqueu, K.; Gornitzka, H.; Dyer, P. W.; Bourissou, D.; Bertrand, G. *J. Am. Chem. Soc.* **2002**, *124*, 11834.
- (125) Canac, Y.; Conejero, S.; Donnadiou, B.; Schoeller, W. W.; Bertrand, G. *J. Am. Chem. Soc.* **2005**, *127*, 7312.
- (126) Lavallo, V.; Mafhouz, J.; Canac, Y.; Donnadiou, B.; Schoeller, W. W.; Bertrand, G. *J. Am. Chem. Soc.* **2004**, *126*, 8670.
- (127) Cattoen, X.; Gornitzka, H.; Bourissou, D.; Bertrand, G. *J. Am. Chem. Soc.* **2004**, *126*, 1342.
- (128) Wanzlick, H. W.; Schoenherr, H. J. *Angew. Chem., Int. Ed. Engl.* **1968**, *7*, 141.
- (129) Oefele, K. *J. Organomet. Chem.* **1968**, *12*, P42.
- (130) Arduengo, A. J., III; Krafczyk, R. *Chem. Z.* **1998**, *32*, 6.
- (131) Dullius, J. E. L.; Suarez, P. A. Z.; Einloft, S.; de Souza, R. F.; Dupont, J.; Fischer, J.; De Cian, A. *Organometallics* **1998**, *17*, 815.
- (132) Arduengo, A. J., III *Acc. Chem. Res.* **1999**, *32*, 913.
- (133) Abernethy, C. D.; Codd, G. M.; Spicer, M. D.; Taylor, M. K. *J. Am. Chem. Soc.* **2003**, *125*, 1128.

- (134) Kernbach, U.; Ramm, M.; Luger, P.; Fehlhammer, W. P. *Angew. Chem., Int. Ed. Engl.* **1996**, *35*, 310.
- (135) Herrmann, W. A.; Munck, F. C.; Artus, G. R. J.; Runte, O.; Anwander, R. *Organometallics* **1997**, *16*, 682.
- (136) Oldham, W. J., Jr.; Oldham, S. M.; Smith, W. H.; Costa, D. A.; Scott, B. L.; Abney, K. D. *Chem. Commun.* **2001**, 1348.
- (137) Kuhn, N.; Kratz, T.; Blaeser, D.; Boese, R. *Inorg. Chim. Acta* **1995**, *238*, 179.
- (138) Grubbs, R. H. *Adv. Synth. Catal.* **2002**, *344*, 569.
- (139) Lee, S.; Hartwig, J. F. *J. Org. Chem.* **2001**, *66*, 3402.
- (140) Marko, I. E.; Sterin, S.; Buisine, O.; Mignani, G.; Branlard, P.; Tinant, B.; Declercq, J.-P. *Science* **2002**, *298*, 204.
- (141) Muehlhofer, M.; Strassner, T.; Herrmann, W. A. *Angew. Chem. Int. Ed.* **2002**, *41*, 1745.
- (142) Viciu, M. S.; Nolan, S. P. *Top. Organomet. Chem.* **2005**, *14*, 241.
- (143) Lee, H. M.; Zeng, J. Y.; Hu, C.-H.; Lee, M.-T. *Inorg. Chem.* **2004**, *43*, 6822.
- (144) Peris, E.; Mata, J.; Loch, J. A.; Crabtree, R. H. *Chem. Commun.* **2001**, 201.
- (145) Loch, J. A.; Albrecht, M.; Peris, E.; Mata, J.; Faller, J. W.; Crabtree, R. H. *Organometallics* **2002**, *21*, 700.

## Chapter Two

# Promoting Dinitrogen Cleavage and Functionalization with Zr(II) and Ti(II) reagents

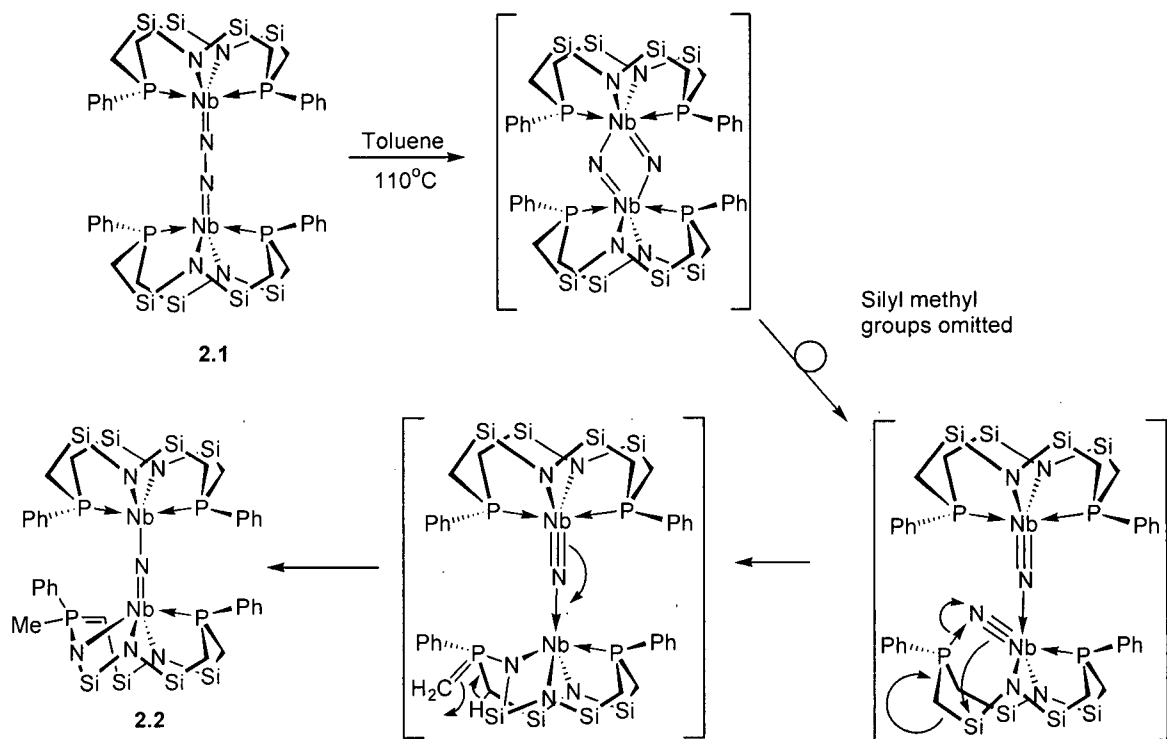
### 2.1. Introduction\*

The conversion of N<sub>2</sub> to ammonia or to certain organic nitrogen-containing products requires the activation and cleavage of the N≡N triple bond. As was highlighted in chapter 1, several early transition metal complexes are capable of performing these kinds of transformations. In some cases, further functionalization of the cleaved nitrogen atoms is possible, forming new element-nitrogen bonds. In each of these examples, an ancillary ligand plays an important role in stabilizing the various transition metal oxidation states necessary for N-N bond reduction.

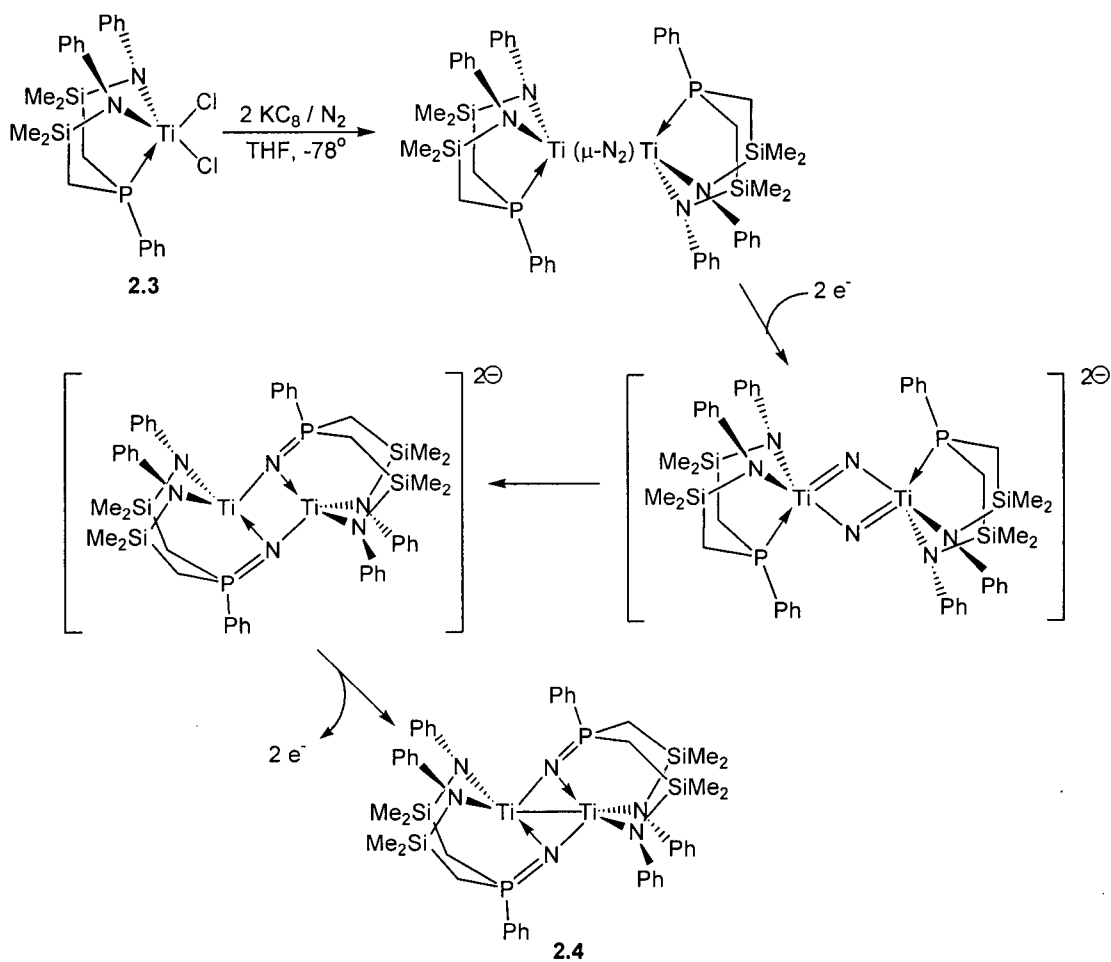
Transition metal complexes employing amidophosphine ancillary ligands have been examined extensively in the Fryzuk group for the cleavage and functionalization of coordinated dinitrogen. For example, a diamidodiphosphine ligand [P<sub>2</sub>N<sub>2</sub>] (where [P<sub>2</sub>N<sub>2</sub>] = (PhP(CH<sub>2</sub>SiMe<sub>2</sub>NSiMe<sub>2</sub>CH<sub>2</sub>)<sub>2</sub>PPh)) has been effectively used to stabilize a dinuclear dinitrogen complex of niobium (**2.1**).<sup>1</sup> Thermolysis of **2.1** promotes N-N bond cleavage to generate a reactive molecular nitride, which immediately reacts with the [P<sub>2</sub>N<sub>2</sub>] ancillary ligand to yield **2.2** (Scheme 2.1). The formation of **2.2** provides a unique

\*A version of this chapter has been accepted for publication (*Proc. Natl. Acad. Sci. USA*).

example of N-N bond cleavage followed by nitrogen atom insertion into the backbone of one of the  $[P_2N_2]$  macrocycles to form a bimetallic bridging nitride complex.

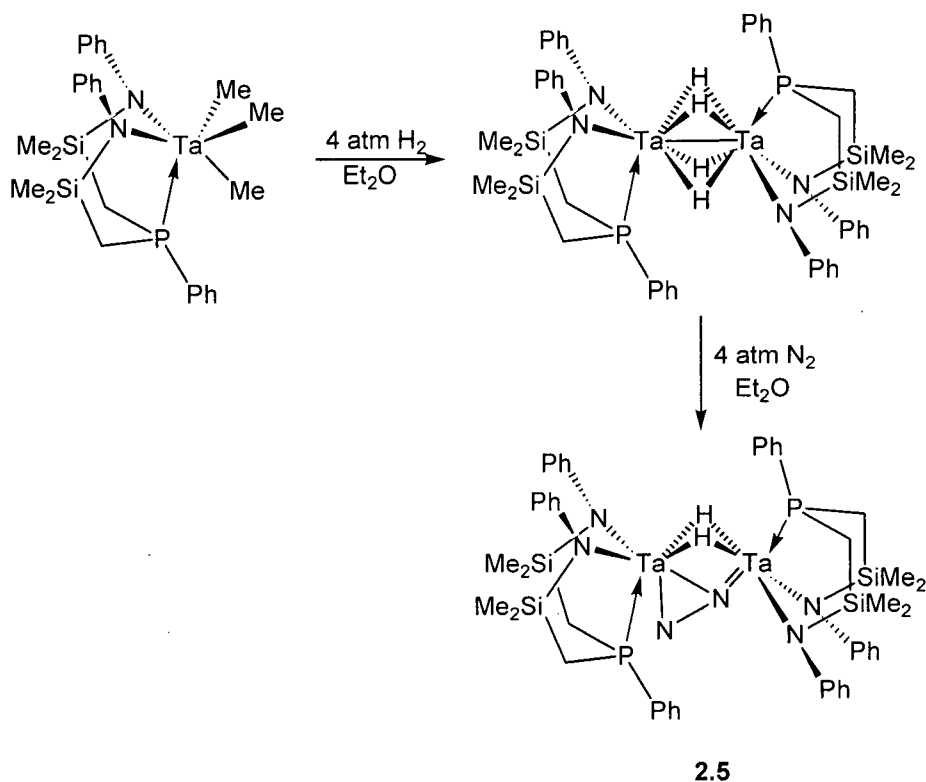


The stabilization of early transition metal dinitrogen complexes has also been investigated in the Fryzuk group using a diamidophosphine [NPN] ancillary ligand (where  $[NPN] = [(PhNSiMe_2CH_2)_2PPh]^{2-}$ ). For example, reduction of a titanium dichloride complex (**2.3**) employing a [NPN] ancillary ligand with 2.2 equivalents of  $KC_8$  under 4 atmospheres of nitrogen yields a dinuclear titanium dinitrogen complex (Scheme 2.2).<sup>2</sup> This species was only identified by  $^1H$  and  $^{31}P$  NMR spectroscopy and mass spectrometry. Thus far, the solid state structure of this dinitrogen complex has yet to be determined. This complex slowly rearranges in solution to form the bis(phosphinimide) titanium (III) dimer **2.4**. The formation of **2.4** occurs as a result of complete N-N bond cleavage, followed by nitrogen atom functionalization by the [NPN] ancillary ligand to yield a new N-P bond.



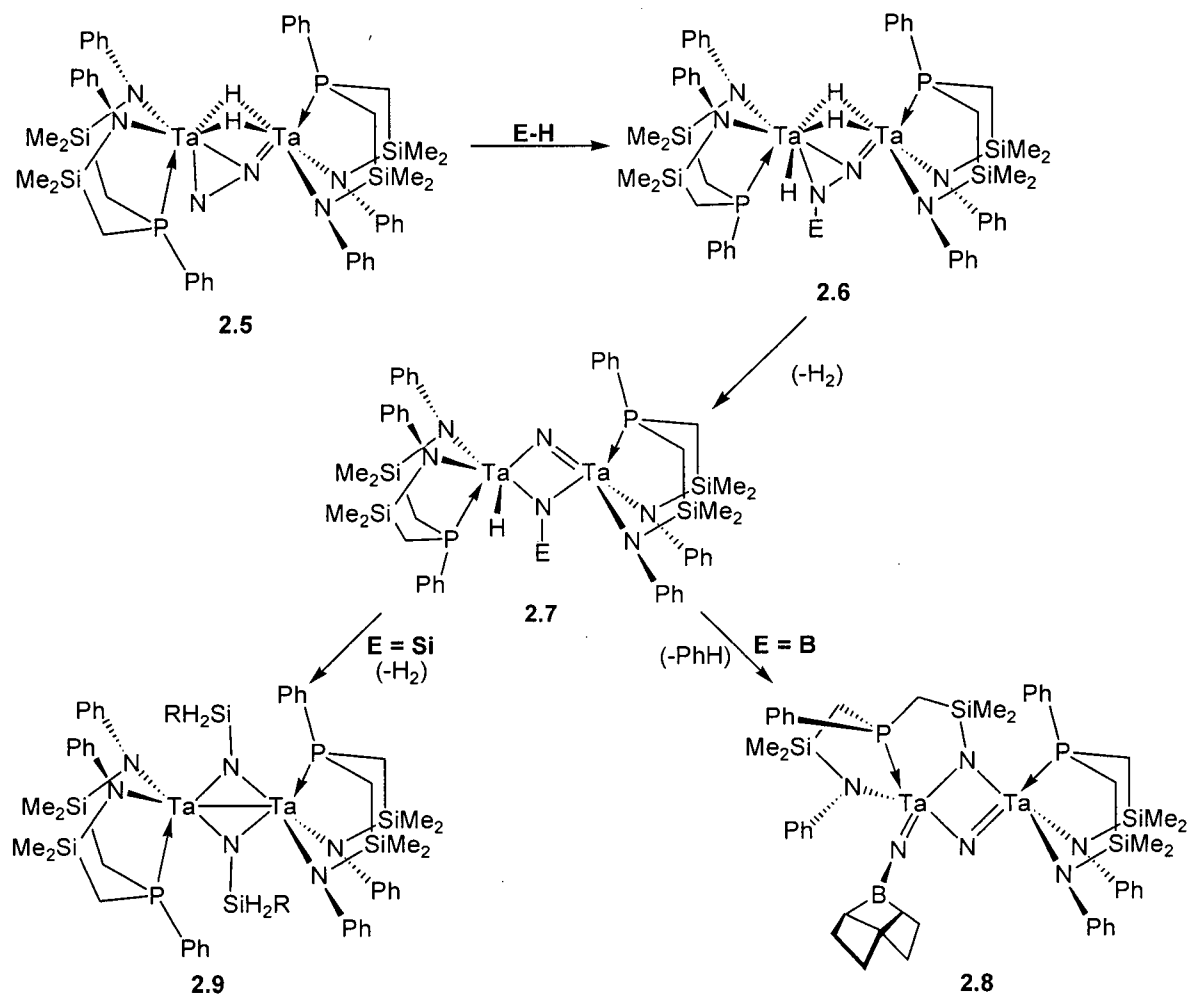
Scheme 2.2.

The diamidophosphine ligand [NPN] has also been used to stabilize a novel side-on end-on coordinated tantalum dinitrogen complex (**2.5**) (Scheme 2.3).<sup>3</sup> The synthesis of this reduced dinitrogen complex is remarkable because it is formed upon exposure of a tetrahydride tantalum derivative to  $N_2$ , a result that is not proliferated by the use of strong reducing reagents such as  $KC_8$ . This dinitrogen complex has been shown to exhibit a wide range of reactivity patterns, which include reactions with electrophiles,<sup>3</sup> adduct formation with Lewis acids,<sup>4</sup> and displacement of the  $N_2$  moiety by terminal alkynes.<sup>5</sup>



Scheme 2.3.

The addition of simple main group hydride reagents (E-H) to the tantalum-dinitrogen complex (**2.5**) has also been studied. These hydride addition reactions feature several common outcomes and are summarized in Scheme 2.4. In every case, E-H addition occurs in a 1,2-addition manner across the exposed end of the coordinated dinitrogen moiety to form, in some cases, an isolable intermediate (**2.6**). This leads to elimination of H<sub>2</sub>, N-N bond cleavage, and subsequent rearrangement to yield **2.7**, a tantalum nitride intermediate. The addition of a second equivalent of E-H reagent to this complex leads to different outcomes, which are dependent on the hydride source. For example, the addition of a B-H reagent leads to ancillary ligand degradation (**2.8**), limiting the overall usefulness of these stoichiometric transformations.<sup>6,7</sup> However, the addition of a Si-H reagent results in a clean conversion to the bis(silylimide) **2.9**, which was observed for the addition of butylsilane.<sup>8</sup>



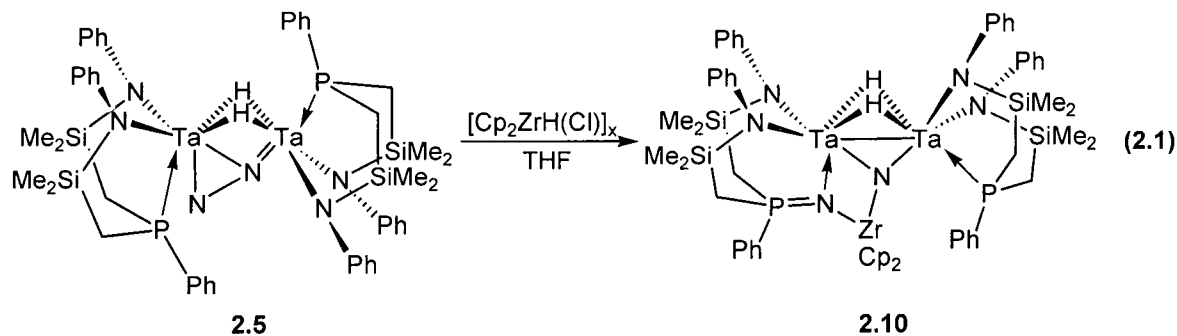
Scheme 2.4.

The extension of this E-H addition chemistry to include transition metal reagents was of particular interest. This would present a unique opportunity to functionalize a coordinated dinitrogen unit with a transition metal atom. In this chapter, the reaction of 2.5 with several zirconium-hydride reagents is examined. What results is an unanticipated reaction that involves N-N bond cleavage without zirconium-hydride addition, or H<sub>2</sub> elimination from 2.5.

## 2.2. Attempted Hydrozirconation of 2.5

Schwartz's reagent or zirconocene chloro-hydride is known to add in a 1,2-addition fashion across the multiple bonds of alkenes, alkynes, ketones, aldehydes, and

nitriles.<sup>9</sup> Given the success of main group hydride additions across the Ta-N bond of **2.5**, a similar process was envisioned that would yield a terminal tantalum hydride moiety and a new Zr-N bond. Stirring a THF solution of sparingly soluble  $[\text{Cp}_2\text{Zr}(\text{Cl})\text{H}]_x$  with **2.5** for 2 weeks generates an intense purple solution from which purple crystals of **2.10** are isolated in 35% yield (Equation 2.1). The  $^1\text{H}$  NMR spectrum reveals a  $C_s$  symmetric species in solution with one single Cp resonance at 5.38 ppm, four inequivalent silyl methyl resonances, and bridging hydrides at 11.4 ppm. Surprisingly, no terminal tantalum hydride resonances are observed indicating that hydrozirconation to form a species similar to **2.6** (Scheme 2.4) had not occurred. The  $^{31}\text{P}\{^1\text{H}\}$  NMR spectrum features two singlets at 7.3 and 46.7 ppm with the downfield resonance split into a doublet ( $^1J_{\text{PN}} = 34.9$  Hz) when  $^{15}\text{N}$ -labelled **3.5** is used. Similar coupling is also observed in the  $^{15}\text{N}\{^1\text{H}\}$  spectrum with the resonance located at  $-185.1$  ppm split into a doublet. A second  $^{15}\text{N}$  resonance is observed at 228.4 ppm. These two resonances are not mutually coupled, implying that N-N bond cleavage has occurred.



The solid state molecular structure of **2.10** was determined by an X-ray diffraction experiment. An ORTEP depiction is shown in Figure 2.1 with selected bond lengths and angles given in Table 2.1 and crystallographic details reported in appendix A. The addition of Schwartz's reagent to **2.5** appears to yield an N-N bond cleaved product in which a zirconocene fragment has inserted between the two nitrogen atoms. No bridging hydrides are observed in the solid state molecular structure; however, these ligands are successfully modeled using XHYDEX<sup>10</sup> and their presence confirmed by  $^1\text{H}$  NMR spectroscopy. A Ta-Ta bond interaction is observed with a Ta1-Ta2 bond distance of

2.7007(6) Å, which is similar to other Ta(IV)-Ta(IV) dinuclear complexes.<sup>11</sup> The phosphinimide P=N bond distance of 1.595(9) Å is also typical of other reported group 5 phosphinimide complexes.<sup>12,13</sup> A bridging zirconium nitride species is also observed. While the formation of this moiety is uncommon, the Zr1-N2 bond length (2.040(9) Å) is shorter than other bridging zirconium nitrides which range from 2.21 to 2.35 Å.<sup>14-16</sup>

The formation of the phosphinimide group in **2.10** is presumably a result of the intramolecular attack of one of the ancillary phosphine donors at an intermediate nitride species. Such an event has been reported earlier in the Fryzuk group in the formation of dinuclear titanium phosphinimide complexes and during the thermolysis of a preformed niobium dinitrogen complex.<sup>1,2</sup> The intermolecular attack of phosphines on metal nitride species also has precedence and is analogous to the formation of **2.10**.<sup>17-19</sup>

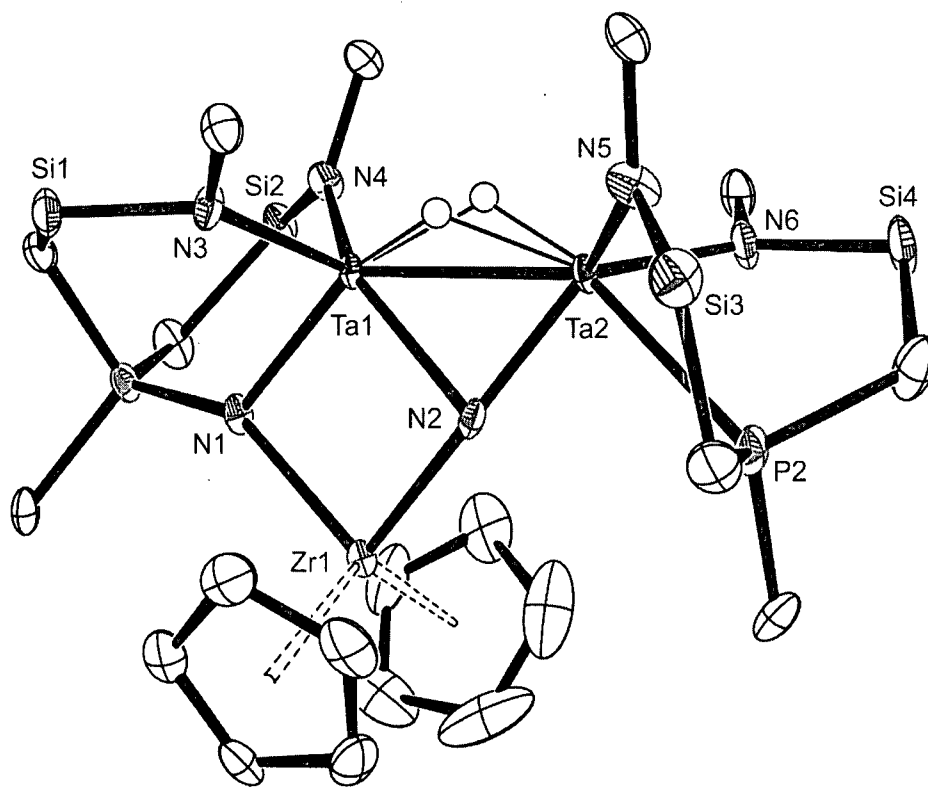


**Figure 2.1.** ORTEP view of  $[\text{NP}(\text{N})\text{N}]\text{Ta}(\mu\text{-H})_2(\mu\text{-N})(\text{Ta}[\text{NPN}])(\text{ZrCp}_2)$  (**2.10**) depicted with 50% ellipsoids; all hydrogen atoms, silyl methyl and phenyl ring carbon atoms except *ipso* carbons have been omitted for clarity.

**Table 2.1.** Selected bond distances (Å) and angles (deg) for  $([\text{NP}(\text{N})\text{N}]\text{Ta}(\mu\text{-H})_2(\mu\text{-N})(\text{Ta}[\text{NPN}])(\text{ZrCp}_2))$  (**2.10**).

Bond Lengths		Bond Angles	
Ta1-Ta2	2.7007(6)	N1-Ta1-N2	87.2(3)
N1...N2	2.925(9)	P1-N1-Ta1	121.5(5)
P1-N1	1.595(9)	N1-Zr1-N2	88.6(3)
Ta1-N1	2.102(9)	Ta1-N2-Ta2	82.9(3)
Ta1-N2	2.139(8)	N3-Ta1-N4	107.0(4)
Ta2-N2	1.935(9)	N5-Ta2-N6	105.6(4)
Zr1-N1	2.146(9)		
Zr1-N2	2.040(9)		
Ta1-N3	2.054(9)		
Ta1-N4	2.102(9)		
Ta2-N5	2.112(10)		
Ta2-N6	2.119(9)		
Ta2-P2	2.624(3)		
Ta1-Zr1	3.0319(11)		

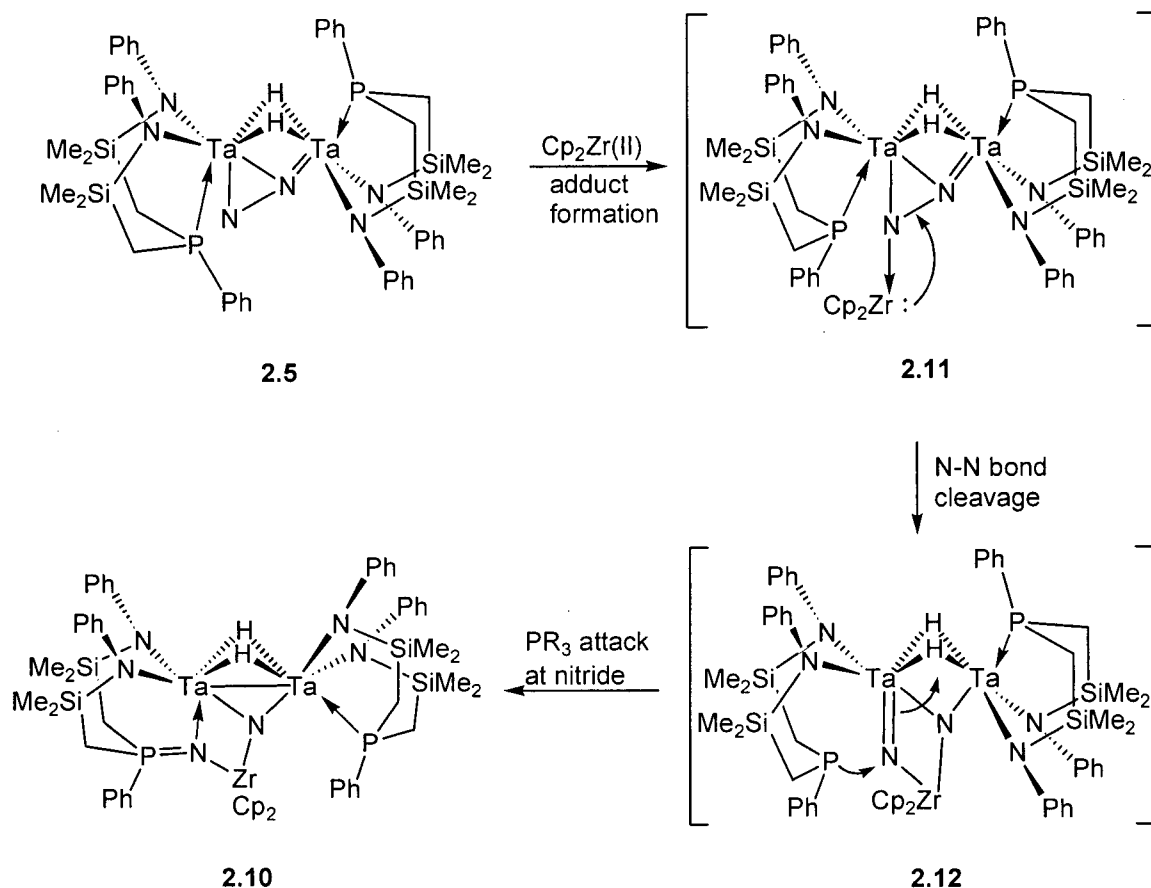
Surprisingly, the addition of  $[\text{Cp}_2\text{Zr}(\text{Cl})\text{H}]_x$  to **2.5** does not result in hydrozirconation of the Ta-N bond. In this reaction, the fate of the hydride and chloride ligands derived from  $[\text{Cp}_2\text{Zr}(\text{Cl})\text{H}]_x$  is not clear. Careful examination of the  $^1\text{H}$  NMR spectrum during the reaction reveals the presence of  $\text{H}_2$  (4.54 ppm in  $\text{C}_6\text{D}_6$ ), although this was not quantified. To probe the origin of  $\text{H}_2$  formation, the addition of  $[\text{Cp}_2\text{ZrH}_2]_2$  to **2.5** was examined and found to yield **2.10** in excellent yield (90% by NMR spectroscopy) in addition to  $\text{H}_2$  liberation. The evolution of  $\text{H}_2$  was further examined with the reaction of the deuterated nitrogen complex  $([\text{NPN}]\text{Ta})_2(\mu\text{-D})_2(\mu\text{-}\eta^1\text{:}\eta^2\text{-N}_2)$  ( $d_2\text{-2.5}$ ) with  $[\text{Cp}_2\text{ZrH}_2]_2$  and found to yield free  $\text{H}_2$  and the absence of a bridging tantalum-hydride signal at 11.4 ppm in the  $^1\text{H}$  NMR spectrum.

Given this information, a rational interpretation of the mechanism likely involves an initial reaction of  $[\text{Cp}_2\text{Zr}(\text{Cl})\text{H}]_x$  with the parent dinitrogen complex **2.5** by chloride for hydride exchange, which generates  $[\text{Cp}_2\text{ZrH}_2]_2$  along with some unknown tantalum chloride species. This chloride for hydride exchange has been observed with the addition of several main group chloride reagents to **2.5** and would account for the low yield of **2.10** when the zirconocene chloro-hydride reagent was used.<sup>20</sup> To examine this hypothesis, the addition of  $\text{Cp}_2\text{ZrCl}_2$  to **2.5** was examined and found to yield the

phosphinimide product in 20% yield (by  $^1\text{H}$  NMR spectroscopy). The low observed yield is consistent with a double chloride for hydride exchange that must occur to generate  $[\text{Cp}_2\text{ZrH}_2]_2$  from  $\text{Cp}_2\text{ZrCl}_2$  and **2.5**.

The observation that free  $\text{H}_2$  is generated during the reaction of  $[\text{Cp}_2\text{ZrH}_2]_2$  with **2.5** suggests that the zirconocene hydride reagent was simply a source of a  $\text{Cp}_2\text{Zr(II)}$  species. To probe this phenomenon, the reaction of a known Zr(II) precursor,  $[\text{Cp}_2\text{Zr(py)}(\text{Me}_3\text{SiC}\equiv\text{CSiMe}_3)]$ , with **2.5** was investigated. The formation of **2.10** is nearly quantitative, which suggests that reductive elimination of  $\text{H}_2$  from  $[\text{Cp}_2\text{ZrH}_2]_2$  occurs to generate a  $\text{Cp}_2\text{Zr(II)}$  species, which can then react with **2.5** to form **2.10**. To the best of our knowledge, this reductive elimination of  $\text{H}_2$  from a Zr(IV) dihydride complex is quite rare.<sup>21,22</sup>

Directed by these experiments, a mechanism for the cleavage and functionalization of the dinitrogen unit in **2.5** can be postulated (Scheme 2.5). The addition of  $[\text{Cp}_2\text{Zr(Cl)H}]_x$  or  $[\text{Cp}_2\text{ZrH}_2]_2$  leads to generation of a  $\text{Cp}_2\text{Zr(II)}$  species in solution, which can form a simple adduct (**2.11**) with the tantalum dinitrogen complex, **2.5**. The two electrons from the zirconium centre can then cleave the N-N bond to form **2.12**, in which the central atom of the metallocene has a formal M(IV) oxidation state. The nitride moiety in this complex can then undergo intramolecular attack with one of the phosphorus atoms on the [NPN] ancillary ligand to generate the final phosphinimide product **2.10**.

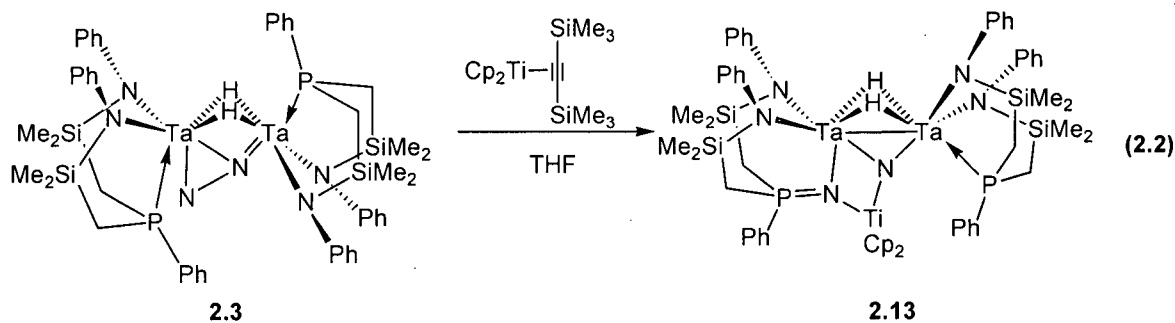


Scheme 2.5.

### 2.3. Reduction and Functionalization of 2.5 with Cp<sub>2</sub>Ti(II)

The cleavage and functionalization of **2.5** with reduced group 4 transition metal derivatives represents a new procedure for the activation of dinitrogen. As an extension, the chemistry with a related titanocene(II) derivative [Cp<sub>2</sub>Ti(Me<sub>3</sub>SiC≡CSiMe<sub>3</sub>)] was examined. The reaction with **2.5** proceeds smoothly in THF at room temperature to generate **2.13** in good yield, which was characterized by NMR spectroscopy and elemental analysis (Equation 2.2). Although no solid state molecular structure was determined, the spectroscopic data is quite similar to **2.10**. A C<sub>s</sub> symmetric species is observed in the <sup>1</sup>H NMR spectrum with equivalent silyl methyl resonances, one single Cp resonance at 5.20 ppm, and bridging hydrides at 12.4 ppm. The <sup>31</sup>P{<sup>1</sup>H} NMR spectrum features two singlets at 8.6 and 46.4 ppm, with the latter resonance split into a doublet

( $^1J_{\text{PN}} = 34 \text{ Hz}$ ) when  $^{15}\text{N}$ -**2.5** is used. Two  $^{15}\text{N}$  resonances are observed in the  $^{15}\text{N}\{^1\text{H}\}$  NMR spectrum at 227.5 and -185.5 ppm with the latter resonance split into a doublet with identical coupling to what was observed in the  $^{31}\text{P}$  NMR spectrum.



#### 2.4. Conclusions

Investigation into the addition of Schwartz's reagent ( $[\text{Cp}_2\text{Zr}(\text{Cl})\text{H}]_x$ ) to the end-on side-on dinitrogen complex **2.5** led to the unanticipated reduction of the dinitrogen moiety without Zr-H addition. This reaction facilitates insertion of a  $\text{Cp}_2\text{Zr}$  fragment into the N-N bond of the dinitrogen ligand. The origin of this zirconocene fragment was probed by a series of experiments, which traced its formation to the elimination of dihydrogen from  $[\text{Cp}_2\text{ZrH}_2]_2$  (formed *in situ* by hydride for chloride exchange). An independent reaction between **2.5** and  $[\text{Cp}_2\text{Zr}(\text{py})(\text{Me}_3\text{SiC}\equiv\text{CSiMe}_3)]$  confirmed that a  $\text{Cp}_2\text{Zr}(\text{II})$  species induces the N-N bond cleavage. This  $\text{Cp}_2\text{Zr}(\text{II})$  species promotes a two-electron inner-sphere reduction of the N-N bond to generate a transient nitride species, which is susceptible to intramolecular attack by a coordinated phosphine atom of the [NPN] ancillary ligand to generate the observed phosphinimide in addition to a trimetallic nitride species. This process represents a new way to cleave and functionalize coordinated dinitrogen.

## 2.5. Experimental

### 2.5.1. General Considerations

Unless otherwise stated, all manipulations were performed under an atmosphere of dry oxygen-free argon or nitrogen by means of standard Schlenk or glovebox techniques. Anhydrous hexanes and toluene were purchased from Aldrich, sparged with dinitrogen, and further dried by passage through a tower of silica followed by passage through a tower of Ridox (or Q-5) catalyst prior to use. Diethyl ether, pentane, and tetrahydrofuran were purchased anhydrous from Aldrich, sparged with nitrogen, and passed through an Innovative Technologies Pure-Solv 400 Solvent Purification System. Nitrogen gas was dried and deoxygenated by passage through a column containing activated molecular sieves and MnO.

$C_6D_6$ ,  $CD_3C_6D_5$ , and  $C_5D_5N$  were dried by refluxing with sodium/potassium alloy in a sealed vessel under partial pressure, then trap-to-trap distilled, and freeze-pump-thawed several times. Deuterated tetrahydrofuran was dried by refluxing with molten potassium metal in a sealed vessel under vacuum, then trap-to-trap distilled, and freeze-pump-thaw-degassed several times. Unless otherwise stated,  $^1H$ ,  $^{31}P$ ,  $^1H\{^{31}P\}$ ,  $^{31}P\{^1H\}$ ,  $^{15}N\{^1H\}$ ,  $^7Li\{^1H\}$  NMR spectra were recorded on a Bruker AMX-400 instrument with a 5mm BBI probe operating at 400.0 MHz for  $^1H$ .  $^{31}P$  NMR spectra were referenced to either external or internal  $P(OMe)_3$  ( $\delta$  141.0 ppm with respect to 85%  $H_3PO_4$  at  $\delta$  0.0 ppm). Elemental analyses and mass spectrometry (EI/MS) were performed at the Department of Chemistry at the University of British Columbia or the Department of Chemistry at the University of Windsor. IR spectroscopy was performed on a Nicolet 4700 FT-IR spectrometer.

### 2.5.2. Materials and Reagents

All materials were purchased from an appropriate supplier and purified by published methods prior to use.  $[(\{NPN\}_2Ta_2)(\mu-H)_2(\mu-\eta^1:\eta^2-N_2)]$ ,<sup>3</sup>  $[(\{NPN\}_2Ta_2)(\mu-D)_2(\mu-\eta^1:\eta^2-N_2)]$ ,<sup>3</sup>  $[Cp_2Zr(py)(Me_3SiC\equiv CSiMe_3)]$ ,<sup>23</sup> and  $[Cp_2Ti(Me_3SiC\equiv CSiMe_3)]$ <sup>24</sup> were all prepared by literature procedures.

### 2.5.3. Synthesis and Characterization of Complexes 2.10 and 2.13

#### Synthesis of $[N(\mu\text{-P}=\text{N})N]Ta(\mu\text{-H})_2(\mu\text{-N}(\text{ZrCp}_2))Ta[NPN]$ (2.10)

##### a) using $[\text{Cp}_2\text{Zr}(\text{Cl})\text{H}]_x$ :

To a mixture of Schwartz's reagent,  $[\text{Cp}_2\text{Zr}(\text{Cl})\text{H}]_x$ , (70 mg, 0.265 mmol) and **2.5** (334 mg, 0.265 mmol, 1 equivalent) in a 50 mL Erlenmeyer flask equipped with a stir bar was added 10 mL toluene and 10 mL THF in a glove box. The mixture was capped and stirred for 1 week at 15°C, after which the red-brown color of **2.5** was converted to a dark purple. The crude purple solid **2.10** was recovered on a frit after evaporation of solvents and trituration with hexanes. X-ray quality crystals were obtained from a cooled solution of THF. Yield = 137 mg, 35%. These were also used for NMR spectroscopy and elemental analysis.

$^1\text{H}\{^{31}\text{P}\}$  NMR ( $\text{C}_6\text{D}_6$ ):  $\delta$  -0.32, -0.04, -0.02, 0.08 (s, 6H each,  $\text{SiCH}_3$ ), 1.17 (AMX,  $^2J_{\text{HH}} = 11$  Hz,  $^2J_{\text{PH}} = 36$  Hz, 4H,  $\text{PCH}_2$ ), 2.19 (AMX,  $^2J_{\text{HH}} = 15$  Hz,  $^2J_{\text{PH}} = 43$  Hz, 4H,  $\text{PCH}_2$ ), 5.38 (s, 10H,  $\eta^5\text{-C}_5\text{H}_5$ ), 6.48, 6.55, 6.74, 6.95, 6.99, 7.62 (d, t, 20 H total,  $\text{N-C}_6\text{H}_5$ ), 7.99, 8.26 (dd, 4H,  $o\text{-PC}_6\text{H}_5$ ), 7.08, 7.12, 7.17, 7.68, (d, t, 6H total,  $\text{PC}_6\text{H}_5$ ), 11.66 (d,  $^2J_{\text{HP}} = 18$  Hz,  $\text{TaHTa}$ ).

$^{13}\text{C}\{^1\text{H}\}$  NMR ( $\text{C}_6\text{D}_6$ ):  $\delta$  0.2, 0.9, 1.0, 1.8 ( $\text{SiCH}_3$ ), 11.9, 20.4 ( $\text{PCH}_2$ ), 106.1 ( $\eta^5\text{-C}_5\text{H}_5$ ), 113.1, 113.9, 114.7, 117.8, 124.7, 125.2 ( $\text{NC}_6\text{H}_5$ ), 123.2, 129.0, 135.4, 137.8 ( $\text{P-C}_6\text{H}_5$ ), 153.2, 155.9 ( $o\text{-PC}_6\text{H}_5$ ).

$^{31}\text{P}\{^1\text{H}\}$  NMR ( $\text{C}_6\text{D}_6$ ):  $\delta$  7.3 ppm (s), 46.7 ppm (s).

Anal. Calc'd for  $\text{C}_{58}\text{H}_{74}\text{N}_6\text{P}_2\text{Si}_4\text{Ta}_2\text{Zr}$ : C 46.99; H 5.03; N 5.67. Found: C 47.12; H 5.21; N 5.51.

##### (b) using $[\text{Cp}_2\text{ZrH}_2]_2$ :

To an intimate mixture of  $[\text{Cp}_2\text{ZrH}_2]_2$  (16 mg, 0.036 mmol) and **2.5** (92 mg, 0.072 mmol) in a J-Young tube was added 2 mL  $d_8$ -THF in a glove box. A sealed capillary tube containing a  $\text{P}(\text{OMe})_3$  standard solution was added and the mixture was sealed and rotated on a mechanical stirrer for 2 weeks at room temperature. The  $^1\text{H}$  and  $^{31}\text{P}$  NMR confirmed the exclusive formation of **2.10** in addition to unreacted **2.5** and  $\text{H}_2$  formation (4.54 in  $d_8$ -THF) (76% yield by  $^{31}\text{P}$  NMR after 2 weeks). A similar experiment with  $D_2$ -

**2.5** and  $[\text{Cp}_2\text{ZrH}_2]_2$  yielded **2.10** and no bridging hydride resonances in the  $^1\text{H}$  NMR.

**c) using  $\text{Cp}_2\text{ZrCl}_2$ :**

To an intimate mixture of  $\text{Cp}_2\text{ZrCl}_2$  (24 mg, 0.081 mmol) and **2.5** (102 mg, 0.081 mmol) in a J-Young tube was added 2 mL  $\text{C}_6\text{D}_6$  in a glove box. A sealed capillary tube containing a  $\text{P}(\text{OMe})_3$  standard solution was added and the mixture was sealed and rotated on a mechanical stirrer for 1 week at room temperature. The  $^1\text{H}$  and  $^{31}\text{P}$  NMR confirmed the formation of **2.10** (20% yield by  $^{31}\text{P}$  NMR after 2 weeks) in addition to  $\text{H}_2$  formation (4.47 ppm in  $\text{C}_6\text{D}_6$ ).

**d) using  $\text{Cp}_2\text{Zr}(\text{py})(\text{Me}_3\text{SiC}\equiv\text{CSiMe}_3)$ :**

To a stirred solution of **2.5** (350 mg, 0.28 mmol) in 20 mL toluene was added  $\text{Cp}_2\text{Zr}(\text{py})(\text{Me}_3\text{SiC}\equiv\text{CSiMe}_3)$  (135 mg, 0.28 mmol) dissolved in 5 mL of toluene. The dark brown solution immediately darkened and the solution stirred for 8 hours. The solvent was removed under vacuum, leaving a purple residue, which was triturated with pentanes until a purple solid was retained. The resulting precipitate was recovered on a glass frit. Yield = 370 mg, 90%.

**Synthesis of  $^{15}\text{N}_2$ - $[\text{N}(\mu\text{-P}=\text{N})\text{N}]\text{Ta}(\mu\text{-H})_2(\mu\text{-N}(\text{ZrCp}_2))\text{Ta}[\text{NPN}]$  ( $^{15}\text{N}_2$ -**2.10**).**

1 equivalent of  $\text{Cp}_2\text{Zr}(\text{py})(\text{Me}_3\text{SiC}\equiv\text{CSiMe}_3)$  was allowed to react with 1 equivalent of  $^{15}\text{N}_2$ -**1** in a manner similar to that outlined above for the synthesis of **2.10**.  $^{15}\text{N}$  NMR ( $\text{C}_6\text{D}_6$ ):  $\delta$  228.4 (d,  $J_{\text{PN}} = 5$  Hz), -185.1 (d,  $^1J_{\text{PN}} = 35$ ).

**Synthesis of  $[\text{N}(\mu\text{-P}=\text{N})\text{N}]\text{Ta}(\mu\text{-H})_2(\mu\text{-N}(\text{TiCp}_2))\text{Ta}[\text{NPN}]$  (**2.13**).**

To a stirred solution of **2.5** (300 mg, 0.24 mmol) in 20 mL toluene was added  $\text{Cp}_2\text{Ti}(\text{Me}_3\text{SiC}\equiv\text{CSiMe}_3)$  (83 mg, 0.24 mmol) dissolved in 5 mL of toluene. The dark brown solution immediately darkened and the solution stirred for 8 hours. The solvent was removed under vacuum, leaving a purple residue, which was triturated with pentanes to yield a purple solid. Yield = 276 mg, 80%.

$^1\text{H}\{^{31}\text{P}\}$  NMR ( $\text{C}_6\text{D}_6$ ):  $\delta$  -0.45, -0.01, 0.07, 0.11 (s, 6H each,  $\text{SiCH}_3$ ), 1.50 (AMX,  $^2J_{\text{HH}} = 10\text{Hz}$ ,  $^2J_{\text{PH}} = 36\text{Hz}$ , 4H,  $\text{PCH}_2$ ), 2.05 (AMX,  $^2J_{\text{HH}} = 15\text{Hz}$ ,  $^2J_{\text{PH}} = 42$  Hz, 4H,  $\text{PCH}_2$ ), 5.20

(s, 8H,  $\eta^5$ -C<sub>5</sub>H<sub>5</sub>), 6.62-7.24 (m, 26H total, -ArH), 9.32 (dd, 4H, *o*-PC<sub>6</sub>H<sub>5</sub>), 12.40 (d, <sup>2</sup>J<sub>HP</sub> = 17 Hz, TaHTa).

<sup>13</sup>C{<sup>1</sup>H} NMR (C<sub>6</sub>D<sub>6</sub>):  $\delta$  0.2, 0.9, 1.1, 1.8 (SiCH<sub>3</sub>), 12.1, 20.6 (PCH<sub>2</sub>), 104.5 ( $\eta^5$ -C<sub>5</sub>H<sub>5</sub>), 112.5, 113.2, 113.5, 118.5, 123.6, 126.2 (NC<sub>6</sub>H<sub>5</sub>), 122.9, 129.6, 136.9, 139.4 (P-C<sub>6</sub>H<sub>5</sub>), 155.6, 156.1 (*o*-PC<sub>6</sub>H<sub>5</sub>).

<sup>31</sup>P{<sup>1</sup>H} NMR (C<sub>6</sub>D<sub>6</sub>):  $\delta$  8.6 ppm (s), 46.4 ppm (s).

Anal. Calc'd for C<sub>58</sub>H<sub>74</sub>N<sub>6</sub>P<sub>2</sub>Si<sub>4</sub>Ta<sub>2</sub>Ti: C 48.40; H 5.18; N 5.84. Found: C 48.23; H 5.10; N 5.49.

**Synthesis of <sup>15</sup>N<sub>2</sub>-[N( $\mu$ -P=N)N]Ta( $\mu$ -H)<sub>2</sub>( $\mu$ -N(TiCp<sub>2</sub>))Ta[NPN] (<sup>15</sup>N<sub>2</sub>-2.13).**

1 equivalent of Cp<sub>2</sub>Ti(Me<sub>3</sub>SiC $\equiv$ CSiMe<sub>3</sub>) was allowed to react with 1 equivalent of <sup>15</sup>N<sub>2</sub>-2.5 in a manner similar to that outlined above for the synthesis of 2.13.

<sup>15</sup>N{<sup>1</sup>H} NMR (C<sub>6</sub>D<sub>6</sub>):  $\delta$  227.5 (d, J<sub>PN</sub> = 5 Hz), -185.5 (d, <sup>1</sup>J<sub>PN</sub> = 34 Hz).

## 2.6. References

- (1) Fryzuk, M. D.; Kozak, C. M.; Bowdridge, M. R.; Patrick, B. O.; Rettig, S. J. *J. Am. Chem. Soc.* **2002**, *124*, 8389.
- (2) Morello, L.; Yu, P.; Carmichael, C. D.; Patrick, B. O.; Fryzuk, M. D. *J. Am. Chem. Soc.* **2005**, *127*, 12796.
- (3) Fryzuk, M. D.; Johnson, S. A.; Patrick, B. O.; Albinati, A.; Mason, S. A.; Koetzle, T. F. *J. Am. Chem. Soc.* **2001**, *123*, 3960.
- (4) Studt, F.; MacKay, B. A.; Johnson, S. A.; Patrick, B. O.; Fryzuk, M. D.; Tucek, F. *Chem. Eur. J.* **2005**, *11*, 604.
- (5) Shaver, M. P.; Johnson, S. A.; Fryzuk, M. D. *Can. J. Chem.* **2005**, *83*, 652.
- (6) MacKay, B. A.; Johnson, S. A.; Patrick, B. O.; Fryzuk, M. D. *Can. J. Chem.* **2005**, *83*, 315.
- (7) Fryzuk, M. D.; MacKay, B. A.; Johnson, S. A.; Patrick, B. O. *Angew. Chem. Int. Ed.* **2002**, *41*, 3709.
- (8) Fryzuk, M. D.; MacKay, B. A.; Patrick, B. O. *J. Am. Chem. Soc.* **2003**, *125*, 3234.
- (9) Bertelo, C. A.; Schwartz, J. *J. Am. Chem. Soc.* **1976**, *98*, 262.
- (10) Orpen, A. G. *Dalton Trans.* **1980**, 2509.
- (11) Shaver, M. P.; Fryzuk, M. D. *Organometallics* **2005**, *24*, 1419.
- (12) Yue, N.; Hollink, E.; Guerin, F.; Stephan, D. W. *Organometallics* **2001**, *20*, 4424.
- (13) Courtenay, S.; Stephan, D. W. *Organometallics* **2001**, *20*, 1442.
- (14) Bai, G.; Mueller, P.; Roesky, H. W.; Uson, I. *Organometallics* **2000**, *19*, 4675.
- (15) Banaszak Holl, M. M.; Wolczanski, P. T. *J. Am. Chem. Soc.* **1992**, *114*, 3854.
- (16) Abarca, A.; Martin, A.; Mena, M.; Yelamos, C. *Angew. Chem. Int. Ed.* **2000**, *39*, 3460.
- (17) Bennett, B. K.; Saganic, E.; Lovell, S.; Kaminsky, W.; Samuel, A.; Mayer, J. M. *Inorg. Chem.* **2003**, *42*, 4127.
- (18) Betley, T. A.; Peters, J. C. *J. Am. Chem. Soc.* **2004**, *126*, 6252.
- (19) Seymore, S. B.; Brown, S. N. *Inorg. Chem.* **2002**, *41*, 462.
- (20) Johnson, S. A., PhD Thesis, University of British Columbia, 2000.
- (21) Chirik, P. J.; Henling, L. M.; Bercaw, J. E. *Organometallics* **2001**, *20*, 534.

- (22) Edelbach, B. L.; Rahman, A. K. F.; Lachicotte, R. J.; Jones, W. D. *Organometallics* **1999**, *18*, 3170.
- (23) Nitschke, J. R.; Zuercher, S.; Tilley, T. D. *J. Am. Chem. Soc.* **2000**, *122*, 10345.
- (24) Varga, V.; Mach, K.; Schmid, G.; Thewalt, U. *J. Organomet. Chem.* **1994**, *475*, 127.

## Chapter Three

# Synthesis of Group 4 Bis(amido)-N-Heterocyclic Carbene Complexes

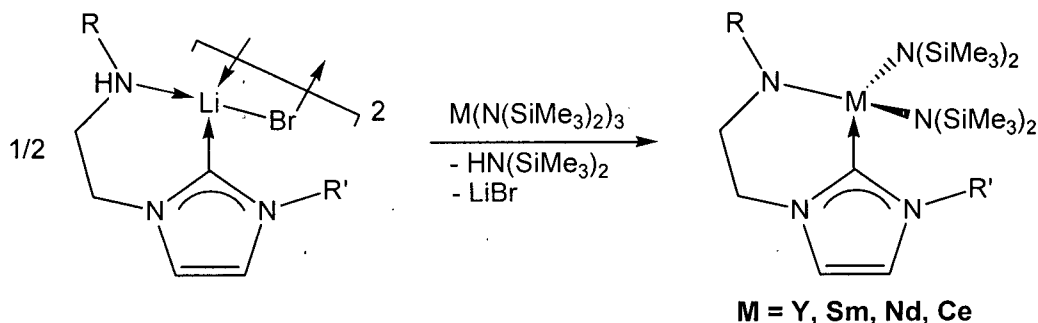
### 3.1 Introduction\*

N-Heterocyclic carbenes have become popular ligands in coordination chemistry and in homogeneous catalysis. In particular, late transition metal complexes employing NHC ligands show strong metal carbene bonds and slow dissociation rates, properties that furnish robust and versatile catalysts.<sup>1-5</sup> However, the use of these ligands in early transition metal chemistry has little precedent. Coordination of neutral donors, such as NHCs, to  $d^0$  metal centres often results in complexes that display enhanced lability of the neutral ligand since back donation from the metal to ligand is not possible. In an effort to examine this tendency, NHCs with pendant anionic donors have been synthesized, in anticipation that this modification would anchor the ligand to the metal centre and enable the strength of the metal-carbene bond to be monitored.

The first systematic study of the lability of ETM and lanthanide NHC complexes was performed utilizing an amido-functionalized NHC ligand.<sup>6</sup> Aminolysis reactions involving a lithium bromide adduct of this bidentate ligand and  $M(N(SiMe_3)_2)_3$  ( $M=Y$ ,

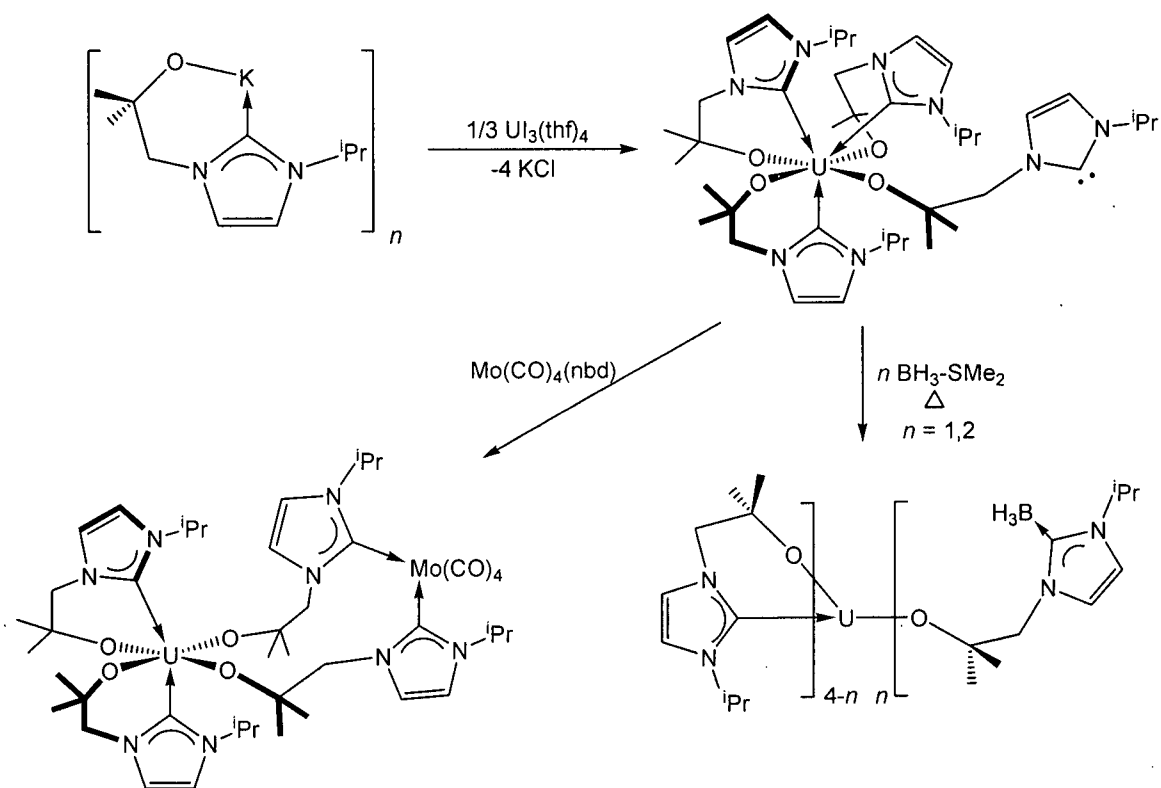
\*A portion of this chapter has been published (Spencer, L.; Winston, S.; Fryzuk, M.D. *Organometallics* 2004, 23, 3372).

samarium and yttrium, the lability of the NHC donor was investigated and found to dissociate from the metal centre in the presence of  $\text{Me}_2\text{NCH}_2\text{CH}_2\text{NMe}_2$  and  $\text{Ph}_3\text{P}=\text{O}$ .



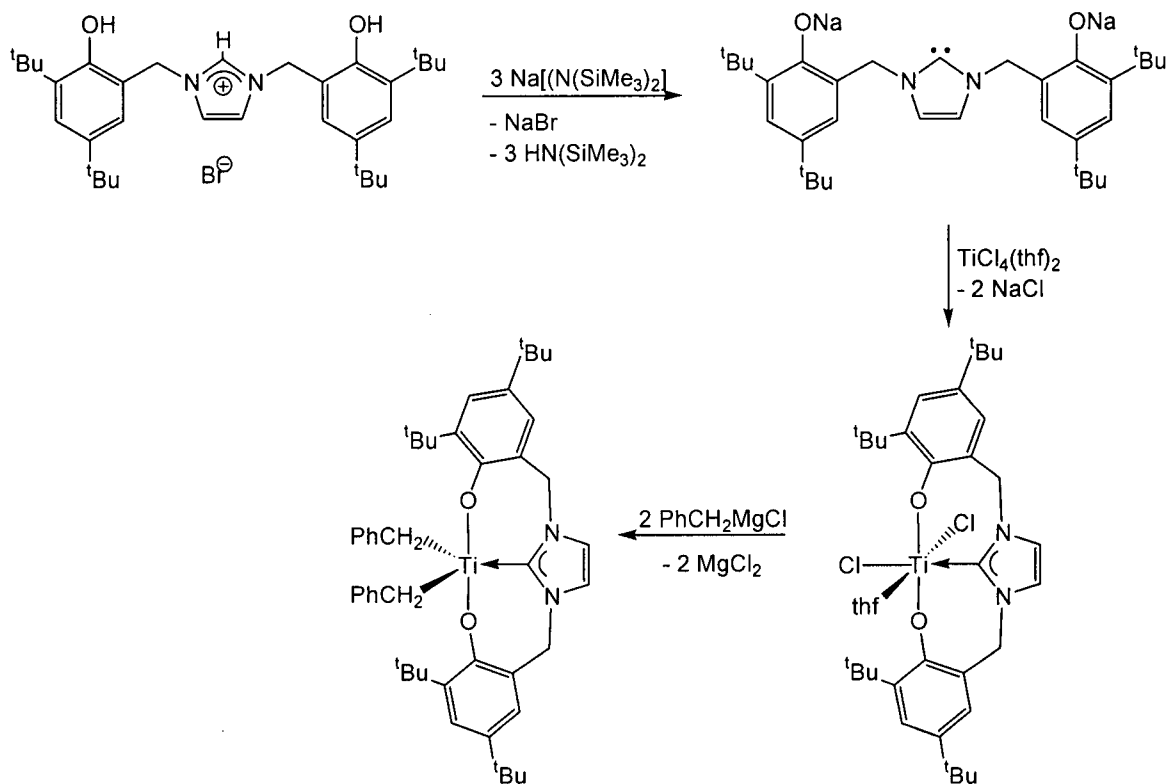
Scheme 3.1

ETM alkoxide-functionalized NHC complexes have also been reported.<sup>7,8</sup> Uranium(IV) complexes bearing this ancillary ligand display a unique example of a metal complex with a free unbound NHC donor (Scheme 3.2).<sup>7</sup> This donor is capable of reacting with other Lewis acids to generate simple acid-base adducts. Further reactivity of the uranium-bound carbenes was observed with the addition of other metal fragments, such as  $\text{Mo}(\text{CO})_4$ , and functional groups like  $\text{BH}_3$ . Although this may be useful for the introduction of molecules into the coordination sphere of the uranium(IV) metal, these results provide further proof of the hemilabile nature of NHCs when coordinated to electropositive metals.



**Scheme 3.2**

Interest in NHC ligands with pendant anionic groups is not limited to bidentate examples. A tridentate carbene donor system has been reported employing two anionic phenoxide donors with a centrally disposed NHC unit (Scheme 3.3).<sup>8</sup> Preliminary research with titanium derivatives has been reported with no mention of NHC dissociation. Although this aspect was not addressed, it seems likely that the central disposition of the NHC in this tridentate binding motif might anchor the NHC donor to an electropositive metal centre.



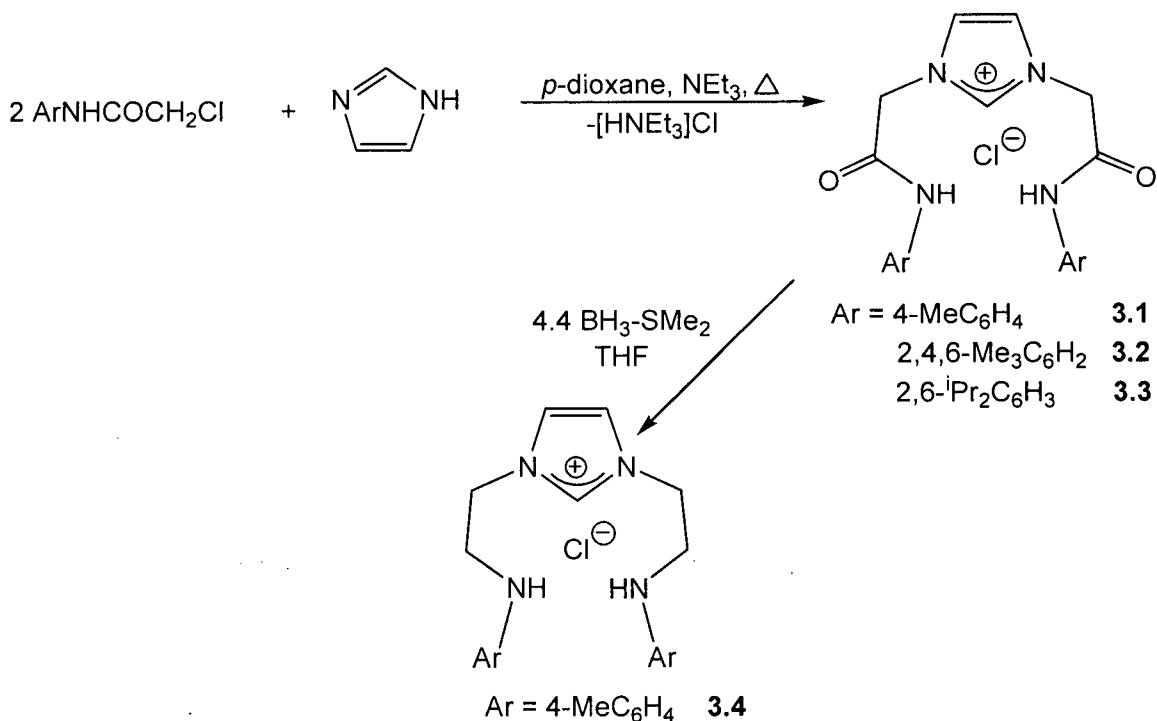
Scheme 3.3

In light of these results, a tridentate donor system was designed that would incorporate an NHC flanked by two anionic amido arms. It was anticipated this pincer architecture would render the carbene stable to dissociation because of its central position between two anionic donors. This design creates a ligand which will be abbreviated by the formula  $^{\text{Ar}}[\text{NCN}]$ , where Ar refers to an aryl substituent on the amido donor and  $[\text{NCN}]$  refers to the diamido-NHC ligand. The synthesis and coordination of this  $^{\text{Ar}}[\text{NCN}]$  ligand to group 4 transition metals is the subject of discussion in this chapter.

### 3.2. Synthesis of $^{\text{Ar}}[\text{NCN}]\text{H}_2$ and Lithium Derivatives

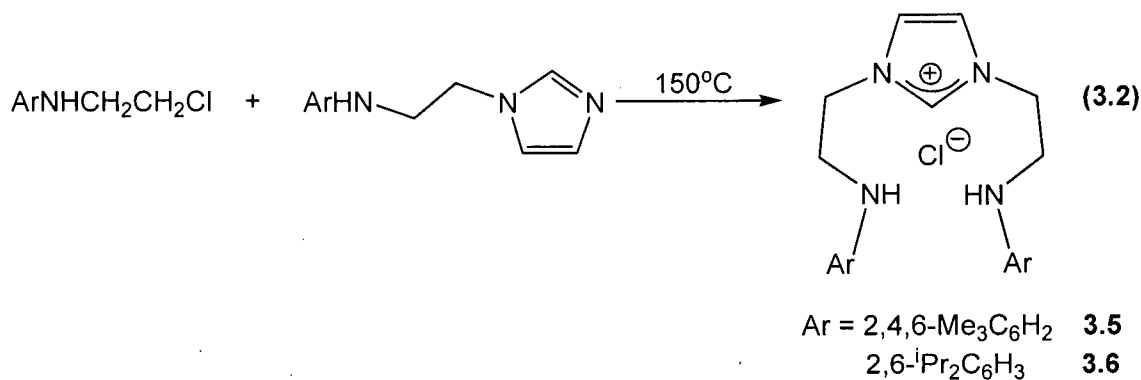
To construct a NHC with two pendant amine arms, the reduction of several bis(amide) imidazolium chloride precursors was examined. Addition of substituted 2-chloroacetamides to imidazole produces **3.1-3.3** in reasonable yields (Scheme 3.4). The  $^{13}\text{C}\{^1\text{H}\}$  NMR spectrum of **3.1** features an amide resonance at 170.5 ppm, in addition to

appropriate imidazolium and aryl resonances. Reduction of the amide derivative **3.1** with borane-dimethylsulfide gives the desired bis(amino)-imidazolium chloride in reasonable yield. Both  $^1\text{H}$  and  $^{13}\text{C}\{^1\text{H}\}$  NMR spectra are consistent with the expected product (**3.4**) as evidenced by the disappearance of the amide  $^{13}\text{C}$  resonance in the  $^{13}\text{C}\{^1\text{H}\}$  NMR spectrum. The  $^1\text{H}$  NMR spectrum shows two multiplets for the newly formed ethylene spacers and an amino  $-\text{NH}$  resonance at 5.74 ppm.



Scheme 3.4.

Incorporation of more sterically demanding aryl amido groups required a different synthetic approach. Unfortunately, the reduction of bis(amide) imidazolium chlorides (**3.2**, **3.3**) with borane was unsuccessful, leading only to decomposition of the starting materials. Introduction of mesityl (2,4,6-Me<sub>3</sub>C<sub>6</sub>H<sub>2</sub>) and 2,6-diisopropyl (2,6-<sup>i</sup>Pr<sub>2</sub>C<sub>6</sub>H<sub>3</sub>) groups was accomplished by melting the appropriately substituted imidazole and N-substituted 2-chloroethylamine. This provided the imidazolium chlorides **3.5** and **3.6** in near quantitative yield (Equation 3.2). The  $^1\text{H}$  and  $^{13}\text{C}\{^1\text{H}\}$  NMR spectra of **3.5** and **3.6** are similar to **3.4** with the presence of symmetrical ethylene spacer and amino groups.



X-ray quality crystals of **3.5** were grown from CH<sub>3</sub>CN and analyzed by X-ray crystallography. An ORTEP depiction of the solid state molecular structure of **3.5** is shown in Figure 3.1. Relevant bond lengths and angles are listed in Table 3.1, and crystallographic details are located in appendix A. The presence of a chloride counterion confirms the synthesis of an imidazolium moiety. In addition, a C1-N1 bond length of 1.326(4) and N1-C1-N2 bond angle of 109.4(3)<sup>o</sup> is observed, typical of other reported imidazolium compounds.<sup>9-11</sup>

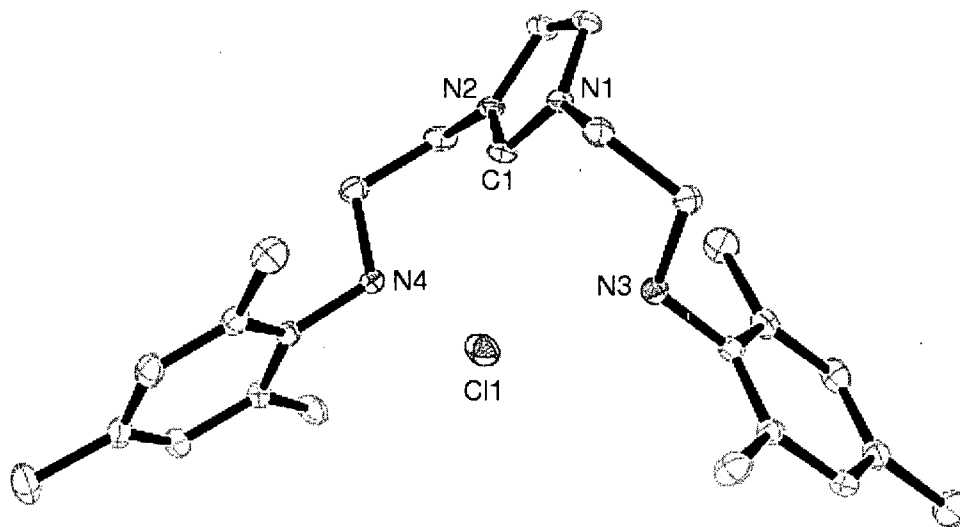
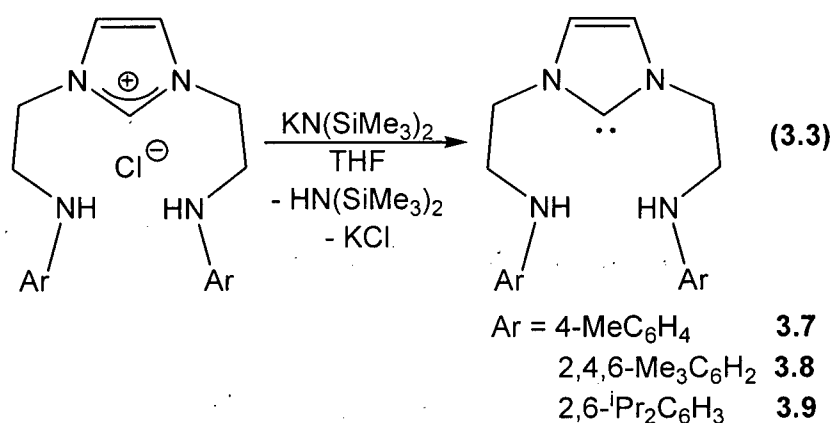


**Figure 3.1.** ORTEP view of <sup>Mes</sup>[NCHN]H<sub>2</sub>·Cl (**3.5**) depicted with 50% thermal ellipsoids; all hydrogen atoms have been omitted for clarity.

**Table 3.1.** Selected Bond Distances (Å) and Bond Angles (°) for <sup>Mes</sup>[NCN]H<sub>2</sub>·Cl (**3.5**) and <sup>Mes</sup>[NCN]H<sub>2</sub> (**3.8**).

Bond Lengths ( <b>3.5</b> )		Bond Angles ( <b>3.5</b> )	
C1-N1	1.326(4)	N1-C1-N2	109.4(3)
C1-N2	1.325(4)		
Bond Lengths ( <b>3.8</b> )		Bond Angles ( <b>3.8</b> )	
C1-N1	1.365(3)	N1-C1-N3	102.2(2)

Deprotonation of imidazolium halide precursors **3.4-3.6** with KN(SiMe<sub>3</sub>)<sub>2</sub> proceeds cleanly to give NHCs **3.7-3.9** in near quantitative yield (Equation 3.3). Both <sup>1</sup>H and <sup>13</sup>C{<sup>1</sup>H} NMR spectra of **3.7** and **3.8** are consistent with a symmetrical molecule. The presence of a carbene moiety is signified by the absence of the resonance attributed to the iminium proton (at C<sub>2</sub>), an upfield shift in the heterocycle protons in the C<sub>4,5</sub> positions, and a weak <sup>13</sup>C resonance at 211.4 ppm (**3.7**) and 215.0 (**3.8**) ppm for the carbene moiety. Deprotonation of **3.6** with one equivalent of KN(SiMe<sub>3</sub>)<sub>2</sub> at -30°C resulted in the isolation of a highly soluble yellow oil. Although <sup>1</sup>H NMR spectroscopy of the oily product confirmed the presence of **3.9**, other unidentifiable resonances were present. Given this observation, the highly soluble carbene **3.9** was generated *in situ* from **3.6** and used as a THF solution for further reactions.



Colourless crystals of **3.8** were grown from a saturated hexane solution and were analyzed by X-ray diffraction. An ORTEP depiction of the solid state molecular structure of **3.8** is given in Figure 3.2. Relevant bond lengths and angles are listed in

Table 3.1, and crystallographic details are located in appendix A. The N1-C1-N3 bond angle is  $102.2(2)^\circ$ , significantly smaller than the imidazolium chloride precursor **3.5**, which is consistent with other reported systems.<sup>9-11</sup>

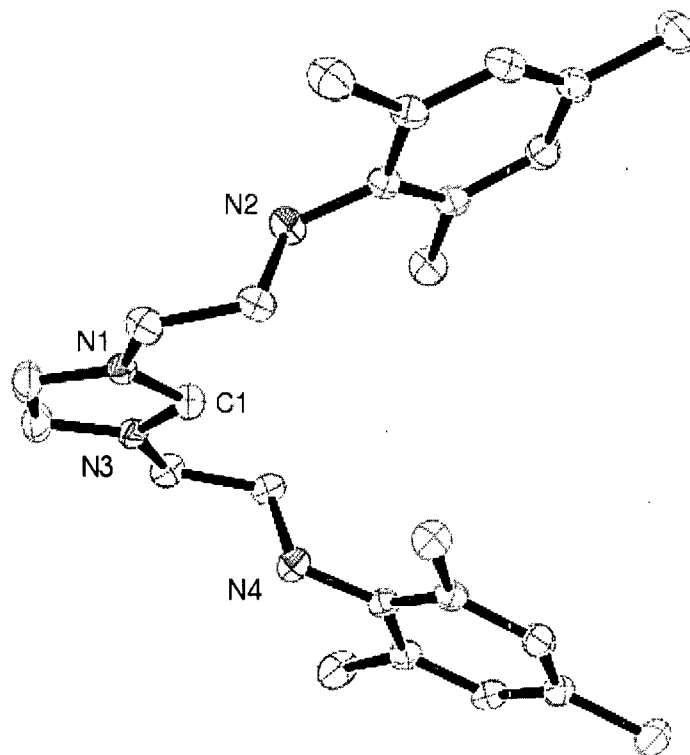
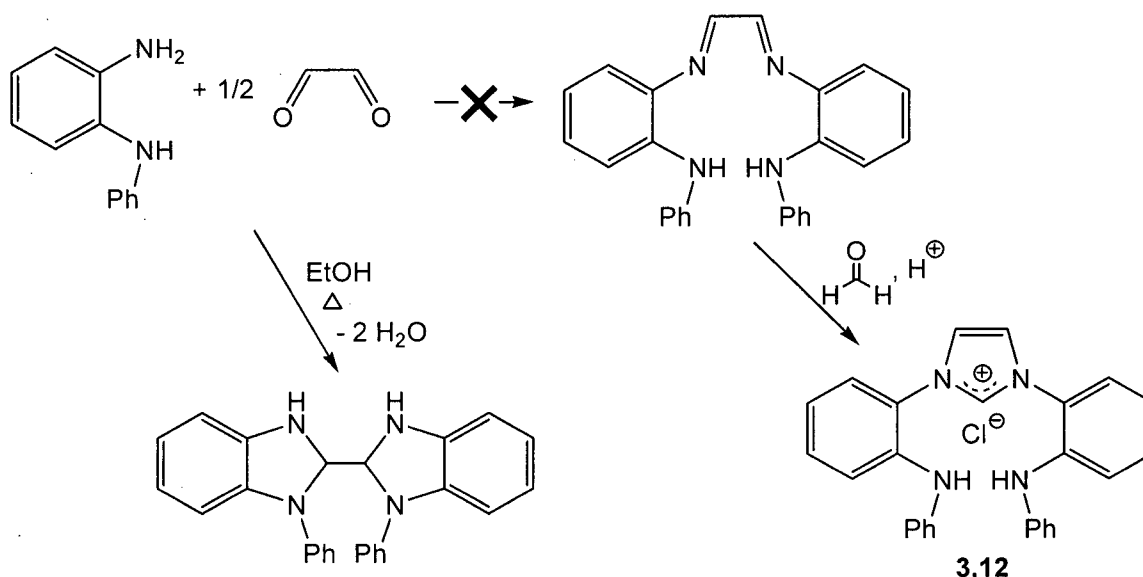


**Figure 3.2.** ORTEP view of  $^{\text{Mes}}[\text{NCN}]\text{H}_2$  (**3.8**) depicted with 50% thermal ellipsoids; all hydrogen atoms have been omitted for clarity.

Metathesis reactions with  $\text{Li}_2[\text{NPN}]$  have successfully been used in the Fryzuk group in the synthesis of  $[\text{NPN}]$  metal complexes.<sup>12</sup> Along this line, the synthesis of  $\text{Li}_2[\text{NCN}]$  was investigated. The addition of two equivalents of *n*-BuLi to **3.7** and **3.8** yielded  $\text{Li}_2^{\text{tol}}[\text{NCN}]$  (**3.10**) and  $\text{Li}_2^{\text{Mes}}[\text{NCN}]$  (**3.11**), respectively (Equation 3.4). Unfortunately, the low solubility of these complexes has prevented a solid state molecular structure determination; however, the  $^1\text{H}$  NMR spectra of both species in *d*<sub>5</sub>-pyridine shows broad resonances indicative of the desired products. For example, the  $^1\text{H}$  NMR spectrum of **3.10** reveals two multiplets assigned to the ethylene spacers, one signal for aryl-methyl and imidazole environments, and two doublets for the *para*-substituted aryl ring. The  $^{13}\text{C}\{^1\text{H}\}$  NMR spectrum shows a weak resonance at 189.9 ppm, which is similar to other reported Li-NHC compounds.<sup>6</sup> Additionally, a broad  $^7\text{Li}$  resonance is

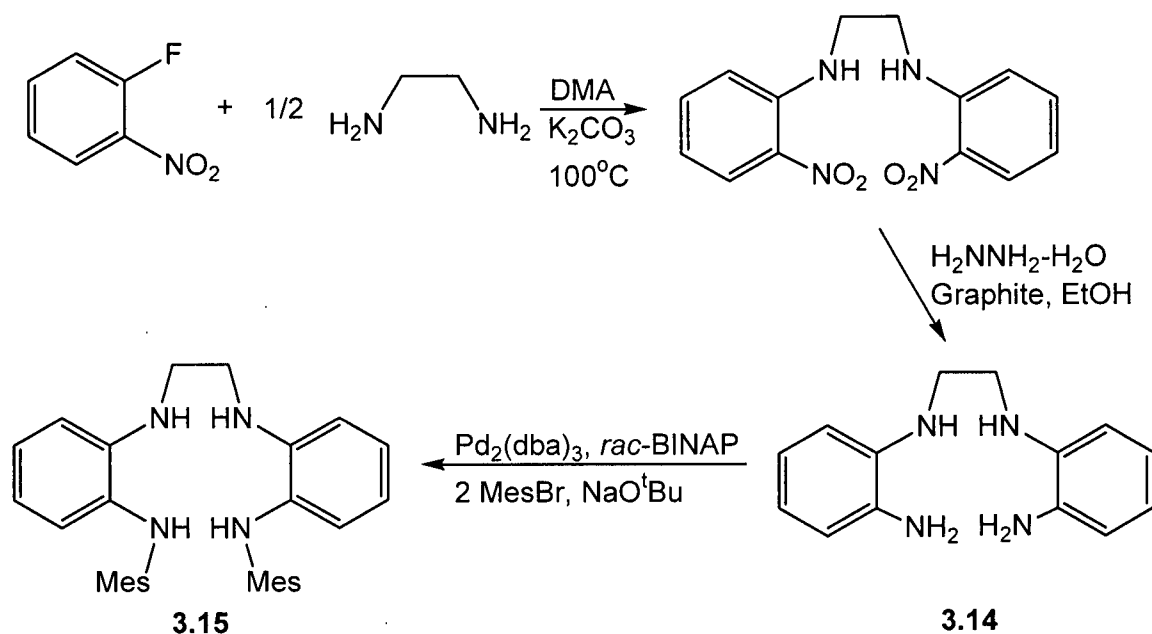


Unfortunately, the synthesis of a substituted diimine precursor has proven to be problematic. The reaction between *N*-phenyl-*ortho*-phenylenediimine with glyoxal was examined and found to yield a bis(benzimidazole) derivative.<sup>14</sup> Substitution of benzil or 2,3-butanedione for glyoxal was also investigated in an attempt to prevent the formation of benzimidazole derivatives. However, no reaction was observed between *N*-phenyl-*ortho*-phenylenediimine and these glyoxal derivatives using experimental conditions that have been successful in the synthesis of diimines.<sup>13</sup>



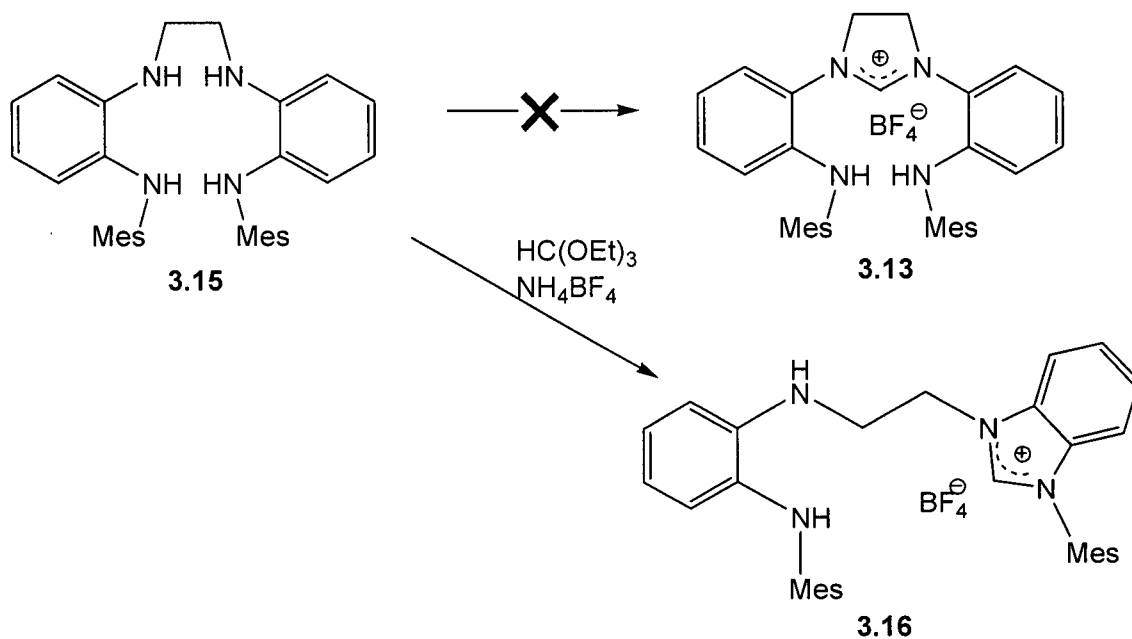
Scheme 3.5.

The synthesis of *N*-substituted diamines was also examined with a goal to ring close these compounds to generate the imidazolium complex **3.13**. A precursor to **3.13**, a substituted tetraamine (**3.14**), was synthesized in several steps from 2-nitrofluorobenzene and 1,2-ethylenediamine (Scheme 3.6).<sup>15</sup> Palladium catalyzed coupling of the aniline **3.14** with two equivalents of mesityl bromide produced the desired mesityl-substituted tetraamine **3.15** in an overall yield of 86%.



Scheme 3.6.

Ring closure of the tetraamine with triethylorthoformate and ammonium tetrafluoroborate was anticipated to yield the imidazolium tetrafluoroborate derivative **3.13**.  $^1H$  and  $^{13}C\{^1H\}$  NMR spectroscopy showed an asymmetric compound in solution with inequivalent ethylene spacer, aryl, and imidazole resonances, in addition to an imidazolium resonance at 10.04 ppm in the  $^1H$  NMR spectrum. Given this spectroscopic evidence, the formation of the asymmetric benzimidazolium tetrafluoroborate compound **3.16** is postulated (Scheme 3.7).

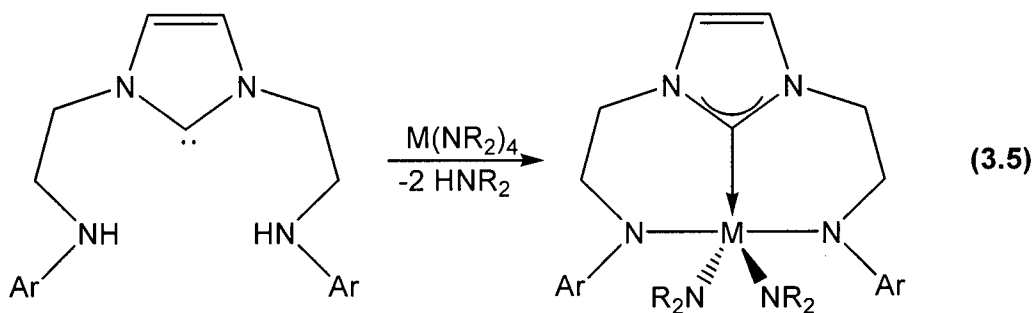


Scheme 3.7.

#### 3.4. Synthesis of Group 4 [NCN] Amido, Chloride, and Alkyl Complexes

The coordination of the [NCN] ancillary ligand onto group 4 transition metals can be easily achieved by either amine or alkyl elimination reactions. For example, treatment of a THF solution  $\text{Zr}(\text{NEt}_2)_4$  with **3.7** proceeded smoothly at room temperature to afford  $^{\text{tol}}[\text{NCN}]\text{Zr}(\text{NEt}_2)_2$  (**3.17**) in high yield (Equation 3.5). Complex **3.17** was characterized by  $^1\text{H}$  and  $^{13}\text{C}\{^1\text{H}\}$  NMR spectroscopy and shows equivalent  $\text{NEt}_2$  moieties along with equivalent amido side arms of the  $^{\text{tol}}[\text{NCN}]$  unit; on the basis of this data a  $C_{2v}$  symmetry can be assigned to this five-coordinate complex. The  $^{13}\text{C}\{^1\text{H}\}$  NMR spectrum shows a resonance at 188.8 ppm indicative of a metal-carbene moiety. The aminolysis reactions of **3.8** and **3.9** with  $\text{Zr}(\text{NEt}_2)_4$  yielded no reaction at room temperature and when heated provided a mixture of intractable materials. The absence of a reaction may be attributed to the increase in steric bulk at the amido nitrogen position on the [NCN] architecture. Incorporation of the bulkier  $^{\text{Mes}}[\text{NCN}]$  and  $^{\text{Dipp}}[\text{NCN}]$  ancillary ligands on zirconium was achieved by aminolysis reactions with  $\text{Zr}(\text{NMe}_2)_4$ . These reactions occurred immediately at room temperature to provide the desired  $^{\text{Ar}}[\text{NCN}]\text{Zr}(\text{NMe}_2)_2$  products **3.18** and **3.19**.

These aminolysis reactions have also been used with  $\text{Ti}(\text{NMe}_2)_4$  and  $\text{Hf}(\text{NMe}_2)_4$  to give **3.20** and **3.21**, respectively.



$M = \text{Zr}, \text{Ar} = 4\text{-MeC}_6\text{H}_4, \text{R} = \text{Et}$       **3.17**

$M = \text{Zr}, \text{Ar} = 2,4,6\text{-Me}_3\text{C}_6\text{H}_2, \text{R} = \text{Me}$       **3.18**

$M = \text{Zr}, \text{Ar} = 2,6\text{-}^i\text{Pr}_3\text{C}_6\text{H}_2, \text{R} = \text{Me}$       **3.19**

$M = \text{Ti}, \text{Ar} = 4\text{-MeC}_6\text{H}_4, \text{R} = \text{Me}$       **3.20**

$M = \text{Hf}, \text{Ar} = 2,4,6\text{-Me}_3\text{C}_6\text{H}_2, \text{R} = \text{Me}$       **3.21**

X-ray quality crystals of **3.17** were grown from  $\text{Et}_2\text{O}$  and the solid state molecular structure was determined by X-ray crystallography. An ORTEP depiction of **3.17** is shown in Figure 3.4. Relevant bond lengths and angles are listed in Table 3.2, and crystallographic details are located in appendix A. The ligand assumes a quasi-planar orientation to produce a distorted trigonal pyramidal metal centre. One of the six-membered chelating rings of [NCN] is nearly planar, with a N1-C1-Zr1-N3 torsion angle of  $-0.8^\circ$ . However, the other six-membered chelate ring is distorted from planarity as noted by the N2-C1-Zr1-N4 torsion angle of  $34.2^\circ$ . The Zr1-C1 bond length of 2.421(6) Å is slightly shorter than previously characterized lengths of Zr-based NHC compounds (2.432(3)-2.456(3) Å),<sup>16,17</sup> most likely a result of the ligand architecture that pulls the carbene donor closer to the metal. The Zr-N amido bond lengths average to 2.113(6) Å and are comparable to other Zr-amide complexes.<sup>18-21</sup>

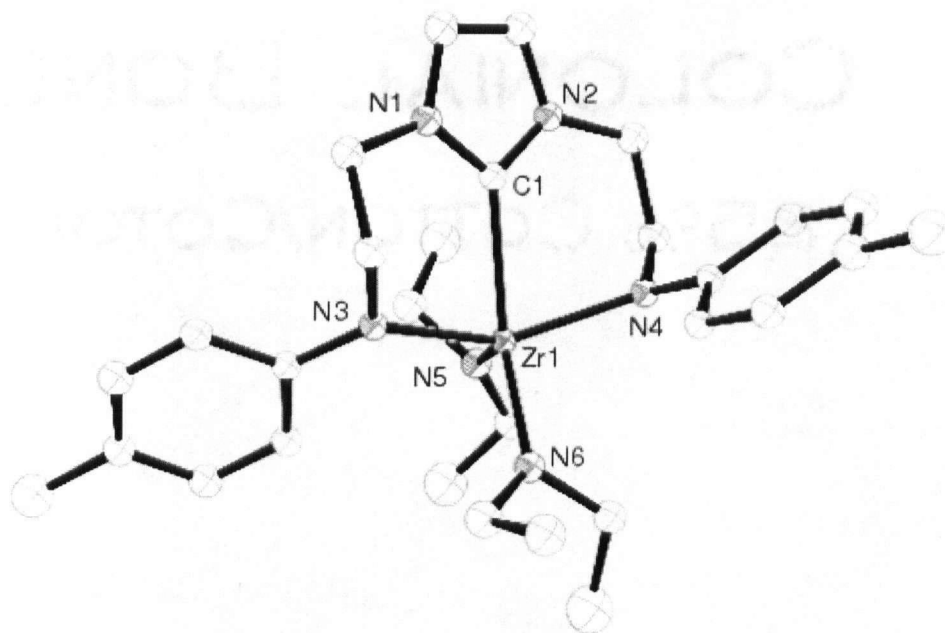
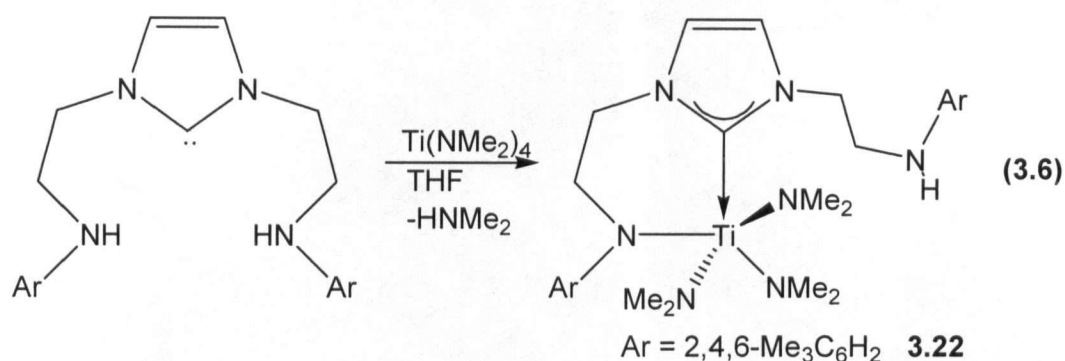


**Figure 3.4.** ORTEP view of  $^{tol}[\text{NCN}]\text{Zr}(\text{NEt}_2)_2$  (**3.17**) depicted with 50% thermal ellipsoids; all hydrogen atoms have been omitted for clarity.

**Table 3.2.** Selected Bond Distances (Å) and Bond Angles ( $^\circ$ ) for  $^{tol}[\text{NCN}]\text{Zr}(\text{NEt}_2)_2$ , (**3.17**).

Bond Lengths		Bond Angles	
Zr1-C1	2.421(6)	N3-Zr1-N4	141.7(4)
Zr1-N3	2.190(6)	N3-Zr1-C1	75.0(2)
Zr1-N4	2.169(5)	N4-Zr1-C1	77.9(2)
Zr1-N5	2.058(6)	N5-Zr1-C1	147.2(4)
Zr1-N6	2.036(6)	N6-Zr1-C1	104.1(3)
		N5-Zr1-N6	108.6(3)
		N1-C1-Zr1-N3	-0.8
		N2-C1-Zr1-N4	34.2 $^\circ$

The reaction of **3.8** with  $\text{Ti}(\text{NMe}_2)_4$  does not produce the expected bis(amide) titanium complex. The  $^1\text{H}$  and  $^{13}\text{C}\{^1\text{H}\}$  NMR spectra showed a product with  $C_s$  symmetry (**3.22**) in solution with four multiplets observed for the ethylene spacers, two doublets for the imidazole groups, two distinct aryl signals, two aryl-methyl signals, and a broad resonance attributed to the  $\text{NMe}_2$  groups. This suggests that the  $[\text{NCN}]$  ligand is present in the amide-amine configuration shown in Equation 3.6.



The solid state molecular structure of **3.22** was determined by an X-ray diffraction experiment from crystals grown from an Et<sub>2</sub>O solution (Figure 3.5). Relevant bond lengths and angles are listed in Table 3.3, and crystallographic details are located in appendix A. The ligand coordinates in an amide-amine donor configuration on a distorted trigonal bipyramidal titanium metal centre. The Ti-N amide bond lengths are typical of other reported titanium amide complexes<sup>22-28</sup> as is the Ti1-C1 NHC bond length.<sup>16,28</sup> Although introduction of the [NCN] ligand is incomplete, the formation of a new Ti-C NHC bond was encouraging. Thus far, all attempts to promote the coordination of the other pendant amine donor by thermolysis have been unsuccessful.

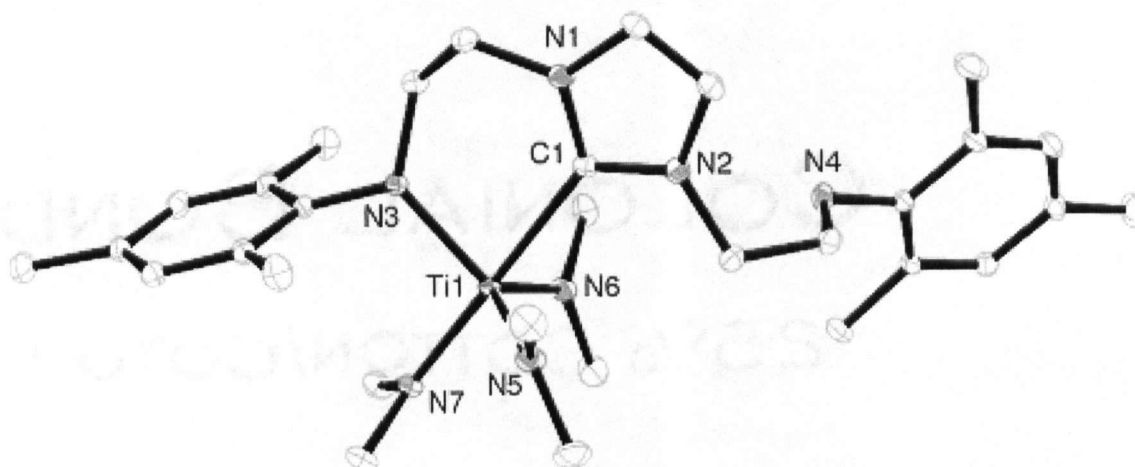
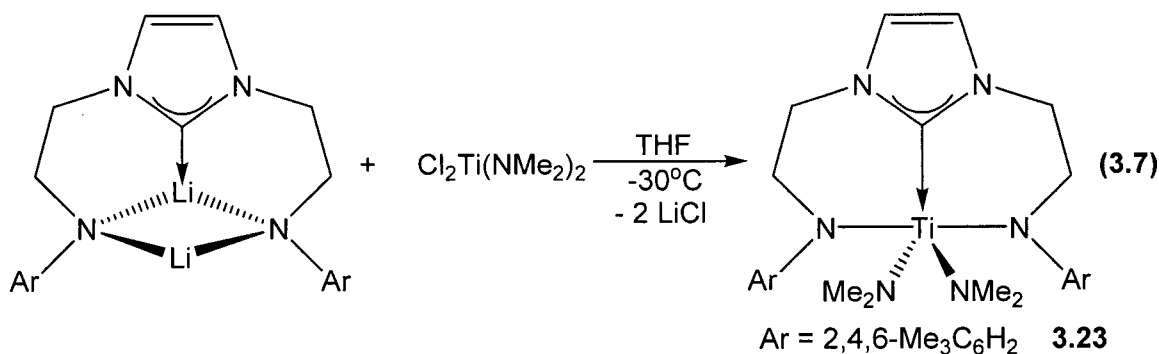


**Figure 3.5.** ORTEP view of <sup>Mes</sup>[NCNH]Ti(NMe<sub>2</sub>)<sub>3</sub> (**3.22**) depicted with 50% thermal ellipsoids; all hydrogen atoms have been omitted for clarity.

**Table 3.3.** Selected Bond Distances (Å) and Bond Angles (°) for  $^{\text{Mes}}[\text{NCNH}]\text{Ti}(\text{NMe}_2)_3$ , (**3.22**).

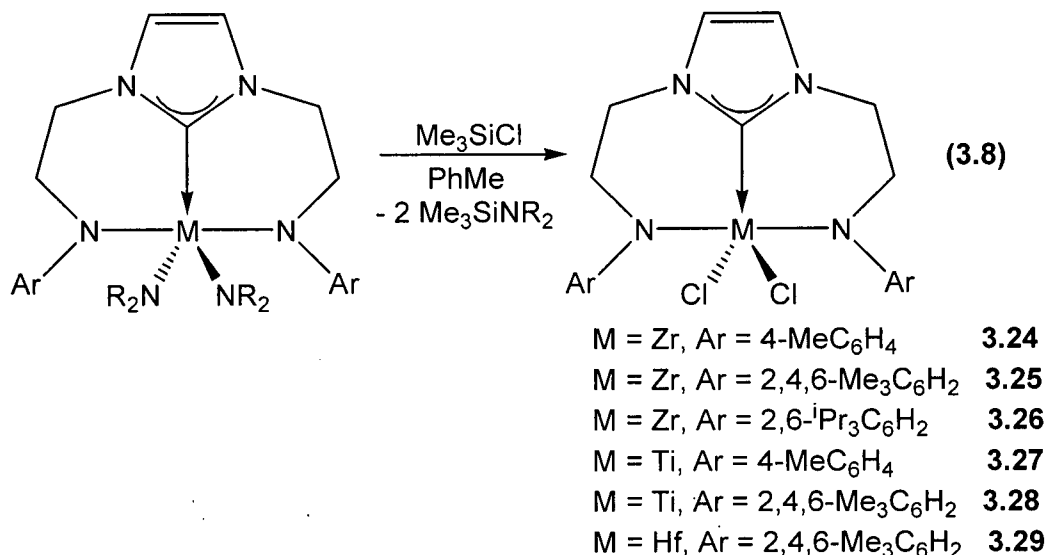
Bond Lengths		Bond Angles	
Ti1-C1	2.3382(18)	N3-Ti1-C1	82.18(6)
Ti1-N3	1.9983(14)	N5-Ti1-C1	88.37(6)
Ti1-N5	1.9650(15)	N7-Ti1-C1	177.91(6)
		N3-Ti1-N5	123.09(6)
		N3-Ti1-N7	97.37(6)

Coordination of both amide donors to form  $^{\text{Mes}}[\text{NCN}]\text{Ti}(\text{NMe}_2)_2$  was achieved by a metathesis reaction between the dilithiated  $[\text{NCN}]$  derivative **3.11** and  $\text{Cl}_2\text{Ti}(\text{NMe}_2)_2$  (Equation 3.7). This reaction proceeded immediately in toluene to give a dark red product in 68% yield. In solution, the  $^1\text{H}$  NMR spectrum is consistent with a symmetrical species in solution with diagnostic  $^{13}\text{C}$  and  $^1\text{H}$  resonances expected for **3.23**. Although elemental analysis studies agree with the formation of **3.23**, attempts to grow crystals suitable for X-ray diffraction study have been unsuccessful.



Treatment of the group 4 bis(amido) metal complexes with excess  $\text{Me}_3\text{SiCl}$  in toluene gave the metal dichloride complexes in quantitative yield (**3.24-3.29**) (Equation 3.8). These complexes are extremely insoluble in many common organic solvents, which may indicate a dimeric structure in the solid state.<sup>29-32</sup> Although no solution spectroscopic data could be obtained, the empirical formulae of **3.24-3.29** were confirmed by mass spectrometry and elemental analysis. The addition of pyridine to a suspension of **3.24** in toluene resulted in the isolation of the pyridine adduct **3.30**. Complex **3.30** is soluble in many common organic solvents, which has allowed full

characterization by spectroscopic and X-ray diffraction studies. The NMR data for **3.30** clearly show the presence of resonances for coordinated pyridine along with ligand resonances. The Zr-carbene carbon in **3.30** appears as a weak singlet at 187.9 ppm in the  $^{13}\text{C}\{^1\text{H}\}$  NMR spectrum.



Crystals of **3.30** were grown from a concentrated benzene solution and analyzed by single-crystal X-ray diffraction. An ORTEP depiction of **3.30** is given in Figure 3.6 with relevant bond lengths and angles listed in Table 3.4, and crystallographic details located in appendix A. In the solid state, the zirconium centre is coordinated by the tridentate <sup>tol</sup>[NCN] ligand in addition to pyridine. The two chlorides adopt a mutually *cis* position with the [NCN] ligand in a meridional orientation to generate a pseudo-octahedral arrangement around the central Zr atom. Both of the six-membered chelating rings of [NCN] are nearly planar, with N2-C1-Zr1-N4 and N1-C1-Zr1-N3 torsion angles of 1.2° and 7.5°, respectively; however, each ring has the carbon  $\alpha$  to the amido donor sitting above or below in the solid state. The Zr-C carbene bond length is similar to **3.17** but still shorter than previously characterized lengths of Zr-based NHC compounds.<sup>17</sup> The Zr-N amido bond lengths average to 2.138(4) Å and are comparable to other Zr-amide complexes.<sup>18-20,33</sup> The Zr-Cl bond distances are not unusual as is the Zr-N bond length of the pyridine donor (2.398(5) Å).

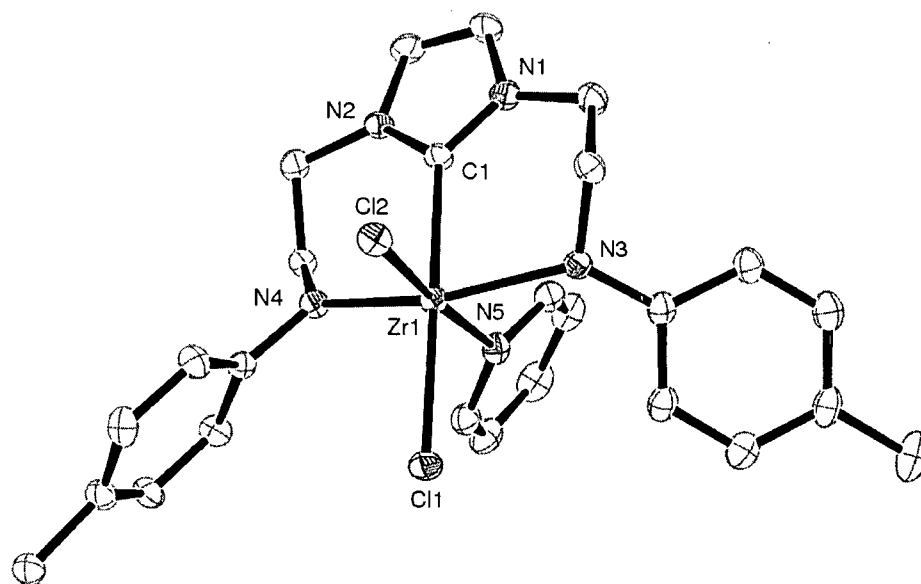


**Figure 3.6.** ORTEP view of  $^{101}\text{[NCN]ZrCl}_2(\text{py})$  (**3.30**) depicted with 50% thermal ellipsoids; all hydrogen atoms have been omitted for clarity.

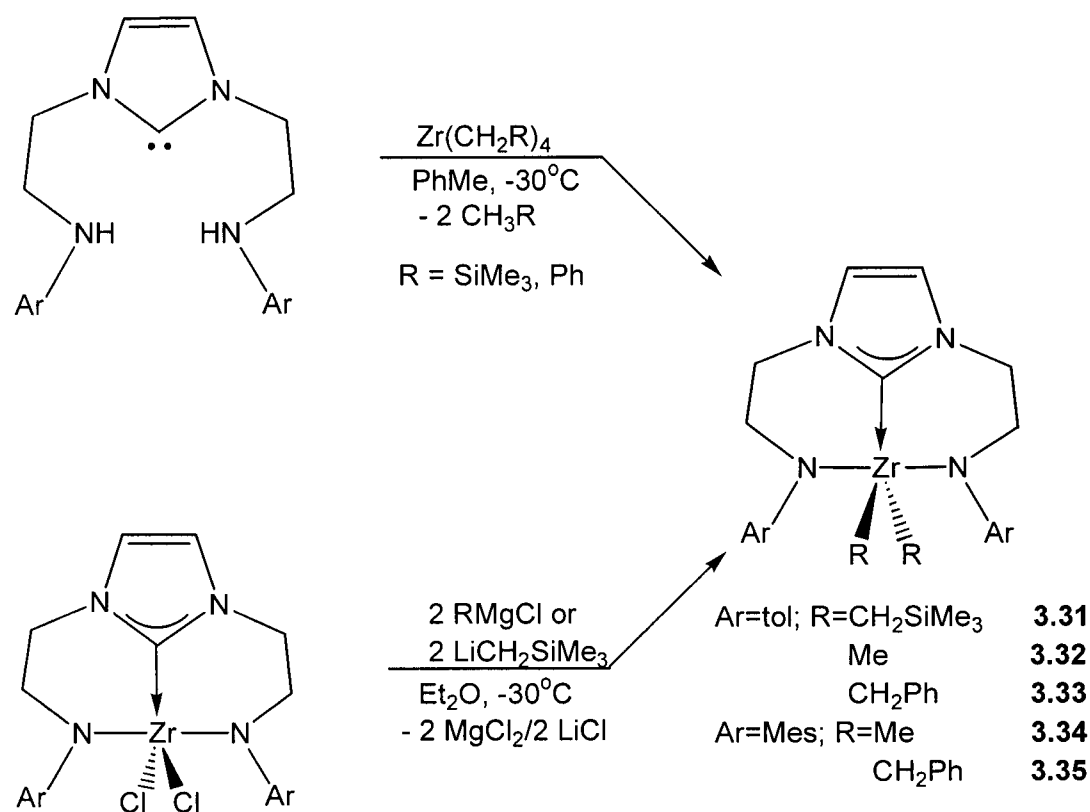
**Table 3.4.** Selected Bond Distances (Å) and Bond Angles ( $^\circ$ ) for  $^{101}\text{[NCN]ZrCl}_2(\text{py})$ , (**3.30**).

Bond Lengths		Bond Angles	
Zr1-C1	2.391(5)	N3-Zr1-N4	155.27(16)
Zr1-N3	2.167(4)	N5-Zr1-C1	84.02(18)
Zr1-N4	2.109(4)	N4-Zr1-Cl1	94.77(14)
		Cl1-Zr1-Cl1	170.38(14)
		N2-C1-Zr1-N4	1.2
		N1-C1-Zr1-N3	7.5

Given the ease of NHC dissociation in reported amide-NHC ETM complexes,<sup>6,7,34</sup> the aspect of carbene lability in  $^{101}\text{[NCN]ZrCl}_2(\text{py})$  was investigated. This was accomplished in two ways: in the first, the  $^{13}\text{C}\{^1\text{H}\}$  NMR spectrum of **3.24** in  $d_5$ -pyridine, a strongly coordinating solvent, was measured. This spectrum is compared to that obtained in non-coordinating  $d_6$ -benzene. In particular the chemical shift of the N-heterocyclic carbene carbon resonance was monitored. In  $d_5$ -pyridine this resonance is

observed at 181.0 ppm while in  $d_6$ -benzene, it appeared at 187.9 ppm; the free carbene resonance observed for **3.7** is found at 211.4 ppm in  $d_6$ -benzene. A second experiment involved the addition of 10 equivalents of  $\text{Me}_2\text{NCH}_2\text{CH}_2\text{NMe}_2$  to a  $d_6$ -benzene solution of **3.24**; in this case no change in the  $^{13}\text{C}\{^1\text{H}\}$  NMR resonance of the carbene carbon is observed. Both of these experiments are consistent with the carbene carbon atom of the NHC in the [NCN] ancillary ligand remaining bound to the Zr centre, confirming that the flanking amido donors do anchor the NHC to the Zr(IV) centre.

The preparation of dialkyl zirconium complexes was performed by both alkylation and protonolysis methods. For example, the reaction of  $\text{Zr}(\text{CH}_2\text{SiMe}_3)_4$  with **3.7** produced the desired product **3.31** via  $\text{SiMe}_4$  elimination (Scheme 3.8). This complex was also synthesized from the reaction of dichloride **3.24** and two equivalents of  $\text{LiCH}_2\text{SiMe}_3$ ; however, a better yield was obtained via the alkane elimination method at  $-30^\circ\text{C}$ .  $^1\text{H}$  and  $^{13}\text{C}\{^1\text{H}\}$  NMR spectroscopy showed the presence of the desired dialkyl groups in addition to expected ligand resonances. For example, the  $^1\text{H}$  NMR spectrum of **3.32** features equivalent zirconium-methyl groups with a single resonance at 0.62 ppm, in addition to equivalent amido side arms of the  $^{101}\text{[NCN]}$  unit. The  $^{13}\text{C}\{^1\text{H}\}$  NMR spectrum shows a resonance at 39.7 ppm, which is characteristic of a zirconium-methyl moiety.



Scheme 3.8.

The X-ray diffraction study of a single crystal of **3.31** revealed a distorted trigonal bipyramidal geometry around the zirconium metal centre. An ORTEP depiction of the solid state molecular structure of **3.31** is shown in Figure 3.7. Relevant bond lengths and angles are listed in Table 3.5, and crystallographic details are located in appendix A. The zirconium-carbene bond length (Zr1-C1) is 2.415(3) Å, which is slightly longer than that found in **3.31** but still shorter than the corresponding bond distances reported for NHC zirconium complexes of the type *trans*-ZrCl<sub>4</sub>L<sub>2</sub> (L = NHC).<sup>17</sup>

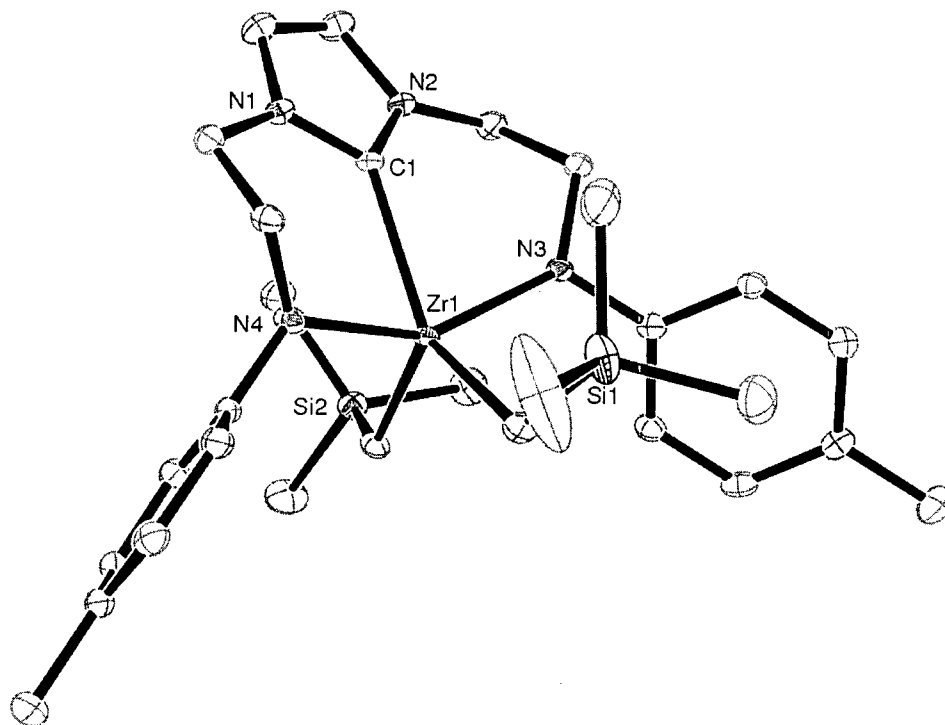
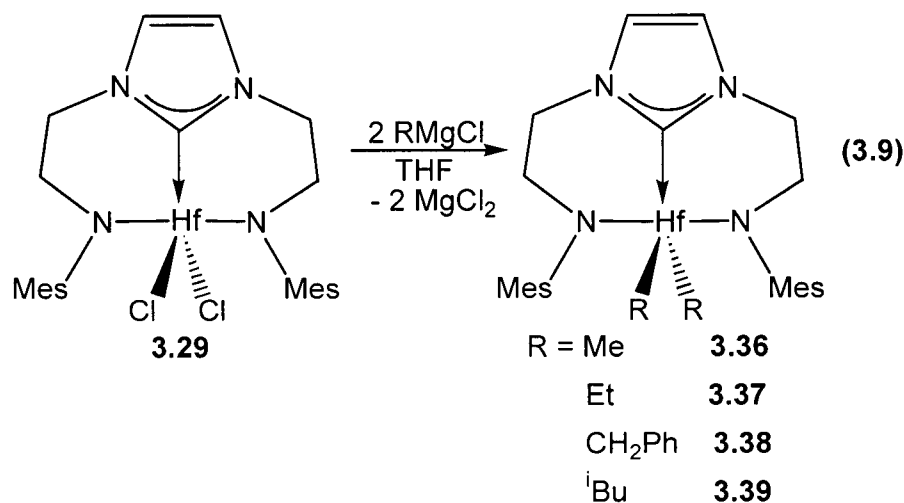


**Figure 3.7.** ORTEP view of  $^{10I}[\text{NCN}]\text{Zr}(\text{CH}_2\text{SiMe}_3)_2$  (**3.31**) depicted with 50% thermal ellipsoids; all hydrogen atoms have been omitted for clarity.

**Table 3.5.** Selected Bond Distances (Å) and Bond Angles ( $^\circ$ ) for  $^{10I}[\text{NCN}]\text{Zr}(\text{CH}_2\text{SiMe}_3)_2$  (**3.31**).

Bond Lengths		Bond Angles	
Zr1-C1	2.415(3)	N3-Zr1-N4	148.73(9)
Zr1-N3	2.173(2)	N3-Zr1-C1	78.23(9)
Zr1-N4	2.135(2)	N4-Zr1-C1	76.27(9)
Zr1-C23	2.238(3)	C24-Zr1-C1	115.29(10)
Zr1-C24	2.254(3)		

Alkylation of the hafnium dichloride **3.29** by Grignard reagents was the optimal method for the synthesis of dialkyl products **3.36-3.39** (Equation 3.9). In solution, the dialkyl products possess  $C_{2v}$  symmetry with diagnostic  $^{13}\text{C}$  and  $^1\text{H}$  resonances in the NMR spectra. For example, the  $^1\text{H}$  NMR spectrum of **3.36** shows equivalent  $^1\text{H}$  resonances for hafnium-methyl groups at 0.12 ppm, in addition to appropriate ethylene spacer, aryl and imidazole resonances.



An ORTEP depiction of the solid state molecular structure of **3.38** is shown in Figure 3.8 and was determined from an X-ray diffraction experiment from crystals grown from Et<sub>2</sub>O. Relevant bond lengths and angles are listed in Table 3.6, and crystallographic details are located in appendix A. The ligand assumes a puckered orientation with respect to a distorted trigonal bipyramidal metal centre. The mesitylamido donors are pseudo *trans* oriented with N4-Hf1-N3 being 151.49(8)°. The hafnium-carbene bond length (2.387(3) Å) is similar to the previously reported zirconium [NCN] complexes as are Hf-N amido (avg. 1.361(3) Å) and Hf-C 2.250(3) Å alkyl bond lengths.

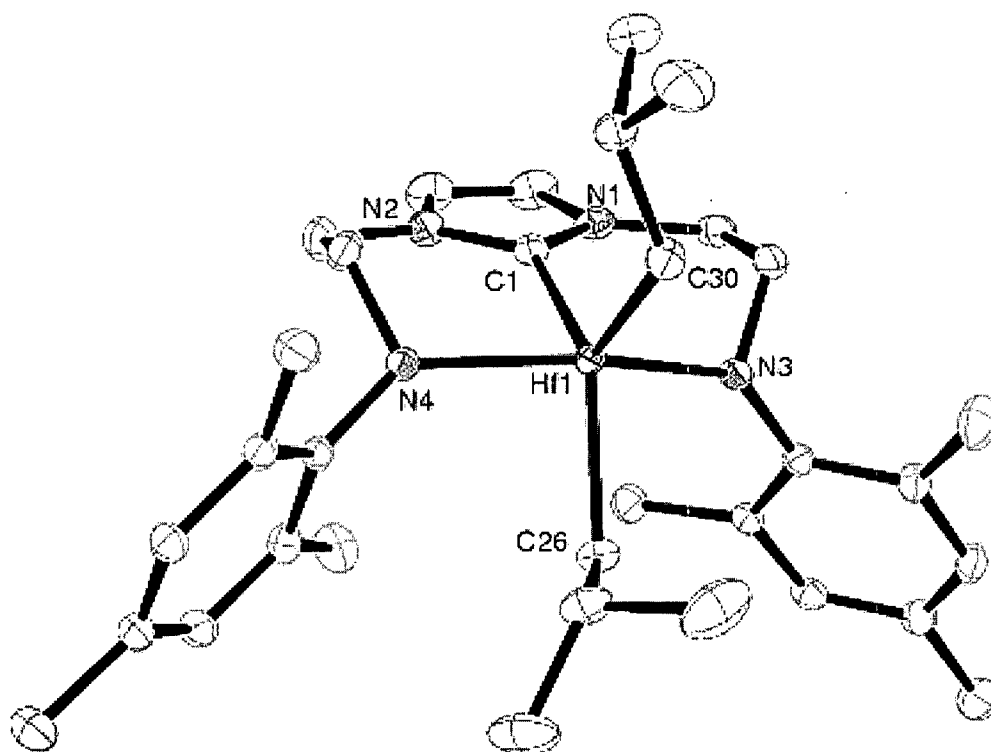


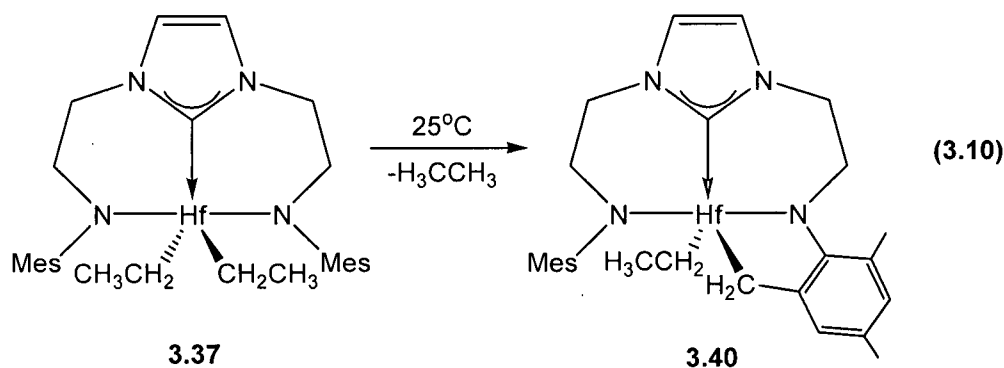
**Figure 3.8.** ORTEP view of  $\text{Mes}[\text{NCN}]\text{Hf}^{\text{t}}\text{Bu}_2$  (**3.39**) depicted with 50% thermal ellipsoids; all hydrogen atoms have been omitted for clarity.

**Table 3.6.** Selected Bond Distances (Å) and Bond Angles ( $^\circ$ ) for  $\text{Mes}[\text{NCN}]\text{Hf}^{\text{t}}\text{Bu}_2$ , (**3.38**).

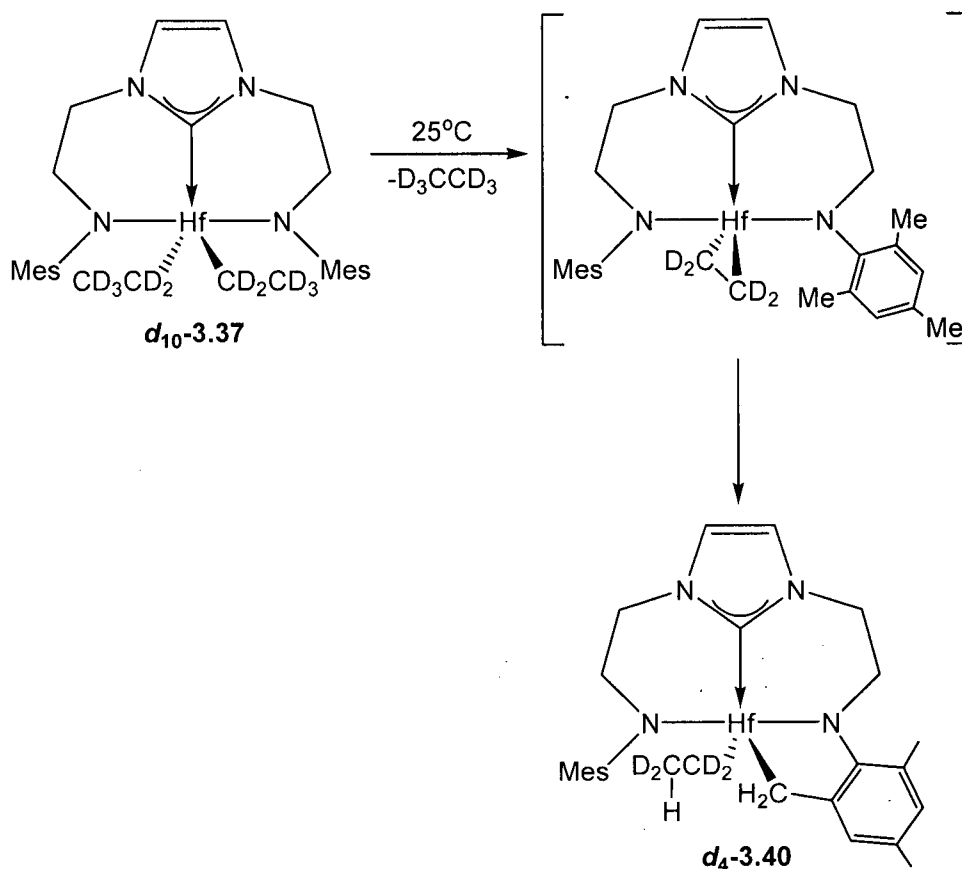
Bond Lengths		Bond Angles	
Hf1-C1	2.385(3)	N3-Hf1-N4	151.49(8)
Hf1-N3	2.101(2)	N3-Hf1-C1	80.30(9)
Hf1-N4	2.126(2)	N4-Hf1-C1	80.30(9)
		C30-Hf1-C1	118.02(9)
		C26-Hf1-C1	134.32(9)

The hafnium dialkyls possess excellent thermal stability. For example, the  $^1\text{H}$  NMR spectrum of **3.39** remains unchanged after heating a  $\text{C}_6\text{D}_6$  solution at  $60^\circ\text{C}$  for several weeks. One exception is the diethyl complex  $\text{Mes}[\text{NCN}]\text{Hf}(\text{CH}_2\text{CH}_3)_2$  (**3.37**), which decomposes at room temperature to give the metallated species **3.40** and ethane (identified by  $^1\text{H}$  NMR spectroscopy) (Equation 3.10). The  $^1\text{H}$  NMR spectrum of **3.40** shows a  $\text{C}_1$  symmetric species in solution with five inequivalent aryl-methyl resonances. There are two doublets at 1.00 and 2.51 ppm indicative of two diastereotopic protons on

the metallated  $-\text{CH}_2$  resonance, consistent with a previously described metallated mesityl group.<sup>35</sup> Furthermore, two multiplets at -0.10 and 0.10 ppm can be assigned to the diastereotopic protons of the remaining  $-\text{HfCH}_2$  group, an observation previously made with a similarly metallated  $-\text{HfCH}_2\text{CH}_3$  system.<sup>36</sup> Further proof of *ortho*-methyl bond activation is observed with a downfield shifted Hf-C  $^{13}\text{C}$  resonance at 72.9 ppm, a chemical shift similar to that found for the benzylic carbons of the hafnium dibenzyl derivative **3.38**.



The decomposition of the deuterated diethyl complex  $^{\text{Mes}}[\text{NCN}]\text{Hf}(\text{CD}_2\text{CD}_3)_2$  ( $d_{10}$ -**3.37**) provides information on the mechanism of this metallation. Decomposition of  $d_{10}$ -**3.37** results in the liberation of  $d_6$ -ethane ( $\text{CD}_3\text{CD}_3$ ; identified by GC-MS), which suggests that  $\beta$ -hydrogen transfer has occurred to give a reactive  $\eta^2$ -ethylene intermediate (Scheme 3.9). This intermediate is not observed in solution but readily undergoes C-H bond activation with a neighboring mesityl-methyl group to give the mono-protonated product,  $d_4$ -**3.40**. The residual  $^1\text{H}$  resonance is observed in the  $^1\text{H}$  NMR spectrum as a broad singlet at 1.5 ppm integrating to one proton. Attempts to trap the  $\eta^2$ -ethylene intermediate with  $\text{PMe}_3$  or pyridine were unsuccessful.



Scheme 3.9.

### 3.5 Conclusions

The synthesis of a potentially dianionic, tridentate NHC ligand system has been described. Incorporation of this ligand on group 4 transition metal was accomplished by protonolysis reactions with  $M(\text{NMe}_2)_4$  and alkane elimination reactions with  $\text{Zr}(\text{CH}_2\text{R})_4$  ( $\text{R} = \text{Ph}, \text{SiMe}_3$ ) to generate bis(amide) and dialkyl derivatives, respectively. The bis(amide) complexes were converted to dichloro or other dialkyl complexes by straightforward procedures. Hafnium dialkyl complexes display excellent stability, with one exception: the hafnium diethyl complex **3.37** undergoes a facile  $\beta$ -hydrogen transfer reaction at room temperature to yield a metallated hafnium species. The addition of strong donors, such as pyridine and  $\text{Me}_2\text{NCH}_2\text{CH}_2\text{NMe}_2$ , to group 4 metal complexes containing the [NCN] ancillary ligand did not show any NHC dissociation. This confirms that the flanking amido donors anchor the NHC to the group 4 metal centre.

The following chapters will investigate the application of these group 4 complexes and extend the coordination chemistry of the [NCN] ligand to include high oxidation state metals such as tantalum.

### 3.6. Experimental Section

#### 3.6.1. General Considerations

Unless otherwise stated, general procedures were performed as described in Section 2.5.1.

#### 3.6.2. Materials and Reagents

All chemicals were purchased from a chemical supplier and used as received. 4-MeC<sub>6</sub>H<sub>4</sub>NHC(O)CH<sub>2</sub>Cl,<sup>37</sup> 2,4,6-Me<sub>3</sub>C<sub>6</sub>H<sub>2</sub>NHC(O)CH<sub>2</sub>Cl,<sup>38</sup> 2,6-<sup>i</sup>Pr<sub>2</sub>C<sub>6</sub>H<sub>3</sub>NHC(O)CH<sub>2</sub>Cl,<sup>39</sup> (H<sub>2</sub>NC<sub>6</sub>H<sub>4</sub>NHCH<sub>2</sub>)<sub>2</sub> (3.14),<sup>15</sup> Zr(CH<sub>2</sub>SiMe<sub>3</sub>)<sub>4</sub><sup>40</sup> and CD<sub>3</sub>CD<sub>2</sub>MgBr<sup>41</sup> were all prepared by literature methods. 2,4,6-Me<sub>3</sub>C<sub>6</sub>H<sub>2</sub>NHCH<sub>2</sub>CH<sub>2</sub>Cl was prepared by a modification of literature procedure.<sup>42</sup>

#### 3.6.3. Synthesis and Characterization of Complexes 3.1 - 3.40

Synthesis of <sup>tol</sup>[NCHN]<sup>CO</sup>H<sub>2</sub>·Cl (3.1), <sup>Mes</sup>[NCHN]<sup>CO</sup>H<sub>2</sub>·Cl (3.2), and <sup>Dipp</sup>[NCHN]<sup>CO</sup>H<sub>2</sub>·Cl (3.3).

The following procedure is representative of the synthesis of 3.1–3.3. To a 500 mL Schlenk flask was added imidazole (1.85 g, 27.1 mmol), 4-MeC<sub>6</sub>H<sub>4</sub>NHC(O)CH<sub>2</sub>Cl (10.0 g, 54.5 mmol), and NEt<sub>3</sub> (8.35 mL, 60.0 mmol). The white slurry was dissolved in 300 mL *p*-dioxane and heated to reflux overnight. After cooling to room temperature, the solvent was removed *in vacuo* and 100 mL CH<sub>2</sub>Cl<sub>2</sub> added to yield a white slurry. This white suspension was filtered and washed with several portions of CH<sub>2</sub>Cl<sub>2</sub> until the washings became clear. The colourless microcrystalline solid was dried *in vacuo* overnight and found to contain one equivalent of CH<sub>2</sub>Cl<sub>2</sub> as determined by the <sup>1</sup>H NMR spectrum. Yield = 7.60 g, 58%.

**3.1:** <sup>1</sup>H NMR (*d*<sub>6</sub>-DMSO): δ 2.24 (s, 6H, -CH<sub>3</sub>), 5.32 (s, 4H, -CH<sub>2</sub>), 7.12 (d, J=8 Hz, 4H, -ArH), 7.52 (d, J=8 Hz, 4H, -ArH), 7.80 (s, 2H, -imidH), 9.24 (s, 1H, -NCHN), 10.90 (s, 2H, -C(O)NH).

$^{13}\text{C}\{^1\text{H}\}$  NMR ( $d_6$ -DMSO):  $\delta$  21.1 (-CH<sub>3</sub>), 55.4 (-CH<sub>2</sub>), 119.5 (-ArC), 125.3 (-imidC), 129.8 (-ArC), 132.7 (-ArC), 134.8 (-ArC), 144.6 (-NCHN), 170.5 (-C(O)NH).

Anal. Calcd for C<sub>22</sub>H<sub>25</sub>Cl<sub>3</sub>N<sub>4</sub>O<sub>2</sub>: C, 54.61; H, 5.21; N, 11.58. Found: C, 54.45; H, 5.02; N, 11.22.

**3.2:**  $^1\text{H}$  NMR ( $d_6$ -DMSO):  $\delta$  2.26 (s, 12H, -*o*-ArCH<sub>3</sub>), 2.36 (s, 6H, -*p*-ArCH<sub>3</sub>), 5.12 (s, 4H, -CH<sub>2</sub>), 7.43 (s, 4H, -ArH), 7.65 (s, 2H, -imidH), 9.10 (s, 1H, -NCHN), 10.54 (s, 2H, -C(O)NH).

$^{13}\text{C}\{^1\text{H}\}$  NMR ( $d_6$ -DMSO):  $\delta$  21.4 (-CH<sub>3</sub>), 22.3 (-CH<sub>3</sub>), 57.2 (-CH<sub>2</sub>), 121.2 (-ArC), 123.8 (-imidC), 130.2 (-ArC), 131.9 (-ArC), 133.7 (-ArC), 145.1 (-NCHN), 172.4 (-C(O)NH).

Anal. Calcd. For C<sub>25</sub>H<sub>31</sub>N<sub>4</sub>O<sub>2</sub>: C, 71.57; H, 7.45; N, 13.35. Found: C, 71.44; H, 7.10; N, 13.46.

**3.3:**  $^1\text{H}$  NMR ( $d_6$ -DMSO):  $\delta$  1.42 (d,  $J = 9$  Hz, 24H, -CH(CH<sub>3</sub>)<sub>3</sub>), 3.78 (sept,  $J = 9$  Hz, 4H, -CH(CH<sub>3</sub>)<sub>2</sub>), 5.24 (s, 4H, -C(O)CH<sub>2</sub>), 7.52-7.60 (m, 6H, -ArH), 7.83 (s, 2H, -imidH), 9.56 (s, 1H, -NCHN), 10.34 (s, 2H, -C(O)NH).

$^{13}\text{C}\{^1\text{H}\}$  NMR ( $d_6$ -DMSO):  $\delta$  18.5 (-CH<sub>3</sub>), 39.5 (-CH), 55.8 (-NCH<sub>2</sub>), 120.8 (-imidC), 124.8 (-ArC), 131.3 (-ArC), 133.4 (-ArC) (-ArC), 139.5 (-ArC), 143.0 (-NCHN), 175.2 (-C(O)NH).

Anal. Calcd. For C<sub>31</sub>H<sub>43</sub>ClN<sub>4</sub>O<sub>2</sub>: C, 69.06; H, 8.04; N, 10.39. Found: C, 69.30; H, 8.31; N, 10.28.

#### Synthesis of $^{101}\text{[NCHN]H}_2\cdot\text{Cl}$ (3.4)

A 250 mL Schlenk flask containing a magnetic stirbar was charged with **3.1**-CH<sub>2</sub>Cl<sub>2</sub> (10.1g, 20.8 mmol) and THF (100 mL) was added. BH<sub>3</sub>-SMe<sub>2</sub> (5.0M in Et<sub>2</sub>O, 18.3 mL) was added, and the white suspension was heated to reflux for 16 h with stirring. Vigorous gas evolution was noted as soon as heating commenced. The solvent was removed under reduced pressure leaving a white residue. Aqueous HCl (1M, 45.7 mL, 45.7 mmol) was added and the suspension refluxed for 1 h. After cooling to room temperature, solid NaOH (7.3 g, 0.18 mol) was added to the clear solution, which caused a white solid to precipitate. Addition of CH<sub>2</sub>Cl<sub>2</sub> (50 mL) caused further precipitation of a white solid. The solid was filtered, washed with CH<sub>2</sub>Cl<sub>2</sub> (3 x 20 mL), and dried in vacuo

overnight to give a white powder. The solid was recrystallized from MeOH giving colorless crystals. Yield = 3.70 g, 48%.

**$^1\text{H}$  NMR (DMSO- $d_6$ ):**  $\delta$  2.13 (s, 6H,  $-\text{CH}_3$ ), 3.40 (t,  $J = 5$  Hz, 4H,  $-\text{CH}_2\text{N}_{\text{Ar}}$ ), 4.28 (t,  $J = 5$  Hz, 4H,  $-\text{CH}_2\text{N}_{\text{imid}}$ ), 5.74 (br s, 2H,  $-\text{NH}$ ), 6.50 (d,  $J = 8$  Hz, 4H,  $-\text{ArH}$ ), 6.88 (d,  $J = 8$  Hz, 4H,  $-\text{ArH}$ ), 7.78 (s, 2H,  $-\text{imidH}$ ), 9.16 (s, 1H,  $-\text{imidH}$ ).

**$^{13}\text{C}\{^1\text{H}\}$  NMR (DMSO- $d_6$ ):**  $\delta$  28.5 ( $-\text{CH}_3$ ), 50.5 ( $-\text{CH}_2\text{N}$ ), 52.1 ( $-\text{CH}_2\text{N}$ ), 115.3 ( $-\text{ArC}$ ), 125.2 ( $-\text{ArC}$ ), 126.1 ( $-\text{ArC}$ ), 130.0 ( $-\text{imidC}$ ), 138.6 ( $-\text{NCHN}$ ), 140.5 ( $-\text{ArC}$ ). EI-MS: 370 [ $\text{M}^+$ ].

Anal. Calcd. for  $\text{C}_{21}\text{H}_{27}\text{ClN}_4$ : C, 68.00; H, 7.34; N, 15.10. Found: C, 67.82; H, 7.10; N, 15.13.

### Synthesis of 2,4,6- $\text{Me}_3\text{C}_6\text{H}_2\text{NHC}(\text{O})\text{CH}_2(\text{imid})$ and 2,6- $^i\text{Pr}_3\text{C}_6\text{H}_2\text{NHC}(\text{O})\text{CH}_2(\text{imid})$

The following procedure is representative of the synthesis of 2,4,6- $\text{Me}_3\text{C}_6\text{H}_2\text{NHC}(\text{O})\text{CH}_2(\text{imid})$  and 2,6- $^i\text{Pr}_3\text{C}_6\text{H}_2\text{NHC}(\text{O})\text{CH}_2(\text{imid})$ . NaH (3.8 g, 158.3 mmol) and imidazole (9.73 g, 142.9 mmol) were combined in DMF (75 mL) and stirred for 30 minutes at 50 °C to give a clear brown solution. 2,4,6- $\text{Me}_3\text{C}_6\text{H}_2\text{NHC}(\text{O})\text{CH}_2\text{Cl}$  (28.2 g, 142.9 mmol) was added portionwise over a period of 30 minutes to give an opaque solution. After stirring for 12 hours, water (20 mL) was added and all solvents were removed under reduced pressure. The resulting brown residue was acidified with 2M HCl (250 mL) and washed with  $\text{Et}_2\text{O}$  (3 x 150 mL). The aqueous solution was made basic with excess NaOH and extracted with  $\text{CH}_2\text{Cl}_2$  (3 x 250 mL). The  $\text{CH}_2\text{Cl}_2$  was removed to give a white crystalline material, which was washed with hexanes. Yield = 28.0 g, 86%.

**2,4,6- $\text{Me}_3\text{C}_6\text{H}_2\text{NHC}(\text{O})\text{CH}_2(\text{imid})$ :**  **$^1\text{H}$  NMR ( $\text{CDCl}_3$ ):**  $\delta$  2.12 (s, 6H,  $-\text{o-ArCH}_3$ ), 2.25 (s, 3H,  $-\text{p-ArCH}_3$ ), 4.75 (s, 2H,  $-\text{NCH}_2$ ), 6.80 (s, 2H,  $-\text{ArH}$ ), 7.05 (s, 1H,  $-\text{imidH}$ ), 7.10 (s, 1H,  $-\text{imidH}$ ), 7.60 (s, 1H,  $-\text{NCHN}$ ).

**$^{13}\text{C}\{^1\text{H}\}$  NMR ( $\text{CDCl}_3$ ):**  $\delta$  18.2 ( $-\text{CH}_3$ ), 20.5 ( $-\text{CH}_3$ ), 57.0 ( $-\text{NCH}_2$ ), 123.0 ( $-\text{imidC}$ ), 123.2 ( $-\text{imidC}$ ), 128.5 ( $-\text{ArC}$ ), 130.5 ( $-\text{ArC}$ ), 130.7 ( $-\text{ArC}$ ), 135.1 ( $-\text{NCHN}$ ), 140.1 ( $-\text{ArC}$ ), 178.1 ( $-\text{C}(\text{O})$ ).

Anal. Calc. for  $\text{C}_{14}\text{H}_{17}\text{N}_3\text{O}$ : C, 69.11; H, 7.04; N, 17.27. Found: C, 69.00; H, 7.01; N, 17.10.

**2,6-<sup>1</sup>Pr<sub>3</sub>C<sub>6</sub>H<sub>2</sub>NHC(O)CH<sub>2</sub>(imid):** <sup>1</sup>H NMR (CDCl<sub>3</sub>): δ 1.16 (d, J=7 Hz, -CH(CH<sub>3</sub>)<sub>2</sub>), 2.86 (sept, J=7 Hz, -CH(CH<sub>3</sub>)<sub>2</sub>), 4.87 (s, 2H, -C(O)CH<sub>2</sub>), 7.10 (s, 1H, -imidH), 7.15 (d, J=8 Hz, 2H, -ArH), 7.21 (s, 1H, -imidH), 7.29 (t, J=8 Hz, 1H, -ArH), 7.64 (s, 1H, -imidH).

<sup>13</sup>C{<sup>1</sup>H} NMR (CDCl<sub>3</sub>): δ 21.3 (-CH<sub>3</sub>), 36.4 (-CH), 58.7 (-NCH<sub>2</sub>), 124.1 (-imidC), 124.6 (-imidC), 127.2 (-ArC), 130.9 (-ArC), 131.8 (-ArC), 137.1 (-NCHN), 142.3 (-ArC), 174.7 (-C(O)).

Anal. Calcd. for C<sub>17</sub>H<sub>23</sub>N<sub>3</sub>O C, 71.55; H, 8.12; N, 14.72. Found: C, 71.23; H, 7.93; N, 14.55.

#### Synthesis of 2,4,6-Me<sub>3</sub>C<sub>6</sub>H<sub>2</sub>NHCH<sub>2</sub>CH<sub>2</sub>(imid) and 2,6-<sup>1</sup>Pr<sub>3</sub>C<sub>6</sub>H<sub>2</sub>HCH<sub>2</sub>CH<sub>2</sub>(imid)

The following procedure is representative of the synthesis of 2,4,6-Me<sub>3</sub>C<sub>6</sub>H<sub>2</sub>NHCH<sub>2</sub>CH<sub>2</sub>(imid) and 2,6-<sup>1</sup>Pr<sub>3</sub>C<sub>6</sub>H<sub>2</sub>HCH<sub>2</sub>CH<sub>2</sub>(imid). 2,4,6-Me<sub>3</sub>C<sub>6</sub>H<sub>2</sub>NHCOCH<sub>2</sub>(imidazole) (13.0 g, 56.8 mmol) and BH<sub>3</sub>-SMe<sub>2</sub> (25.0 mL, 125.0 mmol, 5.0 M in Et<sub>2</sub>O) were combined in THF (500 ml) and refluxed overnight. The THF was removed under reduced pressure and 2 M HCl (63 mL, 2.2 equivalents) was added to the white residue. The solution was made basic with excess NaOH (8 equivalents) and extracted with CH<sub>2</sub>Cl<sub>2</sub> (3 x 250 mL). The CH<sub>2</sub>Cl<sub>2</sub> was removed, and the clear oil recrystallized with boiling hexanes. Yield = 9.8 g, 80%.

**2,4,6-Me<sub>3</sub>C<sub>6</sub>H<sub>2</sub>NHCH<sub>2</sub>CH<sub>2</sub>(imid):** <sup>1</sup>H NMR (d<sub>6</sub>-DMSO): δ 2.03 (s, 6H, -o-ArCH<sub>3</sub>), 2.15 (s, 3H, -p-ArCH<sub>3</sub>), 3.19 (t, J = 8 Hz, -NCH<sub>2</sub>), 3.68 (t, J = 8 Hz, 1H, -NH), 4.13 (t, J=8 Hz, -NCH<sub>2</sub>), 6.80 (s, 2H, -ArH), 6.85 (s, 1H, -imidH), 7.20 (s, 1H, -imidH), 7.64 (s, 1H, -NCHN).

<sup>13</sup>C{<sup>1</sup>H} NMR (d<sub>6</sub>-DMSO): δ 18.9 (-CH<sub>3</sub>), 22.1 (-CH<sub>3</sub>), 48.4 (-NCH<sub>2</sub>), 48.9 (-NCH<sub>2</sub>), 121.0 (-imidC), 121.6 (-imidC), 126.4 (-ArC), 128.8 (-ArC), 129.0 (-ArC), 134.2 (-NCN), 142.1 (-ArC).

Anal. Calc. for C<sub>14</sub>H<sub>19</sub>N<sub>3</sub>: C, 73.33; H, 8.35; N, 18.32. Found: C, 73.05; H, 8.09; N, 18.15.

**2,6-<sup>1</sup>Pr<sub>3</sub>C<sub>6</sub>H<sub>2</sub>HCH<sub>2</sub>CH<sub>2</sub>(imid):** <sup>1</sup>H NMR (d<sub>6</sub>-DMSO): δ 1.10 (d, J=7 Hz, -CH(CH<sub>3</sub>)<sub>2</sub>), 2.95 (sept, J = 7 Hz, -CH(CH<sub>3</sub>)<sub>2</sub>), 3.03 (t, J = 8 Hz, -N<sub>Ar</sub>CH<sub>2</sub>), 3.98 (t, J = 8 Hz, -

$N_{\text{imid}}CH_2$ ), 7.02 (s, 1H, -imidH), 7.11 (d,  $J=8$  Hz, 2H, -ArH), 7.24 (s, 1H, -imidH), 7.35 (t,  $J=8$  Hz, 1H, -ArH), 7.80 (s, 1H, -imidH).

$^{13}C\{^1H\}$  NMR ( $d_6$ -DMSO):  $\delta$  22.5 (-CH<sub>3</sub>), 29.6 (-CH), 50.7 (-NCH<sub>2</sub>), 51.3 (-NCH<sub>2</sub>), 118.7 (-imidC), 120.2 (-imidC), 121.3 (-ArC), 128.3 (-NCN), 129.4 (-ArC), 134.8 (-ArC), 138.4 (-ArC).

Anal. Calcd. for C<sub>17</sub>H<sub>25</sub>N<sub>3</sub> C, 75.23; H, 9.28; N, 15.48. Found: C, 74.97; H, 9.45; N, 15.33.

### Synthesis of 2,6-<sup>i</sup>Pr<sub>2</sub>C<sub>6</sub>H<sub>3</sub>NHCH<sub>2</sub>CH<sub>2</sub>Cl

2,6-<sup>i</sup>Pr<sub>2</sub>C<sub>6</sub>H<sub>3</sub>NHC(O)CH<sub>2</sub>Cl (10 g, 35.1 mmol) and BH<sub>3</sub>-SMe<sub>2</sub> (15.4 mL, 77.1 mmol, 5.0 M in Et<sub>2</sub>O) were dissolved in THF (250 ml) in a 500 mL Schlenk flask and refluxed overnight. The THF was removed under reduced pressure and 2 M HCl (38.6 mL, 2.2 equivalents) was added to the white residue. The solution was made basic with excess NaOH (14.04 g, 8 equivalents) and extracted with CH<sub>2</sub>Cl<sub>2</sub> (3 x 50 mL). The CH<sub>2</sub>Cl<sub>2</sub> was removed and the clear oil was extracted with pentane. The solvent was removed to yield a colorless oil that was used without further purification. Yield = 8.19 g, 86 %.

$^1H$  NMR (CDCl<sub>3</sub>):  $\delta$  1.23 (d,  $J = 7$  Hz, 12H, -CH(CH<sub>3</sub>)<sub>2</sub>), 3.19 (t,  $J = 8$  Hz, 2H, -NCH<sub>2</sub>), 3.18 (sept,  $J = 7$  Hz, 2H, -CH(CH<sub>3</sub>)<sub>2</sub>), 3.73 (t,  $J = 8$  Hz, 2H, -CH<sub>2</sub>Cl), 7.08 (m, 3H, -ArH).

$^{13}C\{^1H\}$  NMR (CDCl<sub>3</sub>): 20.3 (-CH<sub>3</sub>), 30.6 (-CH), 45.8 (-CH<sub>2</sub>Cl), 51.3 (-NCH<sub>2</sub>), 125.7 (-ArC), 128.9 (-ArC), 130.1 (-ArC), 137.9 (-ArC).

### Synthesis of <sup>Mes</sup>[NCHN]<sup>Cl</sup> (3.5) and <sup>Dipp</sup>[NCHN]<sup>Cl</sup> (3.6)

The following procedure is representative of the synthesis of **3.5** and **3.6**. 2,4,6-Me<sub>3</sub>C<sub>6</sub>H<sub>2</sub>NHCH<sub>2</sub>CH<sub>2</sub>Cl (6.0 g, 30.4 mmol) and 2,4,6-Me<sub>3</sub>C<sub>6</sub>H<sub>2</sub>NHCH<sub>2</sub>CH<sub>2</sub>(imid) (6.5 g, 30.4 mmol) were combined and stirred at 150 °C for 2 hours. The resulting white solid was washed with THF (50 mL) and filtered to give a white crystalline powder. Yield = 11.29 g, 87%. Recrystallization with boiling acetonitrile gave long colorless crystals.

**3.5:  $^1\text{H}$  NMR ( $d_6$ -DMSO):**  $\delta$  2.01 (s, 12H,  $-o\text{-ArCH}_3$ ), 2.12 (s, 6H,  $-p\text{-ArCH}_3$ ), 3.15 (q,  $J = 8$  Hz, 4H,  $-\text{N}_{\text{Ar}}\text{CH}_2$ ), 3.92 (t,  $J = 8$  Hz, 1H,  $-\text{NH}$ ), 4.40 (t,  $J = 8$  Hz, 4H,  $-\text{N}_{\text{imid}}\text{CH}_2$ ), 6.81 (s, 4H,  $-\text{ArH}$ ), 7.88 (s, 2H,  $-\text{imidH}$ ), 9.35 (s, 1H,  $-\text{NCHN}$ ).

**$^{13}\text{C}\{^1\text{H}\}$  NMR ( $d_6$ -DMSO):**  $\delta$  17.8 ( $-\text{CH}_3$ ), 20.2 ( $-\text{CH}_3$ ), 47.2 ( $-\text{NCH}_2$ ), 49.2 ( $-\text{NCH}_2$ ), 122.6 ( $-\text{imidC}$ ), 129.0 ( $-\text{ArC}$ ), 130.2 ( $-\text{ArC}$ ), 130.7 ( $-\text{ArC}$ ), 137.2 ( $-\text{NCHN}$ ), 142.4 ( $-\text{ArC}$ ).  
Anal. Calcd. for  $\text{C}_{25}\text{H}_{35}\text{ClN}_4$ : C, 70.32; H, 8.26; N, 13.12. Found: C, 70.15; H, 8.13; N, 13.02.

**3.6:  $^1\text{H}$  NMR ( $d_6$ -DMSO):**  $\delta$  1.19 (d,  $J = 7$  Hz,  $-\text{CH}(\text{CH}_3)_2$ ), 2.92 (sept,  $J = 7$  Hz,  $-\text{CH}(\text{CH}_3)_2$ ), 3.44 (q,  $J = 8$  Hz, 4H,  $-\text{N}_{\text{Ar}}\text{CH}_2$ ), 3.89 (t,  $J = 8$  Hz, 1H,  $-\text{NH}$ ), 4.90 (t,  $J = 8$  Hz, 4H,  $-\text{N}_{\text{imid}}\text{CH}_2$ ), 7.01 (m, 6H,  $-\text{ArH}$ ), 7.76 (s, 2H,  $-\text{imidH}$ ), 9.16 (s, 1H,  $-\text{NCHN}$ ).

**$^{13}\text{C}\{^1\text{H}\}$  NMR ( $d_6$ -DMSO):**  $\delta$  20.2 ( $\text{CH}_3$ ), 33.5 ( $-\text{CH}$ ), 45.9 ( $-\text{NCH}_2$ ), 50.3 ( $-\text{NCH}_2$ ), 121.5 ( $-\text{imidC}$ ), 127.6 ( $-\text{ArC}$ ), 129.7 ( $-\text{ArC}$ ), 131.6 ( $-\text{ArC}$ ), 139.5 ( $-\text{NCHN}$ ), 143.1 ( $-\text{ArC}$ ).  
Anal. Calcd. for  $\text{C}_{31}\text{H}_{47}\text{ClN}_4$ : C, 72.84; H, 9.27; N, 10.96. Found: C, 72.78; H, 9.55; N, 10.74.

### Synthesis of $^{\text{tol}}[\text{NCN}]\text{H}_2$ (3.7) and $^{\text{Mes}}[\text{NCN}]\text{H}_2$ (3.8)

The following procedure is representative of the synthesis of **3.7** and **3.8**. The following procedure was used in the synthesis of **3.9**; however, the product was not isolated. A THF solution (10 mL) of  $\text{KN}(\text{SiMe}_3)_2$  (664 mg, 3.3 mmol) was slowly added dropwise to **3.5** (1.24 g, 3.3 mmol) dissolved in 40 mL THF, creating a slightly yellow suspension. The suspension was stirred for  $\frac{1}{2}$  hr and the solvent removed in vacuo. The pale yellow residue was extracted with toluene (20 mL) and the solution filtered through celite. Removal of the solvent yielded a white solid which was washed several times with hexane and dried in vacuo. Yield = 1.10 g, 100%.

**3.7:  $^1\text{H}$  NMR ( $\text{C}_6\text{D}_6$ ):**  $\delta$  2.13 (s, 6H,  $-\text{CH}_3$ ), 3.40 (t,  $J = \text{Hz}$ , 4H,  $-\text{CH}_2\text{N}$ ), 4.28 (t,  $J = \text{Hz}$ , 4H,  $-\text{CH}_2\text{N}$ ), 5.74 (br s, 2H,  $-\text{NH}$ ), 6.25 (s, 2H,  $-\text{imidH}$ ), 6.53 (d,  $J = \text{Hz}$ , 4H,  $-\text{ArH}$ ), 6.85 (d,  $J = \text{Hz}$ , 4H,  $-\text{ArH}$ ).

**$^{13}\text{C}\{^1\text{H}\}$  NMR ( $\text{C}_6\text{D}_6$ ):**  $\delta$  22.5 ( $-\text{CH}_3$ ), 46.1 ( $-\text{CH}_2\text{N}$ ), 50.9 ( $-\text{CH}_2\text{N}$ ), 114.5 ( $-\text{ArC}$ ), 118.9 ( $-\text{imidC}$ ), 120.6 ( $-\text{ArC}$ ), 130.7 ( $-\text{ArC}$ ), 149.8 ( $-\text{ArC}$ ), 211.4 ( $-\text{NCN}$ ).

Anal. Calcd. for  $\text{C}_{21}\text{H}_{26}\text{N}_4$ : C, 75.41; H, 7.84; N, 16.75. Found: C, 75.20; H, 7.49; N, 16.88.

**3.8:**  $^1\text{H}$  NMR ( $\text{C}_6\text{D}_6$ ):  $\delta$  2.35 (s, 6H, *-p*-ArCH<sub>3</sub>), 2.40 (s, 12H, *-o*-ArCH<sub>3</sub>), 3.22 (q, J = 8Hz, 4H, -NCH<sub>2</sub>), 3.76 (t, J = 8Hz, 4H, -NCH<sub>2</sub>), 4.15 (t, J = 8Hz, 1H, -NH), 6.30 (s, 2H, -imidH), 6.82 (s, 4H, -ArH).

$^{13}\text{C}\{^1\text{H}\}$  NMR ( $\text{C}_6\text{D}_6$ ):  $\delta$  20.0 (*-o*-CH<sub>3</sub>), 24.5 (*-p*-CH<sub>3</sub>), 48.5 (-NCH<sub>2</sub>), 49.1 (-NCH<sub>2</sub>), 121.7 (-imidC), 126.9 (-ArC), 127.5 (-ArC), 130.1 (-ArC), 145.0 (-ArC), 215.0 (-NCN).

Anal. Calc. for C<sub>25</sub>H<sub>34</sub>N<sub>4</sub>: C, 76.88; H, 8.77; N, 14.35. Found: C, 76.54; H, 8.41; N, 14.28

### Synthesis of Li<sub>2</sub><sup>tol</sup>[NCN] (3.10) and Li<sub>2</sub><sup>Mes</sup>[NCN] (3.11),

The following procedure is representative of the synthesis of **3.10** and **3.11**. A toluene solution of **3.7** (530 mg, 1.6 mmol) was cooled to -30°C and 2.0 mL of 1.6M *n*-BuLi (3.2 mmol) was added slowly dropwise. The solution immediately darkened after the first equivalent was added and a white precipitate formed after addition of the second equivalent of base was complete. The white suspension was allowed to warm slowly to room temperature where it is stirred overnight. Filtration yielded a white powder which was washed with several portions of toluene. Yield = 549 mg, 99% yield.

**3.10:**  $^1\text{H}$  NMR ( $\text{C}_5\text{D}_5\text{N}$ ):  $\delta$  2.29 (s, 6H, -ArCH<sub>3</sub>), 3.62(m, 4H, -NCH<sub>2</sub>), 4.13 (m, 4H, -NCH<sub>2</sub>), 6.69 (s, 4H, -ArH), 7.00 (s, 2H, -imidH).

$^{13}\text{C}\{^1\text{H}\}$  NMR ( $\text{C}_5\text{D}_5\text{N}$ ):  $\delta$  21.4 (-CH<sub>3</sub>), 45.6 (-NCH<sub>2</sub>), 47.2 (-NCH<sub>2</sub>), 117.9 (-ArC), 120.5 (-ArC), 122.9 (-imidC), 126.9 (-ArC), 148.6 (-ArC), 189.9 (-NCN).

$^7\text{Li}$  NMR ( $\text{C}_5\text{H}_5\text{N}$ ):  $\delta$  2.86.

Añal. Calcd. for C<sub>21</sub>H<sub>24</sub>Li<sub>2</sub>N<sub>4</sub>: C, 72.83; H, 6.98; N, 16.18; Found: C, 72.79; H, 6.78; N, 16.01.

**3.11:**  $^1\text{H}$  NMR ( $\text{C}_5\text{D}_5\text{N}$ ):  $\delta$  2.35 (s, 6H, *-p*-ArCH<sub>3</sub>), 2.46 (s, 6H, *-o*-ArCH<sub>3</sub>), 4.08 (m, 4H, -NCH<sub>2</sub>), 4.18 (m, 4H, -NCH<sub>2</sub>), 6.81 (s, 4H, -ArH), 6.91 (s, 2H, -imidH).

$^{13}\text{C}\{^1\text{H}\}$  NMR ( $\text{C}_5\text{D}_5\text{N}$ ):  $\delta$  20.4 (-CH<sub>3</sub>), 21.3 (-CH<sub>3</sub>), 46.8 (-NCH<sub>2</sub>), 47.8 (-NCH<sub>2</sub>), 119.5 (-ArC), 119.9 (-ArC), 123.6 (-imidC), 127.9 (-ArC), 149.5 (-ArC), 190.2 (-NCN).

$^7\text{Li}$  NMR ( $\text{C}_5\text{D}_5\text{N}$ ):  $\delta$  2.88.

Anal. Calcd. for C<sub>25</sub>H<sub>32</sub>Li<sub>2</sub>N<sub>4</sub>: C, 74.61; H, 8.01; N, 13.92; Found: C, 74.55; H, 7.95; N, 13.86.

### Synthesis of (2,4,6-Me<sub>3</sub>C<sub>6</sub>H<sub>2</sub>NHC<sub>6</sub>H<sub>4</sub>NHCH<sub>2</sub>)<sub>2</sub> (3.15)

A 100 mL Schlenk was charged with Pd<sub>2</sub>(dba)<sub>3</sub> (151 mg, 0.16 mmol), *rac*-BINAP (103 mg, 0.16 mmol), NaO<sup>t</sup>Bu (1.11 g, 11.6 mmol), **3.14** (1.0 g, 4.1 mmol), mesityl bromide (1.81 g, 9.0 mmol) and 50 mL of toluene. The mixture was slowly warmed to 100°C and stirred overnight. The dark brown suspension was filtered through Celite and the solvent removed to yield a dark red residue. Pentane (10 mL) was added to yield a brown powder that was further purified by dissolving the solid in toluene and filtering through a silica plug. Yield = 1.69 g, 86%.

<sup>1</sup>H NMR (CDCl<sub>3</sub>): δ 2.03 (s, 12H, -*o*-ArCH<sub>3</sub>), 2.27 (s, 12H, -*p*-ArCH<sub>3</sub>), 3.56 (s, 4H, -NCH<sub>2</sub>), 4.60 (br s, 2H, -NH), 6.22 (d, J = 8 Hz, 2H, -ArH), 6.62 (t, J = 8 Hz, 2H, -ArH), 6.80-6.86 (m, 4H, -ArH).

<sup>13</sup>C{<sup>1</sup>H} NMR (CDCl<sub>3</sub>): δ 18.9 (-CH<sub>3</sub>), 20.1 (-CH<sub>3</sub>), 52.2 (-NCH<sub>2</sub>), 116.5 (-ArC), 117.9 (-ArC), 118.5 (-ArC), 120.3 (-ArC), 125.6 (-ArC), 127.9 (-ArC), 130.4 (-ArC), 135.2 (-ArC).

Satisfactory elemental analysis was not obtained.

### Synthesis of Asymmetrical Imidazolinium tetrafluoroborate (3.16)

A 25 mL Schlenk flask was charged with **3.15** (980 mg, 2.0 mmol), NH<sub>4</sub>BF<sub>4</sub> (215 mg, 2.0 mmol), and HC(OEt)<sub>3</sub> (0.31 mL, 2.0 mmol) and slowly heated to 120°C. The slurry was stirred at this temperature for 1 hr, then cooled to room temperature. THF was added to give a white suspension, which was filtered and washed with several portions of THF. The white solid was dried *in vacuo* overnight. Yield = 968 mg, 84 %.

<sup>1</sup>H NMR (d<sub>6</sub>-DMSO): δ 1.87 (s, 6H, -*p*-ArCH<sub>3</sub>), 1.89 (s, 6H, -*p*-ArCH<sub>3</sub>), 2.21 (s, 3H, -*o*-ArCH<sub>3</sub>), 2.37 (s, 6H, -*o*-ArCH<sub>3</sub>), 3.81 (m, 2H, -NCH<sub>2</sub>), 4.89 (m, 2H, -NCH<sub>2</sub>), 5.04 (m, 1H, -NH), 5.71 (m, 1H, -NH), 5.82 (m, 1H, -ArH), 6.40 (m, 1H, -ArH), 6.55 (m, 1H, -ArH), 6.61 (m, 1H, -ArH), 6.87 (s, 2H, -ArH), 7.20 (m, 2H, -ArH), 7.39 (m, 1H, -ArH), 7.66 (m, 1H, -ArH), 7.76 (m, 1H, -ArH), 8.26 (m, 1H, -ArH), 10.04 (s, 1H, -NCHN).

<sup>13</sup>C{<sup>1</sup>H} NMR (d<sub>6</sub>-DMSO): δ 19.6 (-CH<sub>3</sub>), 20.4 (-CH<sub>3</sub>), 20.9 (-CH<sub>3</sub>), 21.8 (-CH<sub>3</sub>), 51.3 (-NCH<sub>2</sub>), 55.0 (-NCH<sub>2</sub>), 113.5 (-ArC), 115.8 (-ArC), 117.9 (-ArC), 118.3 (-ArC), 118.9 (-ArC), 119.5 (-ArC), 120.4 (-ArC), 120.9 (-ArC), 123.3 (-ArC), 124.7 (-ArC), 125.2 (-

ArC), 126.3 (-ArC), 127.5 (-ArC), 128.5 (-ArC), 129.3 (-ArC), 131.6 (-ArC), 132.7 (-ArC), 133.6 (-ArC), 135.2 (-ArC), 137.2 (-ArC), 143.4 (-NCHN).

Satisfactory elemental analysis was not obtained.

**Synthesis of  $\text{Ar}(\text{NCN})\text{M}(\text{NMe}_2)_2$  [(M=Zr, Ar=tol, R=Et (3.17); M=Zr, Ar=Mes, R=Me (3.18); M=Zr, Ar=Dipp, R=Me (3.19); M=Ti, Ar=tol, R=Me (3.20); M=Hf, Ar=Mes, R=Me (3.21)]**

The following procedure is representative of the synthesis of **3.17–3.21**. In the case of **3.19**, the carbene **3.9** was generated in situ and used as a THF solution. A cooled ( $-30^\circ\text{C}$ ) THF (10 mL) solution of  $\text{Hf}(\text{NMe}_2)_4$  (415 mg, 1.17 mmol) was slowly added dropwise to **3.8** dissolved in THF (20 mL). The mixture was warmed to room temperature gradually and stirred overnight. After the solvent was removed *in vacuo* and toluene (15 mL) added, the solution was filtered and the solvent removed to give a pale orange solid, that was recrystallized with  $\text{Et}_2\text{O}$ /hexanes at  $-30^\circ\text{C}$  to give a white powder. Yield = 662 mg, 85%.

**3.17:**  $^1\text{H NMR}$  ( $\text{C}_6\text{D}_6$ ):  $\delta$  1.10 (t,  $J=8$  Hz, 12H,  $-\text{NCH}_2\text{CH}_3$ ), 2.35 (s, 6H,  $-\text{CH}_3$ ), 3.40 (m, 4H,  $-\text{CH}_2\text{N}$ ), 3.44 (q,  $J = 8$  Hz, 8H,  $-\text{NCH}_2\text{CH}_3$ ), 3.92 (m, 4H,  $-\text{CH}_2\text{N}$ ), 5.80 (s, 2H,  $-\text{imidH}$ ), 7.10 (d,  $J=8$  Hz, 4H,  $-\text{ArH}$ ), 7.15 (d,  $J = 8\text{Hz}$ , 4H,  $-\text{ArH}$ ).

$^{13}\text{C}\{^1\text{H}\}$  NMR ( $\text{C}_6\text{D}_6$ ):  $\delta$  17.5 ( $-\text{CH}_2\text{CH}_3$ ), 23.0 ( $-\text{CH}_3$ ), 50.7 ( $-\text{CH}_2\text{N}$ ), 51.2 ( $-\text{CH}_2\text{N}$ ), 53.4 ( $-\text{ZrNCH}_2$ ), 119.9 ( $-\text{ArC}$ ), 120.6 ( $-\text{imidC}$ ), 127.2 ( $-\text{ArC}$ ), 130.1 ( $-\text{ArC}$ ), 157.6 ( $-\text{ArC}$ ), 188.8 ( $-\text{NCN}$ ).

Anal. Calcd. for  $\text{C}_{29}\text{H}_{44}\text{N}_6\text{Zr}$ : C, 61.33; H, 7.81; N, 14.80. Found: C, 61.11; H, 7.74; N, 14.56.

**3.18:**  $^1\text{H NMR}$  ( $\text{C}_6\text{D}_6$ ):  $\delta$  2.21 (s, 6H,  $-\text{p-ArCH}_3$ ), 2.40 (s, 12H,  $-\text{o-ArCH}_3$ ), 2.67 (s, 12H,  $-\text{NMe}_2$ ), 3.34 (m, 4H,  $-\text{NCH}_2$ ), 3.61 (m, 4H,  $-\text{NCH}_2$ ), 6.02 (s, 2H,  $-\text{imidH}$ ), 6.96 (s, 4H,  $-\text{ArH}$ ).

$^{13}\text{C}\{^1\text{H}\}$  NMR ( $\text{C}_6\text{D}_6$ ):  $\delta$  19.6 ( $-\text{o-CH}_3$ ), 23.4 ( $-\text{p-CH}_3$ ), 45.6 ( $-\text{NCH}_3$ ), 48.8 ( $-\text{NCH}_2$ ), 49.2 ( $-\text{NCH}_2$ ), 122.4 ( $-\text{imidC}$ ), 130.5 ( $-\text{ArC}$ ), 132.3 ( $-\text{ArC}$ ), 132.9 ( $-\text{ArC}$ ), 140.2 ( $-\text{ArC}$ ), 190.9 ( $-\text{ZrC}_{\text{carbene}}$ ).

Anal. Calc. for  $\text{C}_{29}\text{H}_{44}\text{N}_6\text{Zr}$ : C, 61.33; H, 7.81; N, 14.80. Found: C, 61.20; H, 7.58; N, 14.45.

**3.19:**  $^1\text{H NMR}$  ( $\text{C}_6\text{D}_6$ ):  $\delta$  1.20 (d,  $J = 8$  Hz, 12H,  $-\text{CH}(\text{CH}_3)_2$ ), 1.35 (d,  $J = 8$  Hz, 12H,  $-\text{CH}(\text{CH}_3)_2$ ), 2.43 (s, 12H,  $-\text{N}(\text{CH}_3)_2$ ), 3.24 (sept,  $J = 8$  Hz, 4H,  $-\text{CH}(\text{CH}_3)_2$ ), 3.86 (m, 4H,  $-\text{NCH}_2$ ), 4.13 (m, 4H,  $-\text{NCH}_2$ ), 5.98 (s, 2H,  $-\text{imidH}$ ), 6.98-7.03 (m, 6H,  $-\text{ArH}$ ).

$^{13}\text{C}\{^1\text{H}\}$  NMR ( $\text{C}_6\text{D}_6$ ):  $\delta$  21.4 ( $\text{CH}_3$ ), 31.6 ( $-\text{CH}$ ), 46.7 ( $-\text{NCH}_3$ ), 49.6 ( $-\text{NCH}_2$ ), 51.5 ( $-\text{NCH}_2$ ), 119.9 ( $-\text{imidC}$ ), 121.2 ( $-\text{ArC}$ ), 125.8 ( $-\text{ArC}$ ), 130.4 ( $-\text{ArC}$ ), 140.2 ( $-\text{ArC}$ ), 192.1 ( $-\text{NCN}$ ).

Anal. Calc. for  $\text{C}_{35}\text{H}_{56}\text{N}_6\text{Zr}$ : C, 64.47; H, 8.66; N, 12.89. Found: C, 64.37; H, 8.83; N, 12.75.

**3.20:**  $^1\text{H NMR}$  ( $\text{C}_6\text{D}_6$ ):  $\delta$  2.38 (s, 6H,  $-\text{CH}_3$ ), 2.65 (s, 12H,  $-\text{N}(\text{CH}_3)_2$ ), 3.45 (m, 4H,  $-\text{CH}_2\text{N}$ ), 4.08 (m, 4H,  $-\text{CH}_2\text{N}$ ), 5.78 (s, 2H,  $-\text{imidH}$ ), 7.11 (d,  $J=8$  Hz, 4H,  $-\text{ArH}$ ), 7.20 (d,  $J = 8$  Hz, 4H,  $-\text{ArH}$ ).

$^{13}\text{C}\{^1\text{H}\}$  NMR ( $\text{C}_6\text{D}_6$ ):  $\delta$  24.3 ( $-\text{CH}_3$ ), 49.6 ( $-\text{CH}_2\text{N}$ ), 51.7 ( $-\text{NCH}_3$ ), 52.4 ( $-\text{CH}_2\text{N}$ ), 118.4 ( $-\text{ArC}$ ), 120.3 ( $-\text{imidC}$ ), 127.2 ( $-\text{ArC}$ ), 132.3 ( $-\text{ArC}$ ), 155.7 ( $-\text{ArC}$ ), 187.2 ( $-\text{NCN}$ ).

Anal. Calc. for  $\text{C}_{25}\text{H}_{36}\text{N}_6\text{Ti}$ : C, 64.10; H, 7.75; N, 17.94. Found: C, 63.98; H, 7.88; N, 17.84.

**3.21:**  $^1\text{H NMR}$  ( $\text{C}_6\text{D}_6$ ):  $\delta$  2.19 (s, 6H,  $-\text{p-ArCH}_3$ ), 2.39 (s, 12H,  $-\text{o-ArCH}_3$ ), 2.70 (s, 12H,  $-\text{NMe}_2$ ), 3.36 (m, 4H,  $-\text{NCH}_2$ ), 3.55 (m, 4H,  $-\text{NCH}_2$ ), 5.95 (s, 2H,  $-\text{imidH}$ ), 6.91 (s, 4H,  $-\text{ArH}$ ).

$^{13}\text{C}\{^1\text{H}\}$  NMR ( $\text{C}_6\text{D}_6$ ):  $\delta$  19.7 ( $-\text{o-CH}_3$ ), 24.3 ( $-\text{p-CH}_3$ ), 44.5 ( $-\text{NCH}_3$ ), 49.0 ( $-\text{NCH}_2$ ), 50.1 ( $-\text{NCH}_2$ ), 122.0 ( $-\text{imidC}$ ), 129.8 ( $-\text{ArC}$ ), 132.8 ( $-\text{ArC}$ ), 133.3 ( $-\text{ArC}$ ), 142.3 ( $-\text{ArC}$ ), 195.7 ( $-\text{HfC}_{\text{carbene}}$ ).

Anal. Calc. for  $\text{C}_{29}\text{H}_{44}\text{HfN}_6$ : C, 53.16; H, 6.77; N, 12.83. Found: C, 52.89; H, 6.44; N, 12.68.

### Synthesis of $^{\text{Mes}}[\text{NCNH}]\text{Ti}(\text{NMe}_2)_3$ (3.22)

A cooled ( $-30^\circ\text{C}$ ) THF (10 mL) solution of  $\text{Ti}(\text{NMe}_2)_4$  (200 mg, 0.89 mmol) was slowly added dropwise to **3.8** (348 mg, 0.89 mmol) dissolved in THF (20 mL). The mixture was warmed to room temperature gradually and stirred overnight. After the solvent was removed *in vacuo* and toluene (15 mL) added, the solution was filtered and the solvent removed to give a dark red solid, that was recrystallized with  $\text{Et}_2\text{O}$ /hexanes at  $-30^\circ\text{C}$  to give a red powder. Yield = 662 mg, 85%.

**<sup>1</sup>H NMR (C<sub>6</sub>D<sub>6</sub>):** δ 2.13 (s, 6H, -*o*-ArCH<sub>3</sub>), 2.18 (s, 3H, -*p*-ArCH<sub>3</sub>), 2.22 (s, 3H, -*p*-ArCH<sub>3</sub>), 2.38 (s, 6H, -*o*-ArCH<sub>3</sub>), 2.6 (t, J = 8 Hz, 1H, -NH), 3.0 (q, J = 8 Hz, 2H, -CH<sub>2</sub>NH), 3.1-3.2 (br s, 18H, -NCH<sub>3</sub>), 3.40 (m, 2H, -NCH<sub>2</sub>), 3.50 (m, 2H, -NCH<sub>2</sub>), 3.77 (t, J = 8 Hz, -NCH<sub>2</sub>), 6.04 (d, J = 2 Hz, 1H, -imidH), 6.42 (d, J = 2 Hz, 1H, -imidH), 6.78 (s, 2H, -ArH), 7.01 (s, 2H, -ArH).

**<sup>13</sup>C{<sup>1</sup>H} NMR (C<sub>6</sub>D<sub>6</sub>):** δ 19.5 (-CH<sub>3</sub>), 20.2 (-CH<sub>3</sub>), 22.6 (-CH<sub>3</sub>), 22.9 (-CH<sub>3</sub>), 45.8 (-NCH<sub>2</sub>), 47.8 (-NCH<sub>2</sub>), 49.8 (-NCH<sub>2</sub>), 51.3 (-NCH<sub>2</sub>), 117.8 (-ArC), 118.5 (-ArC), 119.6 (-imidC), 120.6 (-imidC), 128.9 (-ArC), 129.8 (-ArC), 130.5 (-ArC), 132.6 (-ArC), 148.7 (-ArC), 149.9 (-ArC), 192.6 (-NCN).

Satisfactory elemental analysis was not obtained.

### Synthesis of <sup>Mes</sup>[NCN]Ti(NMe<sub>2</sub>)<sub>2</sub> (3.23)

To a cooled (-30°C) solution of Cl<sub>2</sub>Ti(NMe<sub>2</sub>)<sub>2</sub> (103 mg, 5.0 mmol) in THF (10 mL) was slowly added a THF solution of **3.11** (200 mg, 5.0 mmol). The solution was left to stand at -30°C for 15 minutes and then slowly warmed to room temperature. The red solution was stirred overnight at which time the solvent was removed to dryness, toluene added, and the solution filtered through Celite. The volume was reduced to several mL's and hexane added to yield a dark red powder. Yield = 1.78 g, 68%.

**<sup>1</sup>H NMR (C<sub>6</sub>D<sub>6</sub>):** δ 2.22 (s, 6H, -*p*-ArCH<sub>3</sub>), 2.40 (s, 6H, -*o*-ArCH<sub>3</sub>), 2.78 (br s, 12H, -N(CH<sub>3</sub>)<sub>2</sub>), 3.35 (m, 4H, -CH<sub>2</sub>), 3.60 (m, 4H, -CH<sub>2</sub>), 6.05 (s, 2H, -imidH), 6.95 (s, 4H, -ArH).

**<sup>13</sup>C{<sup>1</sup>H} NMR (C<sub>6</sub>D<sub>6</sub>):** δ 20.5 (-CH<sub>3</sub>), 22.4 (-CH<sub>3</sub>), 50.6 (-NCH<sub>3</sub>), 52.4 (-NCH<sub>2</sub>), 54.1 (-NCH<sub>2</sub>), 117.9 (-imidC), 120.4 (-ArC), 128.0(-ArC), 131.7 (-ArC), 143.7 (-ArC), 193.7 (-NCN).

Anal. Calc. for C<sub>29</sub>H<sub>44</sub>N<sub>6</sub>Ti: C, 66.40; H, 8.45; N, 16.02. Found: C, 66.52; H, 8.80; N, 15.89.

### Synthesis of <sup>Ar</sup>(NCN)MCl<sub>2</sub> [(M=Zr, Ar=tol (3.24), M=Zr, Ar=Mes (3.25), M=Zr, Ar=Dipp (3.26), M=Ti, Ar=tol (3.27), M=Ti, Ar=Mes (3.28), M=Hf, Ar=Mes (3.29)]

The following procedure is representative of the synthesis of **3.24-3.29**. Chlorotrimethylsilane (1.03 mL, 8.14 mmol) was added dropwise to a toluene (20 mL)

solution of **4** (533 mg, 0.81 mmol) with vigorous stirring. The white suspension was stirred overnight and collected by filtration to give a white powder. Yield = 495 mg, 95%.

**3.24:** EI-MS: 494 [ $M^+$ ]

Anal. Calcd. for  $C_{21}H_{24}Cl_2N_4Zr$ : C, 51.00; H, 4.89; N, 11.33. Found: C, 50.65; H, 4.53; N, 11.28.

**3.25:** EI-MS: 562 [ $M^+$ ]

Anal. Calc. for  $C_{25}H_{32}Cl_2N_4Zr$ : C, 54.53; H, 5.86; N, 10.17. Found: C, 54.36; H, 5.44; N, 10.01.

**3.26:** EI-MS: 634 [ $M^+$ ]

Anal. Calcd. for  $C_{31}H_{44}Cl_2N_4Zr$ : C, 58.65; H, 6.99; N, 8.83. Found: C, 58.95; H, 7.21; N, 8.95.

**3.27:** EI-MS: 451 [ $M^+$ ]

Anal. Calcd. for  $C_{21}H_{24}Cl_2N_4Ti$ : C, 55.90; H, 5.36; N, 12.42. Found: C, 55.78; H, 5.52; N, 12.23.

**3.28:** EI-MS: 507 [ $M^+$ ]

Anal. Calcd. for  $C_{25}H_{32}Cl_2N_4Ti$ : C, 59.19; H, 6.36; N, 11.04. Found: C 59.26; H, 6.45; N, 10.89.

**3.29:** EI-MS: 638 [ $M^+$ ]

Anal. Calc. for  $C_{25}H_{32}Cl_2HfN_4$ : C, 47.07; H, 5.06; N, 8.78. Found: C, 46.85; H, 4.86; N, 8.53.

### Synthesis of $^{101}[\text{NCN}]ZrCl_2(\text{py})$ (**3.30**)

The pyridine adduct was formed by suspending a portion of the solid **3.24** in toluene and adding an excess of pyridine. The solution was filtered, and the solvent was reduced in volume (~ 2 mL). Hexane was then added to precipitate a red-orange solid. Further recrystallization from a saturated solution of benzene afforded red-orange crystals of **3.30**- $1/2C_6H_6$ .

$^1\text{H NMR}$  ( $C_6D_6$ ):  $\delta$  2.18 (s, 6H,  $-CH_3$ ), 3.60 (m, 4H,  $-CH_2N$ ), 4.15 (m, 4H,  $-CH_2N$ ), 5.92 (s, 2H,  $-imidH$ ), 6.42 (br s, 2H,  $-pyH$ ), 6.74 (br s, 1H,  $-pyH$ ), 6.90 (d,  $J = \text{Hz}$ , 4H,  $-ArH$ ), 7.49 (d,  $J = \text{Hz}$ , 4H,  $-ArH$ ), 8.58 (br s, 2H,  $-pyH$ ).

$^{13}\text{C}\{^1\text{H}\}$  NMR ( $\text{C}_6\text{D}_6$ ):  $\delta$  23.0 (-CH<sub>3</sub>), 51.4 (-CH<sub>2</sub>N), 52.9 (-CH<sub>2</sub>N), 119.3 (-ArC), 121.3 (-imidC), 124.1 (-ArC), 126.9 (-ArC), 131.4 (-ArC), 136.3 (-ArC), 150.4 (-ArC), 156.1 (-ArC), 187.9 (-NCN).

Anal. Calcd. for  $\text{C}_{29}\text{H}_{32}\text{Cl}_2\text{N}_5\text{Zr}$ : C, 56.85; H, 5.26; N, 11.43. Found: C, 56.80; H, 5.33; N, 11.40.

**Synthesis of  $^{\text{Ar}}[\text{NCN}]\text{ZrR}_2$  [(Ar = tol, R = CH<sub>2</sub>SiMe<sub>3</sub> (3.31), Me (3.32), CH<sub>2</sub>Ph (3.33); Ar = Mes, R = Me (3.34), CH<sub>2</sub>Ph (3.35)]**

**Method A (SiMe<sub>4</sub> elimination):** To a cooled (-30°C) THF solution (10 mL) of **3.7** (90 mg, 0.27 mmol) was added dropwise a cooled (-30°C) THF solution (5 mL) of Zr(CH<sub>2</sub>SiMe<sub>3</sub>)<sub>4</sub> (121 mg, 0.27 mmol). The solution was kept at the reduced temperature for ½ hour then gradually warmed to room temperature for 15 min. The solvent was removed and the yellow residue was extracted with hexane/toluene (5:1) (3 x 10 mL). The extracts were cooled to -30°C over a period of 1 week giving a large portion of pale yellow crystal. Yield = 110 mg, 67%.

**Method B (Alkylation):** A suspension of **3.24** (103 mg, 0.21 mmol) in Et<sub>2</sub>O was cooled to -30°C and an Et<sub>2</sub>O solution of LiCH<sub>2</sub>SiMe<sub>3</sub> (39 mg, 0.42 mmol) was slowly added dropwise. The solution was allowed to gradually warm to room temperature where stirring was continued for ½ hour. The solvent was removed and the yellow residue extracted with hexane/toluene (5:1) (3 x 10 mL). The extracts were cooled to -30°C over a period of 1 week to give the same pale yellow crystalline material described above. Yield = 50 mg, 40%.

**3.31: (Method A)  $^1\text{H}$  NMR ( $\text{C}_6\text{D}_6$ ):**  $\delta$  0.11 (s, 18H, -CH<sub>2</sub>SiMe<sub>3</sub>), 0.95 (s, 4H, -CH<sub>2</sub>SiMe<sub>3</sub>), 2.23 (s, 6H, -CH<sub>3</sub>), 3.40 (m, 4H, -CH<sub>2</sub>N), 3.95 (m, 4H, -CH<sub>2</sub>N), 5.79 (s, 2H, -imidH), 7.18 (d, J = 8 Hz, 4H, -ArH), 7.30 (d, J = 8 Hz, 4H, -ArH).

$^{13}\text{C}\{^1\text{H}\}$  NMR ( $\text{C}_6\text{D}_6$ ):  $\delta$  1.4 (-SiC), 23.5 (-CH<sub>3</sub>), 50.9 (-CH<sub>2</sub>N), 54.6 (-CH<sub>2</sub>N), 69.0 4 (-ZrCH<sub>2</sub>), 121.0 (-ArC), 121.4 (-imidC), 129.4 (-ArC), 132.7 (-ArC), 155.2 (-ArC), 186.8 (-NCN). Anal. Calcd. For  $\text{C}_{29}\text{H}_{46}\text{N}_4\text{Si}_2\text{Zr}$ : C, 58.24; H, 7.75; N, 9.37. Found: C, 58.05; H, 7.66; N, 9.20.

**3.32: (Method B)  $^1\text{H}$  NMR ( $\text{C}_6\text{D}_6$ ):**  $\delta$  0.62 (s, 6H,  $-\text{ZrCH}_3$ ), 2.35 (s, 6H,  $-\text{CH}_3$ ), 4.01 (m, 4H,  $-\text{CH}_2\text{N}$ ), 4.33 (m, 4H,  $-\text{CH}_2\text{N}$ ), 5.86 (s, 2H,  $-\text{imidH}$ ), 6.93 (d,  $J = 8$  Hz, 4H,  $-\text{ArH}$ ), 7.05 (d,  $J = 8$  Hz, 4H,  $-\text{ArH}$ ).

**$^{13}\text{C}\{^1\text{H}\}$  NMR ( $\text{C}_6\text{D}_6$ ):**  $\delta$  19.9 ( $-\text{CH}_3$ ), 39.7 ( $-\text{ZrCH}_3$ ), 50.2 ( $-\text{CH}_2\text{N}$ ), 51.4 ( $-\text{CH}_2\text{N}$ ), 118.5 ( $-\text{ArC}$ ), 120.4 ( $-\text{imidC}$ ), 127.8 ( $-\text{ArC}$ ), 130.2 ( $-\text{ArC}$ ), 148.6 ( $-\text{ArC}$ ), 193.5 ( $-\text{NCN}$ ).

Anal. Calc. for  $\text{C}_{23}\text{H}_{30}\text{N}_4\text{Zr}$  C, 60.88; H, 6.66; N, 12.35. Found: C, 60.53; H, 6.78; N, 12.14.

**3.33: (Method A)  $^1\text{H}$  NMR ( $\text{C}_6\text{D}_6$ ):**  $\delta$  1.85 (s, 4H,  $-\text{ZrCH}_2$ ), 2.35 (s, 12H,  $-\text{p-ArCH}_3$ ), 3.14 (m, 4H,  $-\text{NCH}_2$ ), 3.47 (m, 4H,  $-\text{NCH}_2$ ), 5.89 (s, 2H,  $-\text{imidH}$ ), 6.79 (d,  $J = 8$  Hz, 4H,  $-\text{o-CH}_2\text{Ph}$ ), 6.90 (t,  $J = 8$  Hz, 2H,  $-\text{p-CH}_2\text{Ph}$ ), 7.01 (s, 4H,  $-\text{ArH}$ ), 7.26 (t,  $J = 8$  Hz, 4H,  $-\text{m-CH}_2\text{Ph}$ ).

**$^{13}\text{C}\{^1\text{H}\}$  NMR ( $\text{C}_6\text{D}_6$ ):**  $\delta$  23.4 ( $-\text{p-CH}_3$ ), 48.3 ( $-\text{NCH}_2$ ), 54.6 ( $-\text{NCH}_2$ ), 70.3 ( $-\text{ZrCH}_2$ ), 119.8 ( $-\text{imidC}$ ), 123.1 ( $-\text{ArC}$ ), 129.6 ( $-\text{ArC}$ ), 130.8 ( $-\text{ArC}$ ), 137.6 ( $-\text{ArC}$ ), 145.8 ( $-\text{ArC}$ ), 150.1 ( $-\text{ArC}$ ), 195.3 ( $-\text{ZrC}_{\text{Carbene}}$ ). Some aromatic resonances obscured by  $\text{C}_6\text{D}_6$  solvent.

Anal. Calc. for  $\text{C}_{33}\text{H}_{38}\text{N}_4\text{Zr}$  C, 68.11; H, 6.58; N, 9.63. Found: C, 68.22; H, 6.67; N, 9.52.

**3.34: (Method B)  $^1\text{H}$  NMR ( $\text{C}_6\text{D}_6$ ):**  $\delta$  0.33 (s, 6H,  $-\text{ZrCH}_3$ ), 2.20 (s, 6H,  $-\text{p-ArCH}_3$ ), 2.43 (s, 12H,  $-\text{o-ArCH}_3$ ), 3.37 (m, 4H,  $-\text{NCH}_2$ ), 3.45 (m, 4H,  $-\text{NCH}_2$ ), 5.88 (s, 2H,  $-\text{imidH}$ ), 6.98 (s, 4H,  $-\text{ArH}$ ).

**$^{13}\text{C}\{^1\text{H}\}$  NMR ( $\text{C}_6\text{D}_6$ ):**  $\delta$  18.6 ( $-\text{o-CH}_3$ ), 20.0 ( $-\text{p-CH}_3$ ), 48.4 ( $-\text{ZrCH}_3$ ), 51.7 ( $-\text{NCH}_2$ ), 52.3 ( $-\text{NCH}_2$ ), 118.5 ( $-\text{imidC}$ ), 129.9 ( $-\text{ArC}$ ), 133.3 ( $-\text{ArC}$ ), 135.0 ( $-\text{ArC}$ ), 148.9 ( $-\text{ArC}$ ), 189.8 ( $-\text{ZrC}_{\text{Carbene}}$ ).

Anal. Calc. for  $\text{C}_{27}\text{H}_{38}\text{N}_4\text{Zr}$ : C, 63.61; H, 7.51; N, 10.99. Found: C, 63.33; H, 7.32; N, 10.75.

**3.35: (Method B)  $^1\text{H}$  NMR ( $\text{C}_6\text{D}_6$ ):**  $\delta$  1.92 (s, 4H,  $-\text{ZrCH}_2$ ), 2.24 (s, 6H,  $-\text{p-ArCH}_3$ ), 2.31 (s, 12H,  $-\text{o-ArCH}_3$ ), 3.03 (m, 4H,  $-\text{NCH}_2$ ), 3.56 (m, 4H,  $-\text{NCH}_2$ ), 5.77 (s, 2H,  $-\text{imidH}$ ), 6.84 (d,  $J=8$  Hz, 4H,  $-\text{o-CH}_2\text{Ph}$ ), 6.92 (t,  $J=8$  Hz, 2H,  $-\text{p-CH}_2\text{Ph}$ ), 6.98 (s, 4H,  $-\text{ArH}$ ), 7.17 (t,  $J=8$  Hz, 4H,  $-\text{m-CH}_2\text{Ph}$ ).

**$^{13}\text{C}\{^1\text{H}\}$  NMR ( $\text{C}_6\text{D}_6$ ):**  $\delta$  20.2 ( $-\text{o-CH}_3$ ), 24.3 ( $-\text{p-CH}_3$ ), 49.3 ( $-\text{NCH}_2$ ), 52.7 ( $-\text{NCH}_2$ ), 65.6 ( $-\text{ZrCH}_2$ ), 121.6 ( $-\text{imidC}$ ), 122.4 ( $-\text{ArC}$ ), 130.3 ( $-\text{ArC}$ ), 131.5 ( $-\text{ArC}$ ), 136.6 ( $-\text{ArC}$ ),

148.4 (-ArC), 156.3 (-ArC), 190.1 (-ZrC<sub>Carbene</sub>). Some aromatic resonances obscured by C<sub>6</sub>D<sub>6</sub> solvent.

Anal. Calc. for C<sub>39</sub>H<sub>46</sub>N<sub>4</sub>Zr: C, 70.75; H, 7.00; N, 8.46. Found: C, 70.43; H, 6.92; N, 8.35.

**Synthesis of <sup>Mes</sup>(NCN)Hf(R)<sub>2</sub> [R=Me (3.36), CH<sub>2</sub>CH<sub>3</sub> (3.37), CD<sub>2</sub>CD<sub>3</sub> (*d*<sub>10</sub>-3.37), CH<sub>2</sub>Ph (3.38), CH<sub>2</sub>CH(CH<sub>3</sub>)<sub>2</sub> (3.39)]**

The following procedure is representative of the synthesis of **3.36-3.39**. **3.29** (400 mg, 0.63 mmol) was dissolved in 5 mL THF and cooled to -30 °C. MeMgBr (0.42 mL, 1.3 mmol, 3M in Et<sub>2</sub>O) was added dropwise and the slightly yellow solution was stirred in the dark for 30 minutes. The THF was removed under reduced pressure and to the resulting residue was added a few drops 1,4-dioxane and Et<sub>2</sub>O (5 mL). The resulting suspension was filtered through Celite and volatiles were removed to give a white solid, **3.36**, which was recrystallized with Et<sub>2</sub>O. Yield = 293 mg, 78 %.

**3.36:** <sup>1</sup>H NMR (C<sub>6</sub>D<sub>6</sub>): δ 0.12 (s, 6H, -HfCH<sub>3</sub>), 2.17 (s, 6H, -*p*-ArCH<sub>3</sub>), 2.49 (s, 12H, -*o*-ArCH<sub>3</sub>), 3.40 (m, 4H, -NCH<sub>2</sub>), 3.49 (m, 4H, -NCH<sub>2</sub>), 5.90 (s, 2H, -imidH), 6.99 (s, 4H, -ArH).

<sup>13</sup>C{<sup>1</sup>H} NMR (C<sub>6</sub>D<sub>6</sub>): δ 19.6 (-CH<sub>3</sub>), 20.7 (-CH<sub>3</sub>), 52.2 (-NCH<sub>2</sub>), 54.1 (-HfCH<sub>3</sub>), 54.2 (-NCH<sub>2</sub>), 119.5 (-imidC), 129.6 (-ArC), 132.3 (-ArC), 135.3 (-ArC), 152.1 (-ArC), 196.1 (-HfC<sub>Carbene</sub>).

Anal. Calc. for C<sub>27</sub>H<sub>38</sub>HfN<sub>4</sub>: C, 54.31; H, 6.41; N, 9.38. Found: C, 54.22; H, 6.26; N, 9.16.

**3.37:** <sup>1</sup>H NMR (C<sub>6</sub>D<sub>6</sub>): δ 0.62 (q, J = 8Hz, 4H, -HfCH<sub>2</sub>), 1.49 (t, J = 8Hz, 6H, -CH<sub>2</sub>CH<sub>3</sub>), 2.24 (s, 6H, -*p*-ArCH<sub>3</sub>), 2.46 (s, 12H, -*o*-ArCH<sub>3</sub>), 3.32 (m, 2H, -NCH<sub>2</sub>), 3.55 (m, 4H, -NCH<sub>2</sub>), 5.90 (s, 2H, -imidH), 6.70 (s, 4H, -ArH).

<sup>13</sup>C{<sup>1</sup>H} NMR (C<sub>6</sub>D<sub>6</sub>): δ 12.8 (-HfCH<sub>2</sub>CH<sub>3</sub>), 19.7 (-CH<sub>3</sub>), 20.9 (-CH<sub>3</sub>), 51.4 (-NCH<sub>2</sub>), 52.5 (-NCH<sub>2</sub>), 66.1 (-HfCH<sub>2</sub>CH<sub>3</sub>), 119.9 (-imidC), 129.6 (-ArC), 131.8 (-ArC), 134.9 (-ArC), 152.9 (-ArC), 196.4 (-HfC<sub>Carbene</sub>).

Anal. Calc. for C<sub>29</sub>H<sub>42</sub>HfN<sub>4</sub>: C, 55.72; H, 6.77; N, 8.96. Found: C, 55.24; H, 6.59; N, 8.87.

***d*<sub>10</sub>-3.37:** <sup>1</sup>H and <sup>13</sup>C NMR spectra identical to **11** with the absence of -HfCH<sub>2</sub>CH<sub>3</sub> resonances.

**3.38:** <sup>1</sup>H NMR (C<sub>6</sub>D<sub>6</sub>): δ 1.85 (s, 4H, -HfCH<sub>2</sub>), 2.26 (s, 6H, -*p*-ArCH<sub>3</sub>), 2.36 (s, 12H, -*o*-ArCH<sub>3</sub>), 3.04 (m, 4H, -NCH<sub>2</sub>), 3.46 (m, 4H, -NCH<sub>2</sub>), 5.73 (s, 2H, -imidH), 6.82 (d, J = 8Hz, 4H, -*o*-CH<sub>2</sub>Ph), 6.90 (t, J = 8Hz, 2H, -*p*-CH<sub>2</sub>Ph), 7.02 (s, 4H, -ArH), 7.18 (t, J = 8Hz, 4H, -*m*-CH<sub>2</sub>Ph).

<sup>13</sup>C{<sup>1</sup>H} NMR (C<sub>6</sub>D<sub>6</sub>): δ 21.2 (-CH<sub>3</sub>), 22.1 (-CH<sub>3</sub>), 50.0 (-NCH<sub>2</sub>), 51.4 (-NCH<sub>2</sub>), 73.5 (-HfCH<sub>2</sub>), 121.3 (-ArC), 122.9 (-imidC), 129.6 (-ArC), 130.9 (-ArC), 135.5 (-ArC), 147.9 (-ArC), 155.6 (-ArC), 196.5 (-HfC<sub>Carbene</sub>). Some aromatic resonances obscured by C<sub>6</sub>D<sub>6</sub> resonances.

Anal. Calc. for C<sub>39</sub>H<sub>46</sub>HfN<sub>4</sub>: C, 62.51; H, 6.19; N, 7.48. Found: C, 62.42; H, 6.14; N, 7.42.

**3.39:** <sup>1</sup>H NMR (C<sub>6</sub>D<sub>6</sub>): δ 0.68 (d, J = 8Hz, 4H, -HfCH<sub>2</sub>), 1.02 (d, J = 8Hz, 12H, -CH(CH<sub>3</sub>)<sub>2</sub>), 2.24 (s, 6H, -*p*-ArCH<sub>3</sub>), 2.35 (n, J = 8Hz, 2H, -CH<sub>2</sub>CH(CH<sub>3</sub>)<sub>2</sub>), 2.46 (s, 12H, -*o*-ArCH<sub>3</sub>), 3.23 (m, 2H, -NCH<sub>2</sub>), 3.67 (m, 4H, -NCH<sub>2</sub>), 5.86 (s, 2H, -imidH), 7.00 (s, 4H, -ArH).

<sup>13</sup>C{<sup>1</sup>H} NMR (C<sub>6</sub>D<sub>6</sub>): δ 13.7 (-CH<sub>2</sub>CH(CH<sub>3</sub>)<sub>2</sub>), 19.4 (-*o*-CH<sub>3</sub>), 20.5 (-*p*-CH<sub>3</sub>), 32.3 (-CH<sub>2</sub>CH(CH<sub>3</sub>)<sub>2</sub>), 50.5 (-NCH<sub>2</sub>), 52.1 (-NCH<sub>2</sub>), 68.4 (-HfCH<sub>2</sub>), 118.4 (-imidC), 128.4 (-ArC), 132.1 (-ArC), 133.9 (-ArC), 148.4 (-ArC), 194.9 (-HfC<sub>Carbene</sub>).

Anal. Calc. for C<sub>33</sub>H<sub>50</sub>HfN<sub>4</sub>: C, 58.18; H, 7.40; N, 8.22. Found: C, 57.91; H, 7.05; N, 8.01.

#### Decomposition of <sup>Mes</sup>(NCN)Hf(CH<sub>2</sub>CH<sub>3</sub>)<sub>2</sub> to form **3.40** and *d*<sub>4</sub>-**3.40**.

**3.37** (110 mg, 0.18 mmol) was dissolved in Et<sub>2</sub>O (20 mL) and the pale yellow solution was stirred for 5 days. The Et<sub>2</sub>O was removed under reduced pressure and hexanes added to precipitate a dark orange powder. Yield = 99 mg, 95 %.

<sup>1</sup>H NMR (C<sub>6</sub>D<sub>6</sub>): δ -0.10 (dq, J = 5, 8Hz, 1H, -HfCH<sub>2</sub>CH<sub>3</sub>), 0.010 (dq, J = 5, 8Hz, 1H, -HfCH<sub>2</sub>CH<sub>3</sub>), 1.00 (d, J = 12Hz, 1H, -HfCH<sub>2</sub>Ar), 1.01 (t, J = 8Hz, 3H, -HfCH<sub>2</sub>CH<sub>3</sub>), 2.23 (s, 3H, -CH<sub>3</sub>), 2.25 (s, 3H, -CH<sub>3</sub>), 2.37 (s, 3H, -CH<sub>3</sub>), 2.47 (s, 3H, -CH<sub>3</sub>), 2.51 (d, J = 12Hz, 1H, -HfCH<sub>2</sub>Ar), 2.58 (s, 3H, -CH<sub>3</sub>), 3.19 (m, 3H, -NCH<sub>2</sub>), 3.22 (m, 3H, -NCH<sub>2</sub>), 3.27-3.31 (m, 3H, -NCH<sub>2</sub>), 3.47 (m, 3H, -NCH<sub>2</sub>), 3.62 (m, 3H, -NCH<sub>2</sub>), 3.93 (m, 3H, -

NCH<sub>2</sub>), 4.16 (m, 3H, -NCH<sub>2</sub>), 5.89 (d, J=2Hz, 1H, -imidH), 5.92 (d, J=2Hz, 1H, -imidH), 6.77 (s, 1H, -ArH), 6.97 (s, 1H, -ArH), 7.04 (s, 2H, -ArH).

<sup>13</sup>C{<sup>1</sup>H} NMR (C<sub>6</sub>D<sub>6</sub>): δ 9.7 (-HfCH<sub>2</sub>CH<sub>3</sub>), 19.1 (-ArCH<sub>3</sub>), 19.3 (-ArCH<sub>3</sub>), 21.1 (-ArCH<sub>3</sub>), 21.3 (-ArCH<sub>3</sub>), 52.1 (-NCH<sub>2</sub>), 53.8 (-NCH<sub>2</sub>), 55.2 (-NCH<sub>2</sub>), 55.3 (-NCH<sub>2</sub>), 58.2 (-HfCH<sub>2</sub>CH<sub>3</sub>), 72.9 (-HfCH<sub>2</sub>Ar), 119.5 (-imidC), 129.3 (-ArC), 129.9 (-ArC), 135.0 (-ArC), 138.5 (-ArC), 138.6 (-ArC), 142.9 (-ArC), 145.6 (-ArC), 197.3 (-HfC<sub>Carbene</sub>). Some aromatic resonances obscured by C<sub>6</sub>D<sub>6</sub> solvent.

Anal. Calc. for C<sub>27</sub>H<sub>36</sub>HfN<sub>4</sub>: C, 54.49; H, 6.10; N, 9.41. Found: C, 54.13; H, 5.86; N, 9.12.

**d<sub>4</sub>-3.40**: <sup>1</sup>H and <sup>13</sup>C NMR spectra identical to **3.40** with the absence of -HfCH<sub>2</sub>CH<sub>3</sub> resonances.

### 3.7. References

- (1) Regitz, M. *Angew. Chem., Int. Ed. Engl.* **1996**, *35*, 725.
- (2) Herrmann, W. A.; Kocher, C. *Angew. Chem., Int. Ed. Engl.* **1997**, *36*, 2162.
- (3) Dullius, J. E. L.; Suarez, P. A. Z.; Einloft, S.; de Souza, R. F.; Dupont, J.; Fischer, J.; De Cian, A. *Organometallics* **1998**, *17*, 815.
- (4) Arduengo, A. J., III *Acc. Chem. Res.* **1999**, *32*, 913.
- (5) Arduengo, A. J., III; Krafczyk, R. *Chem. Z.* **1998**, *32*, 6.
- (6) Arnold, P. L.; Mungur, S. A.; Blake, A. J.; Wilson, C. *Angew. Chem. Int. Ed.* **2003**, *42*, 5981.
- (7) Arnold, P. L.; Blake, A. J.; Wilson, C. *Chem. Eur. J.* **2005**, *11*, 6095.
- (8) Aihara, H.; Matsuo, T.; Kawaguchi, H. *Chem. Commun.* **2003**, 2204.
- (9) Arduengo, A. J., III; Dias, H. V. R.; Calabrese, J. C.; Davidson, F. *J. Am. Chem. Soc.* **1992**, *114*, 9724.
- (10) Arduengo, A. J., III; Dias, H. V. R.; Harlow, R. L.; Kline, M. *J. Am. Chem. Soc.* **1992**, *114*, 5530.
- (11) Arduengo, A. J., III; Harlow, R. L.; Kline, M. *J. Am. Chem. Soc.* **1991**, *113*, 361.
- (12) Fryzuk, M. D.; Johnson, S. A.; Patrick, B. O.; Albinati, A.; Mason, S. A.; Koetzle, T. F. *J. Am. Chem. Soc.* **2001**, *123*, 3960.
- (13) Arduengo, A. J., III; Krafczyk, R.; Schmutzler, R.; Craig, H. A.; Goerlich, J. R.; Marshall, W. J.; Unverzagt, M. *Tetrahedron* **1999**, *55*, 14523.
- (14) Malek, A.; Fresco, J. M. *Can. J. Chem.* **1973**, *51*, 1981.
- (15) Chandra, S.; Kumar, R. *Transition Met. Chem.* **2004**, *29*, 269.
- (16) Niehues, M.; Erker, G.; Kehr, G.; Schwab, P.; Froehlich, R.; Blacque, O.; Berke, H. *Organometallics* **2002**, *21*, 2905.
- (17) Niehues, M.; Kehr, G.; Erker, G.; Wibbeling, B.; Frohlich, R.; Blacque, O.; Berke, H. *J. Organomet. Chem.* **2002**, *663*, 192.
- (18) Zhang, X.; Zhu, Q.; Guzei, I. A.; Jordan, R. F. *J. Am. Chem. Soc.* **2000**, *122*, 8093.
- (19) Skinner, M. E. G.; Li, Y.; Mountford, P. *Inorg. Chem.* **2002**, *41*, 1110.

- (20) Schrock, R. R.; Seidel, S. W.; Schrodi, Y.; Davis, W. M. *Organometallics* **1999**, *18*, 428.
- (21) Scott, M. J.; Lippard, S. J. *Inorg. Chim. Acta* **1997**, *263*, 287.
- (22) Petersen, J. R.; Hoover, J. M.; Kassel, W. S.; Rheingold, A. L.; Johnson, A. R. *Inorg. Chim. Acta* **2005**, *358*, 687.
- (23) Straus, D. A.; Kamigaito, M.; Cole, A. P.; Waymouth, R. M. *Inorg. Chim. Acta* **2003**, *349*, 65.
- (24) Lee, Y.-J.; Lee, J.-D.; Ko, J.; Kim, S.-H.; Kang, S. O. *Chem. Commun.* **2003**, 1364.
- (25) Novak, A.; Blake, A. J.; Wilson, C.; Love, J. B. *Chem. Commun.* **2002**, 2796.
- (26) Harris, S. A.; Ciszewski, J. T.; Odom, A. L. *Inorg. Chem.* **2001**, *40*, 1987.
- (27) Boisson, C.; Berthet, J. C.; Ephritikhine, M.; Lance, M.; Nierlich, M. J. *Organomet. Chem.* **1997**, *531*, 115.
- (28) Mungur, S. A.; Blake, A. J.; Wilson, C.; McMaster, J.; Arnold, P. L. *Organometallics*, ACS ASAP.
- (29) Arndt, S.; Okuda, J. *Chem. Rev.* **2002**, *102*, 1953.
- (30) Fagan, P. J.; Manriquez, J. M.; Marks, T. J.; Day, C. S.; Vollmer, S. H.; Day, V. W. *Organometallics* **1982**, *1*, 170.
- (31) Okuda, J. *Dalton Trans.* **2003**, 2367.
- (32) Evans, W. J.; Drummond, D. K.; Grate, J. W.; Zhang, H.; Atwood, J. L. *J. Am. Chem. Soc.* **1987**, *109*, 3928.
- (33) Scott, M. J.; Lippard, S. J. *Organometallics* **1997**, *16*, 5857.
- (34) Arnold, P. L.; Liddle, S. T. *Chem. Commun.* **2005**, 5638.
- (35) Warren, T. H.; Schrock, R. R.; Davis, W. M. *Organometallics* **1996**, *15*, 562.
- (36) Alt, H. G.; Denner, C. E.; Milius, W. *Inorg. Chim. Acta* **2004**, *357*, 1682.
- (37) Matulenko, M. A.; Hakeem, A. A.; Kolasa, T.; Nakane, M.; Terranova, M. A.; Uchic, M. E.; Miller, L. N.; Chang, R.; Donnelly-Roberts, D. L.; Namovic, M. T.; Moreland, R. B.; Brioni, J. D.; Stewart, A. O. *Bioorg. Med. Chem.* **2004**, *12*, 3471.
- (38) Gowda, B. T.; Svoboda, I.; Fuess, H. *Z. Naturforsch., A: Phys. Sci.* **2000**, *55*, 779.

- (39) Wilde, R. G.; Billheimer, J. T.; Germain, S. J.; Hausner, E. A.; Meunier, P. C.; Munzer, D. A.; Stoltenborg, J. K.; Gillies, P. J.; Burcham, D. L.; et al. *Bioorg. Med. Chem.* **1996**, *4*, 1493.
- (40) McAlexander, L. H.; Li, L.; Yang, Y.; Pollitte, J. L.; Xue, Z. *Inorg. Chem.* **1998**, *37*, 1423.
- (41) Whitesides, G. M.; Hackett, M.; Brainard, R. L.; Lavalleye, J. P. P. M.; Sowinski, A. F.; Izumi, A. N.; Moore, S. S.; Brown, D. W.; Staudt, E. M. *Organometallics* **1985**, *4*, 1819.
- (42) Bird, R.; Knipe, A. C.; Stirling, C. J. M. *J. Chem. Soc., Perkin Trans. 2* **1973**, 1215.

## Chapter Four

# Reactivity and Applications of Group 4 [NCN] Transition Metal Complexes

### 4.1. Introduction\*

To date, research with NHC donors has focused on the application of late transition metal NHC complexes in areas such as homogeneous catalysis. In general, the chemistry of electropositive NHC complexes, which include groups 4, 5, and the *s*- and *f*-block metals, has been limited to studying the binding of the NHC donor and the coordination properties of the metal complexes. Surprisingly, little is known about the application and reactivity of these complexes in homogeneous catalysis and small molecule activation.<sup>1</sup> In chapter 3, we demonstrated that by flanking a centrally disposed NHC with two pendant amido donors in a tridentate motif, the carbene donor has been forced to bind to group 4 transition metals by virtue of its position in the chelate array. Given this stability, we were interested in the reactivity and application of these complexes in fundamental processes such as homogeneous catalysis and small molecule activation.

\*A portion of this chapter has been published (Spencer, L.; Fryzuk, M.D. *J. Organomet. Chem.* **2005**, *690*, 5788).

In this chapter, the applications of group 4 transition metal [NCN] complexes in olefin polymerization and migratory insertion processes will be presented. In addition, the attempted syntheses of coordinated dinitrogen complexes will be outlined. As the topics discussed are unique from each other, separate introductions are included in each section for each reactivity pattern investigated.

#### 4.2. Hf and Zr Cation Formation and Polymerization Studies

Group 4 transition metal complexes with substituted amide ligands have been extensively examined as olefin polymerization catalysts.<sup>2-9</sup> Perhaps the most recognized examples of highly active amide-based olefin polymerization complexes are the constrained geometry catalysts (CGC's) (**4.1**, M = Ti, Zr, Figure 4.1).<sup>10</sup> This catalyst and derivatives thereof are active for both ethylene and 1-hexene polymerization. Group 4 complexes stabilized by NHC ligands (**4.2-4.3**) have also been investigated for the polymerization of  $\alpha$ -olefins (Figure 4.1).<sup>11</sup> These simple N-alkyl substituted NHC supported complexes exhibit moderate ethylene polymerization activity at room temperature. The activity dramatically decreases at elevated temperatures, which is potentially a result of NHC dissociation from the metal centre. Another example of an NHC-based polymerization catalyst is the bis(aryloxido)NHC stabilized titanium complex described in chapter 3.1, which exhibits high ethylene polymerization activity upon MMAO activation.<sup>12</sup>

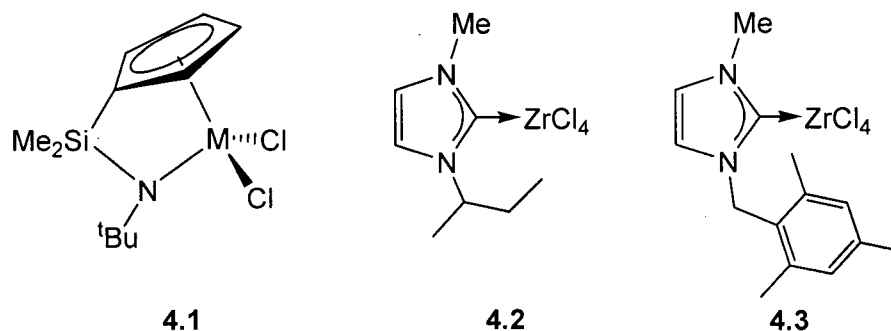
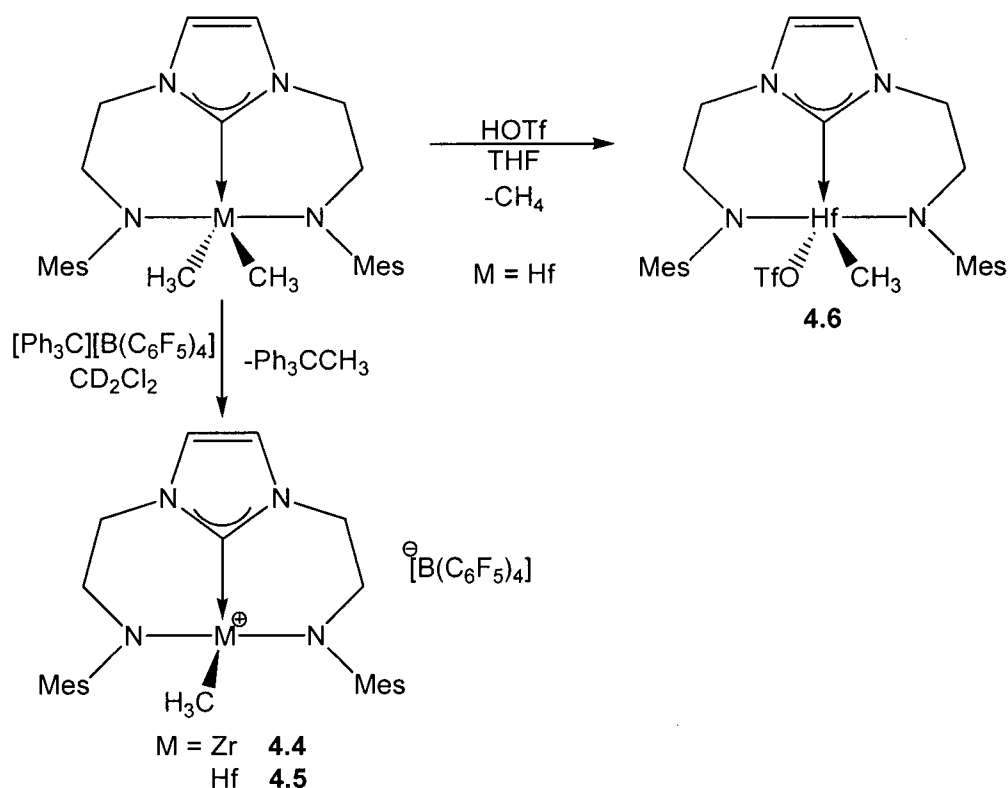


**Figure 4.1.** Examples of Group 4 olefin polymerization catalysts.

In light of the success with the CGC design and spurred by the recent accomplishments of NHC supported complexes, the synthesis of activated zirconium and hafnium [NCN] complexes was investigated. The methyl cations,  $\{\text{Mes}[\text{NCN}]M(\text{CH}_3)\}[\text{B}(\text{C}_6\text{F}_5)_4]$ , ( $M = \text{Zr}$ , **4.4**;  $M = \text{Hf}$ , **4.5**) were generated *in situ* from dimethyl precursors **3.33** and **3.35** at  $-10^\circ\text{C}$  with  $[\text{Ph}_3\text{C}][\text{B}(\text{C}_6\text{F}_5)_4]$  (Scheme 4.1). Due to the thermal sensitivity of the species, the products were identified by  $^1\text{H}$  NMR spectroscopy in solution and not isolated.  $^1\text{H}$  NMR spectroscopy of both species shows anticipated ligand resonances for  $C_s$  symmetric products in solution with  $M\text{-CH}_3$  resonances at 0.50 ppm for **4.4** and 0.26 ppm for **4.5**.

Treatment of **3.35** with triflic acid generates the hafnium methyl-triflate complex,  $\text{Mes}[\text{NCN}]\text{Hf}(\text{OTf})(\text{CH}_3)$  (**4.6**), which is isolable at room temperature (Scheme 4.1). The  $^1\text{H}$  NMR spectrum of **4.6** shows similar ligand resonances to **4.4** and **4.5**, indicative of a  $C_s$  symmetric species in solution with a  $\text{Hf-CH}_3$  resonance at 0.19 ppm. These findings are similar to those of previously described hafnium triflate complexes.<sup>13</sup>



Scheme 4.1.

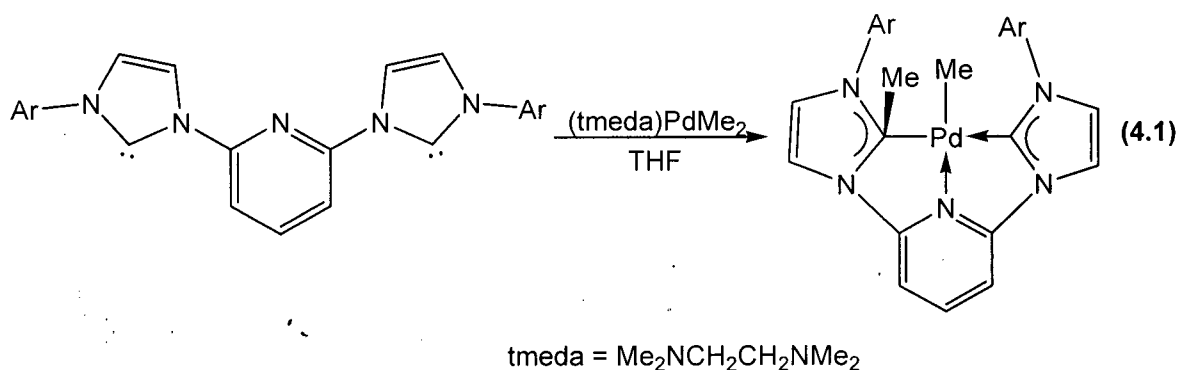
Cationic complexes **4.4** and **4.5** were evaluated as 1-hexene polymerization catalysts. The addition of ~500 equivalents of 1-hexene to a chlorobenzene solution of **4.4** resulted in the isolation of a viscous oily polymer.  $^{13}\text{C}\{^1\text{H}\}$  NMR spectroscopy of the substance reveals the formation of atactic poly-1-hexene in 4% yield.<sup>14</sup> The low yield observed is quite surprising in light of the many active amido-based non-metallocene group 4 catalysts.<sup>2-9</sup> It was recently found that 1-hexene polymerization with group 4 metal bearing diamido  $^{\text{Mes}}[\text{N}(\text{NMe})\text{N}]$  ancillary ligands underwent *ortho*-methyl C-H bond activation during polymerization.<sup>15</sup> Investigation of the decomposition products revealed an *ortho*-methyl C-H bond activated compound similar to **3.39**, in addition to other unidentifiable materials.

The exposure of **4.4** to ethylene in toluene resulted in a different outcome. A large amount of polyethylene was recovered, which shows that **4.4** is a moderately active catalyst for the polymerization of ethylene ( $125 \text{ g mmol}^{-1} \text{ h}^{-1} \text{ atm}^{-1}$ ). It is important to note that immediately after exposure to ethylene, a noticeable exothermic event was observed. Halting the polymerization experiment at increasingly longer times resulted in a decreased activity. This suggests that the active species, albeit catalytically active, is short-lived in solution.

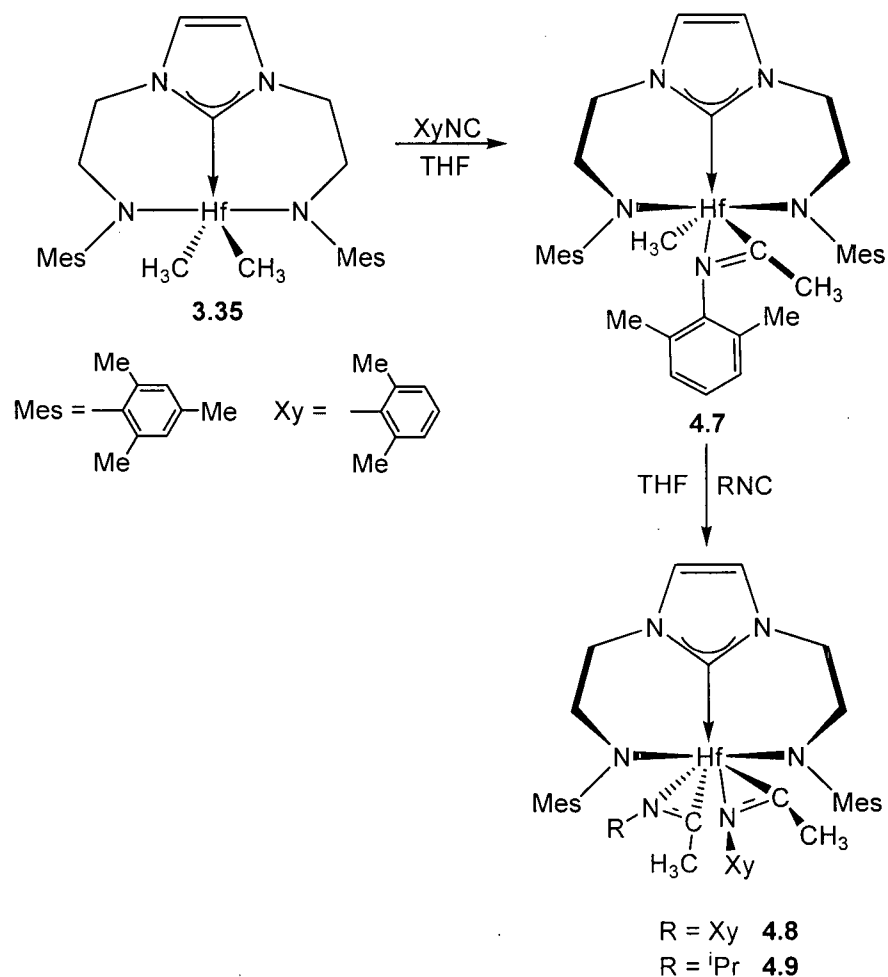
#### 4.3. Formation of [NCN] Hafnium $\eta^2$ -Iminoacyls and an Eneamidolate metallacycle

The migratory insertion of carbon monoxide into metal alkyl and hydride bonds represents a fundamental reaction type in organometallic chemistry.<sup>16</sup> Interest in this area stems from the importance of carbonylation reactions where the migratory insertion of CO is a key step in the catalytic cycle.<sup>17</sup> CO insertion into transition metal alkyls normally generates  $\eta^1$  or  $\eta^2$ -acyl derivatives, with the latter binding mode typically occurring in electron-deficient early d-block, actinide and lanthanide metal centres. Analogous reactivity has been observed in the migratory insertion of isocyanides, isoelectronic equivalents of CO, generating  $\eta^2$ -iminoacyl groups.<sup>16</sup>

Migratory insertion reactions involving transition metal NHC complexes have also been investigated and, in some cases, the destructive modification of the NHC donor has been observed.<sup>18,19</sup> For example, the facile insertion of an NHC group into a Pd-Me bond was recently reported (Equation 4.1).<sup>19</sup> DFT calculations on model complexes suggests all three functionalities of the tridentate ligand coordinate to the palladium centre prior to methyl migration from the metal centre to the NHC moiety.



With respect to early transition metal (ETM) complexes and migratory insertion reactions, the participation of the metal-NHC bond during these reactions has yet to be addressed. Along this line, the migratory insertion of substituted isocyanides into the hafnium-alkyl bonds of **3.35** was investigated. The hafnium dimethyl derivative reacts immediately in solution with one equivalent of xylyl isocyanide (XyNC) to give the mono-insertion product **4.7** (Scheme 4.2). The <sup>1</sup>H NMR spectrum is consistent with a C<sub>s</sub> symmetric structure (equivalent N-mesityl groups and backbone linkers); the remaining hafnium-methyl resonance is found at 0.17 ppm. The η<sup>2</sup> coordination of the iminoacyl group is confirmed by <sup>13</sup>C{<sup>1</sup>H} NMR (N=C, 259 ppm) and IR (ν<sub>C=N</sub> 1575 cm<sup>-1</sup>) spectroscopy and is a typical outcome for this kind of reaction.<sup>16</sup> In solution, only one of the two possible orientations of the η<sup>2</sup>-iminoacyl unit is observed. NOE measurements show a through space enhancement of the *ortho*-methyls of the N-xylyl group upon irradiation of the remaining Hf-Me resonance, which supports the isomer having the N-xylyl group pointing towards the Hf-Me.



Scheme 4.2.

The solid-state molecular structure of **4.7** determined by an X-ray diffraction experiment also verified the  $\eta^2$ -iminoacyl coordination mode. An ORTEP depiction of **4.7** is shown in Figure 4.2 with relevant bond lengths and angles listed in Table 4.1 and crystallographic details given in appendix A. The imino carbon atom is directly bound to the hafnium centre with the Hf1-C36 bond length at 2.251(2) Å, which is similar to related iminoacyl-zirconium complexes (2.23-2.25 Å).<sup>16</sup> The bond angles of the triangle defined by Hf-C26-N5 are typical of other structurally characterized group 4  $\eta^2$ -iminoacyl complexes as is the imino N5-C26 bond length.<sup>16</sup> Surprisingly, the ancillary [NCN] ligand is distorted towards facial coordination with the N4-Hf1-N3 angle being 133.65(7)°.

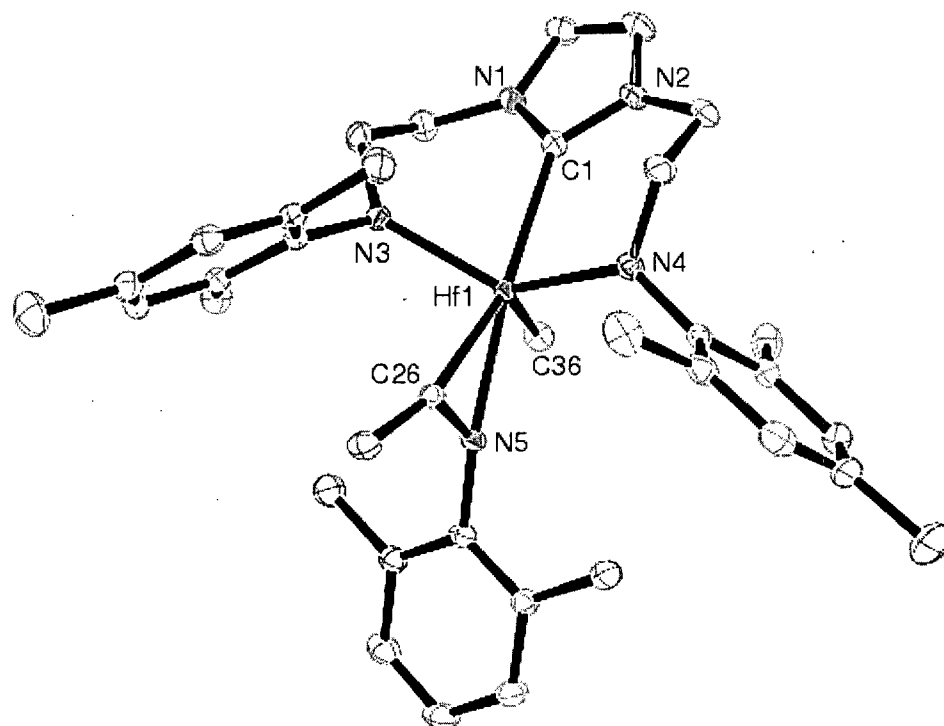


**Figure 4.2.** ORTEP view of  $^{\text{Mes}}[\text{NCN}]\text{Hf}(\eta^2\text{-XyNCCH}_3)(\text{CH}_3)$  (**4.7**) (THF omitted), depicted with 50% ellipsoids; all hydrogen atoms have been omitted for clarity.

**Table 4.1.** Selected Bond Distances (Å) and Bond Angles ( $^\circ$ ) for  $^{\text{Mes}}[\text{NCN}]\text{Hf}(\eta^2\text{-XyNCCH}_3)(\text{CH}_3)$ , (**4.7**).

Bond Lengths		Bond Angles	
Hf1-C1	2.387(2)	N3-Hf1-N4	133.65(7)
Hf1-N3	2.1352(18)	N5-C26-Hf1	73.05(11)
Hf1-N4	2.1117(18)	N4-Hf1-C1	77.25(7)
Hf1-C26	2.251(2)	N3-Hf1-C1	77.72(7)
Hf1-N5	2.2461(16)		
N5-C26			

Addition of a second equivalent of xylyl isocyanide to **4.7** resulted in an immediate color change from pale yellow to dark purple, with the exclusive formation of the bis( $\eta^2$ -iminoacyl) product **4.8** (Scheme 4.2). The presence of an  $\eta^2$ -iminoacyl group is noted by a  $\nu_{\text{C=N}}$  band at  $1568\text{ cm}^{-1}$ . The room temperature  $^1\text{H}$  NMR spectrum of **4.8** in  $\text{CD}_2\text{Cl}_2$  is consistent with a  $C_s$  symmetric species (four inequivalent ethylene spacer

resonances); however, cooling the solution to  $-40^{\circ}\text{C}$  is necessary to fully resolve all resonances. At this lower temperature, two unique environments are observed for each  $\eta^2$ -iminoacyl group consistent with the solid-state molecular structure of **4.8**. An ORTEP depiction of **4.8** is shown in Figure 4.3. Bond lengths and angles for **4.8** are given in Table 4.2 and crystallographic details are given in appendix A. The characteristic iminoacyl  $^{13}\text{C}$  resonance ( $\sim 260$  ppm) was not observed in the  $^{13}\text{C}$  NMR spectrum. This is likely due to fast exchange under the normal acquisition conditions.

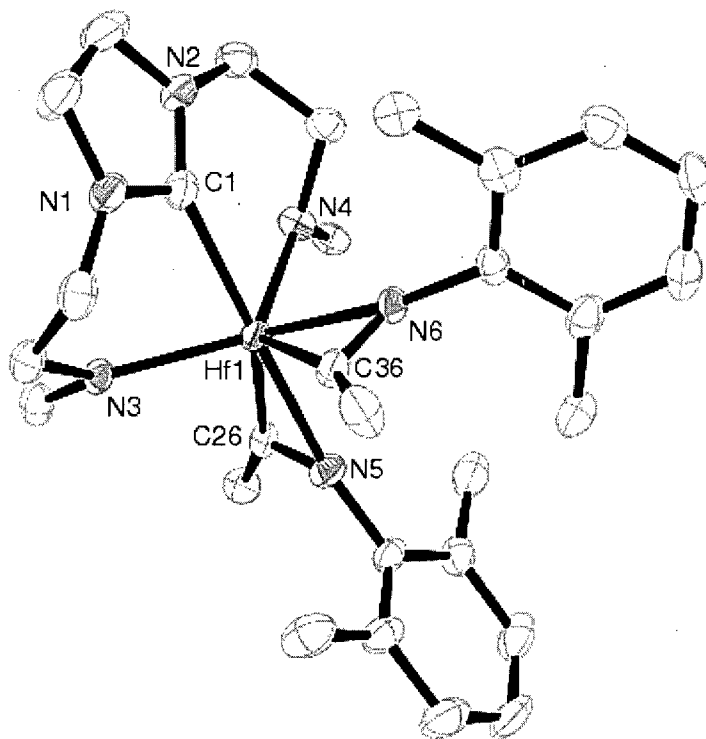


**Figure 4.3.** ORTEP view of  $^{\text{Mes}}[\text{NCN}]\text{Hf}(\eta^2\text{-XyNCCH}_3)_2$  (**4.8**) ( $\text{CH}_2\text{Cl}_2$  omitted), depicted with 50% ellipsoids; all hydrogen atoms and mesityl groups have been omitted for clarity.

**Table 4.2.** Selected Bond Distances (Å) and Bond Angles (°) for <sup>Mes</sup>[NCN]Hf(η<sup>2</sup>-XyNCCH<sub>3</sub>)<sub>2</sub>, (**4.8**).

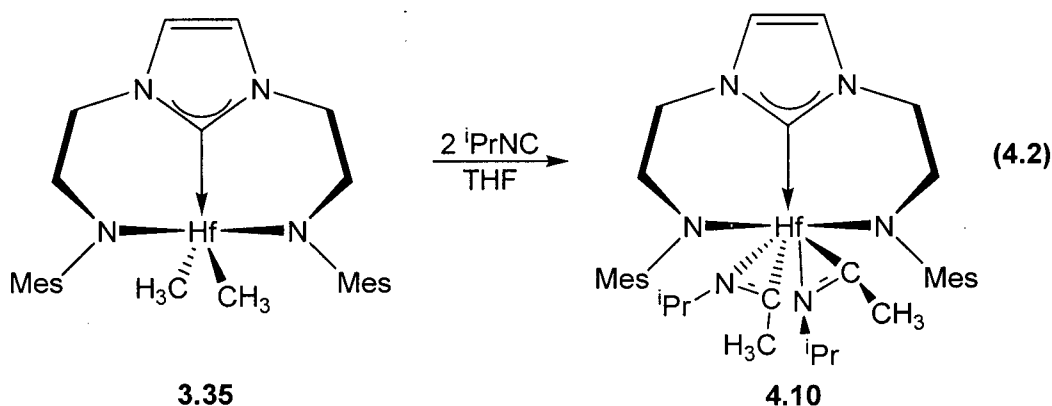
Bond Lengths		Bond Angles	
Hf1-C1	2.377(10)	N3-Hf1-N4	122.6(3)
Hf1-N3	2.154(7)	C26-Hf1-N5	34.0(3)
Hf1-N4	2.146(8)	N4-Hf1-C1	78.2(3)
Hf1-C26	2.249(9)	N3-Hf1-C1	76.2(3)
Hf1-N5	2.250(8)	N6-Hf1-C36	32.3(3)
Hf1-N6	2.305(7)		
Hf1-C36	2.306(10)		

In the solid state, there are two independent molecules in the unit cell with subtle variations in the η<sup>2</sup>-iminoacyl bond lengths (only one of the molecules is used for structural analysis described below). Although formally seven-coordinate, **4.8** is best described as distorted trigonal bipyramidal about hafnium, with each of the η<sup>2</sup>-iminoacyl groups occupying a single coordination site, one axial and one equatorial. The <sup>Mes</sup>[NCN] ligand is puckered towards a facial orientation with N4-Hf1-N3 being 122.6(3)°, presumably to accommodate the additional steric constraints of two xylyl units. The two iminoacyl groups are oriented perpendicular to each other, which is further evidence of the considerable steric interactions in the solid state.

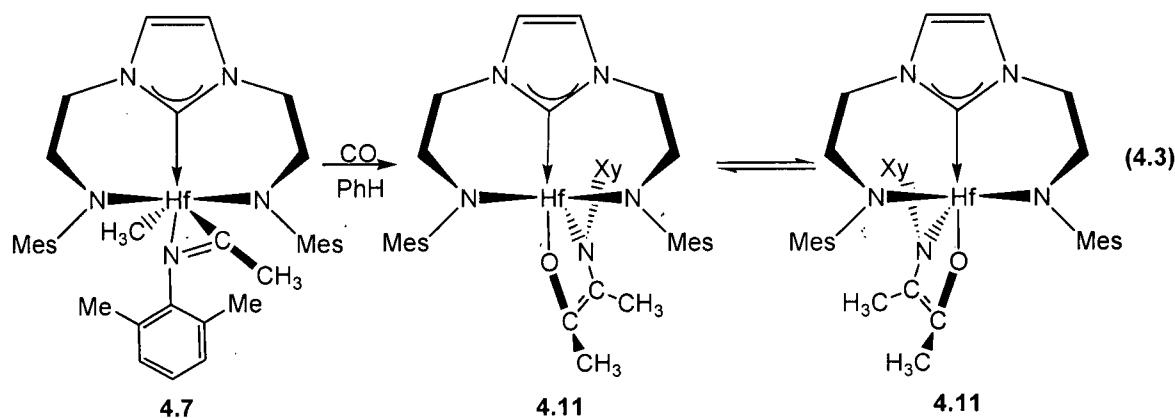
In general, thermolysis of groups 4 and 5 bis(η<sup>2</sup>-iminoacyl) complexes results in the formation of enediamido metallacycles.<sup>20,21</sup> No reaction was observed by <sup>1</sup>H NMR spectroscopy when **4.8** was heated in toluene (110°C for >8h). This is somewhat surprising given that this transformation is reported to be facilitated by lowering the π\*<sub>C=N</sub> orbital via the presence of electron-withdrawing substituents or by having a relatively electron-rich metal centre.<sup>16</sup> Because NHCs are considered strongly σ-donating,<sup>22,23</sup> this should have facilitated this C-C bond coupling process.

To probe the effects of sterics on this process, isopropylisocyanide (<sup>i</sup>PrNC) was added to **4.7** to generate the mixed bis(iminoacyl) species **4.9** (Scheme 4.2). Thermolysis of this material did not result in the formation of an enediamido metallacycle even after extended reaction times at 110°C. Finally, the bis(isopropyl) iminoacyl was prepared by the addition of two equivalents of isopropyl isocyanide to the dimethyl complex **3.35** to generate **4.10** in excellent yield (Equation 4.2). This compound also turned out to be

stable to thermolysis as evidenced by no change in the  $^1\text{H}$  NMR spectrum after one day at  $110^\circ\text{C}$ . Formation of an enediamido metallacycle is known to be affected by the steric bulk located on the nitrogen atom.<sup>24,25</sup> Moreover, for enediamide formation to occur, both  $\eta^2$ -iminoacyls must rotate into the preferred coplanar configuration, which would appear to be difficult in complexes **4.8–4.10** due to the increased steric bulk around the metal centre.<sup>20,21,26-28</sup>



The insertion of carbon monoxide into the remaining metal-alkyl bond in **4.7** was investigated with a view that this smaller molecule would insert and facilitate C=C bond formation. Indeed, a facile reaction is observed when the hafnium methyl-iminoacyl complex **4.7** is exposed to one atmosphere of CO. Interestingly, the product was identified as the enamidolate complex **4.11** (Equation 4.3). The likely first step is insertion of CO into the remaining Hf-CH<sub>3</sub> bond; however, monitoring this process by NMR spectroscopy did not provide any evidence for the presence of a mixed acyl-iminoacyl compound implying that the C=C bond formation process is quite facile. To our knowledge, only one other example of enamidolate synthesis has been reported; however, in contrast to our work, forcing conditions (200-1000 psi of CO) were required.<sup>20</sup>



The solid-state molecular structure of **4.11** was determined by an X-ray diffraction experiment and an ORTEP depiction is shown in Figure 4.4. Relevant bond lengths and angles are listed in Table 4.3, and crystallographic details are located in appendix A. The C=C bond length (1.340(9) Å) compares well with previously described metallocyclopentene metallocycles.<sup>20,29</sup> The eneamidolate ring is distorted from a planar coordination, an observation prominent in most enediolate, eneamidolate and enediamides systems. This bending has been attributed to a  $\eta^2, \pi$  bonding interaction between the electron deficient metal centre and the olefinic portion of the metallacyclic backbone, a phenomenon observed in a similar Zr-butadiene system.<sup>29</sup> A fold angle of 24.0° was found for **4.11**, significantly less than the previously reported fold angles (~50°) of other compounds.<sup>20,30</sup> As a result, the Hf1...C26 and Hf1...C27 distances (2.728(7) and 2.660(6) Å, respectively) are significantly longer than a previously reported eneamidolate complex (2.549(8) and 2.581(8) Å).<sup>21</sup> Once again, the <sup>Mes</sup>[NCN] ancillary ligand is distorted towards facial coordination as evidenced by the N4-Hf1-N3 bond angle of 124.5(2)°. The molecule possesses  $C_1$  symmetry in the solid state as a result of a weak  $\eta^2, \pi$  interaction from the olefin; however,  $C_3$  symmetry is observed in solution at room temperature due to ring flipping of this eneamidolate ring on the NMR time scale. The  $\Delta G^\ddagger$  of 54.1 kJ mol<sup>-1</sup> for the ring flipping process (Equation 4.4) is estimated from the coalescence temperature (268 K), and is very similar to the value estimated for a Hf-enediamide complex (59.4 kJ mol<sup>-1</sup>).<sup>20</sup> Broad resonances for the O-C(CH<sub>3</sub>)= and O-C(CH<sub>3</sub>)= carbon nuclei are observed in the <sup>13</sup>C{<sup>1</sup>H} NMR spectrum at room temperature at 137.0 ppm and 19.4 ppm, respectively.

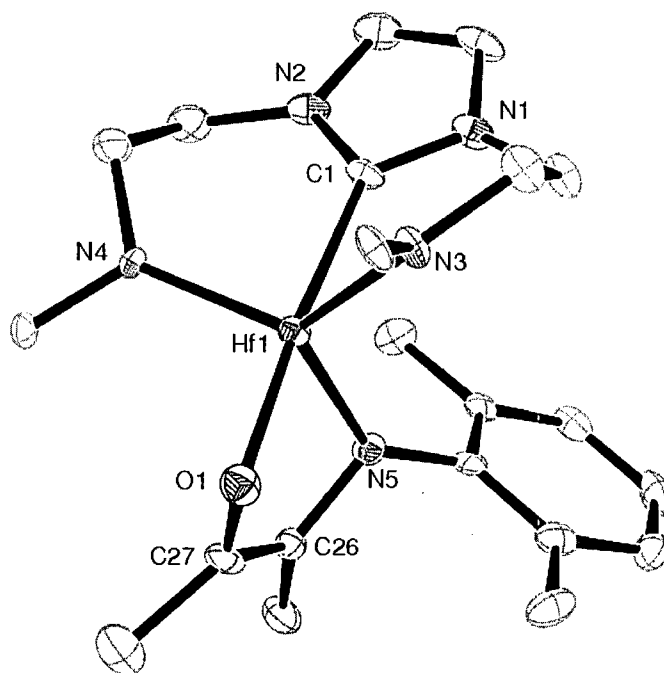


**Figure 4.4.** ORTEP view of  $\text{Mes}[\text{NCN}]\text{Hf}(\text{OC}(\text{CH}_3)=\text{C}(\text{CH}_3)\text{NXy})$ , (**4.11**) ( $1/2 \text{ Et}_2\text{O}$  omitted), depicted with 50% ellipsoids; all hydrogen atoms and mesityl groups have been omitted for clarity.

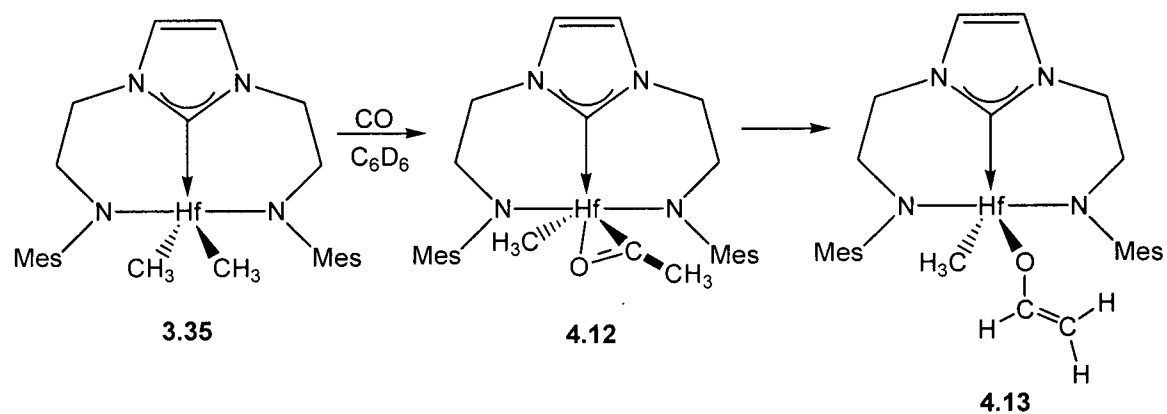
**Table 4.3.** Selected Bond Distances (Å) and Bond Angles ( $^\circ$ ) for  $\text{Mes}[\text{NCN}]\text{Hf}(\text{OC}(\text{CH}_3)=\text{C}(\text{CH}_3)\text{NXy})$ , (**4.11**).

Bond Lengths		Bond Angles	
Hf1-C1	2.348(6)	O1-Hf1-N5	83.14(19)
Hf1-N3	2.077(5)	N3-Hf1-N4	124.5(2)
Hf1-N4	2.082(5)	N3-Hf1-C1	78.1(2)
Hf1-N5	2.061(5)	N4-Hf1-C1	81.2(2)
Hf1-C26	2.728(7)		
Hf1-C27	2.660(6)		
Hf1-O1	2.032(4)		
C6-C27	1.340(9)		
Hf1...C26	2.728(7)		
Hf1...C27	2.660(6)		

#### 4.4. Formation of a Hafnium Vinyl-enolate and Enediolate Metallacycle

Due to its ease of preparation and its enhanced thermal stability relative to zirconium dialkyl complexes, the hafnium dimethyl derivative **3.35** was chosen for

reactivity studies with CO. Exposure of **3.35** to one atmosphere of carbon monoxide for one day results in the formation of  $^{\text{Mes}}[\text{NCN}]\text{Hf}(\text{CH}_3)(\text{O}-\text{CH}=\text{CH}_2)$  (**4.13**), a hafnium vinyl-enolate (Scheme 4.3). Diagnostic resonances appear in the  $^1\text{H}$  NMR spectrum at 3.47 ppm, 3.54 ppm, and 5.75 ppm, with appropriate geminal and vicinal coupling constants. The downfield resonance at 5.75 ppm, assigned to the  $\alpha$ -O-CH= proton, splits further when  $^{13}\text{CO}$  is substituted, giving typical  $^1J_{^{13}\text{C}-^1\text{H}}$  coupling of 145 Hz.<sup>31</sup> The  $^{\text{Mes}}[\text{NCN}]$  ligand resonances are diagnostic of a  $C_s$  symmetric compound and also consistent with the Hf-CH<sub>3</sub> resonance located at 0.37 ppm. The  $^{13}\text{C}\{^1\text{H}\}$  NMR spectrum reveals a Hf-NHC carbene signal at 196.2 ppm, as well as vinyl  $^{13}\text{C}$  resonances at 120.2 ppm and 139.0 ppm. From the solution NMR data, a definitive orientation of the ligand remains unknown, and for this reason, a *mer* geometry is shown, despite the fact that the mono insertion adduct of XyNC (**4.7**) has a facial coordination of the ancillary ligand.

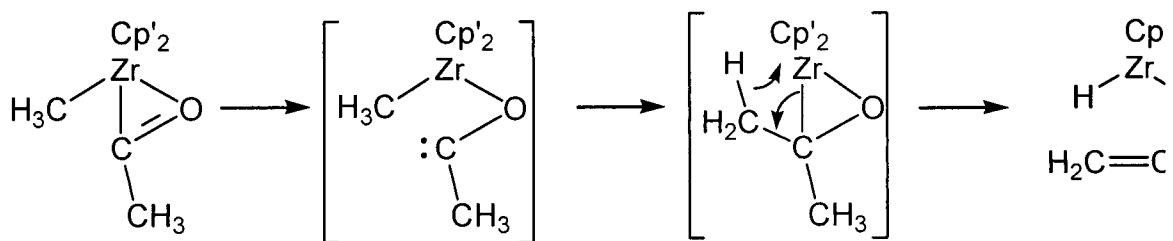


Scheme 4.3.

Monitoring the reaction of CO with the dimethyl complex showed the formation of the  $\eta^2$ -acyl intermediate  $^{\text{Mes}}[\text{NCN}]\text{Hf}(\eta^2\text{-COCH}_3)(\text{CH}_3)$  **4.12**, as evidenced by a singlet at 1.62 ppm for the acetyl methyl protons. This resonance splits into a doublet with the use of  $^{13}\text{CO}$  ( $^1J_{^{13}\text{C}-^1\text{H}} = 7$  Hz), confirming that simple insertion has occurred. The  $^{13}\text{C}\{^1\text{H}\}$  NMR spectrum features a resonance at 339.6 ppm, and is typical for the acyl carbonyl carbon of reported Hf( $\eta^2$ -acyl) complexes.<sup>16</sup> IR spectroscopy was also useful in

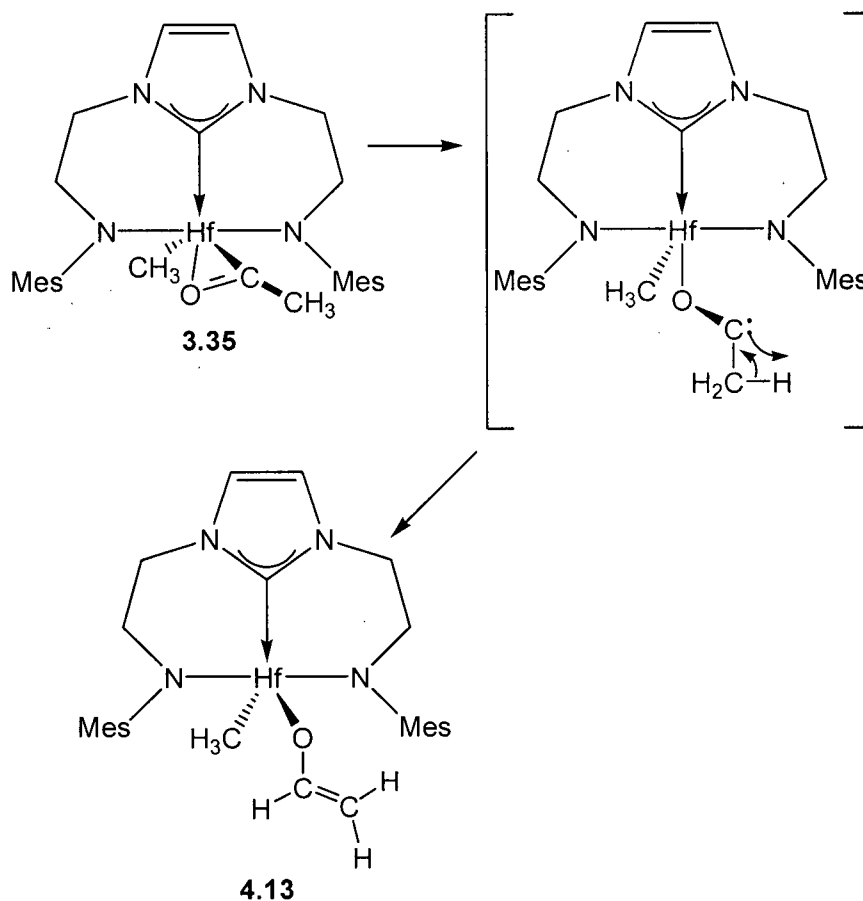
the determination of the  $\text{Hf}(\eta^2\text{-acetyl})$  moiety with a  $\nu_{\text{C=O}}$  stretch observed at  $1540\text{ cm}^{-1}$ , characteristic of similar compounds.

The rearrangement of the hafnium methyl-acetyl complex **4.12** to the methyl-vinyl enolate derivative **4.13** was unexpected. The high reactivity of group 4 methyl-acetyl complexes has been ascribed to the oxy-carbene resonance form of the  $\eta^2\text{-acetyl}$  moiety.<sup>31,32</sup> This species can undergo intramolecular coupling with the adjacent methyl group,<sup>33</sup> which is followed by hydrogen abstraction by the metal to generate a hydridomethylvinyl-enolate complex (Scheme 4.4).



Scheme 4.4.

In the case of the hafnium methyl-acetyl complex **4.12**, the formation of the vinyl enolate suggests that the oxy-carbene resonance form preferentially undergoes a hydrogen-atom shift from the methyl substituent of the carbene carbon to generate the observed vinyl enolate (Scheme 4.5). Presumably, the  $\eta^2\text{-acetyl}$  unit of **4.12** is oriented in such a way as to disfavor C-C coupling with the  $\text{Hf-CH}_3$  unit, and instead, hydrogen transfer from the methyl occurs. Whether or not this is a result of a geometric constraint caused by the different ancillary ligands or an electronic effect is unknown. Similar hydrogen and silyl group migrations have been reported for  $\text{Cp}_3\text{ThR}$  and  $\text{Cp}_2^*\text{ThR}(\text{Cl})$  derivatives upon reaction with  $\text{CO}$ .<sup>34</sup>



Scheme 4.5.

Continued exposure of **4.13** to CO results in the formation of an insoluble, white powder. ES-MS shows a molecular ion peak at 652  $m/z$  indicative of a second CO insertion; however, the insolubility of this product has hampered further characterization efforts.

It has been shown that the nature of carbonylation products is dependent on substituents on the metal.<sup>35</sup> With this in mind, the carbonylation of the hafnium diisobutyl complex, **3.38**, was investigated. Exposure of **3.38** to one atmosphere of CO for an extended period (5 days) results in the precipitation of colorless crystals in reasonable yield. Analysis of these crystals by solid-state X-ray diffraction indicated that this material is the dihafnium bis(enediolate) complex,  $(^{\text{Mes}}[\text{NCN}]\text{Hf})_2(\mu\text{-OC}(\text{tBu})=\text{C}(\text{tBu})\text{O})_2$ , **4.16** (Equation 4.6). The ORTEP diagram is shown in Figure 4.5, bond lengths and angles are shown in Table 4.4, and crystallographic details are located

in appendix A. Examination of the C-C bond length suggests double bond character (avg. 1.342(15) Å) and is similar to other early transition metal enediolate complexes.<sup>36</sup> The [NCN] ligand distorts to a facial geometry having an N4-Hf1-N3 bond angle of 124.4(3)°. Hf-C alkyl and Hf-N amido bond lengths are similar to previously discussed complexes. The <sup>1</sup>H NMR spectrum is consistent with a C<sub>s</sub> symmetric species in solution with two distinct *iso*-butyl resonances. In addition, **4.16** exhibits a weak <sup>13</sup>C resonance at 140.0 ppm characteristic of an olefinic C=C bond (<sup>1</sup>J<sub>C-<sup>13</sup>C</sub> = 20 Hz with <sup>13</sup>CO).

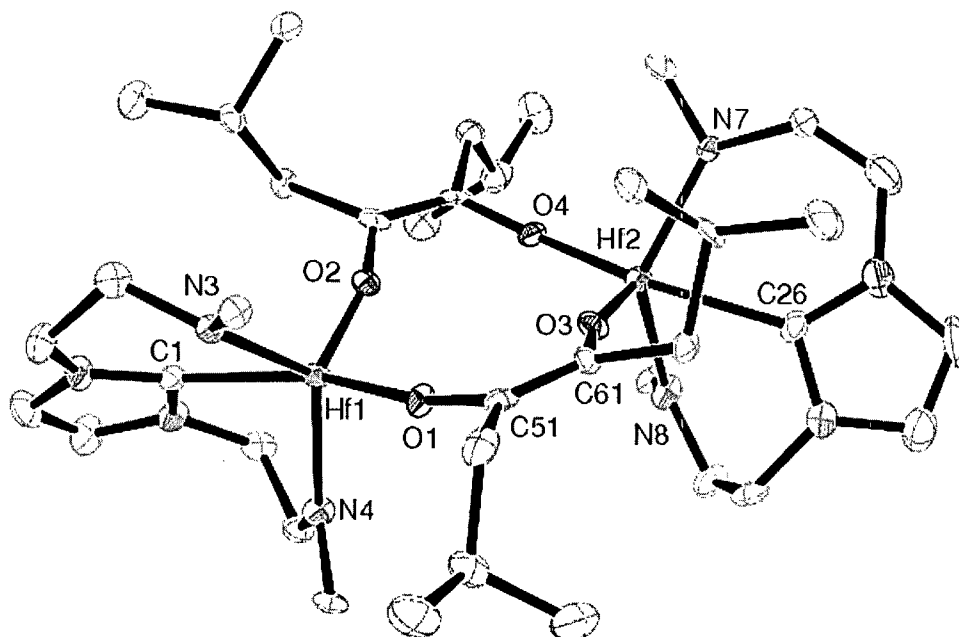
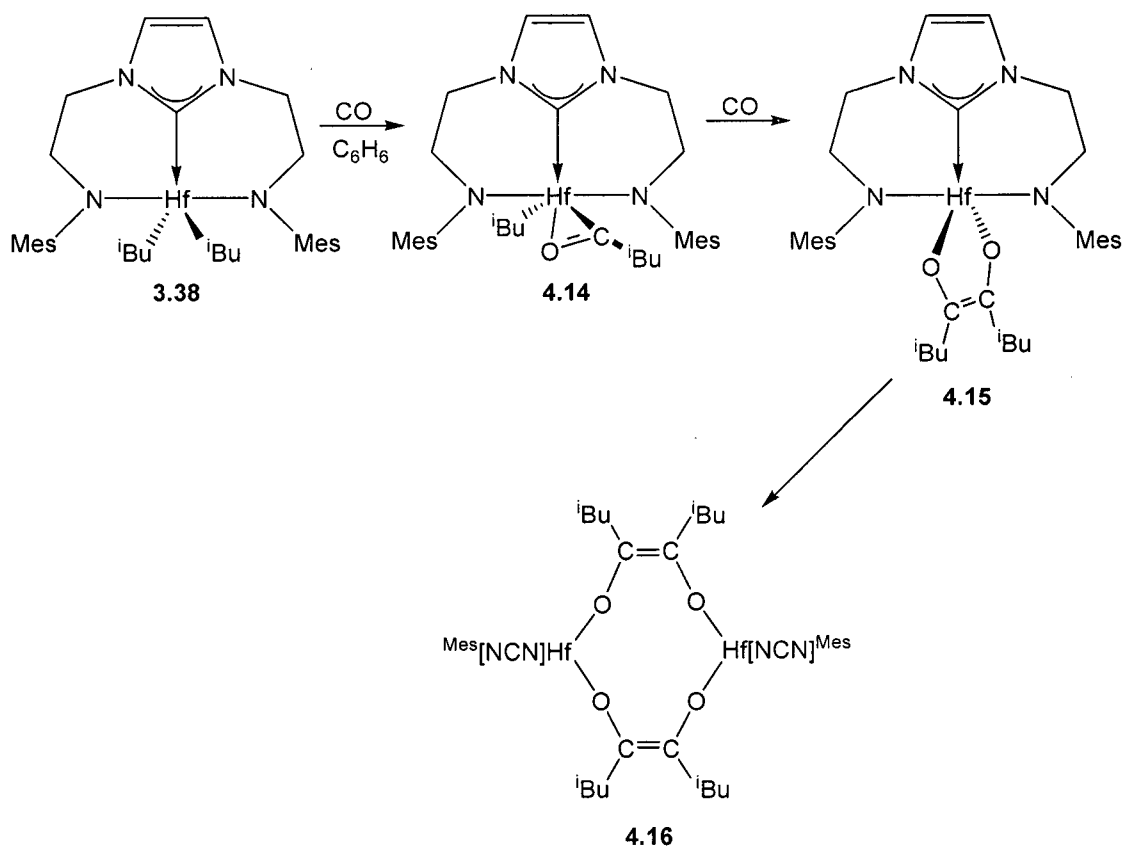


**Figure 4.5.** ORTEP view of (<sup>Mes</sup>[NCN]Hf)<sub>2</sub>(μ-OC(<sup>i</sup>Bu)=C(<sup>i</sup>Bu)O)<sub>2</sub>, (**4.16**) (4 C<sub>6</sub>H<sub>6</sub> omitted), depicted with 50% ellipsoids; all hydrogen atoms and mesityl groups have been omitted for clarity.

**Table 4.4.** Selected Bond Distances (Å) and Bond Angles (°) for (<sup>Mes</sup>[NCN]Hf)<sub>2</sub>(μ-OC(<sup>i</sup>Bu)=C(<sup>i</sup>Bu)O)<sub>2</sub>, (**4.16**).

Bond Lengths		Bond Angles	
Hf1-C1	2.387(9)	O1-Hf1-O2	105.4(2)
Hf1-N3	2.109(7)	N3-Hf1-N4	124.4(3)
Hf1-N4	2.097(7)	N3-Hf1-C1	77.8(3)
Hf1-O1	1.937(5)	N4-Hf1-C1	77.1(3)
Hf1-O2	1.912(6)	C51-O1-Hf1	169.4(6)
C51-C61	1.341(12)	C52-O1-Hf1	163.1(6)

The mechanism of the formation of the dinuclear bis(enediolate) was examined by monitoring the reaction of **3.38** with CO as a function of time using NMR spectroscopy. The first intermediate formed is the hafnium isobutyl-acyl species, **4.14**, clearly distinguished by a  $^{13}\text{C}\{^1\text{H}\}$  NMR singlet at 338.4 ppm, attributed to a  $\text{Hf}(\text{O}=\text{C}^i\text{Bu})$  resonance. This finding is analogous to other early transition metal  $\eta^2$ -acyl complexes (Scheme 4.6).<sup>16</sup> The  $^1\text{H}$  NMR spectrum reveals a  $C_s$  symmetric species in solution with two distinct *iso*-butyl resonances. An upfield resonance at 1.68 ppm, assigned to the methylene protons  $\alpha$  to the acyl carbonyl of one *iso*-butyl unit, splits into a doublet of doublets when  $^{13}\text{CO}$  was used ( $^2J_{^{13}\text{C}-^1\text{H}} = 4.7$  Hz). Again, the coordination mode of the  $^{\text{Mes}}[\text{NCN}]$  ligand in **4.14**, *mer* vs *fac*, is not assignable with the NMR data available.

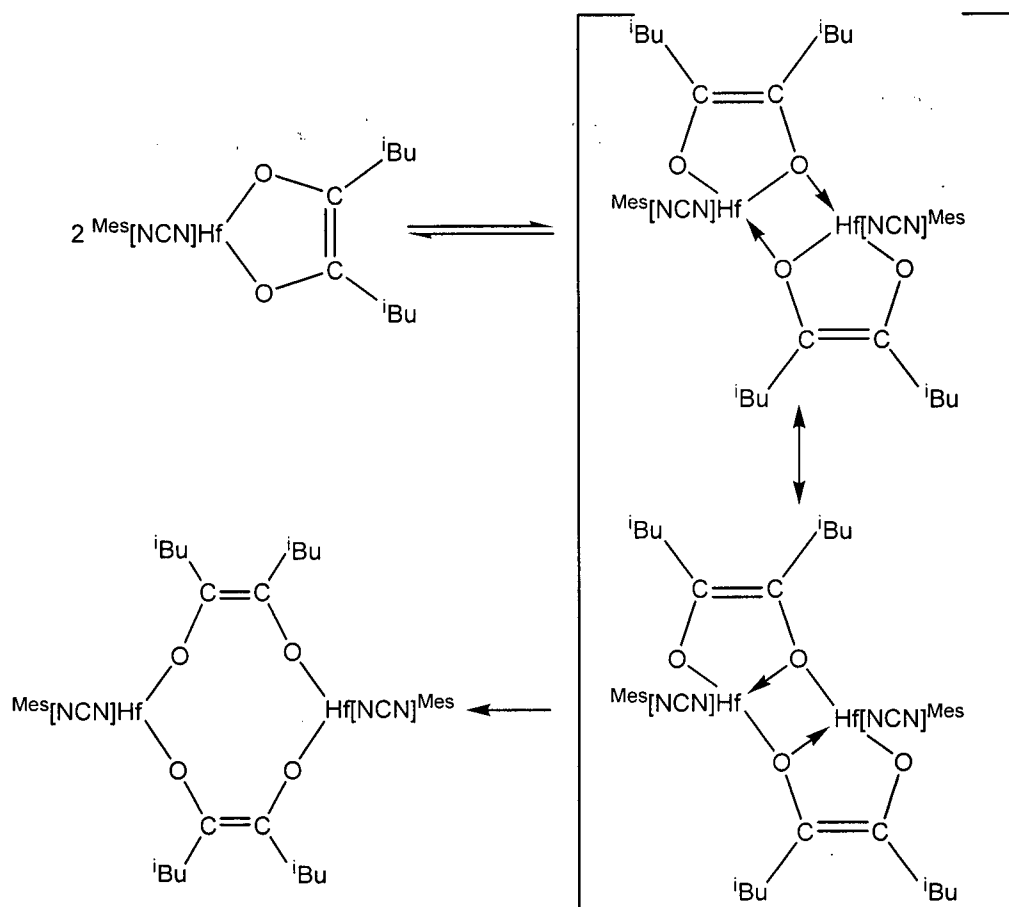


Scheme 4.6.

Continued exposure of **4.14** to CO results in the formation of a new product having  $C_{2v}$  symmetry (one set of *iso*-butyl resonances) in solution and distinct from the

final dihafnium macrocycle **4.16** (Scheme 4.6). Only one *iso*-butyl resonance is present in the  $^1\text{H}$  NMR spectrum at room temperature, suggestive of a CO insertion into the remaining Hf-CH<sub>2</sub> alkyl bond of **4.14**. The  $^{13}\text{C}\{^1\text{H}\}$  NMR spectrum of this species displays a weak resonance at 140.6 ppm which suggests that a new C=C bond is formed. This spectroscopic evidence is consistent with the formation of the mononuclear hafnium-enediolate, **4.15** (Scheme 4.6). The synthesis of this enediolate likely proceeds through a bis( $\eta^2$ -acyl) species, the presence of which was not observed by  $^1\text{H}$  NMR studies. In solution, the nuclearity of the enediolate **4.15** is assumed to be mononuclear; however, there are early transition metal enediolates reported in both monomeric and dimeric forms, depending on the steric bulk of the alkyl group.<sup>35</sup> For example, when the alkyl group is bulky (R=CH<sub>2</sub>C(CH<sub>3</sub>)<sub>3</sub>, CH<sub>2</sub>Si(CH<sub>3</sub>)<sub>3</sub>) monomeric species have been observed, and with smaller groups (R=H, CH<sub>3</sub>, CH<sub>2</sub>Ph), higher nuclearity species have been reported. Indeed, there are several reports of monomeric enediolates dimerizing to form dinuclear complexes (Scheme 4.7).<sup>37,38</sup> In one example, such complexes show dynamic behavior interconverting oxygen atoms through a low activation-energy process by a ten-membered metallacycle intermediate, similar in structure to the final product **4.16**.<sup>37</sup>

A reasonable proposal for the formation of **4.16** is shown in Scheme 4.7, and involves dimerization of **4.15** via dative oxygen-hafnium interactions that are converted to covalent bonds. This dimerization is followed by ring-opening to generate the 10-membered dihafnium macrocycle. The driving force for the formation of the dinuclear complex **4.16** may be the better oxygen-to-hafnium  $\pi$ -donation, an overlap that is more difficult in the mononuclear complex **4.15** with the five-membered enediolate ring.<sup>39-41</sup> Examination of the solid state structure of **4.16** reveals an average Hf-O-C bond angle of 163.5(3) $^\circ$  and reflects such a  $\pi$ -donation. The reason for the differences in reactivity between alkyl substituents may be attributed to competitive dimerization and insertion pathways. Such considerations have been attributed to the nucleophilic character of the alkoxy-carbene moiety and have been well-documented in actinide and tantalum metallocene systems.<sup>34,42</sup>

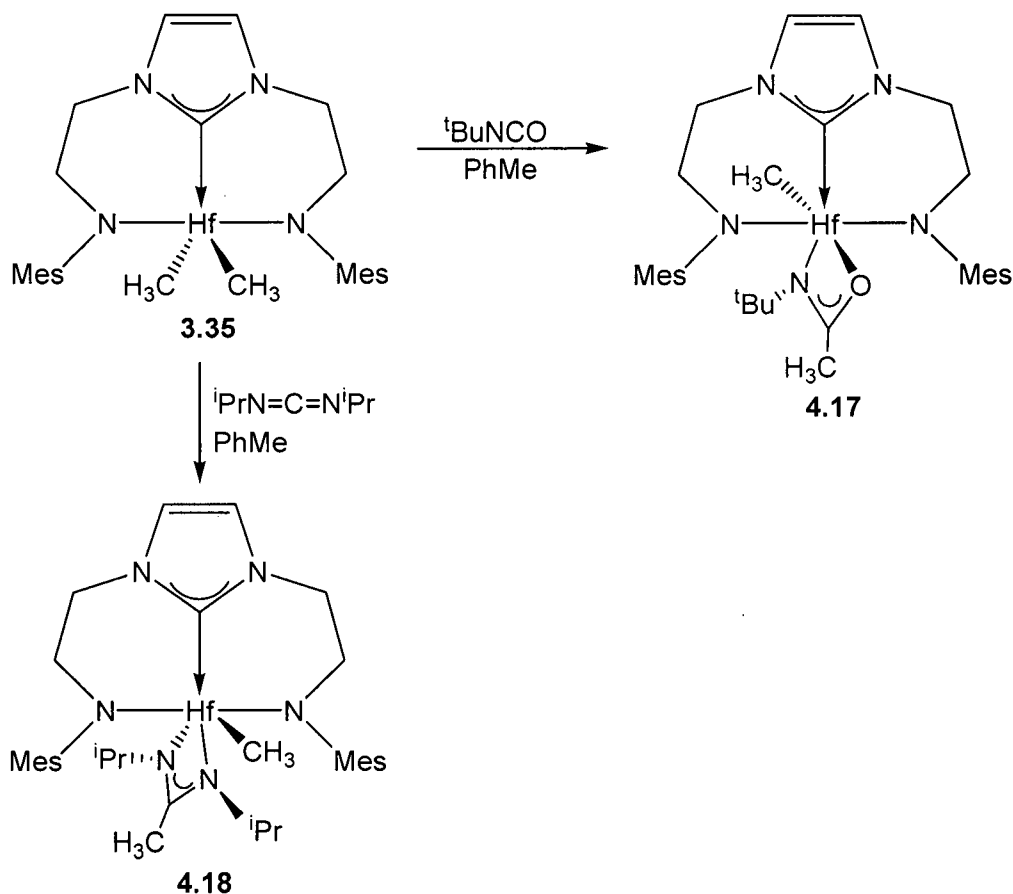


Scheme 4.7.

#### 4.5. Formation of Amidate and Amidinate Metallacycles

The transition-metal-assisted formation of new C-C bonds from insertion reactions with other simple organic molecules was also investigated. The insertion of cumulenes, such as isocyanates and carbodiimides, into zirconium-alkyl bonds has been shown to yield amidate<sup>43</sup> and amidinate<sup>43-46</sup> ligands, respectively. With this in mind, the reaction of *tert*-butyl isocyanate with the hafnium-dimethyl complex **3.35** was investigated (Scheme 4.8). This reaction proceeds immediately at room temperature to yield **4.17** as an off-white powder in 84% yield. The  $^1\text{H}$  and  $^{13}\text{C}\{^1\text{H}\}$  NMR spectra are consistent with the symmetrical bidentate coordination of an amidate ligand. Most notably, a  $^{13}\text{C}$  resonance at 180.4 ppm is indicative of an  $-\text{NC}(\text{Me})\text{O}$  moiety, which is similar to other reported metal amidate compounds.<sup>43</sup> Interestingly, the addition of

excess isocyanate did not produce a bis(amidate) product, which could result from increased steric interactions at the metal centre.



**Scheme 4.8.**

A single crystal X-ray diffraction experiment confirmed the identity of the product as **4.17**. An ORTEP depiction of **4.17** is shown in Figure 4.6 with relevant bond lengths and angles listed in Table 4.5 and crystallographic details located in appendix A. The geometry about the hafnium metal centre is a distorted trigonal bipyramid with the amidate group occupying one of the coordination sites. The metallacycle core as defined by N5-Hf1-O1-C26 is essentially planar (torsion angle of N-Hf-O-C = 8.9°). The N5-C26 and O1-C26 bond lengths (1.299(3) Å and 2.1351(17) Å, respectively) are similar to previously reported group 4 amidate compounds as is the amidate bite angle defined by O1-Hf1-N5 bond angle (58.02(8)°).<sup>43</sup>

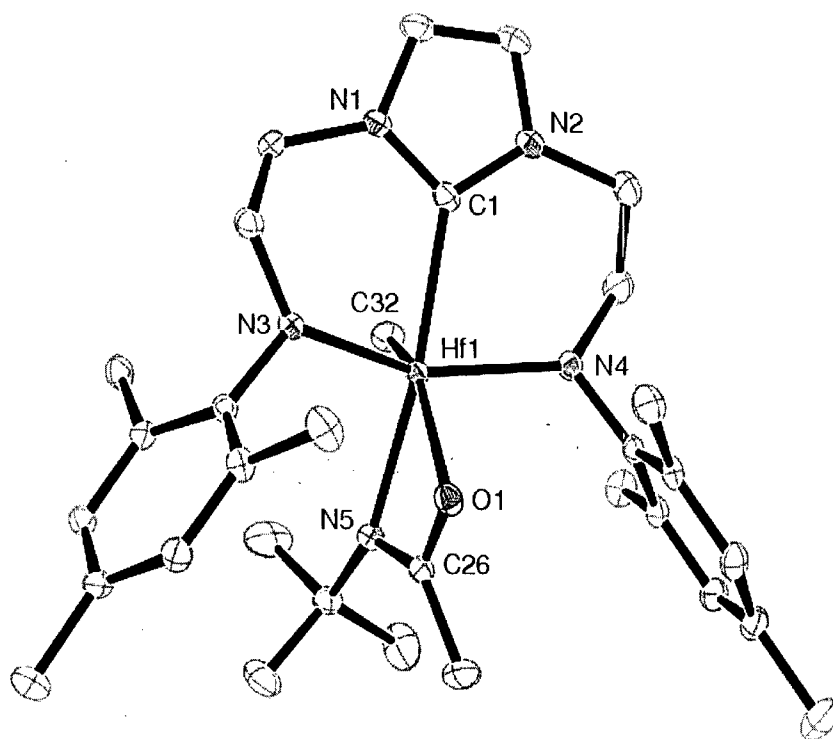


**Figure 4.6.** ORTEP view of  $\text{Mes}[\text{NCN}]\text{Hf}(\text{Me})(\eta^3\text{-}^t\text{BuNC}(\text{Me})\text{O})$  (**4.17**) depicted with 50% ellipsoids; all hydrogen atoms have been omitted for clarity.

**Table 4.5.** Selected Bond Distances (Å) and Bond Angles ( $^\circ$ ) for  $\text{Mes}[\text{NCN}]\text{Hf}(\text{Me})(\eta^3\text{-}^t\text{BuNC}(\text{Me})\text{O})$ , (**4.17**).

Bond Lengths		Bond Angles	
Hf1-C1	2.385(3)	N3-Hf1-N4	145.47(8)
Hf1-N3	2.116(2)	N3-Hf1-C1	78.59(9)
Hf1-N4	2.124(2)	N4-Hf1-C1	78.35(8)
Hf1-N5	2.374(2)	Hf1-N5-C26	87.02(8)
Hf1-O1	2.1351(17)	Hf1-O1-C26	97.65(8)
Hf1-C26	2.646(3)	O1-C26-N5	115.04(8)
Hf1-C32	2.270(3)	O1-Hf1-N5	58.02(8)
C26-N5	1.299(3)	C26-N5-Hf1-O1	8.9
C26-O1	1.305(3)		

Carbodiimides have also been shown to insert into titanium- and zirconium-alkyl bonds to form amidinate complexes.<sup>43</sup> Indeed, the addition of one equivalent of  $^i\text{PrN}=\text{C}=\text{N}^i\text{Pr}$  to a toluene solution of **3.35** results in the formation of **4.18** as the exclusive product (Scheme 4.8). The  $^1\text{H}$  NMR spectrum reveals that the desired

amidinate was produced with no evidence of multiple insertions of the carbodiimide molecule. In solution, a single hafnium-methyl resonance was observed at  $-0.06$  ppm in addition to a methyl resonance at  $1.74$  ppm. Two inequivalent isopropyl moieties are also observed, implying the orientation of the amidinate ligand shown in Scheme 4.8. The  $^{13}\text{C}\{^1\text{H}\}$  NMR spectrum is also informative with a  $^{13}\text{C}$  resonance at  $179.4$  ppm, indicative of a  $-\text{NC}(\text{Me})\text{N}$  group.

The formation of **4.18** was confirmed by an X-ray diffraction experiment performed on crystals grown from a concentrated  $\text{Et}_2\text{O}$  solution. An ORTEP depiction of **4.18** is shown in Figure 4.7 with bond lengths and angles given in Table 4.6 and crystallographic details located in appendix A. Although formally six-coordinate, the geometry at the hafnium centre is best described as a distorted trigonal bipyramid, with the amidinate moiety occupying one coordination site. The N3-Hf1-N4 and N3-Hf1-C1 bond angles in **4.18** are similar to the amidate complex **4.17**. The amidinate bite angle defined by the N5-Hf1-N6 bond angle is  $58.45(7)^\circ$ , similar to other reported metal-amidinate complexes.<sup>44,47,48</sup> The metal carbene bond length is  $2.418(3)$  Å, typical of other [NCN] Hf complexes. The  $\text{RC}(\text{NR}')_2\text{Hf}$  core forms a nearly planar metallacycle as defined by the torsion angle formed by C27-N5-Hf1-N6. The C-N bond distances are approximately equal and are intermediate between C=N double bond distances in carbodiimides ( $1.16$ - $1.22$  Å)<sup>49</sup> and  $\text{C}(\text{sp}^2)\text{-N}$  single bond distances ( $1.47$  Å).<sup>50</sup>

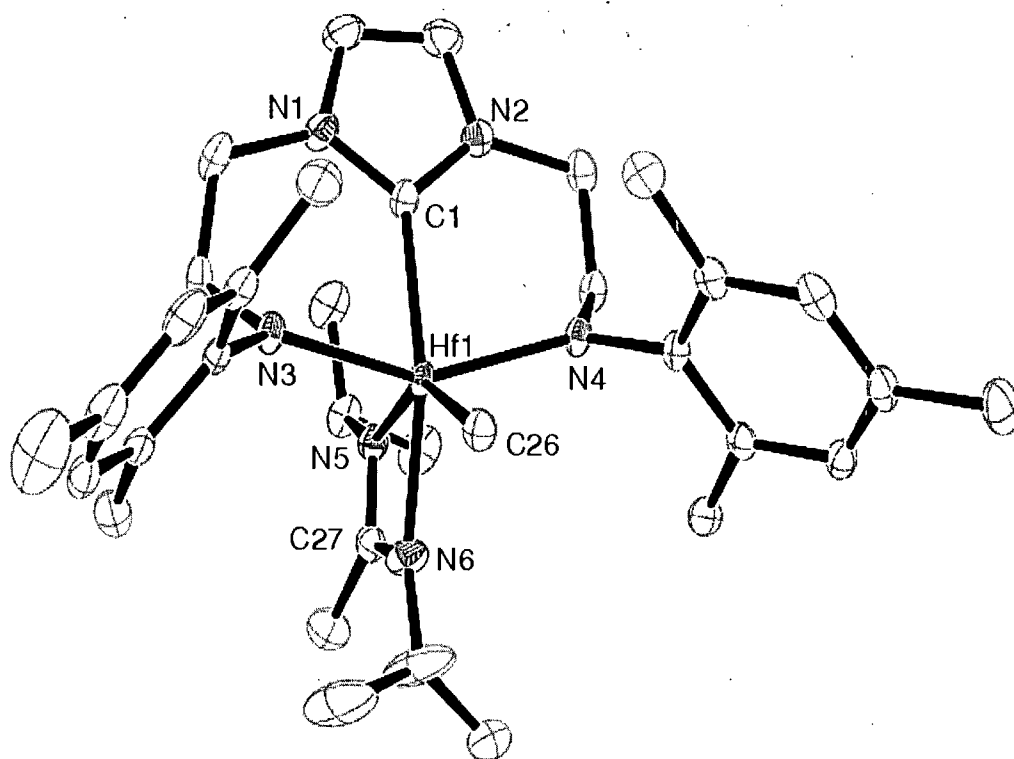


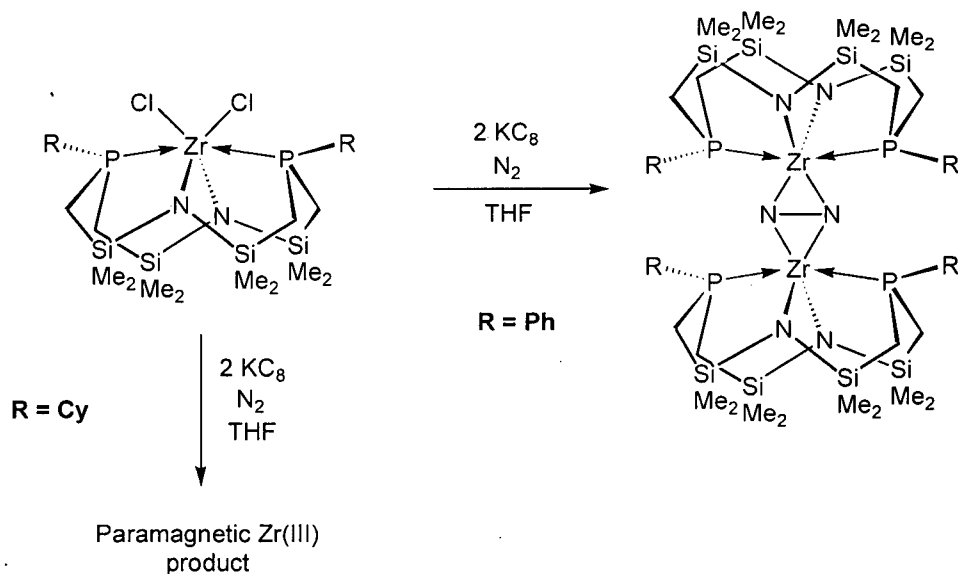
**Figure 4.7.** ORTEP view of  $\text{Mes}[\text{NCN}]\text{Hf}(\text{Me})(\eta^3\text{-}^i\text{PrNC}(\text{Me})\text{N}^i\text{Pr})$  (**4.18**) depicted with 50% ellipsoids; all hydrogen atoms have been omitted for clarity.

**Table 4.6.** Selected Bond Distances (Å) and Bond Angles (°) for  $\text{Mes}[\text{NCN}]\text{Hf}(\text{Me})(\eta^3\text{-}^i\text{PrNC}(\text{Me})\text{N}^i\text{Pr})$ , (**4.18**).

Bond Lengths		Bond Angles	
Hf1-C1	2.418(3)	N3-Hf1-N4	147.38(7)
Hf1-N3	2.130(2)	N3-Hf1-C1	78.91(6)
Hf1-N4	2.120(2)	N4-Hf1-C1	77.88(7)
Hf1-N5	2.235(2)	Hf1-N5-C27	92.80(7)
Hf1-N6	2.292(2)	Hf1-N6-C27	96.06(8)
Hf1-C26	2.282(2)	N6-C27-N5	112.05(8)
Hf1-C(7)	2.714(2)	N5-Hf1-N6	58.45(7)
C27-N5	1.345(2)	C7-N5-Hf1-N6	4.9
C27-N6	1.321(2)		

## 4.6. Attempted Synthesis of Group 4 [NCN] Dinitrogen Complexes

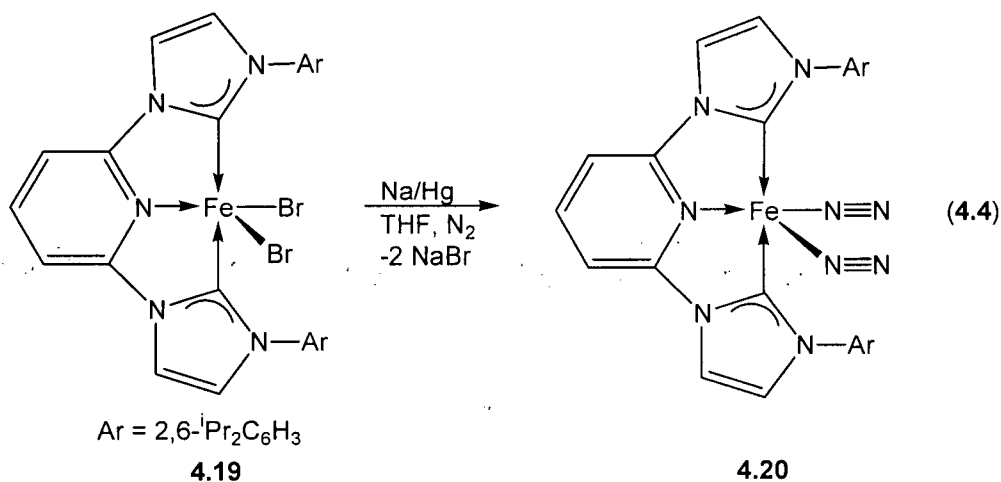
Research in the Fryzuk group has centered on the use of [PNP], [P<sub>2</sub>N<sub>2</sub>] and [NPN] ligands for the preparation of early transition metal dinitrogen complexes. In particular, the reduction of metal chlorides with strong reducing agents in the presence of dinitrogen generally affords dinitrogen complexes with different N<sub>2</sub> binding modes.<sup>51-57</sup> For example, the reduction of [P<sub>2</sub>N<sub>2</sub>]ZrCl<sub>2</sub> with KC<sub>8</sub> in the presence of dinitrogen yields the side-on dinitrogen complex ([P<sub>2</sub>N<sub>2</sub>]Zr)(μ-η<sup>2</sup>:η<sup>2</sup>-N<sub>2</sub>) in good yields (Scheme 4.9).<sup>54</sup> Although this reduction method is successful for many amidophosphine stabilized ETM complexes, reduction of the cyclohexyl-substituted analog <sup>Cy</sup>[P<sub>2</sub>N<sub>2</sub>]ZrCl<sub>2</sub> fails to yield a dinitrogen complex, instead producing a paramagnetic Zr(III) complex.<sup>58</sup> Evidently, a slight modification in the electronic nature of the ligand can influence the products obtained from the reduction process.



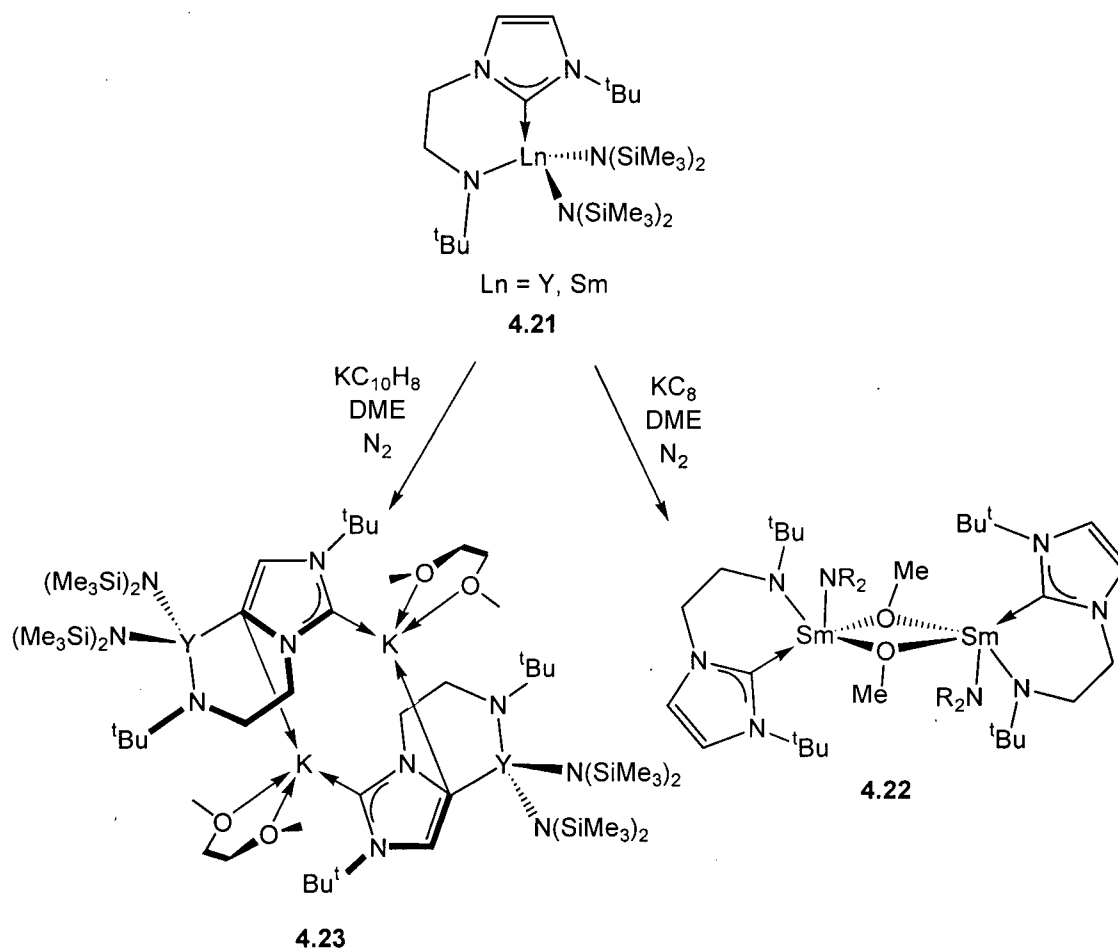
Scheme 4.9.

The first molecular dinitrogen complex stabilized by an NHC ligand was recently reported.<sup>59</sup> The reduction of the iron complex **4.19** with an excess of Na/Hg amalgam in THF under dinitrogen gives the bis-dinitrogen complex **4.20** (Equation 4.4). Like many

LTM dinitrogen complexes, the nitrogen ligands are weakly activated by the iron centre and display N-N bond lengths (avg. 1.114 Å) that are similar to free N<sub>2</sub> (1.0975 Å).

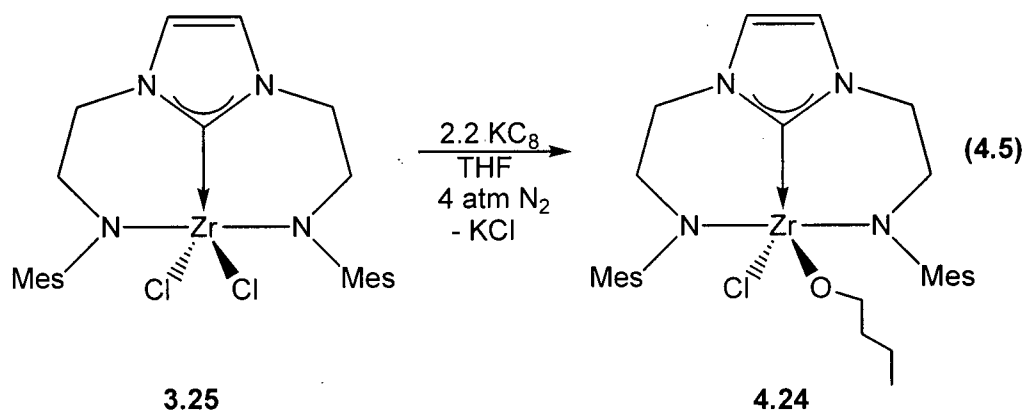


The reduction of metal-NHC complexes does not necessarily result in the formation of dinitrogen complexes.<sup>60,61</sup> Treatment of the samarium derivative of **4.21** with 2.2 equivalents of KC<sub>8</sub> in the presence of DME results in the isolation of **4.22**, a bridging ether cleavage product (Scheme 4.10). The formation of **4.22** was postulated to proceed via a reduced Sm(II) intermediate, which could activate the DME solvent. The reduction of an yttrium derivative of **4.21** reveals that the NHC is also capable of participating in this reduction chemistry. The olefinic carbon backbone of the five-membered NHC ring undergoes reduction during the reaction of KC<sub>8</sub>H<sub>10</sub> with the yttrium derivative **4.21**, which facilitates deprotonation of the NHC ring to generate **4.23**. These results suggest that both the metal centre and the NHC unit are capable of engaging in reduction chemistry.



Scheme 4.10.

The addition of 2.2 equivalents of potassium graphite to **3.25** in a solution of THF under 4 atmospheres of nitrogen results in the immediate formation of a yellow solution. A small amount of a yellow crystalline solid was obtained upon removal of the solvent, addition of Et<sub>2</sub>O, and filtration through Celite (Equation 4.5). Surprisingly, the <sup>1</sup>H NMR spectrum is consistent with a C<sub>s</sub> symmetric species in solution with the appropriate ligand resonances and unexpected alkyl resonances between 1.0 and 1.5 ppm. Additionally, a triplet is observed at 3.5 ppm indicative of a –OCH<sub>2</sub> moiety. The <sup>13</sup>C{<sup>1</sup>H} NMR spectrum confirms a metal-carbene interaction in addition to a downfield –OCH<sub>2</sub> <sup>13</sup>C resonance. The presence of these functionalities in the NMR spectra suggests that THF is incorporated in the final product.



Single crystals of **4.24** were grown from a concentrated Et<sub>2</sub>O solution and the molecular solid state structure was determined by X-ray crystallography. An ORTEP depiction is shown in Figure 4.8 with bond lengths and angles given in Table 4.7 and crystallographic details located in appendix A. Remarkably, the solid state structure shows the presence of an *n*-butoxide group, in addition to the typical arrangement of the [NCN] ligand. The ligand assumes a meridional orientation with respect to a distorted trigonal bipyramidal zirconium metal centre. The Zr1-O1 bond distance of 1.912(3) Å is similar to other reported Zr-alkoxide complexes,<sup>62,63</sup> as are the Zr-N amide and Zr-C NHC bond distances.

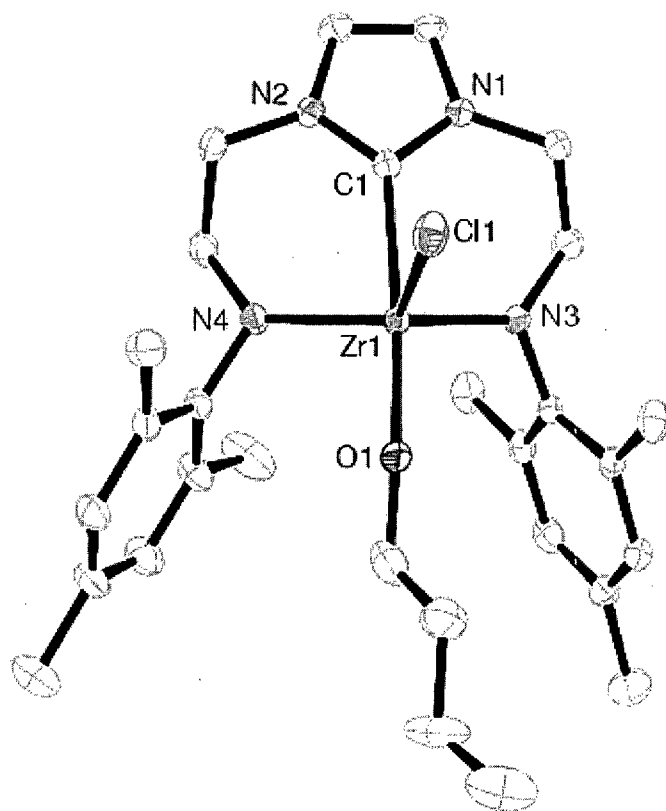


**Figure 4.8.** ORTEP view of  $^{\text{Mes}}[\text{NCN}]\text{Zr}(\text{Cl})(\text{OCH}_2\text{CH}_2\text{CH}_2\text{CH}_3)$  (**4.24**) depicted with 50% ellipsoids; all hydrogen atoms have been omitted for clarity.

**Table 4.7.** Selected Bond Distances (Å) and Bond Angles ( $^\circ$ ) for  $^{\text{Mes}}[\text{NCN}]\text{Zr}(\text{Cl})(\text{OCH}_2\text{CH}_2\text{CH}_2\text{CH}_3)$ , (**4.24**).

Bond Lengths		Bond Angles	
Zr1-C1	2.379(3)	N3-Zr1-N4	126.35(11)
Zr1-N3	2.101(3)	N3-Zr1-C1	78.70(11)
Zr1-N4	2.103(3)	N4-Zr1-C1	78.84(10)
Zr1-O1	1.912(2)	O1-Zr1-C1	167.44(12)
Zr1-Cl1	2.4649(14)	Cl1-Zr1-C1	87.85(8)

This phenomenon of reductive ring-opening of THF has precedent in several reduced early transition metal complexes.<sup>64-66</sup> For example, a titanium(III) hydride dimer  $[\text{Cp}_2\text{TiH}]_2$  was reported to add THF to form solvated monomers that add the O-C $_{\alpha}$  bond of THF across the Ti-H bond in a concerted step.<sup>64</sup> In light of these findings and the C-O bond activation reported in the NHC-derived complex **4.24**, it is plausible that reduction of **3.25** generates a monochloro Zr(III) intermediate, which could promote scission of the

C-O bond in THF. It is important to note that no conclusive evidence of this intermediate was observed as attempts to trap or observe a Zr(III) intermediate were not performed.

Given that the reduction of **3.25** in the presence of THF yielded a species that reacts with the solvent, the reduction in toluene was examined. Unfortunately, no reaction between **3.25** and  $\text{KC}_8$  was observed, potentially a result of the insolubility of **3.25** in toluene. In an attempt to increase the solubility of the metal dichlorides in toluene, the diisopropylphenyl-substituted **3.26** was used in the same reduction conditions, however, no reaction was observed. Other reducing reagents such as Mg, Na/Hg amalgam, and Na have been investigated in similar conditions described above, however, no tractable materials were recovered.

#### 4.7. Synthesis of Hydrazido(1-) Hafnium [NCN] Complexes

The coordination of hydrazine and substituted hydrazines has generated considerable interest, in particular for modeling transition metal intermediates in the biological fixation of dinitrogen.<sup>67-69</sup> In light of our inability to isolate a dinitrogen complex using the [NCN] ancillary ligand, the coordination of substituted hydrazines was investigated. It was hoped that such studies would form N-N bonded complexes that resemble intermediates in the metal-mediated reduction of dinitrogen to ammonia.

Hydrazido ligands have been reported to coordinate to a metal centre in a variety of binding modes. This coordination is classified according to the charge carried by the hydrazido donor.<sup>70,71</sup> Widespread examples of this ligand include hydrazido(1-) ( $\text{NRNR}_2$ ), hydrazido(2-) ( $\text{NNR}_2$ ) (where R signifies an organic group or H), and hydrazido(4-) complexes. Examples of the known coordination modes are given in Figure 4.9.

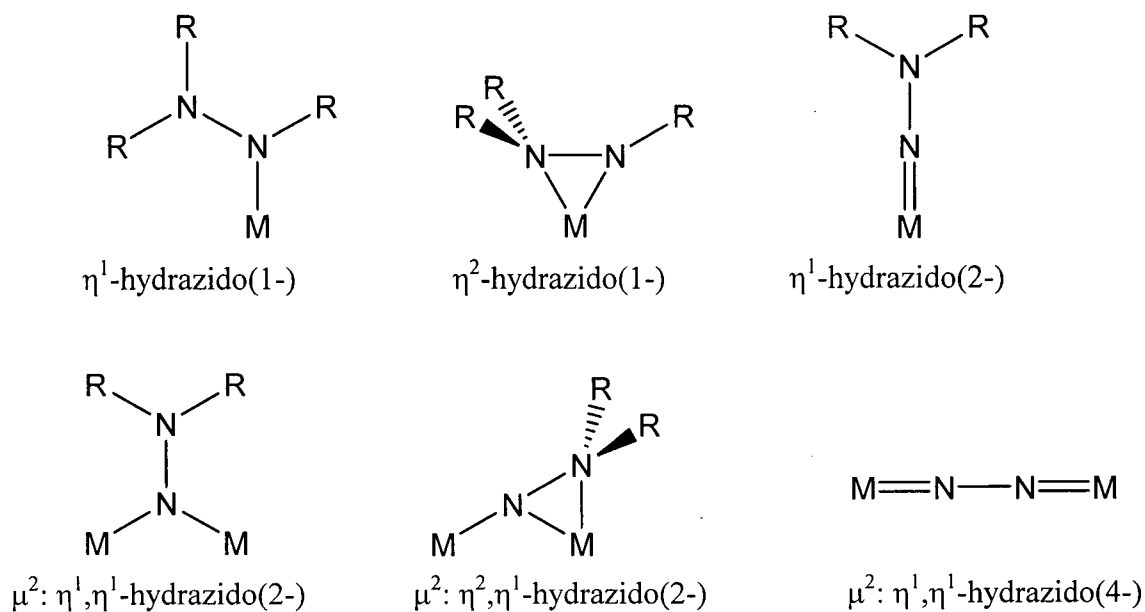


**Figure 4.9.** Coordination modes of hydrazido ligands.

Despite many advances in the area of hydrazido transition metal chemistry, there are relatively few reports of early transition metal complexes incorporating this ligand. For example, mononuclear titanium cyclopentadienyl and porphyrin-supported complexes have been reported with  $\eta^2$ -hydrazido(1-) ligands.<sup>72-74</sup> A slight modification of the supporting ligand can result in a dinuclear complex, as has been observed with a *N,N*-di(pyrrolyl- $\alpha$ -methyl)-*N*-methylamine (dpma) titanium complexes (Figure 4.10).<sup>71</sup> The synthesis of hydrazido(2-) ligands also has precedent in ETM chemistry with reports of both terminal mononuclear complexes<sup>71</sup> and binuclear bridging hydrazido(2-) derivatives.<sup>75</sup>

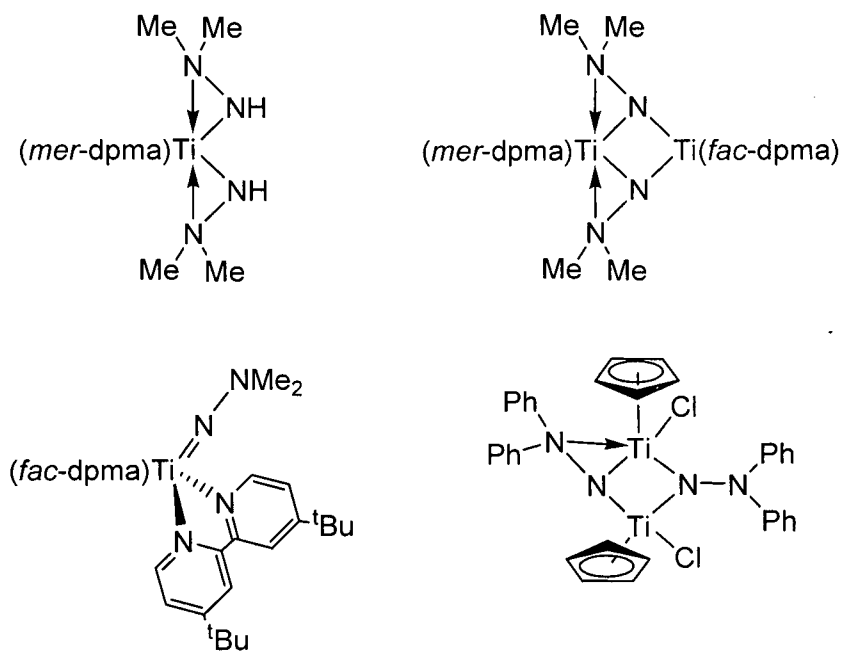


**Figure 4.10.** Examples of hydrazido(1-) and hydrazido(2-) titanium complexes.

The addition of 1 equivalent of 1,1-Me<sub>2</sub>NNH<sub>2</sub> to **3.35** at -30°C resulted in the formation of **4.25**, which was identified by NMR spectroscopy (Equation 4.6). The <sup>1</sup>H NMR spectrum reveals the presence of one amino -NH moiety as a singlet at 4.13 ppm and a -NMe<sub>2</sub> resonance at 2.0 ppm. Based on this data, the exact coordination mode of the hydrazido(1-) moiety cannot be determined, although given the coordination mode of the amidate ligands in **4.17** and **4.18**, an η<sup>2</sup>-orientation of the hydrazido(1-) group might be expected. This η<sup>2</sup> coordination mode has precedent in hydrazido (1-) early transition metal complexes (Figure 4.10).<sup>71</sup>

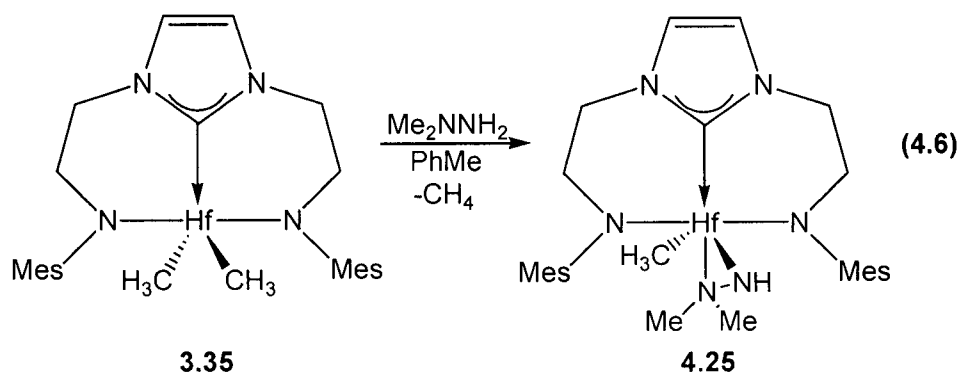
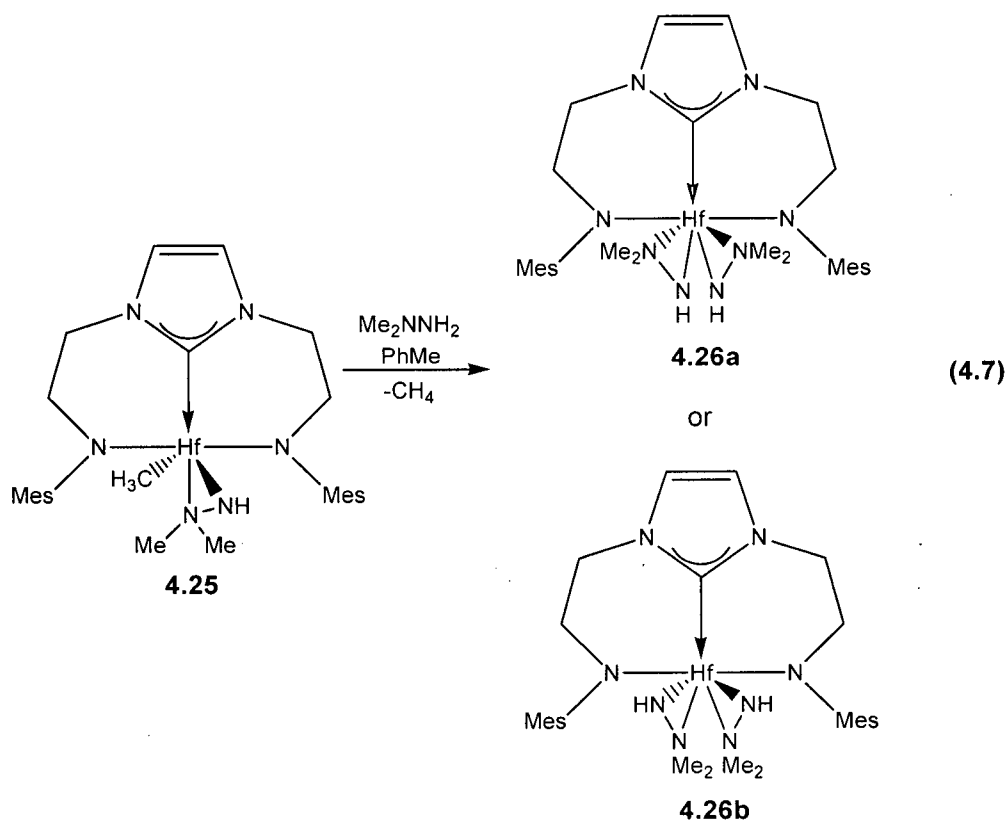




**Table 4.8.** Selected Bond Distances (Å) and Bond Angles (°) for  $\text{Mes}[\text{NCN}]\text{Hf}(\text{Me})(\eta^2\text{-NHNMe}_2)$ , (**4.25**).

Bond Lengths		Bond Angles	
Hf1-C1	2.423(4)	N3-Hf1-N4	153.11(14)
Hf1-N3	2.123(3)	N3-Hf1-C1	78.06(7)
Hf1-N5	2.042(4)	Hf1-N5-N6	83.3(2)
Hf1-N6	2.355(3)	Hf1-N6-N5	59.5(2)
Hf1-C14	2.232(4)	N5-Hf1-N6	37.2(2)
N5-N6	1.437(5)		

The addition of a second equivalent of 1,1-Me<sub>2</sub>NNH<sub>2</sub> to **4.25** at -30°C produced **4.26**, a bis(hydrazido)(1-) complex (Equation 4.7). The <sup>1</sup>H NMR spectrum reveals equivalent -N(CH<sub>3</sub>)<sub>2</sub>, aryl, and imidazole resonances, suggestive of a species with C<sub>2v</sub> symmetry in solution. Although the solid state molecular structure of **4.26** remains unknown, two possible structural isomers could exist in solution which are consistent with the symmetry observed in the <sup>1</sup>H NMR spectrum. The two possibilities are: 1) the -NMe<sub>2</sub> moieties of the η<sup>2</sup>-NHNMe<sub>2</sub> ligands are *trans* to each other (structure **4.26a**, Equation 4.7); or 2) the -NMe<sub>2</sub> moieties of the η<sup>2</sup>-NHNMe<sub>2</sub> ligands are *cis* to each other (structure **4.26b**, Equation 4.7). Unfortunately, NOE measurements did not shed insight into the configuration of the hydrazido(1-) groups, but based on possible steric interactions between -NMe<sub>2</sub> groups, and the reported structures of other bis(hydrazido)(1-) complexes,<sup>71</sup> the structure is most likely **4.26a**.



#### 4.8. Conclusions

In chapter 3, it was demonstrated that having the NHC situated between two anionic amide donors prevented the dissociation of a carbene moiety from an early transition metal. What was not known was how stable early transition metal NHC interactions would be during processes such as olefin polymerization and migratory insertion. Driven by the precedent for activated NHC-derived group 4 catalysts to polymerize  $\alpha$ -olefins, the potential of several [NCN] group 4 metal alkyl compounds was investigated. Activation of the zirconium-dimethyl derivative with  $[\text{Ph}_3\text{C}][\text{B}(\text{C}_6\text{F}_5)_4]$  in the presence of ethylene yielded a moderately active polymerization catalyst. In the presence of 1-hexene, the activated zirconium- and hafnium-dimethyl catalysts yielded a marginal amount of polymer. Investigation into the migratory insertion of isocyanides and CO into the hafnium- $\text{sp}^3$ -carbon bond of several hafnium-alkyl derivatives revealed the NHC moiety remains coordinated to the metal centre and does not participate in a manner that would alter the NHC donor. Multiple insertions of substrates was

accomplished; in some examples further C-C bond coupling was observed to generate new enamidolate and enediolate metallacycles. Attempts to synthesize zirconium [NCN] dinitrogen complexes by previously successful reduction methods were unsuccessful. In one case, an ether cleavage product was recovered (**4.22**), which is a result of solvent C-O bond activation. In the next chapter, the coordination of the [NCN] ligand to tantalum will be examined in an attempt to promote the reduction of dinitrogen.

## 4.9. Experimental

### 4.9.1. General Considerations

Unless otherwise stated, general procedures were performed as described in Section 2.5.1.

### 4.9.2. Materials and Reagents

All materials were purchased from an appropriate supplier and purified by published methods prior to use.  $\text{KC}_8$  was synthesized by the method described in the literature.<sup>77</sup>

### 4.9.3. Synthesis and Characterization of Complexes 4.4 - 4.18, 4.24 - 4.26

*In situ* generation of  $[\text{Mes}[\text{NCN}]\text{M}(\text{CH}_3)][\text{B}(\text{C}_6\text{F}_5)_4]$  (M=Zr (4.4), Hf (4.5)).

The following procedure is representative of the synthesis of 4.4 and 4.5. To a cooled solution of 3.33 (35 mg, 0.069 mmol) in  $\text{CD}_2\text{Cl}_2$  (0.5 mL) was added a cooled  $\text{CD}_2\text{Cl}_2$  (0.5 mL) solution of  $[\text{Ph}_3\text{C}][\text{B}(\text{C}_6\text{F}_5)_4]$  (64 mg, 0.069 mmol). The pale orange solution was immediately transferred to an NMR tube and then frozen in liquid  $\text{N}_2$ . The NMR spectrum was taken immediately after warming the solution to  $-10^\circ\text{C}$ .

**4.4:  $^1\text{H}$  NMR ( $\text{CD}_2\text{Cl}_2$ ):**  $\delta$  0.50 (s, 3H,  $-\text{ZrCH}_3$ ), 2.10 (br s, 12H, *o*-Ar $\text{CH}_3$ ), 2.15 (s, 6H, *p*-Ar $\text{CH}_3$ ), 3.45 (m, 2H,  $-\text{NCH}_2$ ), 3.94 (m, 2H,  $-\text{NCH}_2$ ), 4.14 (m, 2H,  $-\text{NCH}_2$ ), 4.29 (m, 2H,  $-\text{NCH}_2$ ), 6.85 (br s, 4H,  $-\text{ArH}$ ), 7.04 (s, 2H,  $-\text{imidH}$ ).

**4.5:  $^1\text{H}$  NMR ( $\text{CD}_2\text{Cl}_2$ ):**  $\delta$  0.26 (s, 3H,  $-\text{HfCH}_3$ ), 2.15 (br s, 12H, *o*-Ar $\text{CH}_3$ ), 2.20 (s, 6H, *p*-Ar $\text{CH}_3$ ), 3.70 (m, 2H,  $-\text{NCH}_2$ ), 4.05 (m, 2H,  $-\text{NCH}_2$ ), 4.28 (m, 2H,  $-\text{NCH}_2$ ), 4.60 (m, 2H,  $-\text{NCH}_2$ ), 6.99 (br s, 4H,  $-\text{ArH}$ ), 7.15 (s, 2H,  $-\text{imidH}$ ).

### Synthesis of $[\text{Mes}[\text{NCN}]\text{Hf}(\text{OTf})(\text{CH}_3)]$ (4.6)

To a cooled ethereal solution (5 mL) of 3.35 (200 mg, 0.33 mmol) was added an ethereal solution (2 mL) of  $\text{CF}_3\text{SO}_3\text{H}$  (48 mg, 0.32 mmol). The solution was gradually allowed to warm to room temperature and stirred overnight. The solvent was removed

and the residue recrystallized from Et<sub>2</sub>O/hexane at -30°C to give a colorless solid. Yield = 205 mg, 85%.

**<sup>1</sup>H NMR (CD<sub>2</sub>Cl<sub>2</sub>):** δ 0.19 (s, 3H, -HfCH<sub>3</sub>), 2.19 (br s, 12H, *o*-ArCH<sub>3</sub>), 2.21 (s, 6H, *p*-ArCH<sub>3</sub>), 3.34 (m, 2H, -NCH<sub>2</sub>), 4.00 (m, 2H, -NCH<sub>2</sub>), 4.13 (m, 2H, -NCH<sub>2</sub>), 4.55 (m, 2H, -NCH<sub>2</sub>), 6.87 (br s, 4H, -ArH), 7.09 (s, 2H, -imidH).

Anal. Calcd. for C<sub>27</sub>H<sub>35</sub>F<sub>3</sub>HfN<sub>4</sub>O<sub>3</sub>S: C, 44.35; H, 4.83; N, 7.66. Found: C, 43.85; H, 4.61; N, 7.09.

#### Synthesis of <sup>Mes</sup>[NCN]Hf(η<sup>2</sup>-XyNCCH<sub>3</sub>)(CH<sub>3</sub>) (4.7)

To a cooled toluene (5 mL) solution of **3.35** (200 mg, 0.33 mmol) was added a cooled toluene (2 mL) solution of xylyl isocyanide (44 mg, 0.33 mmol). The pale yellow solution was allowed to gradually warm to room temperature and stirred overnight. The solvent was removed and suspended in cold (-30°C) hexanes. The solid was filtered and washed with cold hexanes to give a white powder. The solid was further recrystallized with Et<sub>2</sub>O at -30°C. Yield = 183 mg, 74%.

**<sup>1</sup>H NMR (C<sub>6</sub>D<sub>6</sub>):** δ 0.17 (s, 3H, -HfCH<sub>3</sub>), 1.61 (s, 6H, -xylylCH<sub>3</sub>), 1.63 (s, 3H, -CCH<sub>3</sub>), 2.21 (s, 6H, -*p*-Ar<sub>Mes</sub>-CH<sub>3</sub>), 2.39 (s, 6H, -*o*-Ar<sub>Mes</sub>-CH<sub>3</sub>), 2.48 (s, 6H, -*o*-Ar<sub>Mes</sub> CH<sub>3</sub>), 3.08 (m, 2H, -NCH<sub>2</sub>), 3.18 (m, 2H, -NCH<sub>2</sub>), 3.81 (m, 2H, -NCH<sub>2</sub>), 4.07 (m, 2H, -NCH<sub>2</sub>), 6.06 (s, 2H, -imidH), 6.82-6.92 (m, 7H, -ArH).

**<sup>13</sup>C{<sup>1</sup>H} NMR (C<sub>6</sub>D<sub>6</sub>):** δ 18.2 (-ArCH<sub>3</sub>), 19.7 (-ArCH<sub>3</sub>), 19.8 (-ArCH<sub>3</sub>), 20.5 (-ArCH<sub>3</sub>), 22.4 (-ArCH<sub>3</sub>), 34.2 (-HfCH<sub>3</sub>), 52.2 (-NCH<sub>2</sub>), 56.9 (-NCH<sub>2</sub>), 118.7 (-imidC), 124.3 (-ArC), 128.8 (-ArC), 129.2 (-ArC), 129.6 (-ArC), 131.1 (-ArC), 134.4 (-ArC), 134.6 (-ArC), 147.2 (-ArC), 154.8 (-ArC), 197.5 (-HfC<sub>carbene</sub>), 259.0 (-HfC<sub>iminoacyl</sub>).

**IR (nujol):** ν(C=N) 1575 cm<sup>-1</sup>.

Anal. Calc. for C<sub>36</sub>H<sub>47</sub>N<sub>5</sub>Hf: C, 59.37; H, 6.50; N, 9.62. Found: C, 59.23; H, 6.33; N, 9.46.

#### Synthesis of <sup>Mes</sup>[NCN]Hf(η<sup>2</sup>-RNCCH<sub>3</sub>)<sub>2</sub> (R = Xy (4.8); R = <sup>i</sup>Pr (4.10))

The following procedure is representative of the synthesis of **4.8** and **4.10**. To a toluene (2 mL) solution of **4.7** (200 mg, 0.33 mmol) was added a toluene (2 mL) solution

of xylyl isocyanide (92 mg, 0.70 mmol). The pale yellow solution gradually turned dark purple (or orange in the case of **4.8**) and was stirred overnight, whereupon the solvent was removed quickly and Et<sub>2</sub>O (2 mL) added to precipitate a white solid. Cooling of the solution, followed by filtration yielded colorless microcrystals. Yield = 260 mg, 92%.

**4.8:** <sup>1</sup>H NMR (CD<sub>2</sub>Cl<sub>2</sub>): δ 1.45 (br s, 18H, -CCH<sub>3</sub> and -Ar<sub>Xy</sub>CH<sub>3</sub>), 1.85 (br s, 12H, -o-Ar<sub>Mes</sub>CH<sub>3</sub>), 2.14 (br s, 6H, -p-Ar<sub>Mes</sub>CH<sub>3</sub>), 4.2 (br s, 8H, -NCH<sub>2</sub>), 6.60 (br s, 4H, -Ar<sub>Mes</sub>H), 6.80-6.85 (br s, 6H, -Ar<sub>Xy</sub>H). <sup>1</sup>H NMR (CD<sub>2</sub>Cl<sub>2</sub>, 233 K): δ 1.21 (s, 3H, -CCH<sub>3</sub>), 1.27 (s, 6H, -Ar<sub>Xy</sub>CH<sub>3</sub>), 1.57 (s, 6H, -Ar<sub>Xy</sub>CH<sub>3</sub>), 1.78 (s, 6H, -o-Ar<sub>Mes</sub>CH<sub>3</sub>), 1.85 (s, 6H, -o-Ar<sub>Mes</sub>CH<sub>3</sub>), 2.10 (s, 6H, -p-Ar<sub>Mes</sub>CH<sub>3</sub>), 2.24 (s, 3H, -CCH<sub>3</sub>), 2.80 (m, 2H, -NCH<sub>2</sub>), 3.98 (m, 4H, -NCH<sub>2</sub>), 4.27 (m, 1H, -NCH<sub>2</sub>), 6.56 (s, 2H, -Ar<sub>Mes</sub>H), 6.64 (s, 2H, -Ar<sub>Mes</sub>H), 6.81 (m, 1H, -Ar<sub>Xy</sub>H), 6.85 (m, 2H, -Ar<sub>Xy</sub>H), 6.90 (s, 2H, -imidH).

<sup>13</sup>C{<sup>1</sup>H} NMR (C<sub>6</sub>D<sub>6</sub>): δ 18.5 (-ArCH<sub>3</sub>), 20.4 (-ArCH<sub>3</sub>), 20.8 (-ArCH<sub>3</sub>), 23.6 (-ArCH<sub>3</sub>), 52.7 (-NCH<sub>2</sub>), 57.9 (-NCH<sub>2</sub>), 118.5 (-imidC), 124.7 (-ArC), 125.6 (-ArC), 129.1 (-ArC), 129.9 (-ArC), 130.3 (-ArC), 135.1 (-ArC), 156.5 (-ArC), 196.5 (-HfC<sub>carbene</sub>).

IR(nujol): ν(C=N) 1568 cm<sup>-1</sup>.

Anal. Calc. for C<sub>45</sub>H<sub>56</sub>HfN<sub>6</sub>: C, 62.89; H, 6.57; N, 9.78. Found:

**4.9:** <sup>1</sup>H NMR (C<sub>6</sub>D<sub>6</sub>): δ 0.88 (d, J=7Hz, 12H, -CH(CH<sub>3</sub>)<sub>2</sub>), 1.32 (s, 6H, η<sup>2</sup>-<sup>i</sup>PrNCCH<sub>3</sub>), 2.25 (s, 12H, -o-Ar<sub>Mes</sub>-CH<sub>3</sub>), 2.31 (s, 6H, -p-Ar<sub>Mes</sub>-CH<sub>3</sub>), 3.28 (m, 2H, -N<sub>Ar</sub>CH<sub>2</sub>), 3.47 (sept, J=7Hz, 2H, -CH(CH<sub>3</sub>)<sub>2</sub>), 3.55 (m, 2H, -NCH<sub>2</sub>), 3.67 (m, 2H, -NCH<sub>2</sub>), 4.01 (m, 2H, -NCH<sub>2</sub>), 6.07 (s, 2H, -imidH), 6.93-7.07 (m, 13H, -ArH).

<sup>13</sup>C{<sup>1</sup>H} NMR (C<sub>6</sub>D<sub>6</sub>): δ 20.4 (-ArCH<sub>3</sub>), 20.9 (-ArCH<sub>3</sub>), 21.1 (-CCH<sub>3</sub>) 23.2, 48.8 (-NCH), 53.3 (-NCH<sub>2</sub>), 56.4 (-NCH<sub>2</sub>), 119.4 (-imidC), 128.7 (-ArC), 129.8 (-ArC), 135.3 (-ArC), 157.6 (-ArC), 194.5 (-HfC<sub>carbene</sub>) 266.2 (-HfC<sub>iminoacyl</sub>).

IR(nujol): ν(C=N) 1562 cm<sup>-1</sup>.

Anal. Calc. for C<sub>35</sub>H<sub>52</sub>HfN<sub>6</sub>: C, 57.17; H, 7.13; N, 11.43. Found: C, 56.89; H, 7.00; N, 11.26.

#### Synthesis of <sup>Mes</sup>[NCN]Hf(η<sup>2</sup>-XyNCCH<sub>3</sub>)(η<sup>2</sup>-<sup>i</sup>PrNCCH<sub>3</sub>) (**4.9**).

To a toluene (2 mL) solution of **4.7** (100 mg, 0.14 mmol) was added a toluene (2 mL) solution of <sup>i</sup>PrNC (10 mg, mmol). No observable color change was noted. The

solution was stirred for 1 hour, whereupon the solvent was removed quickly and Et<sub>2</sub>O (2 mL) added to precipitate a white solid, which was washed with hexanes and dried *in vacuo*. Yield = 96 mg, 86%.

<sup>1</sup>H NMR (C<sub>6</sub>D<sub>6</sub>): δ 0.97 (d, J=7Hz, 6H, -CH(CH<sub>3</sub>)<sub>2</sub>), 1.23 (s, 3H, η<sup>2</sup>-<sup>i</sup>PrNCCH<sub>3</sub>), 1.91 (s, 6H, -xylylCH<sub>3</sub>), 2.26 (s, 6H, -*p*-Ar<sub>Mes</sub>-CH<sub>3</sub>), 2.38 (s, 6H, -*o*-Ar<sub>Mes</sub>-CH<sub>3</sub>), 2.39 (s, 6H, -*o*-Ar<sub>Mes</sub>-CH<sub>3</sub>), 2.47 (s, 3H, -η<sup>2</sup>-XyNCCH<sub>3</sub>), 3.10 (m, 2H, -NCH<sub>2</sub>), 3.43 (m, 2H, -NCH<sub>2</sub>), 3.56 (sept, J=7Hz, 1H, -CH(CH<sub>3</sub>)<sub>2</sub>), 3.69 (m, 2H, -NCH<sub>2</sub>), 3.88 (m, 2H, -NCH<sub>2</sub>), 6.01 (s, 2H, -imidH), 6.89 (s, 2H, -Ar<sub>Mes</sub>H), 6.95 (s, 2H, -Ar<sub>Mes</sub>H), 6.97-7.04 (m, 3H, -Ar<sub>xylyl</sub>H).

<sup>13</sup>C{<sup>1</sup>H} NMR (C<sub>6</sub>D<sub>6</sub>): δ 18.5 (-CCH<sub>3</sub>), 18.7 (-CCH<sub>3</sub>), 20.3 (-CH(CH<sub>3</sub>)<sub>2</sub>), 20.7 (-ArCH<sub>3</sub>), 20.9 (-ArCH<sub>3</sub>), 26.0 (-ArCH<sub>3</sub>), 50.3 (-NCH), 52.6 (-NCH<sub>2</sub>), 56.5 (-NCH<sub>2</sub>), 118.7 (-imidC), 124.3 (-ArC), 128.9 (-ArC), 129.4 (-ArC), 130.2 (-ArC), 134.7 (-ArC), 135.8 (-ArC), 148.9 (-ArC), 157.4 (-ArC), 195.1 (-HfC<sub>carbene</sub>), 262.4 (-HfC<sub>iminoacyl</sub>), 264.1 (-HfC<sub>iminoacyl</sub>).

IR (nujol): ν(C=N) 1558, 1570 cm<sup>-1</sup>.

Anal. Calc. for C<sub>40</sub>H<sub>54</sub>HfN<sub>6</sub>: C, 60.25; H, 6.83; N, 10.54. Found: C, 60.01; H, 6.82; N, 10.36.

#### Synthesis of <sup>Mes</sup>[NCN]Hf(OC(CH<sub>3</sub>)=C(CH<sub>3</sub>)NXy) (4.11).

A toluene (10 mL) solution of 4.7 (102 mg, 0.14 mmol) was freeze-pumped-thawed with 1 atm CO several times and left to stand for 1 day. The solvent was removed *in vacuo* and the yellow powder was washed with hexane (5 mL). The yellow solid was recrystallized from Et<sub>2</sub>O at -30°C to give crystals suitable for X-ray diffraction. Yield = 88 mg, 83%.

<sup>1</sup>H NMR (C<sub>6</sub>D<sub>6</sub>, 298K): δ 1.37 (s, 3H, -NCCH<sub>3</sub>), 1.59 (s, 3H, -OCCH<sub>3</sub>), 2.21 (s, 6H, -CH<sub>3</sub>), 2.37 (s, 6H, -CH<sub>3</sub>), 3.01 (m, 4H, -NCH<sub>2</sub>), 3.51 (m, 2H, -N<sub>i</sub>CH<sub>2</sub>), 3.77 (m, 2H, -NCH<sub>2</sub>), 5.81 (s, 2H, -imidH), 6.90-6.96 (m, 5H, -ArH), 7.07-7.09 (m, 2H, -ArH).

<sup>1</sup>H NMR (CD<sub>3</sub>C<sub>6</sub>D<sub>5</sub>, 223 K): δ 1.31 (s, 3H, -NCCH<sub>3</sub>), 1.60 (s, 3H, -OCCH<sub>3</sub>), 1.98 (s, 6H, -ArCH<sub>3</sub>), 2.24 (s, 6H, -ArCH<sub>3</sub>), 2.38 (s, 6H, -ArCH<sub>3</sub>), 2.69 (s, 6H, -ArCH<sub>3</sub>), 2.94 (m, 4H, -NCH<sub>2</sub>), 3.47 (m, 2H, -NCH<sub>2</sub>), 3.73 (m, 2H, -NCH<sub>2</sub>), 5.74 (s, 2H, -imidH), 6.81 (s, 2H, -Ar<sub>Mes</sub>H), 6.99 (m, 3H, -Ar<sub>xy</sub>H), 7.08 (s, 2H, -Ar<sub>Mes</sub>H).

$^{13}\text{C}\{^1\text{H}\}$  NMR ( $\text{C}_6\text{D}_6$ , 298K):  $\delta$  15.2 (-NCCH<sub>3</sub>), 17.4 (-ArCH<sub>3</sub>), 19.0 (-OCCH<sub>3</sub>), 19.4 (-ArCH<sub>3</sub>), 20.9 (-ArCH<sub>3</sub>), 52.9 (-NCH<sub>2</sub>), 57.3 (-NCH<sub>2</sub>), 116.2 (-CN), 118.7 (-imidC), 123.1 (-ArC), 129.6 (-ArC), 131.5 (-ArC), 133.0 (-ArC), 136.0 (-ArC), 137.0 (-CO), 147.9 (-ArC), 149.6 (-ArC), 196.7 (-HfC<sub>carbene</sub>).

Anal. Calc. for C<sub>37</sub>H<sub>47</sub>HfN<sub>5</sub>O: C, 58.76; H, 6.26; N, 9.26. Found: C, 58.29; H, 6.05; N, 9.33.

#### Synthesis of $^{\text{Mes}}(\text{NCN})\text{Hf}(\eta^2\text{-C}(\text{O})\text{CH}_3)(\text{CH}_3)$ (4.12), $^{13}\text{C}$ -4.12

The product was identified *in situ* by NMR and IR spectroscopy. A  $\text{C}_6\text{D}_6$  solution (1 mL) of **3.35** was freeze-pumped-thawed three times with CO, and the solution left at 1 atmosphere. The solution was left to stand for 6 hours and the solvent removed *in vacuo* to yield a pale yellow solid. The product was contaminated with ~5% **4.13**.

$^1\text{H}$  NMR ( $\text{C}_6\text{D}_6$ ):  $\delta$  0.56 (s, 3H, -HfCH<sub>3</sub>), 1.62 (s, 3H, -HfC(O)CH<sub>3</sub>), 2.11 (s, 6H, -*p*-ArCH<sub>3</sub>), 2.34 (s, 6H, -*o*-ArCH<sub>3</sub>), 2.44 (s, 6H, -*o*-ArCH<sub>3</sub>), 2.92 (m, 2H, -CH<sub>2</sub>), 3.20 (m, 2H, -CH<sub>2</sub>), 3.65 (m, 2H, -CH<sub>2</sub>), 3.96 (m, 2H, -CH<sub>2</sub>), 6.01 (s, 2H, -imidH), 6.76 (s, 2H, -ArH), 6.86 (s, 2H, -ArH).

$^{13}\text{C}\{^1\text{H}\}$  NMR ( $\text{C}_6\text{D}_6$ ):  $\delta$  19.7 (-ArCH<sub>3</sub>), 19.8 (-ArCH<sub>3</sub>), 20.8 (-ArCH<sub>3</sub>), 31.1 (-HfC(O)CH<sub>3</sub>), 34.7 (-HfCH<sub>2</sub>), 53.7 (-NCH<sub>2</sub>), 55.9 (-NCH<sub>2</sub>), 119.1 (-imidC), 128.8 (-ArC), 129.5 (-ArC), 130.0 (-ArC), 132.1 (-ArC), 134.9 (-ArC), 135.5 (-ArC), 151.5 (-ArC), 153.0 (-ArC), 195.6 (-HfC<sub>carbene</sub>), 339.6 (-HfC<sub>acyl</sub>).

IR (nujol):  $\nu(\text{C}=\text{O})$  1540  $\text{cm}^{-1}$ .

$^{13}\text{C}$ -4.12:  $^1\text{H}$  and  $^{13}\text{C}$  NMR spectra identical to **19** except 1.62 (d,  $J=7\text{Hz}$ , 3H, -HfC(O)CH<sub>3</sub>).

#### Synthesis of $^{\text{Mes}}(\text{NCN})\text{Hf}(\text{OCH}=\text{CH}_2)(\text{CH}_3)$ (4.13) and $^{13}\text{C}$ -4.13

A benzene solution (10 mL) of **3.35** (250 mg, 0.42 mmol) was freeze-pumped-thawed three times with CO, and the solution left to stir under 1 atmosphere for three days. The solvent was removed residue recrystallized with Et<sub>2</sub>O/hexanes at -30°C. Yield = 162 mg, 62%.

**<sup>1</sup>H NMR (C<sub>6</sub>D<sub>6</sub>):** δ 0.37 (s, 3H, -HfCH<sub>3</sub>), 2.21 (s, 6H, -*p*-ArCH<sub>3</sub>), 2.34 (s, 6H, -*o*-ArCH<sub>3</sub>), 2.62 (s, 6H, -*o*-ArCH<sub>3</sub>), 2.92 (m, 2H, -NCH<sub>2</sub>), 3.15 (m, 2H, -NCH<sub>2</sub>), 3.47 (d, J = 14Hz, -CH), 3.54 (d, J = 6 Hz, -CH), 3.74 (m, 2H, -NCH<sub>2</sub>), 3.96 (m, 2H, -NCH<sub>2</sub>), 5.75 (dd, J = 6, 14 Hz, 1H, -CH), 5.94 (s, 2H, -imidH), 6.95 (s, 2H, -ArH), 7.01 (s, 2H, -ArH).

**<sup>13</sup>C{<sup>1</sup>H} NMR (C<sub>6</sub>D<sub>6</sub>):** δ 19.5 (-*o*-CH<sub>3</sub>), 20.9 (-*p*-CH<sub>3</sub>), 38.4 (-HfCH<sub>3</sub>), 52.1 (-NCH<sub>2</sub>), 55.1 (-NCH<sub>2</sub>), 117.4 (-imidC), 120.2 (-HfOCH=CH<sub>2</sub>), 129.4 (-ArC), 130.4 (-ArC), 133.7 (-ArC), 139.0 (-HfOCH=CH<sub>2</sub>), 145.3 (-ArC), 196.2 (-HfC<sub>carbene</sub>).

Anal. Calcd. for C<sub>28</sub>H<sub>38</sub>HfN<sub>4</sub>O: C, 53.80; H, 6.13; N, 8.96. Found: C, 53.53; H, 5.89; N, 8.61.

**<sup>13</sup>C-4.13:** <sup>1</sup>H NMR resonances are identical except δ 5.75 (ddd, J= 6,14,145 Hz, 2H, -HfO<sup>13</sup>CH=CH<sub>2</sub>).

#### *In situ* generation of <sup>Mes</sup>[NCN]Hf(η<sup>2</sup>-CO(<sup>t</sup>Bu))(<sup>t</sup>Bu) (4.14) and <sup>13</sup>C-4.14.

A C<sub>6</sub>D<sub>6</sub> (1 mL) solution of **3.38** was freeze-pumped-thawed three times with CO. The reaction was followed by <sup>1</sup>H NMR spectroscopy and upon complete conversion to the monoacyl complex, a <sup>13</sup>C NMR spectroscopy experiment was performed.

**<sup>1</sup>H NMR (C<sub>6</sub>D<sub>6</sub>):** δ 0.66 (d, J = 7Hz, 6H, -CH(CH<sub>3</sub>)<sub>2</sub>), 1.06 (d, J = 7Hz, 2H, -HfCH<sub>2</sub>), 1.40 (d, J = 7Hz, 6H, -C(O)CH(CH<sub>3</sub>)<sub>2</sub>), 1.68 (d, J = 7Hz, 2H, -HfC(O)CH<sub>2</sub>), 1.80 (sept, J = 7Hz, 1H, -CH(CH<sub>3</sub>)<sub>2</sub>), 2.18 (-ArCH<sub>3</sub>), 2.34 (-ArCH<sub>3</sub>), 2.38 (-ArCH<sub>3</sub>), 2.75 (sept, J = 7Hz, 1H, -C(O)CH(CH<sub>3</sub>)<sub>2</sub>), 3.07 (m, 2H, -NCH), 3.28 (m, 2H, -NCH), 3.51 (m, 2H, -NCH), 4.00 (m, 2H, -NCH), 6.01 (s, 2H, -imidH), 6.78 (s, 2H, -ArH), 6.85 (s, 2H, -ArH).

**<sup>13</sup>C{<sup>1</sup>H} NMR (C<sub>6</sub>D<sub>6</sub>):** δ 19.8 (-ArCH<sub>3</sub>), 20.0 (-ArCH<sub>3</sub>), 21.2 (-ArCH<sub>3</sub>), 32.3 (-HfC(O)CH<sub>2</sub>), 36.4 (-HfCH<sub>2</sub>), 54.2 (-NCH<sub>2</sub>), 55.6 (-NCH<sub>2</sub>), 118.4 (-imidC), 128.4 (-ArC), 128.6 (-ArC), 129.2 (-ArC), 130.4 (-ArC), 131.2 (-ArC), 132.4 (-ArC), 149.8 (-ArC), 153.2 (-ArC), 196.1 (-HfC<sub>carbene</sub>), 338.4 (-HfC<sub>acyl</sub>).

**<sup>13</sup>C-21:** <sup>1</sup>H NMR resonances are identical except δ 1.68 (dd, J=4,7Hz, 2H, -Hf<sup>13</sup>C(O)CH<sub>2</sub>).

**In situ generation of  $^{\text{Mes}}[\text{NCN}]\text{Hf}(\text{OC}(\text{iBu})=\text{C}(\text{iBu})\text{O})$  (4.15) and  $^{13}\text{C}$ -4.15.**

The same procedure was followed as described in the synthesis of 4.14; however the reaction was further monitored by  $^1\text{H}$  NMR spectroscopy after conversion to the monoacyl complex. Within 1 day, the presence of 4.15 was noted.

$^1\text{H}$  NMR ( $\text{C}_6\text{D}_6$ ):  $\delta$  1.06 (d,  $J = 8\text{Hz}$ , 12H,  $-\text{CH}(\text{CH}_3)_2$ ), 1.99 (n,  $J = 8\text{Hz}$ , 2H,  $-\text{CH}_2\text{CH}(\text{CH}_3)_2$ ), 2.02 (d,  $J = 8\text{Hz}$ , 4H,  $-\text{OCCH}_2$ ), 2.22 (s, 6H,  $-p\text{-ArCH}_3$ ), 2.40 (s, 12H,  $-o\text{-ArCH}_3$ ), 3.41 (m, 4H,  $-\text{NCH}_2$ ), 3.61 (m, 4H,  $-\text{NCH}_2$ ), 5.89 (s, 2H,  $-\text{imidH}$ ), 6.92 (s, 4H,  $-\text{ArH}$ ).

$^{13}\text{C}\{^1\text{H}\}$  NMR ( $\text{C}_6\text{D}_6$ ):  $\delta$  15.5 ( $-\text{CH}(\text{CH}_3)_2$ ), 19.0 ( $-o\text{-CH}_3$ ), 21.2 ( $-p\text{-CH}_3$ ), 33.8 ( $-\text{CH}(\text{CH}_3)_2$ ), 38.3 ( $-\text{CCH}_2$ ), 49.4 ( $-\text{NCH}_2$ ), 52.1 ( $-\text{NCH}_2$ ), 120.4 ( $-\text{imidC}$ ), 129.2 ( $-\text{ArC}$ ), 132.1 ( $-\text{ArC}$ ), 134.3 ( $-\text{ArC}$ ), 140.6 ( $-\text{C}=\text{C}$ ), 153.5 ( $-\text{ArC}$ ), 198.5 ( $-\text{HfC}_{\text{carbene}}$ ).

$^{13}\text{C}$ -4.15:  $^{13}\text{C}$  NMR resonances are identical except  $\delta$  140.6 (d;  $J=30\text{Hz}$ ,  $-\text{C}=\text{C}$ ).

**Synthesis of  $^{\text{Mes}}[\text{NCN}]\text{Hf}(\text{OC}(\text{iBu})=\text{C}(\text{iBu})\text{O})_2$  (4.16) and  $^{13}\text{C}$ -4.16.**

A benzene solution (20 mL) of 3.38 (115 mg, 0.17 mmol) was freeze-pumped-thawed three times with  $\text{CO}$ , and the solution left to stand under 1 atmosphere for five days. Colorless crystalline material began to precipitate after three days. The solution was filtered and the crystalline material was washed with pentane. Yield = 82 mg, 66%.

$^1\text{H}$  NMR ( $\text{C}_6\text{D}_6$ ):  $\delta$  0.79 (d,  $J = 8\text{Hz}$ , 6H,  $-\text{CH}(\text{CH}_3)_2$ ), 0.87 (d,  $J = 8\text{Hz}$ , 6H,  $-\text{CH}(\text{CH}_3)_2$ ), 1.09 (m, 2H,  $-\text{CCH}_2\text{CH}$ ), 1.51 (m, 2H,  $-\text{CCH}_2\text{CH}$ ), 2.21 (s, 6H,  $-\text{ArCH}_3$ ), 2.33 (s, 6H,  $-\text{ArCH}_3$ ), 2.74 (s, 6H,  $-\text{ArCH}_3$ ), 3.40 (m, 4H,  $-\text{NCH}_2$ ), 3.55 (m, 2H,  $-\text{NCH}_2$ ), 4.16 (m, 2H,  $-\text{NCH}_2$ ), 6.01 (s, 2H,  $-\text{imidH}$ ), 6.96 (s, 2H,  $-\text{ArH}$ ), 7.05 (s, 2H,  $-\text{ArH}$ ) (multiplet from  $-\text{CH}_2\text{CH}(\text{CH}_3)_2$  obscured by aryl resonances).

$^{13}\text{C}\{^1\text{H}\}$  NMR ( $\text{C}_6\text{D}_6$ ):  $\delta$  14.6 ( $-\text{CH}(\text{CH}_3)_2$ ), 14.8 ( $-\text{CH}(\text{CH}_3)_2$ ), 19.6 ( $-\text{ArCH}_3$ ), 19.7 ( $-\text{ArCH}_3$ ), 20.4 ( $-\text{ArCH}_3$ ), 34.3 ( $-\text{CH}(\text{CH}_3)_2$ ), 34.6 ( $-\text{CH}(\text{CH}_3)_2$ ), 39.4 ( $-\text{CCH}_2$ ), 39.6 ( $-\text{CCH}_2$ ), 51.3 ( $-\text{NCH}_2$ ), 54.4 ( $-\text{NCH}_2$ ), 119.8 ( $-\text{imidC}$ ), 130.4 ( $-\text{ArC}$ ), 131.6 ( $-\text{ArC}$ ), 131.8 ( $-\text{ArC}$ ), 133.4 ( $-\text{ArC}$ ), 134.1 ( $-\text{ArC}$ ), 140.0 ( $-\text{C}=\text{C}$ ), 149.4 ( $-\text{ArC}$ ), 153.2 ( $-\text{ArC}$ ), 195.4 ( $-\text{HfC}_{\text{carbene}}$ ).

$^{13}\text{C}$ -4.16:  $^{13}\text{C}$  NMR resonances are identical except  $\delta$  140.0 (d,  $J=30\text{Hz}$ ,  $-\text{C}=\text{C}$ ).

Anal. Calc. for  $C_{70}H_{100}Hf_2N_8O_4$ : C, 57.02; H, 6.84; N, 7.60. Found: 56.72; H, 6.59; N, 7.43.

**Synthesis of  $Mes[NCN]Hf(Me)(\eta^3-N(^tBu)C(Me)O)$  (4.17),  $Mes[NCN]Hf(Me)(\eta^3-N(^iPr)C(Me)N(^iPr))$  (4.18)**

The following procedure is representative of the synthesis of **4.17** and **4.18**. In a 50 mL Erlenmeyer flask, **3.35** (100 mg, 0.17 mmol) was dissolved in 10 mL toluene and cooled to  $-30^\circ C$ . At this temperature, a toluene (3 mL) solution of  $^tBuNCO$  (17 mg, 0.17 mmol) was added dropwise and the colorless solution was slowly warmed to room temperature. Upon warming, the solution turned a pale yellow color and was stirred overnight. The solution was filtered through Celite and solvent was reduced in volume. Addition of hexane and cooling to  $-30^\circ C$  resulted in the formation of colorless crystals which were recovered by filtration. Yield = 99 mg, 84%.

**4.17:  $^1H$  NMR ( $C_6D_6$ ):**  $\delta$  0.26 (s, 3H,  $-HfCH_3$ ), 1.05 (s, 9H,  $-C(CH_3)_3$ ), 1.30 (s, 3H,  $-CCH_3$ ), 2.21 (s, 6H,  $-p-ArCH_3$ ), 2.35 (s, 6H,  $-o-ArCH_3$ ), 2.52 (s, 6H,  $-o-ArCH_3$ ), 3.42 (m, 2H,  $-NCH_2$ ), 3.45 (m, 2H,  $-NCH_2$ ), 3.59 (m, 2H,  $-NCH_2$ ), 3.64 (m, 2H,  $-NCH_2$ ), 6.07 (s, 2H,  $-imidH$ ), 6.91 (s, 4H,  $-ArH$ )

**$^{13}C\{^1H\}$  NMR ( $C_6D_6$ ):**  $\delta$  17.7 ( $-CH_3$ ), 20.3 ( $-CH_3$ ), 21.7 ( $-CH_3$ ), 23.2 ( $-CH_3$ ), 40.1 ( $-C(CH_3)_3$ ), 48.3 ( $-NCH_2$ ), 52.9 ( $-NCH_2$ ), 118.6 ( $-ArC$ ), 119.0 ( $-imidC$ ), 128.2 ( $-ArC$ ), 131.4 ( $-ArC$ ), 148.9 ( $-ArC$ ), 180.4 ( $-NCO$ ), 193.8 ( $-NCN$ ).

Anal Calcd. for  $C_{32}H_{47}HfN_5O$ : C, 55.20; H, 6.80; N, 10.06. Found: C, 55.35; H, 6.64; N, 10.30.

**4.18:  $^1H$  NMR ( $C_6D_6$ ):**  $\delta$   $-0.06$  (s, 3H,  $-HfCH_3$ ), 0.88 (d,  $J = 9$  Hz, 6H,  $-CH(CH_3)_2$ ), 0.90 (d,  $J = 9$  Hz, 6H,  $-CH(CH_3)_2$ ), 1.74 (s, 3H,  $-CCH_3$ ), 2.26 (s, 6H,  $-p-ArCH_3$ ), 2.46 (s, 6H,  $-o-ArCH_3$ ), 2.49 (s, 6H,  $-o-ArCH_3$ ), 3.32 (m, 2H,  $-NCH_2$ ), 3.41 (m, 2H,  $-NCH_2$ ), 3.50 (sept,  $J = 9$  Hz, 1H,  $-CH(CH_3)_2$ ), 3.68 (m, 2H,  $-NCH_2$ ), 3.78 (sept,  $J = 9$  Hz, 1H,  $-CH(CH_3)_2$ ), 4.34 (m, 2H,  $-NCH_2$ ), 6.06 (s, 2H,  $-imidH$ ), 6.97 (s, 2H,  $-ArH$ ), 7.01 (s, 2H,  $-ArH$ ).

$^{13}\text{C}\{^1\text{H}\}$  NMR ( $\text{C}_6\text{D}_6$ ):  $\delta$  19.6 (-CH<sub>3</sub>), 20.4 (-CH<sub>3</sub>), 21.9 (-CH<sub>3</sub>), 30.2 (-CH<sub>3</sub>), 30.4 (-CH<sub>3</sub>), 38.6 (-CH), 38.9 (-CH), 49.7 (-NCH<sub>2</sub>), 54.8 (-NCH<sub>2</sub>), 117.9 (-ArC), 120.4 (-imidC), 127.9 (-ArC), 132.6 (-ArC), 150.2 (-ArC), 179.5 (-NCN), 193.8 (-NCN).

Anal Calcd. for  $\text{C}_{34}\text{H}_{52}\text{HfN}_6$ : C, 56.46; H, 7.25; N, 11.62. Found: C, 56.21; H, 7.35; N, 11.42.

#### Synthesis of $^{\text{Mes}}[\text{NCN}]\text{ZrCl}(\text{OCH}_2\text{CH}_2\text{CH}_2\text{CH}_3)$ (4.24)

To a 250 mL thick-walled bomb charged with **3.25** (500 mg, 0.91 mmol) and  $\text{KCl}$  (270 mg, 2.0 mmol) was vacuum transferred 40 mL THF at  $-196^\circ\text{C}$ . The frozen solution was freeze-pump-thawed three times with  $\text{N}_2$  and sealed at  $-196^\circ\text{C}$ . The brown slurry was slowly warmed to room temperature to yield a dark black suspension. After stirring for three days, the pressure in the bomb was reduced to one atmosphere and filtered through Celite. The solvent was removed and the yellow residue was extracted with  $\text{Et}_2\text{O}$ . The solvent was concentrated and left to stand at  $-30^\circ\text{C}$  upon which time yellow block crystals formed. Yield = 187 mg, 35%.

$^1\text{H}$  NMR ( $\text{C}_6\text{D}_6$ ):  $\delta$  0.9-1.1 (m, 7H,  $-\text{CH}_2\text{CH}_2\text{CH}_3$ ), 2.06 (s, 12H,  $-o\text{-ArCH}_3$ ), 2.24 (s, 6H,  $-p\text{-ArCH}_3$ ), 3.42 (m, 2H,  $-\text{NCHH}$ ), 3.50 (t,  $J = 8$  Hz, 2H,  $-\text{OCH}_2$ ), 3.78 (m, 2H,  $-\text{NCHH}$ ), 3.89 (m, 2H,  $-\text{NCHH}$ ), 4.03 (m, 2H,  $-\text{NCHH}$ ), 5.82 (s, 2H,  $-\text{imidH}$ ), 6.89 (s, 2H,  $-\text{ArH}$ ), 6.94 (s, 2H,  $-\text{ArH}$ ).

$^{13}\text{C}\{^1\text{H}\}$  NMR ( $\text{C}_6\text{D}_6$ ):  $\delta$  16.9 (-CH<sub>3</sub>), 20.2 (-CH<sub>3</sub>), 20.9 (-CH<sub>3</sub>), 21.2 (-CH<sub>3</sub>), 22.4 (-CH<sub>3</sub>), 48.9 (-NCH<sub>2</sub>), 51.3 (-NCH<sub>2</sub>), 60.4 (-OCH<sub>2</sub>), 118.5 (-ArC), 120.3 (-imidC), 128.6 (-ArC), 130.5 (-ArC), 149.2 (-ArC), 192.5 (-NCN).

Anal Calcd. for  $\text{C}_{29}\text{H}_{41}\text{ClN}_4\text{OZr}$ : C, 59.20; H, 7.02; N, 9.52. Found: C, 59.35; H, 7.33; N, 9.67.

#### Synthesis of $^{\text{Mes}}[\text{NCN}]\text{Hf}(\text{Me})(\text{NHNMe}_2)$ (4.25), $^{\text{Mes}}[\text{NCN}]\text{Hf}(\text{NHNMe}_2)_2$ (4.26)

The following procedure is representative of the synthesis of **4.25** and **4.26**. In a 50 mL Erlenmeyer flask, **3.35** (200 mg, 0.33 mmol) was dissolved in 10 mL of toluene and cooled to  $-30^\circ\text{C}$ . A toluene solution of  $\text{Me}_2\text{NNH}_2$  (20 mg, 0.33 mmol) was carefully added dropwise at this temperature and the colorless solution was slowly warmed to room

temperature. After stirring overnight, the solution was filtered through Celite, and the solvent removed *in vacuo*. Et<sub>2</sub>O was added and the solution was carefully concentrated and cooled to -30°C to yield large block colorless crystals. Yield = 131 mg, 62%.

**4.25: <sup>1</sup>H NMR (C<sub>6</sub>D<sub>6</sub>):** δ 0.35 (s, 3H, -HfCH<sub>3</sub>), 2.00 (s, 6H, -N(CH<sub>3</sub>)<sub>2</sub>), 2.32 (s, 6H, -*o*-ArCH<sub>3</sub>), 2.44 (s, 6H, -*o*-ArCH<sub>3</sub>), 2.63 (s, 6H, -*p*-ArCH<sub>3</sub>), 3.44 (m, 2H, -NCH<sub>2</sub>), 3.62-3.70 (m, 6H, -NCH<sub>2</sub>), 4.13 (s, 1H, -NH), 6.08 (s, 2H, -imidH), 7.05 (s, 2H, -ArH), 7.09 (s, 2H, -ArH).

**<sup>13</sup>C{<sup>1</sup>H} NMR (C<sub>6</sub>D<sub>6</sub>):** δ 22.4 (-CH<sub>3</sub>), 23.1 (-CH<sub>3</sub>), 35.2 (-NCH<sub>3</sub>), 49.6 (-NCH<sub>2</sub>), 50.2 (-HfCH<sub>3</sub>), 53.1 (-NCH<sub>2</sub>), 118.6 (-ArC), 119.2 (-imidC), 128.4 (-ArC), 130.1 (-ArC), 143.2 (-ArC), 191.4 (-NCN).

Anal Calcd. for C<sub>28</sub>H<sub>42</sub>HfN<sub>6</sub>: C, 52.45; H, 6.60; N, 13.11. Found: C, 52.58; H, 6.51; N, 13.29.

**4.26: <sup>1</sup>H NMR (C<sub>6</sub>D<sub>6</sub>):** 2.12 (s, 12H, -N(CH<sub>3</sub>)<sub>2</sub>), 2.31 (s, 6H, -*p*-ArCH<sub>3</sub>), 2.50 (s, 12H, -*o*-ArCH<sub>3</sub>), 3.60 (m, 4H, -NCH<sub>2</sub>), 3.78 (m, 4H, -NCH<sub>2</sub>), 6.04 (s, 2H, -imidH), 7.02 (s, 4H, -ArH).

**<sup>13</sup>C{<sup>1</sup>H} NMR (C<sub>6</sub>D<sub>6</sub>):** δ 20.3 (-CH<sub>3</sub>), 21.5 (-CH<sub>3</sub>), 39.5 (-NCH<sub>3</sub>), 48.6 (-NCH<sub>2</sub>), 52.3 (-NCH<sub>2</sub>), 53.8 (-HfCH<sub>3</sub>), 118.0 (-ArC), 118.5 (-imidC), 127.9 (-ArC), 133.2 (-ArC), 145.9 (-ArC), 192.5 (-NCN).

Anal Calcd. for C<sub>29</sub>H<sub>46</sub>HfN<sub>8</sub>: C, 50.83; H, 6.77; N, 16.35. Found: C, 50.77; H, 6.93; N, 16.18.

#### 4.8.4. Polymerization protocols

**a) Ethylene polymerization:** A 100 mL Schlenk flask was charged with 50 mL toluene inside a glove box and attached to a vacuum line. The toluene was degassed with ethylene for 30 minutes at room temperature, whereby a toluene (5mL) solution of [Ph<sub>3</sub>C][B(C<sub>6</sub>F<sub>5</sub>)<sub>4</sub>] was syringed into the flask. The orange solution was stirred for 5 minutes under ethylene. A toluene (5 mL) solution of the catalyst was quickly added and the opaque solution stirred for 15 minutes. The experiment was stopped by venting the ethylene and quenching the reaction with 10% methanolic HCl. The resulting

polyethylene was filtered and washed with 10% methanolic HCl and methanol and air-dried overnight.

**b) 1-hexene polymerization:** **4.4** and **4.5** were generated in chlorobenzene and 1-hexene was added immediately (~500 equivalents) by syringe. The solution was stirred for 1 hour and quenched with 10% methanolic HCl. The solvents were removed, the residue dissolved in pentane, and filtered through silica gel. The solvents were removed *in vacuo* to yield a minor amount of a viscous gel.

#### 4.10. References

- (1) Arnold, P. L.; Mungur, S. A.; Blake, A. J.; Wilson, C. *Angew. Chem. Int. Ed.* **2003**, *42*, 5981.
- (2) Scollard, J. D.; McConville, D. H.; Vittal, J. J. *Organometallics* **1997**, *16*, 4415.
- (3) Keaton, R. J.; Jayaratne, K. C.; Fettinger, J. C.; Sita, L. R. *J. Am. Chem. Soc.* **2000**, *122*, 12909.
- (4) Tshuva, E. Y.; Groysman, S.; Goldberg, I.; Kol, M.; Goldschmidt, Z. *Organometallics* **2002**, *21*, 662.
- (5) Tian, J.; Hustad, P. D.; Coates, G. W. *J. Am. Chem. Soc.* **2001**, *123*, 5134.
- (6) Jeon, Y.-M.; Park, S. J.; Heo, J.; Kim, K. *Organometallics* **1998**, *17*, 3161.
- (7) Killian, C. M.; Tempel, D. J.; Johnson, L. K.; Brookhart, M. *J. Am. Chem. Soc.* **1996**, *118*, 11664.
- (8) Mashima, K.; Fujikawa, S.; Tanaka, Y.; Urata, H.; Oshiki, T.; Tanaka, E.; Nakamura, A. *Organometallics* **1995**, *14*, 2633.
- (9) Mitani, M.; Mohri, J.; Yoshida, Y.; Saito, J.; Ishii, S.; Tsuru, K.; Matsui, S.; Furuyama, R.; Nakano, T.; Tanaka, H.; Kojoh, S.-i.; Matsugi, T.; Kashiwa, N.; Fujita, T. *J. Am. Chem. Soc.* **2002**, *124*, 3327.
- (10) Stevens, J. C.; Timmers, F. J.; Wilson, D. R.; Schmidt, G. F.; Nickias, P. N.; Rosen, R. K.; Knight, G. W.; Lai, S. Y.; (Dow Chemical Co., USA). Application: EP, 1991, p 58 pp.
- (11) Niehues, M.; Kehr, G.; Erker, G.; Wibbeling, B.; Frohlich, R.; Blacque, O.; Berke, H. *J. Organomet. Chem.* **2002**, *663*, 192.
- (12) Aihara, H.; Matsuo, T.; Kawaguchi, H. *Chem. Commun.* **2003**, 2204.
- (13) Skoog, S. J.; Mateo, C.; Lavoie, G. G.; Hollander, F. J.; Bergman, R. G. *Organometallics* **2000**, *19*, 1406.
- (14) Asakura, T.; Demura, M.; Nishiyama, Y. *Macromolecules* **1991**, *24*, 2334.
- (15) Warren, T. H.; Schrock, R. R.; Davis, W. M. *Organometallics* **1996**, *15*, 562.
- (16) Durfee, L. D.; Rothwell, I. P. *Chem. Rev.* **1988**, *88*, 1059.

- (17) Ford, P. C.; Editor *ACS Symposium Series, Vol. 152: Catalytic Activation of Carbon Monoxide*, 1981.
- (18) Grundemann, S.; Kovacevic, A.; Albrecht, M.; Faller Jack, W.; Crabtree Robert, H. *J. Am. Chem. Soc.* **2002**, *124*, 10473.
- (19) Danopoulos, A. A.; Tsoureas, N.; Green, J. C.; Hursthouse, M. B. *Chem. Commun.* **2003**, 756.
- (20) Chamberlain, L. R.; Durfee, L. D.; Fanwick, P. E.; Kobriger, L. M.; Latesky, S. L.; McMullen, A. K.; Steffey, B. D.; Rothwell, I. P.; Foltin, K.; Huffman, J. C. *J. Am. Chem. Soc.* **1987**, *109*, 6068.
- (21) Berg, F. J.; Petersen, J. L. *Tetrahedron* **1992**, *48*, 4749.
- (22) Herrmann, W. A. *Angew. Chem. Int. Ed.* **2002**, *41*, 1290.
- (23) Bourissou, D.; Guerret, O.; Gabbaie, F. P.; Bertrand, G. *Chem. Rev.* **2000**, *100*, 39.
- (24) Chamberlain, L. R.; Durfee, L. D.; Fanwick, P. E.; Kobriger, L.; Latesky, S. L.; McMullen, A. K.; Rothwell, I. P.; Foltin, K.; Huffman, J. C.; et al. *J. Am. Chem. Soc.* **1987**, *109*, 390.
- (25) Lappert, M. F.; Ngoc Tuyet Luong, T.; Milne, C. R. C. *J. Organomet. Chem.* **1979**, *174*, C35.
- (26) Durfee, L. D.; McMullen, A. K.; Rothwell, I. P. *J. Am. Chem. Soc.* **1988**, *110*, 1463.
- (27) Latesky, S. L.; McMullen, A. K.; Niccolai, G. P.; Rothwell, I. P.; Huffman, J. C. *Organometallics* **1985**, *4*, 1896.
- (28) Chamberlain, L. R.; Rothwell, I. P.; Huffman, J. C. *J. Chem. Soc., Chem. Commun.* **1986**, 1203.
- (29) Erker, G.; Engel, K.; Krueger, C.; Mueller, G. *Organometallics* **1984**, *3*, 128.
- (30) Bristow, G. S.; Lappert, M. F.; Martin, T. R.; Atwood, J. L.; Hunter, W. F. *J. Chem. Soc., Dalton Trans.* **1984**, 399.
- (31) Manriquez, J. M.; McAlister, D. R.; Sanner, R. D.; Bercaw, J. E. *J. Am. Chem. Soc.* **1978**, *100*, 2716.
- (32) Wolczanski, P. T.; Bercaw, J. E. *Acc. Chem. Res.* **1980**, *13*, 121.

- (33) Choukroun, R.; Douziech, B.; Soleil, F. *J. Chem. Soc., Chem. Commun.* **1995**, 2017.
- (34) Sonnenberger, D. C.; Mintz, E. A.; Marks, T. J. *J. Am. Chem. Soc.* **1984**, *106*, 3484.
- (35) Marks, T. J. *Science* **1982**, *217*, 989.
- (36) Manriquez, J. M.; Fagan, P. J.; Marks, T. J.; Day, C. S.; Day, V. W. *J. Am. Chem. Soc.* **1978**, *100*, 7112.
- (37) Erker, G.; Noe, R. *J. Chem. Soc., Dalton Trans.* **1991**, 685.
- (38) S. Gambarotta, C. F., A. Chiesi-Villa, C. Guastini *J. Am. Chem. Soc.* **1983**, 1690.
- (39) Erker, G.; Petrenz, R. *J. Chem. Soc., Chem. Commun.* **1989**, 345.
- (40) Erker, G.; Sosna, F.; Zwettler, R.; Krueger, C. *Organometallics* **1989**, *8*, 450.
- (41) Erker, G.; Engel, K.; Atwood, J. L.; Hunter, W. E. *Angew. Chem., Int. Ed.* **1983**, *95*, 506.
- (42) Meyer, T. Y.; Garner, L. R.; Baenziger, N. C.; Messerle, L. *Inorg. Chem.* **1990**, *29*, 4045.
- (43) Gambarotta, S.; Strologo, S.; Floriani, C.; Chiesi-Villa, A.; Guastini, C. *Inorg. Chem.* **1985**, *24*, 654.
- (44) Koterwas, L. A.; Fettinger, J. C.; Sita, L. R. *Organometallics* **1999**, *18*, 4183.
- (45) Sita, L. R.; Babcock, J. R. *Organometallics* **1998**, *17*, 5228.
- (46) Jayaratne, K. C.; Sita, L. R. *J. Am. Chem. Soc.* **2000**, *122*, 958.
- (47) Littke, A.; Sleiman, N.; Bensimon, C.; Richeson, D. S.; Yap, G. P. A.; Brown, S. *J. Organometallics* **1998**, *17*, 446.
- (48) Coles, M. P.; Swenson, D. C.; Jordan, R. F.; Young, V. G., Jr. *Organometallics* **1997**, *16*, 5183.
- (49) Obermeyer, A.; Kienzle, A.; Weidlein, J.; Riedel, R.; Simon, A. *Z. Anorg. Allg. Chem.* **1994**, *620*, 1357.
- (50) Sutton, L. E.; Editor *Tables of Interatomic Distances and Configuration in Molecules and Ions: Supplement 1956-1959 (Chemical Society (London) Special Publication No. 18)*, 1965.

- (51) Fryzuk, M. D.; Johnson, S. A.; Patrick, B. O.; Albinati, A.; Mason, S. A.; Koetzle, T. F. *J. Am. Chem. Soc.* **2001**, *123*, 3960.
- (52) Morello, L.; Yu, P.; Carmichael, C. D.; Patrick, B. O.; Fryzuk, M. D. *J. Am. Chem. Soc.* **2005**, *127*, 12796.
- (53) Fryzuk, M. D.; Yu, P.; Patrick, B. O. *Can. J. Chem.* **2001**, *79*, 1194.
- (54) Basch, H.; Musaev, D. G.; Morokuma, K.; Fryzuk, M. D.; Love, J. B.; Seidel, W. W.; Albinati, A.; Koetzle, T. F.; Klooster, W. T.; Mason, S. A.; Eckert, J. *J. Am. Chem. Soc.* **1999**, *121*, 523.
- (55) Cohen, J. D.; Fryzuk, M. D.; Loehr, T. M.; Mylvaganam, M.; Rettig, S. J. *Inorg. Chem.* **1998**, *37*, 112.
- (56) Cohen, J. D.; Mylvaganam, M.; Fryzuk, M. D.; Loehr, T. M. *J. Am. Chem. Soc.* **1994**, *116*, 9529.
- (57) Fryzuk, M. D.; Haddad, T. S.; Mylvaganam, M.; McConville, D. H.; Rettig, S. J. *J. Am. Chem. Soc.* **1993**, *115*, 2782.
- (58) Fryzuk, M. D.; Jin, W. *Unpublished Results* **1998**.
- (59) Danopoulos, A. A.; Wright, J. A.; Motherwell, W. B. *Chem. Commun.* **2005**, 784.
- (60) Arnold, P. L.; Liddle, S. T. *Organometallics* **2006**, *25*, 1485.
- (61) Arnold, P. L.; Liddle, S. T. *Chem. Commun.* **2005**, 5638.
- (62) Fandos, R.; Hernandez, C.; Otero, A.; Rodriguez, A.; Ruiz, M. J.; Terreros, P. *J. Organomet. Chem.* **2000**, *606*, 156.
- (63) Chang, S.-J.; Liu, H.-J.; Chen, C.-T.; Shih, W.-E.; Lin, C.-C.; Gau, H.-M. *J. Organomet. Chem.* **1996**, *523*, 47.
- (64) Sobota, P.; Janas, Z. *J. Organomet. Chem.* **1983**, *243*, 35.
- (65) Covert, K. J.; Mayol, A.-R.; Wolczanski, P. T. *Inorg. Chim. Acta* **1997**, *263*, 263.
- (66) Miller, R. L.; Toreki, R.; LaPointe, R. E.; Wolczanski, P. T.; Van Duyne, G. D.; Roe, D. C. *J. Am. Chem. Soc.* **1993**, *115*, 5570.
- (67) Burgess, B. K. *Chem. Rev.* **1990**, *90*, 1377.
- (68) Malinak, S. M.; Coucouvanis, D. *Prog. Inorg. Chem.* **2001**, *49*, 599.
- (69) Einsle, O.; Tezcan, F. A.; Andrade, S. L. A.; Schmid, B.; Yoshida, M.; Howard, J. B.; Rees, D. C. *Science* **2002**, *297*, 1696.

- (70) Nugent, W. A.; Haymore, B. L. *Coord. Chem. Rev.* **1980**, *31*, 123.
- (71) Li, Y.; Shi, Y.; Odom, A. L. *J. Am. Chem. Soc.* **2004**, *126*, 1794.
- (72) Wiberg, N.; Haering, H. W.; Huttner, G.; Friedrich, P. *Chem. Ber.* **1978**, *111*, 2708.
- (73) Blake, A. J.; McInnes, J. M.; Mountford, P.; Nikonov, G. I.; Swallow, D.; Watkin, D. J. *J. Chem. Soc., Dalton Trans.* **1999**, 379.
- (74) Thorman, J. L.; Woo, L. K. *Inorg. Chem.* **2000**, *39*, 1301.
- (75) Hughes, D. L.; Latham, I. A.; Leigh, G. J. *J. Chem. Soc., Dalton Trans.* **1986**, 393.
- (76) Yamaguchi, A.; Ichishima, I.; Shimanouchi, T.; Mizushima, S. *J. Chem. Phys.* **1959**, *31*, 843.
- (77) Podall, H. E.; Foster, W. E.; Giraitis, A. P. *J. Org. Chem.* **1958**, *23*, 82.

## Chapter Five

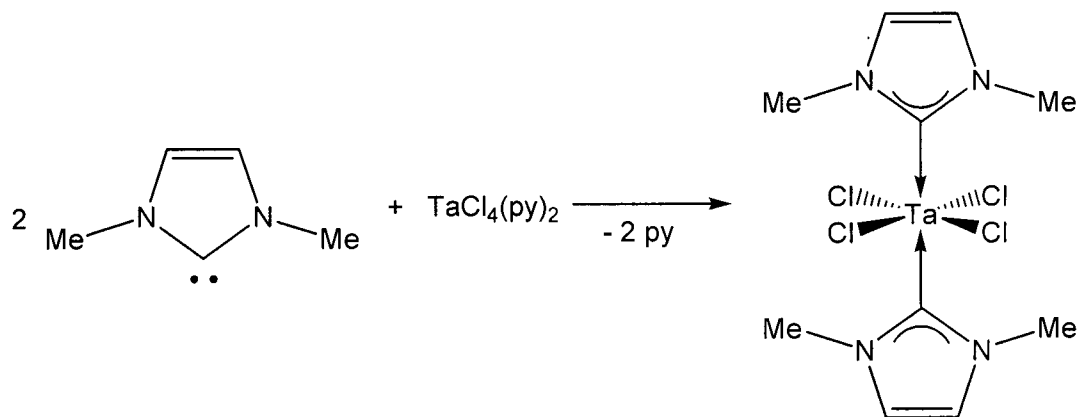
# Synthesis and DFT Studies of Tantalum [NCN] Transition Metal Complexes

### 5.1. Introduction\*

Given the absence of NHC dissociation in group 4 [NCN] complexes discussed in chapter 4, we were interested in the synthesis of other early transition metal [NCN] complexes. As was previously discussed in chapter 2, a tantalum [NPN] complex has been isolated displaying a unique side-on end-on coordination mode for dinitrogen. The synthesis of this complex is quite remarkable as this occurs in the absence of strong reducing agents such as  $KC_8$  or Na/Hg amalgam. In chapter 4, the synthesis of group 4 [NCN] dinitrogen complexes was attempted; however, no dinitrogen containing products were recovered. While the reasons for this are unclear, the potential for other [NCN] transition metal complexes to promote dinitrogen activation is of interest. Tantalum [NCN] complexes are of particular appeal, in light of the successful synthesis of the tantalum [NPN] dinitrogen complex **2.5**.

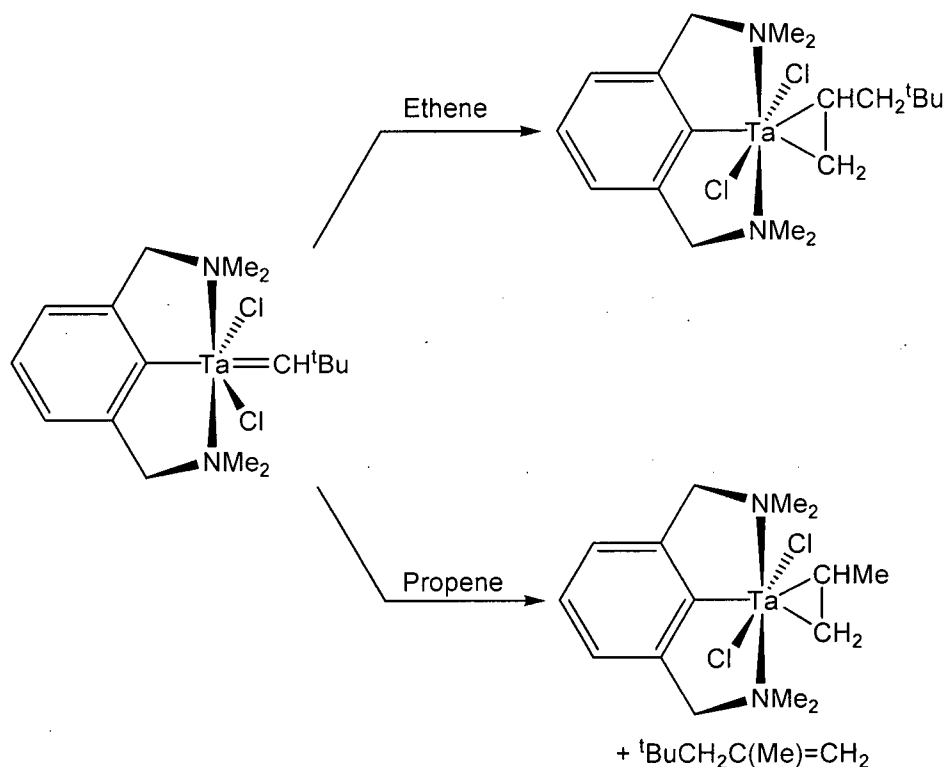
\*A version of this chapter has been accepted for publication (*J. Am. Chem. Soc.*).

To the best of our knowledge, only one previous report describes the chemistry of tantalum-NHC complexes.<sup>1</sup> The addition of a simple alkyl-substituted NHC to  $\text{TaCl}_4(\text{py})_2$  results in the displacement of both pyridine ligands to give  $\text{TaCl}_4(\text{NHC})_2$  (Scheme 5.1). Although these results appear promising, no solid state molecular structures, reactivity, or applications of the complexes were mentioned.



**Scheme 5.1.**

Pincer {NCN}-based ligands that have an anionic aryl group flanked by two amino donors have also been a subject of investigation in organotantalum chemistry (Scheme 5.2).<sup>2-8</sup> In particular, a monoanionic {NCN} ligand has been found to be an excellent spectator ligand that stabilizes and controls tantalum centered reactions. For example, the central metal-aryl unit of the {NCN} ligand was found to be chemically inert during a variety of alkylidene-based transformations reactions that resulted in the formation of reactive tantalum alkene adducts.



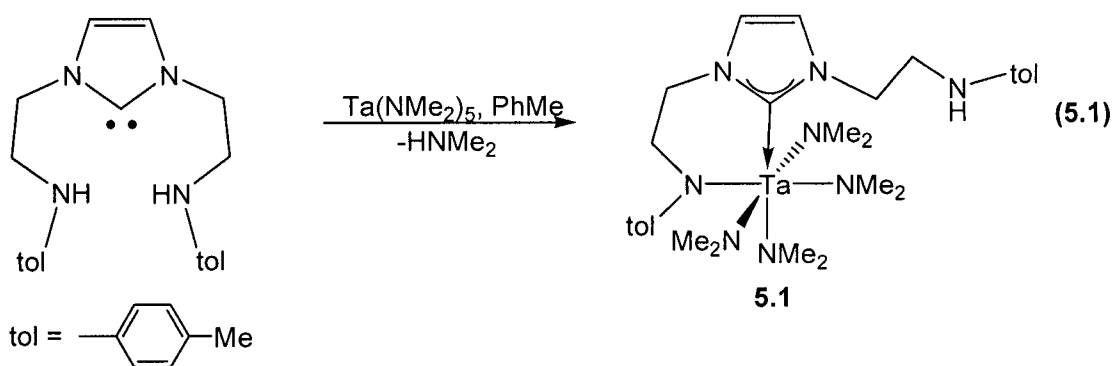
Scheme 5.2.

This chapter details the synthesis of tantalum-amide, -halide, and -alkyl compounds bearing an [NCN] ancillary ligand. In addition, our unsuccessful attempts to prepare a coordinated dinitrogen stabilized by this ligand are also included. In the case of tantalum alkyl compounds, an unexpected C-H activation process occurs, which was investigated by DFT calculations and NMR experiments using deuterium labeled compounds.

## 5.2. Synthesis of Amine-Amide [NCNH] Tantalum Derivatives

In light of the success using aminolysis reactions described in chapter 3, a similar approach was examined as a convenient entry into tantalum [NCN] derivatives. Disappointingly, there was no reaction between  ${}^{\text{Mes}}[\text{NCN}]\text{H}_2$  (**3.8**) and  $\text{Ta}(\text{NMe}_2)_5$ , even at elevated temperatures. Decreasing the steric bulk on the amide donors did promote a reaction. The addition of  ${}^{\text{tol}}[\text{NCN}]\text{H}_2$  (**3.7**) to  $\text{Ta}(\text{NMe}_2)_5$  in toluene yielded a product

that displayed a set of  $^1\text{H}$  and  $^{13}\text{C}$  resonances in the NMR spectra indicative of  $C_s$  symmetric species (**5.1**). This is in contrast to the expected  $C_{2v}$  symmetry anticipated for  $^{\text{tol}}[\text{NCN}]\text{Ta}(\text{NMe}_2)_3$ . NMR spectroscopy shows four multiplets for the ethylene spacers, two doublets for the imidazole groups, two distinct sets of doublets typical of *para*-substituted aryl rings, two aryl-methyl signals, and a broad resonance attributable to the  $-\text{NMe}_2$  groups. Furthermore, a triplet at 3.32 ppm is observed which can be ascribed to an amino  $-\text{NH}$  group. The  $^{13}\text{C}\{^1\text{H}\}$  NMR spectrum features a weak downfield resonance at 198.5 ppm, typical of a metal-carbene carbon atom. From these results, it appears coordination of the [NCN] ligand to tantalum is incomplete, one amine donor is still present, giving the molecule an overall  $C_s$  symmetry in solution (Equation 5.1).



Orange crystals of **5.1** were grown from a saturated solution of toluene and were studied by X-ray crystallography. An ORTEP depiction of the solid state molecular structure **5.1** is shown in Figure 5.1, with selected bond angles and lengths given in Table 5.1 and crystallographic details located in appendix A. The ligand assumes an amide-amine donor configuration with respect to a distorted octahedral metal centre. The Ta-alkyl carbene bond length is 2.407(4) Å and represents, to the best of our knowledge, the first crystallographically characterized Ta-C NHC bond. The Ta-N amido bond lengths are similar to other reported compounds.<sup>9-13</sup> Although introduction of the [NCN] ligand is incomplete, we were encouraged by the formation of a new Ta-C NHC bond. Thus far, all attempts to promote the coordination of the other pendant amine donor have been unsuccessful.

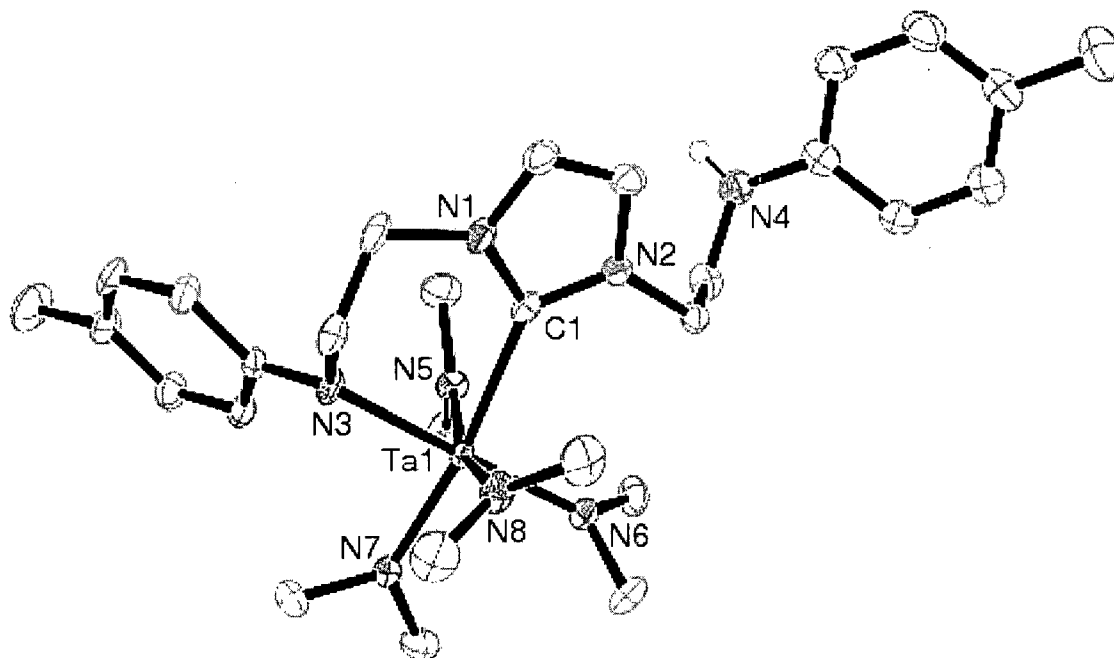


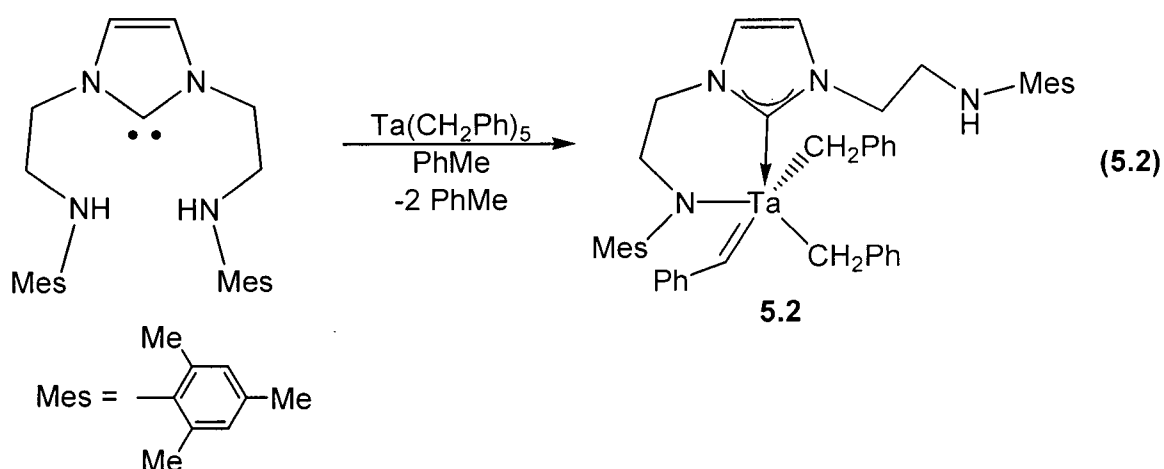
**Figure 5.1.** ORTEP view of  $^{10l}[\text{NCNH}]\text{Ta}(\text{NMe}_2)_4$  (**5.1**) ( $\text{CH}_3\text{C}_6\text{H}_5$  omitted) depicted with 50% thermal ellipsoids; all hydrogen atoms have been omitted for clarity.

**Table 5.1.** Selected bond distances (Å) and angles ( $^\circ$ ) for  $^{10l}[\text{NCNH}]\text{Ta}(\text{NMe}_2)_4$ , **5.1**.

Bond Lengths		Bond Angles	
Ta1-C1	2.407(4)	N8-Ta1-N3	90.58(12)
Ta1-N3	2.181(3)	N6-Ta1-N3	178.48(11)
Ta1-N8	2.050(3)	N3-Ta1-C1	80.14(11)

In chapter 3, alkyl elimination reactions between **3.7** and  $\text{Zr}(\text{CH}_2\text{R})_4$  ( $\text{R} = \text{SiMe}_3$ , Ph) provided the desired five-coordinate dialkyl  $^{10l}[\text{NCN}]\text{Zr}(\text{CH}_2\text{R})_2$  complexes. A similar approach was examined with  $^{\text{Mes}}[\text{NCN}]\text{H}_2$  (**3.8**) and  $\text{Ta}(\text{CH}_2\text{Ph})_5$ . The reaction proceeds immediately in toluene to give dark brown **5.2**, which displays a  $^1\text{H}$  NMR spectrum with inequivalent imidazole and aryl resonances (Equation 5.2). A benzyldiene resonance is observed at 4.81 ppm and correlates with a  $^{13}\text{C}$  resonance located at 236.3 ppm in the  $^{13}\text{C}\{^1\text{H}\}$  NMR spectrum. Presumably, alkylidene formation proceeds through a tetraalkyl  $^{\text{Mes}}(\text{NCNH})\text{Ta}(\text{CH}_2\text{Ph})_4$  intermediate, which is not observed in solution. This species undergoes  $\alpha$ -hydrogen abstraction to generate the benzyldiene product, a phenomenon that has been observed in other tantalum alkyl complexes.<sup>14</sup> Interestingly,

there is no change in the  $^{13}\text{C}$  carbene resonance (or that in **5.1**) in the presence of pyridine over a long period of time, a surprising result despite the carbene dissociation reported in similar bidentate amido-carbene early transition metal complexes.<sup>15</sup>



An ORTEP depiction of the solid state molecular structure for **5.2** is shown in Figure 5.2 as determined by an X-ray diffraction experiment. Relevant bond lengths and angles are listed in Table 5.2, and crystallographic details are located in Appendix A. A benzylidene moiety is clearly observed in addition to an amide-amine ligand configuration on a distorted square pyramidal metal centre. The alkylidene moiety is clearly defined by a large Ta-C-C bond angle of  $164.5(4)^\circ$  and a short Ta-C alkyl bond ( $1.940(4) \text{ \AA}$ ), with the latter being significantly shorter than that of the other two Ta-C alkyl bonds ( $\sim 2.26 \text{ \AA}$ ). The Ta=C bond compares well with previously described Ta-alkylidene complexes.<sup>16</sup> The Ta-C carbene and Ta-N amido bond lengths are similar to **5.1**. Attempts to promote coordination of the pendant amine arm by thermolysis have proven futile leading only to decomposition.

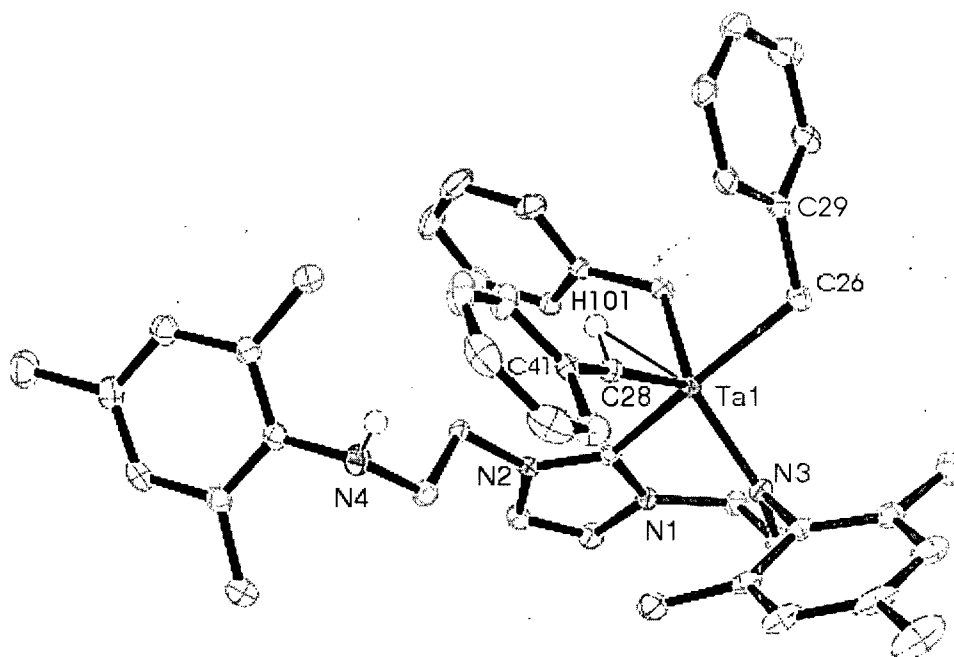


**Figure 5.2.** ORTEP view of  $^{\text{Mes}}[\text{NCNH}]\text{Ta}(\text{CHPh})(\text{CH}_2\text{Ph})_2$  (**5.2**), depicted with 50% thermal ellipsoids; all hydrogen atoms have been omitted for clarity with the exception of H101.

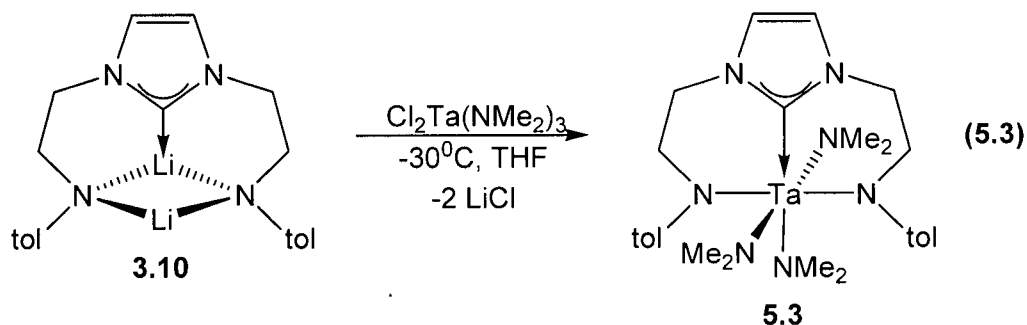
**Table 5.2.** Selected bond distances (Å) and angles ( $^\circ$ ) for  $^{\text{Mes}}[\text{NCNH}]\text{Ta}(\text{CHPh})(\text{CH}_2\text{Ph})_2$  (**5.2**).

Bond Lengths		Bond Angles	
Ta1-C28	1.940(3)	N3-Ta1-C1	80.90(9)
Ta1-N3	2.011(2)	C41-C28-Ta1	164.5(2)
Ta1-C26	2.243(3)	C29-C26-Ta1	126.44(18)
Ta1-C27	2.259(3)		
Ta1-C1	2.290(3)		

### 5.3 Successful Synthesis of Ta[NCN] Amide Complexes

Given the difficulty of coordinating both amide donors to a Ta(V) centre by aminolysis and alkane elimination reactions, an alternative method was sought as a means to generate the desired tridentate coordination mode for this ligand system. Metathesis reactions with  $\text{Li}_2[\text{NPN}]$  have successfully been used by many groups

including our own in the synthesis of tantalum [NPN] metal complexes.<sup>17</sup> The metathesis reaction of **3.10** and  $\text{Cl}_2\text{Ta}(\text{NMe}_2)_3$  proceeds at  $-30^\circ\text{C}$  to produce  $^{101}\text{[NCN]Ta}(\text{NMe}_2)_3$  (**5.3**) in good yield. The  $^1\text{H}$  NMR spectrum features two multiplets for the ethylene spacers and one set of resonances for the imidazole, aryl, and *para*-methyl aryl groups. There are two sets of resonances for the N-methyl protons of the  $\text{NMe}_2$  groups in a ratio of 2:1 at 3.22 and 3.68 ppm. A weak  $^{13}\text{C}$  resonance in the  $^{13}\text{C}\{^1\text{H}\}$  NMR spectrum is also observed at 186.7 ppm, indicative of a metal-carbene carbon atom (Equation 5.3).



Crystals suitable for an X-ray diffraction experiment were grown from toluene and an ORTEP depiction of the solid state molecular structure of **5.3** is shown in Figure 5.3. Relevant bond lengths and angles are listed in Table 5.3, and crystallographic details are located in appendix A. Clearly the ligand exists in a dianionic state with both pendant amide donors coordinating to a single tantalum centre. The ligand adopts a meridional orientation with respect to a distorted octahedral metal centre as evidenced by the *cis* oriented amido donors ( $\text{N}2\text{-Ta}1\text{-N}3 = 89.25(4)^\circ$  and  $\text{N}2\text{-Ta}1\text{-N}4 = 98.46(4)^\circ$ ). The Ta-C carbene and Ta-N amido bond lengths are similar to previously discussed complexes.

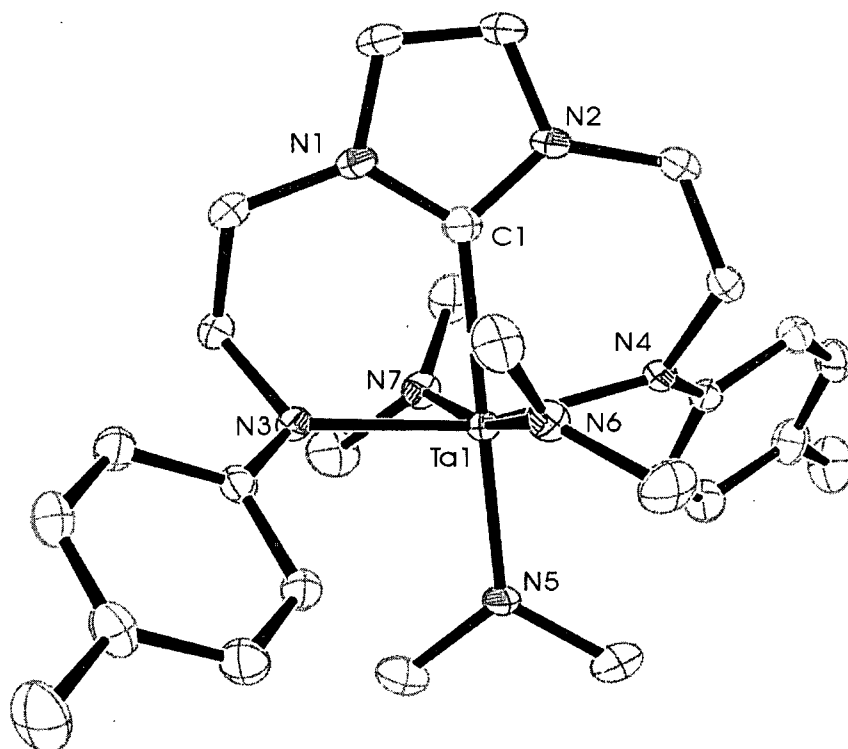


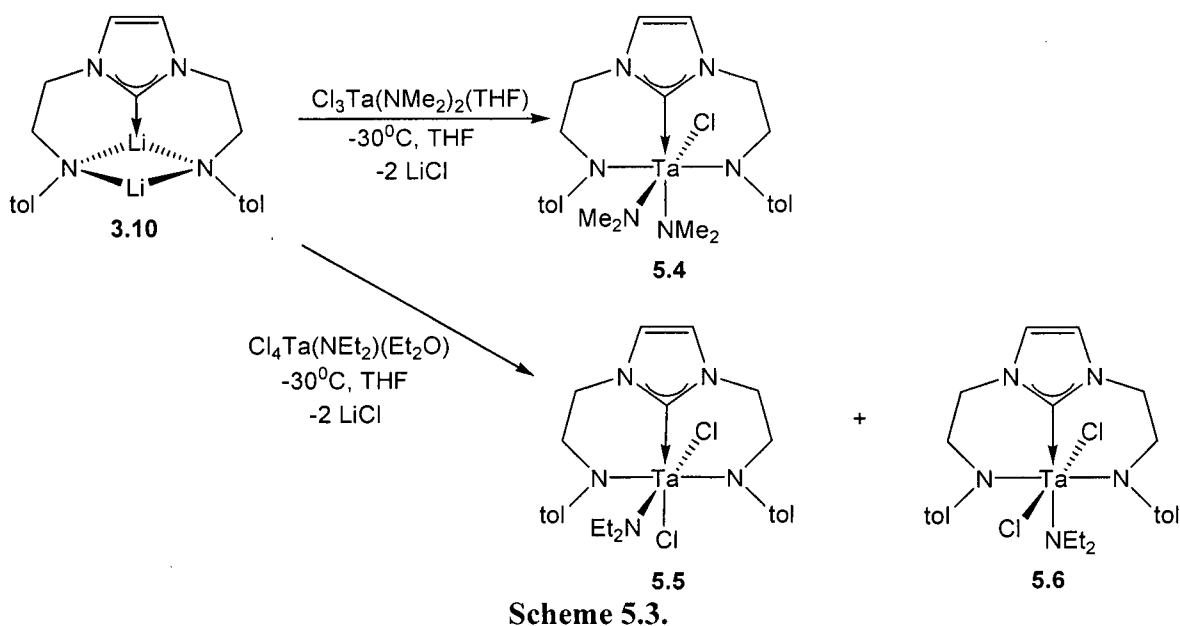
**Figure 5.3.** ORTEP view of  $^{101}\text{[NCN]Ta(NMe}_2\text{)}_3$  (**5.3**), depicted with 50% thermal ellipsoids; all hydrogen atoms have been omitted for clarity.

**Table 5.3.** Selected bond distances (Å) and angles ( $^\circ$ ) for  $^{101}\text{[NCN]Ta(NMe}_2\text{)}_3$  (**5.3**).

Bond Lengths		Bond Angles	
Ta1-N3	2.055(3)	N3-Ta1-N2	89.25(13)
Ta1-N4	2.078(4)	N3-Ta1-C1	82.93(10)
Ta1-N2	2.132(3)	N2-Ta1-C1	81.54(9)
Ta1-C1	2.365(6)	N4-Ta1-C1	180.000(2)

Modification of the tantalum starting material serves as a useful entry into mixed amide-chloride metal complexes. The reaction of **3.10** and  $\text{Cl}_3\text{Ta(NMe}_2\text{)}_2(\text{THF})$  yields the expected product  $^{101}\text{[NCN]TaCl(NMe}_2\text{)}_2$  (**5.4**) (Scheme 5.3). The  $^1\text{H}$  NMR spectrum reveals a  $C_s$  symmetric species in solution with four sets of multiplets for the ethylene spacers and most noticeably three singlets integrating to six protons each. This evidence suggests a *cis* arrangement of  $\text{NMe}_2$  groups on the tantalum centre. Although no crystals of the product could be recovered, NMR evidence is quite compelling given that *trans* deposited  $\text{NMe}_2$  groups would yield a species with  $C_{2v}$  symmetry in solution. A similar reaction with **3.10** and  $\text{TaCl}_4(\text{NEt}_2)(\text{Et}_2\text{O})$  also yields the expected  $^{101}\text{[NCN]TaCl}_2(\text{NEt}_2)$  product. The  $^1\text{H}$  NMR spectrum reveals the presence of two structural isomers in

solution. The minor species possesses  $C_s$  symmetry, a result that would be expected with *cis* deposited chloride groups on the tantalum centre (5.5). The major species possesses  $C_{2v}$  symmetry, indicative of *trans* oriented chloride groups on the metal centre (5.6).



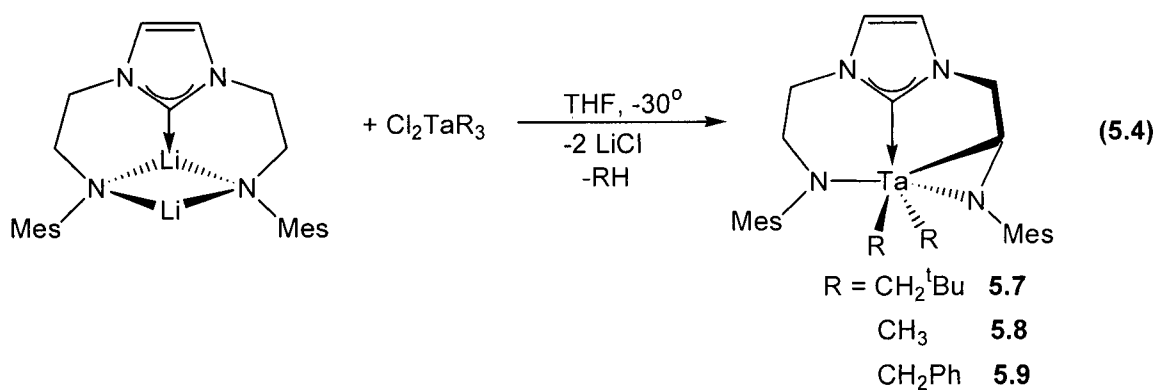
Scheme 5.3.

The reactivity of these amide-substituted Ta[NCN] complexes was investigated, in particular the synthesis of [NCN]TaCl<sub>3</sub> and alkyl derivatives. These complexes could be used in reductive processes to activate N<sub>2</sub>. Unfortunately, attempts to convert the amide groups of 5.3-5.6 to chloride ligands with TMSCl, BCl<sub>3</sub>, or NEt<sub>3</sub>-HCl yields a mixture of intractable materials. Similar results were found when alkylation of 5.3-5.6 was attempted with Al<sub>2</sub>Me<sub>6</sub>, MeLi, MeMgBr, or (<sup>t</sup>BuCH<sub>2</sub>)<sub>2</sub>Zn. The reduction of 5.3-5.6 with strong reducing reagents under N<sub>2</sub> was also investigated; however, no dinitrogen containing products were identified.

#### 5.4. Isolation of Cyclometallated [NCCN]Ta Dialkyl Derivatives

One of the precursors for the synthesis of the [NPN] tantalum dinitrogen complex 2.5 is an [NPN]-substituted tantalum trialkyl derivative. Given the success of coordinating the [NCN] ligand to tantalum by metathesis reactions with mixed alkyl-

chloro precursors of Ta(V),  $\text{Cl}_2\text{TaR}_3$  ( $\text{R} = \text{CH}_2^t\text{Bu}$ , Me,  $\text{CH}_2\text{Ph}$ ), was examined. The reaction of **3.11** with  $\text{Cl}_2\text{Ta}(\text{CH}_2^t\text{Bu})_3$  is representative of these metathesis reactions and proceeds immediately at  $-30^\circ\text{C}$  in THF to give a brown solution. The  $^1\text{H}$  NMR spectrum of the product reveals a complicated set of resonances indicative of a low-symmetry species. The ethylene arms of the ligand backbone are observed as sets of complex, coupled resonances. The asymmetry of the product is further exemplified by inequivalent imidazole-hydrogen resonances at 5.82 and 5.88 ppm. Two different tantalum alkyl  $^1\text{H}$  resonances are also observed, which is unexpected for the anticipated  $\text{Mes}[\text{NCN}]\text{Ta}(\text{CH}_2^t\text{Bu})_3$  product. The  $^{13}\text{C}\{^1\text{H}\}$  NMR spectrum shows two distinct Ta-C alkyl resonances around 70 ppm, and one weak resonance at 85 ppm suggestive of another Ta-C moiety (Equation 5.4).



The solid state molecular structure of **5.7** was determined from an X-ray diffraction experiment and an ORTEP depiction is shown in Figure 5.4. Selected bond angles and lengths are given in Table 5.4 and crystallographic details are located in appendix A. Surprisingly, one of the six-membered metallacycles has undergone cyclometallation to form new five- and three-membered rings. In lieu of the amide C-H bond activation, only two neopentyl groups are observed rather than the expected trialkyl substitution. The C-H bond activated ligand (denoted [NCCN]) adopts a distorted facial orientation about a distorted trigonal bipyramidal metal centre. The bond angles defined by Ta1-C7-N4 are typical of another structurally characterized metallazaaziridine tantalum

complex.<sup>18</sup> All Ta-C alkyl bonds are similar in length (~2.24 Å), and are representative of other reported Ta-C alkyl bond lengths.<sup>16,17,19</sup>

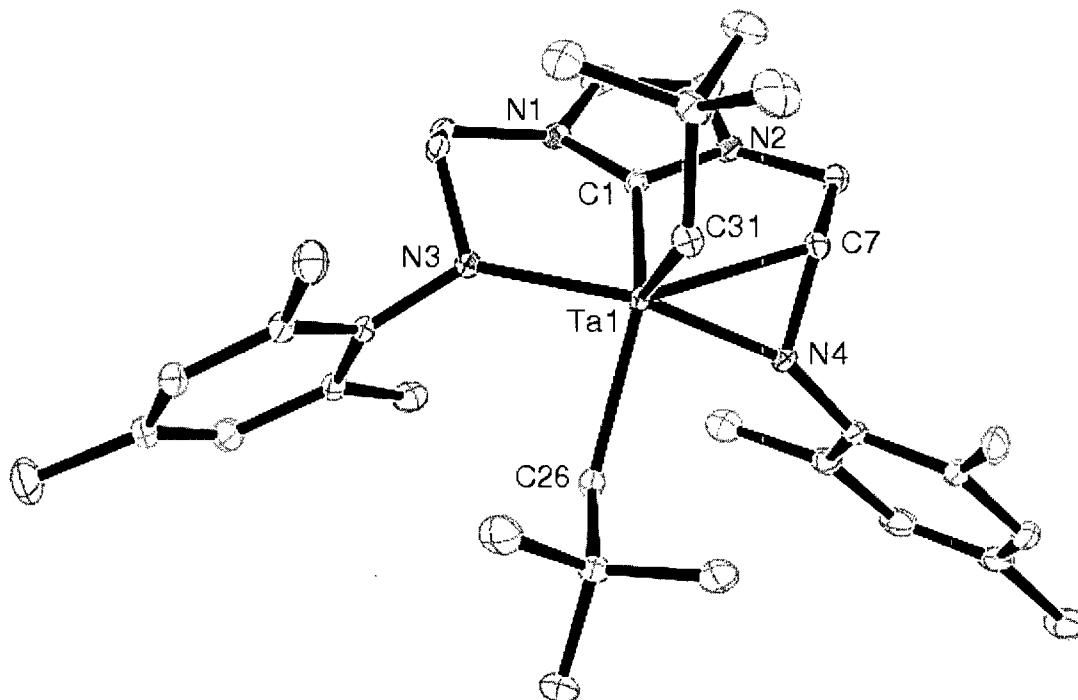


**Figure 5.4.** ORTEP view of <sup>Mes</sup>[NCCN]Ta(CH<sub>2</sub><sup>t</sup>Bu)<sub>2</sub> (**5.7**), depicted with 50% thermal ellipsoids; all hydrogen atoms have been omitted for clarity.

**Table 5.4.** Selected bond distances (Å) and angles (°) for <sup>Mes</sup>[NCCN]Ta(CH<sub>2</sub><sup>t</sup>Bu)<sub>2</sub> (**5.7**).

Bond Lengths		Bond Angles	
Ta1-N4	1.9877(15)	N4-Ta1-N3	153.91(6)
Ta1-N3	2.0738(17)	N4-Ta1-C1	89.46(6)
Ta1-C31	2.1833(17)	N3-Ta1-C1	79.59(6)
Ta1-C1	2.2247(17)	N4-Ta1-C7	39.37(6)
Ta1-C7	2.2257(19)	N4-C7-Ta1	61.34(9)
Ta1-C26	2.255(2)	C7-N4-Ta1	79.29(10)

### 5.5. Mechanistic Insight Into the Formation of 5.7-5.9

Intramolecular C-H bond activation of ligands in Ta complexes is relatively common,<sup>20,21</sup> particularly with amido-based systems.<sup>18,19,22-25</sup> Among these reports, the formation of metallaaziridine rings by exocyclic<sup>18,24,25</sup> C-H bond activation is known; the only example of endocyclic<sup>19</sup> C-H bond activation involves a tripodal tris(aryloxy)amine system that activates next the amine donor. In most examples, metallaaziridine ring formation appears to follow a  $\sigma$ -bond metathesis mechanism involving direct elimination of an alkane,<sup>24</sup> although in some cases the mechanism was not fully investigated.<sup>19</sup>

Two plausible mechanisms were explored for the formation of 5.7-5.9. Assuming that metathesis reactions between  $\text{Li}_2^{\text{Ar}}[\text{NCN}]$  and  $\text{Cl}_2\text{TaR}_3$  provide the trialkyl  $\text{Ar}[\text{NCN}]\text{TaR}_3$  derivatives, the ligand backbone  $\beta$ -H abstraction process may occur by either a one-step  $\sigma$ -bond metathesis pathway (Path 1, Figure 5.5) or a two-step pathway that involves  $\alpha$ -H abstraction to produce a  $[\text{NCN}]\text{Ta}(=\text{CHR}')\text{R}$  alkylidene intermediate (Path 2, Figure 5.5). This alkylidene intermediate could then mediate C-H bond activation of the ligand backbone. Given the literature precedence for both mechanisms, density functional calculations and isotopic labeling experiments were used to elucidate a mechanism for the formation of 5.7-5.9.

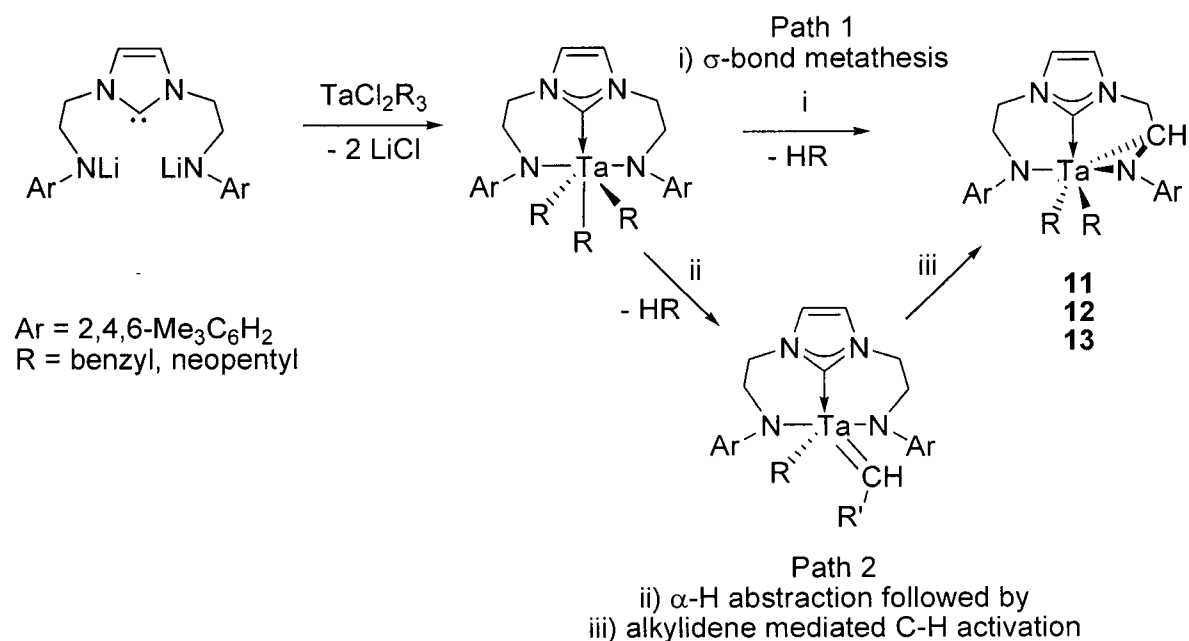


**Figure 5.5.** Potential pathways for ligand  $\beta$ -H abstraction.

### 5.6. Determination of Mechanism by DFT Calculations

DFT calculations were performed using the model complex shown in Figure 5.6 and the B3LYP/BS1 level of theory. All the DFT calculations were performed by Dr. Chad Beddie at the Texas A&M University under the supervision of Professor Michael Hall. The proposed mechanisms were investigated by calculating the structures and energies of intermediates and transition state structures along both pathways (Figure 5.5). The results of these calculations are discussed in detail in appendix B.

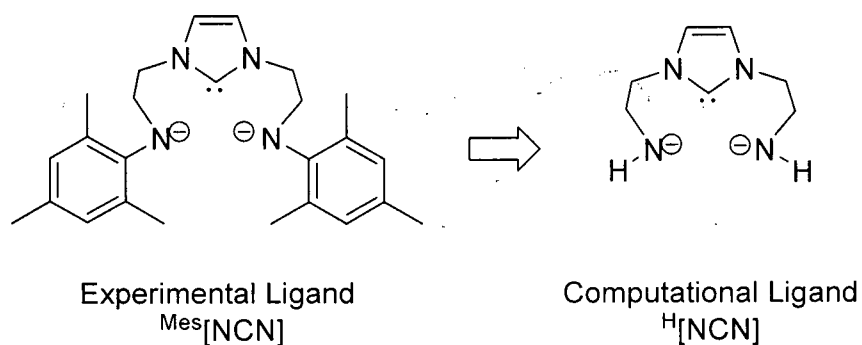
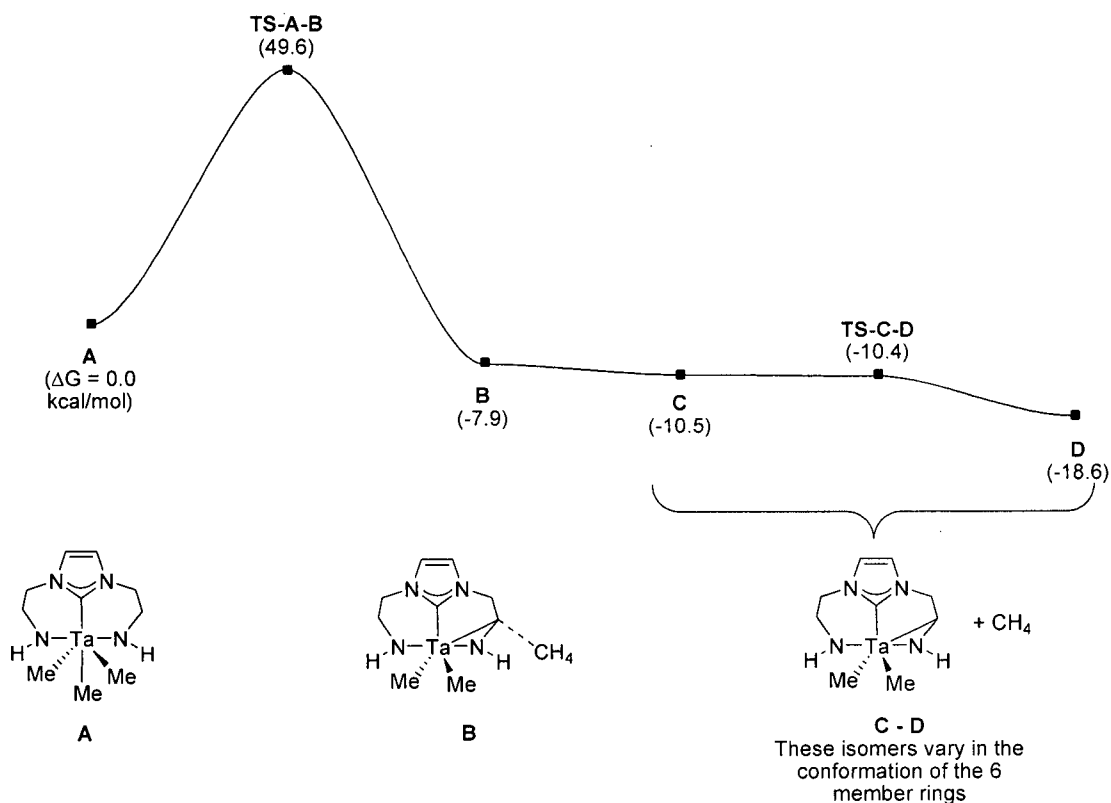


**Figure 5.6.** Computational model of the trimethyl tantalum starting complex.

The computational results suggest the lowest energy pathway involves a tantalum alkylidene intermediate, which can then mediate C-H bond activation with a neighboring backbone linker C-H group to form a new metallazaaziridine. The energies of the intermediates and transition states for both path 1 and 2 are shown in Figures 5.7 and 5.9, respectively. The structures of the energy minimized transition states are given in Figures 5.8 (Path 1) and 5.10 (Path 2).



<sup>a</sup> Gas-phase relative free energies at the B3LYP/BS1 level of theory based on the energy of separated **1** set to 0.0 kcal/mol are provided in parentheses in kcal/mol. Electronic energies, corrected zero-point energies, enthalpies, and free energies are provided in Table 1.

**Figure 5.7.** Relative energies of the intermediates and transition states in a potential  $\sigma$ -bond metathesis mechanism.

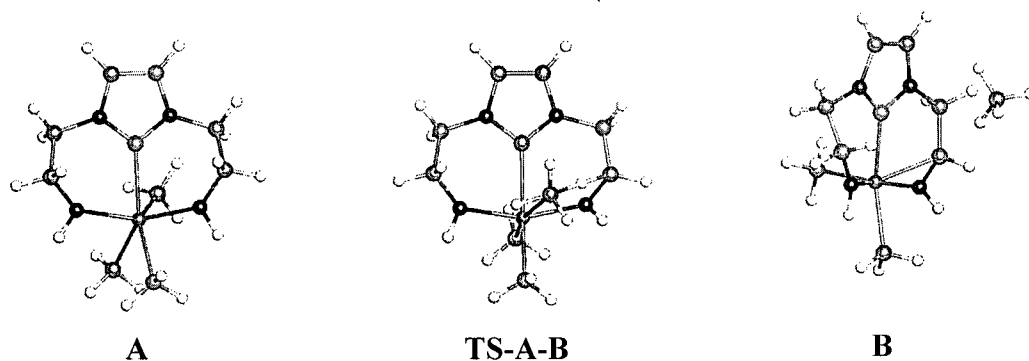
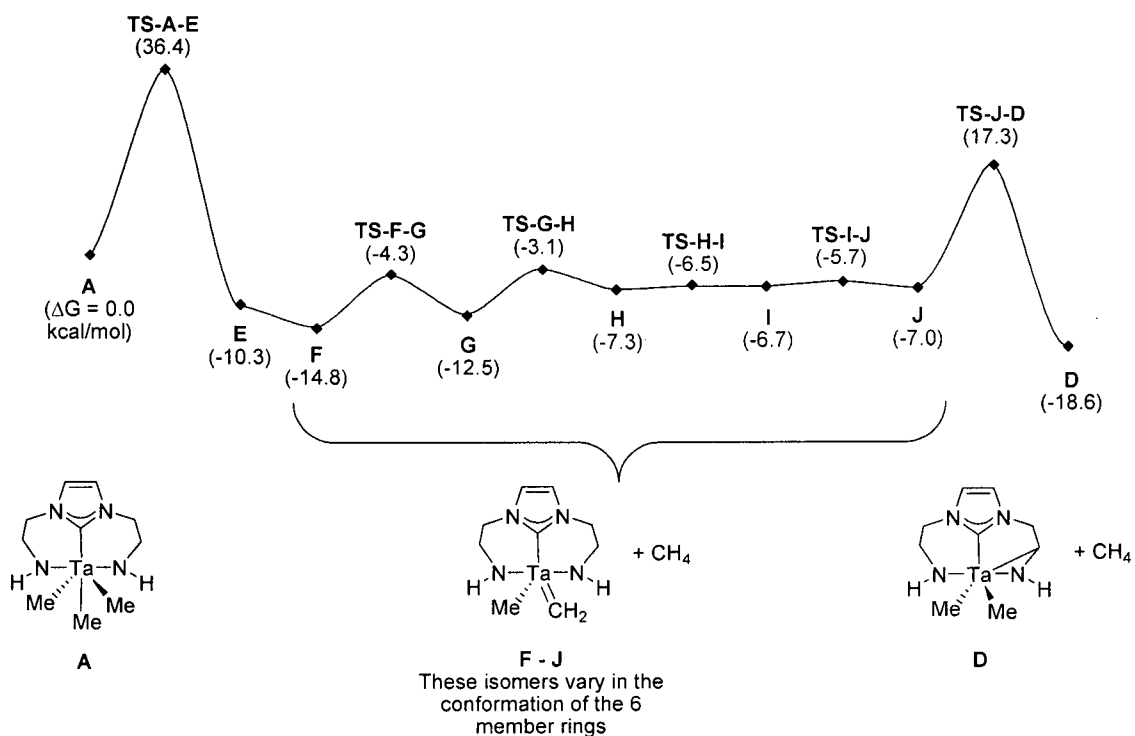


**Figure 5.8.** JIMP<sup>26</sup> Pictures of the one-step  $\sigma$ -bond metathesis pathway.



<sup>a</sup> Gas-phase relative free energies at the B3LYP/BS1 level of theory based on the energy of separated **1** set to 0.0 kcal/mol are provided in parentheses in kcal/mol. Electronic energies, corrected zero-point energies, enthalpies, and free energies are provided in Table 1.

**Figure 5.9.** Relative energies of the intermediates and transition states in a potential two-step  $\alpha$ -H abstraction/alkylidene mediated C-H activation mechanism.

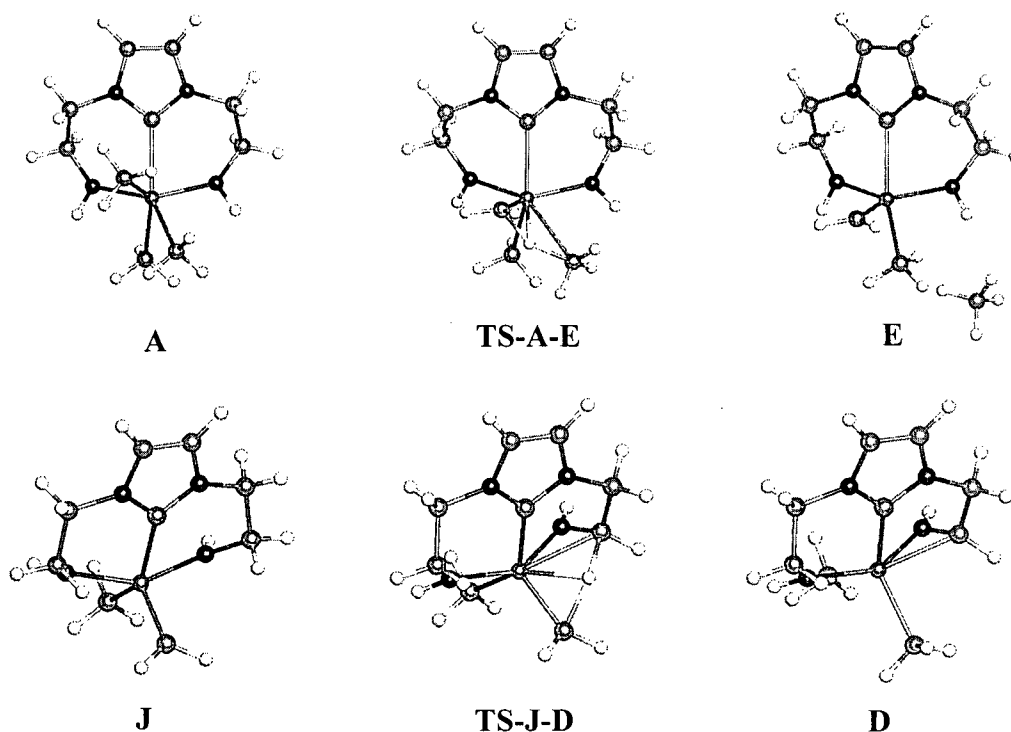
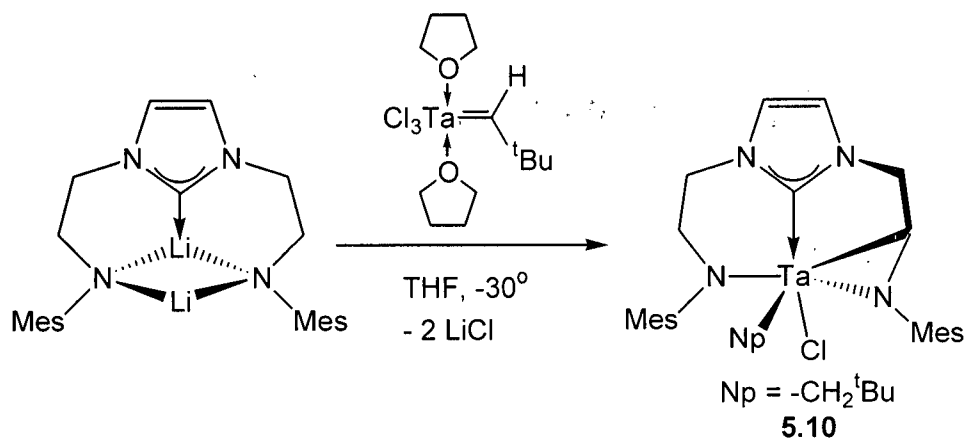


**Figure 5.10.** JIMP<sup>26</sup> Pictures of alkylidene mediated C-H activation of the ligand backbone.

### 5.7. Verification of the Mechanism proposed by DFT Calculations

Based on the computational support for the intermediacy of a tantalum alkylidene in the endocyclic C-H activation process, the synthesis of an [NCN] tantalum alkylidene complex was attempted. Beginning with  $\text{Cl}_3\text{Ta}=\text{CH}^t\text{Bu}(\text{THF})_2$ , the reaction with **3.11** proceeds to give **5.10** in good yield (Scheme 5.4). Both the  $^1\text{H}$  and  $^{13}\text{C}\{^1\text{H}\}$  NMR spectra display resonances similar to the previous cyclometallated complexes **5.7-5.9**. Examination of the  $^1\text{H}$  NMR spectrum during the reaction reveals the presence of 2,2-dimethylpropane formation and no observable intermediate.



Scheme 5.4.

An X-ray diffraction experiment was performed on crystals grown from  $\text{Et}_2\text{O}$  with an ORTEP depiction of **5.10** given in Figure 5.11. Relevant bond lengths and angles are listed in Table 5.5, and crystallographic details are located in appendix A. The solid state molecular structure reveals an endocyclic C-H bond activated complex with similar structural characteristics to **5.7**. Clearly, there is no neopentylidene present as the Ta-C alkyl bonds from both complexes are of similar length. The Ta1-C5 alkyl bond length of 2.216(4) Å is similar to length to **5.7**, as are the bond angles defined by the N3-C5-Ta1 metallaaziridine ring.

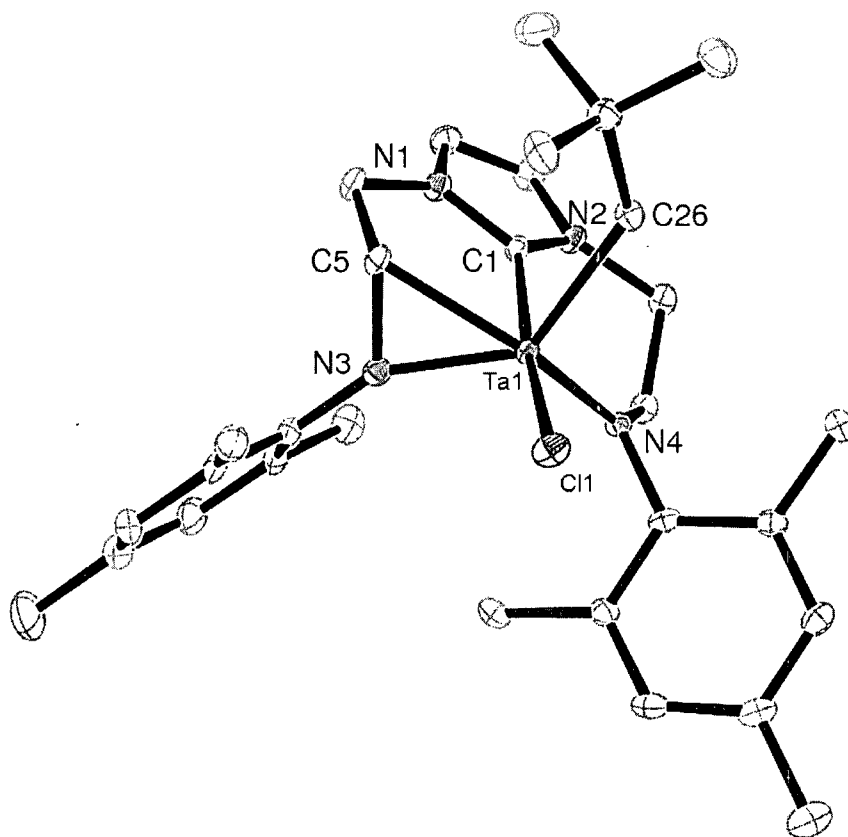


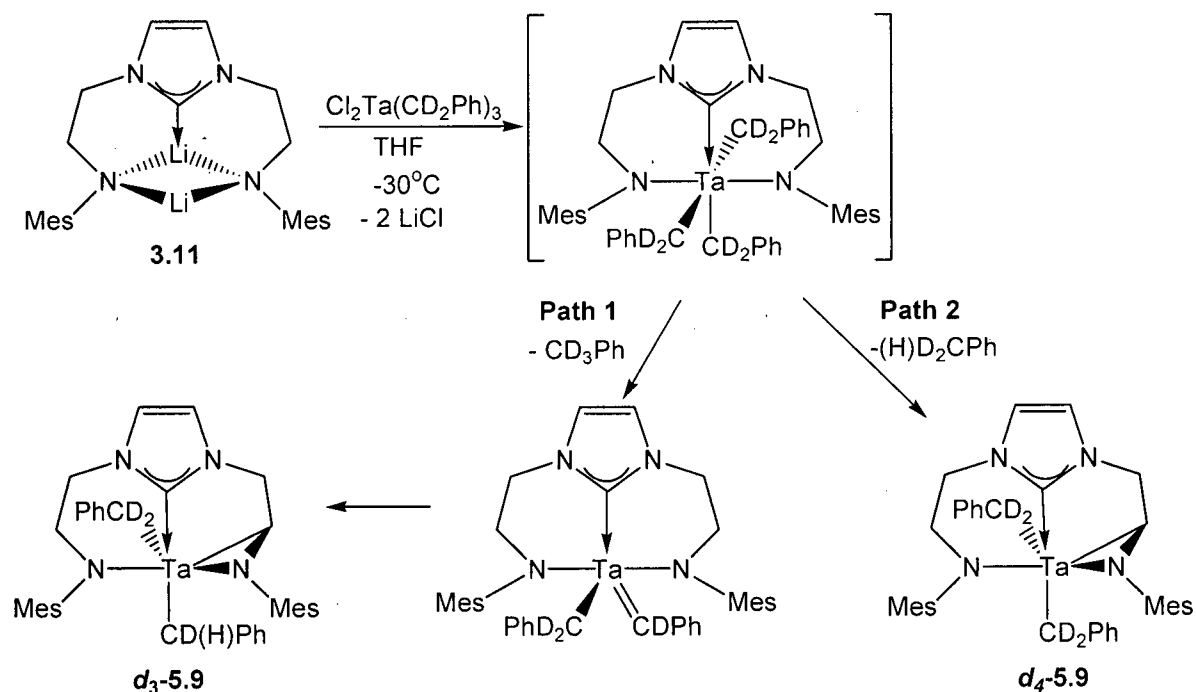
**Figure 5.11.** ORTEP view of  $^{\text{Mes}}[\text{NCCN}]\text{Ta}(\text{Cl})(\text{CH}_2^t\text{Bu})$  (**5.10**), depicted with 50% thermal ellipsoids; all hydrogen atoms have been omitted for clarity.

**Table 5.5.** Selected bond distances (Å) and angles ( $^\circ$ ) for  $^{\text{Mes}}[\text{NCCN}]\text{Ta}(\text{Cl})(\text{CH}_2^t\text{Bu})$  (**5.10**).

Bond Lengths		Bond Angles	
Ta1-N3	1.967(4)	N3-Ta1-N4	115.35(15)
Ta1-N4	2.010(3)	N3-Ta1-C5	39.64(16)
Ta1-C5	2.216(4)	N3-Ta1-C1	84.96(15)
Ta1-C26	2.224(4)	N4-Ta1-C1	77.84(15)
Ta1-C1	2.241(4)	C5-N3-Ta1	79.6(2)
Ta1-Cl1	2.3996(11)	N3-C5-Ta1	60.8(2)

Although these experimental results cannot confirm the presence of an alkylidene intermediate in the decomposition of  $[\text{NCN}]\text{Ta}(\text{alkyl})_3$  complexes, they infer that an alkylidene species can undergo rapid amido C-H bond activation. Further evidence for the mechanism postulated by DFT calculations was observed in NMR experiments using deuterium labeled complexes. Utilizing  $\text{Cl}_2\text{Ta}(\text{CD}_2\text{Ph})_3$  as a starting material, we can examine the proton distribution in the final C-H bond activated product was examined

(Scheme 5.5). If the mechanism proceeds as suggested by calculations, the tantalum alkylidene intermediate would abstract a proton from the ethylene spacer to yield a TaCH(D)Ph moiety (Path 1, Scheme 5.5). If a concerted  $\sigma$ -bond metathesis was the operant mechanism, this reaction would yield two -CD<sub>2</sub>Ph groups and no benzylic proton resonances would be observed (*d*<sub>4</sub>-5.9, Path 2, Scheme 5.5). The reaction of 3.11 with Cl<sub>2</sub>Ta(CD<sub>2</sub>Ph)<sub>3</sub> yields *d*<sub>3</sub>-5.9. The <sup>1</sup>H NMR spectrum clearly shows a 1:1:1 triplet at 2.70 ppm, evidence for the -TaCH(D)Ph moiety in *d*<sub>3</sub>-5.9. This result suggests DFT calculations are correct and implies that the decomposition of [NCN]Ta(alkyl)<sub>3</sub> complexes proceeds through an alkylidene intermediate which rapidly undergoes C-H bond activation with an amido donor.



Scheme 5.5.

## 5.8. Conclusions

In this chapter, the potential of the [NCN] ligand architecture to stabilize tantalum amide, halide, and alkyl complexes has been presented. Aminolysis and alkyl

elimination reactions, which were previously successful in the synthesis of group 4 [NCN] complexes, provided a route to incorporate one flanking amido arm. Thus far, attempts to promote coordination of the second pendant amine arm have been unsuccessful. Coordination of both pendant amide donors was achieved by metathesis reactions between  $\text{Li}_2^{\text{Ar}}[\text{NCN}]$  and substituted tantalum chlorides. In the case of trialkyl tantalum derivatives, amide C-H bond activation occurs to generate a new cyclometallated metallaaziridine. DFT calculations on model complexes suggested that the mechanism for this phenomenon proceeds through a tantalum alkylidene intermediate, which can then mediate C-H bond activation with a neighboring amido group to form a new metallaaziridine. In light of these findings, we examined the synthesis of tantalum alkylidene complexes stabilized by an [NCN] ancillary ligand and found that similar amide C-H bond activation occurs. While this result cannot confirm the mechanism postulated by DFT calculations, deuterium labeling experiments have shown that a tantalum alkylidene intermediate is involved during this process.

## 5.9. Experimental Section

### 5.9.1. General Considerations

Unless otherwise stated, general procedures were performed as described in Section 2.5.1. DFT calculations were performed at the Department of Chemistry at the University of Texas A&M by Dr. Chad Beddie.

### 5.9.2. Materials and Reagents

Ta(NMe<sub>2</sub>)<sub>5</sub> were purchased from Strem Chemicals and used as received. All other chemicals were purchased from Aldrich and used as received. Ta(CH<sub>2</sub>Ph)<sub>5</sub>,<sup>27</sup> Cl<sub>2</sub>Ta(NMe<sub>2</sub>)<sub>3</sub>,<sup>13</sup> Cl<sub>3</sub>Ta(NMe<sub>2</sub>)<sub>2</sub>(THF),<sup>28</sup> Cl<sub>4</sub>Ta(NEt<sub>2</sub>)(Et<sub>2</sub>O),<sup>28</sup> Cl<sub>2</sub>TaMe<sub>3</sub>,<sup>29</sup> Cl<sub>2</sub>Ta(CH<sub>2</sub>Ph)<sub>3</sub>,<sup>30</sup> Cl<sub>2</sub>Ta(CD<sub>2</sub>Ph)<sub>3</sub>,<sup>30</sup> Cl<sub>2</sub>Ta(CH<sub>2</sub><sup>t</sup>Bu)<sub>3</sub>,<sup>31</sup> Cl<sub>3</sub>Ta=CH<sup>t</sup>Bu(THF)<sub>2</sub><sup>32</sup> were all synthesized by literature methods.

### 5.9.3. Synthesis and Characterization of Complexes 5.1 - 5.10

#### Synthesis of <sup>101</sup>[NCNH]Ta(NMe<sub>2</sub>)<sub>4</sub> (5.1)

To a stirred toluene solution (5 mL) of Ta(NMe<sub>2</sub>)<sub>5</sub> (216 mg, 0.54 mmol) in a 50 mL Erlenmeyer flask was added a toluene solution (5 mL) of **3.7** (181 mg, 0.54 mmol). The orange solution was stirred overnight and filtered thru Celite. The solvent was removed until the volume was ~2 mL, and then cooled to -30°C to yield orange blocks. Yield = 246 mg, 66%.

<sup>1</sup>H NMR (C<sub>6</sub>D<sub>6</sub>): 2.22 (s, 3H, -ArCH<sub>3</sub>), 2.44 (s, 3H, -ArCH<sub>3</sub>), 3.06 (br s, 12H, -NCH<sub>3</sub>), 3.16 (m, 2H, -NCH<sub>2</sub>), 3.27 (m, 2H, -NCH<sub>2</sub>), 3.32 (br m, 1H, -NH), 3.52 (br s, 6H, -NCH<sub>3</sub>), 3.75 (br s, 6H, -NCH<sub>2</sub>), 4.03 (m, 2H, -NCH<sub>2</sub>), 4.19 (m, 2H, -NCH<sub>2</sub>), 5.98 (br s, 1H, -imidH), 6.29 (br s, 1H, -imidH), 6.38 (d, J=7 Hz, 2H, -ArH), 6.91 (d, J=7 Hz, 2H, -ArH), 7.01 (d, J=7 Hz, 2H, -ArH), 7.24 (d, J=7 Hz, 2H, -ArH).

<sup>13</sup>C{<sup>1</sup>H} NMR (C<sub>6</sub>D<sub>6</sub>): 18.1 (-CH<sub>3</sub>), 20.2 (-CH<sub>3</sub>), 45.5 (br, -NCH<sub>3</sub>), 46.9 (-NCH<sub>2</sub>), 47.0 (-NCH<sub>2</sub>), 47.5 (-NCH<sub>2</sub>), 48.9 (-NCH<sub>2</sub>), 118.6 (-ArC), 119.3 (-ArC), 120.5 (-imidC), 122.6

(-imidC), 124.8 (-ArC), 124.9 (-ArC), 128.7 (-ArC), 129.2 (-ArC), 140.5 (-ArC), 141.6 (-ArC), 198.5 (-NCN).

Anal. Calcd. for C<sub>29</sub>H<sub>49</sub>N<sub>8</sub>Ta: C, 50.43; H, 7.15; N, 16.22; Found: C, 50.11; H, 7.00; N, 15.95.

### Synthesis of <sup>Mes</sup>[NCNH]Ta=CHPh(CH<sub>2</sub>Ph)<sub>2</sub> (5.2)

To a stirred toluene solution (5 mL) of Ta(CH<sub>2</sub>Ph)<sub>5</sub> (328 mg, 0.51 mmol) was added a toluene solution (5 mL) of **3.8** (200 mg, 0.51 mmol) in a 50 mL Erlenmeyer flask. The dark brown solution was stirred overnight and filtered thru Celite. The solvent was removed to yield a brown residue, which was triturated with hexanes (10 mL) to yield a brown powder. Yield = 327 mg, 76%. X-ray quality crystals were obtained from a cooled (-30°C) toluene solution.

<sup>1</sup>H NMR (C<sub>6</sub>D<sub>6</sub>): 2.02 (s, 3H, -*p*-ArCH<sub>3</sub>), 2.08 (s, 6H, -*o*-ArCH<sub>3</sub>), 2.20 (s, 6H, -*o*-ArCH<sub>3</sub>), 2.31 (s, 3H, -*p*-ArCH<sub>3</sub>), 2.42 (m, 4H, -TaCH<sub>2</sub>), 2.43-3.10 (m, 7H, -NH and -NCH<sub>2</sub>) and 3.58 (dt, J = 6Hz, 1H, -NCH), 4.40 (dt, J = 6Hz, 1H, -NCH), 4.81 (s, 1H, -CHPh), 5.81 (d, J=2 Hz, 1H, -imidH), 6.23 (d, J=2 Hz, 1H, -imidH), 6.60-6.85 (m, H, -ArH), 7.42 (d, J=8 Hz, 4H, -ArH).

<sup>13</sup>C{<sup>1</sup>H} NMR (C<sub>6</sub>D<sub>6</sub>): 17.9 (-CH<sub>3</sub>), 18.2 (-CH<sub>3</sub>), 20.7 (-CH<sub>3</sub>), 21.0 (-CH<sub>3</sub>), 48.7 (-NCH<sub>2</sub>), 48.8 (-NCH<sub>2</sub>), 51.6 (-NCH<sub>2</sub>), 54.5 (-NCH<sub>2</sub>), 69.9 (-TaCH<sub>2</sub>), 85.0 (-TaCH<sub>2</sub>), 119.6 (-ArC), 120.3 (-ArC), 121.2 (-imidC), 123.7 (-imidC), 125.6 (-ArC), 129.3 (-ArC), 129.8 (-ArC), 129.9 (-ArC), 130.6 (-ArC), 131.0 (-ArC), 132.0 (-ArC), 136.1 (-ArC), 137.6 (-ArC), 137.8 (-ArC), 138.2 (-ArC), 142.7 (-ArC), 147.8 (-ArC), 148.7 (-ArC), 155.3 (-ArC), 205.0 (-NCN), 236.3 (-TaCH).

Anal. Calcd. for C<sub>46</sub>H<sub>53</sub>N<sub>4</sub>Ta: C, 65.55; H, 6.34; N, 6.65; Found: C, 65.26; H, 6.22; N, 6.59.

### Synthesis of <sup>tol</sup>[NCN]Ta(NMe<sub>2</sub>)<sub>3</sub> (5.3), <sup>tol</sup>[NCN]Ta(NMe<sub>2</sub>)<sub>2</sub>Cl (5.4), <sup>tol</sup>[NCN]Ta(NEt<sub>2</sub>)Cl<sub>2</sub> (5.5-5.6)

The following procedure is representative of the synthesis of **5.3-5.6**. To a cooled (-30°C) THF solution (5 mL) of Cl<sub>2</sub>Ta(NMe<sub>2</sub>)<sub>3</sub> (288 mg, 0.75 mmol) was added a chilled (-30°C) THF solution (5 mL) of **3.10** (408 mg, 0.75 mmol) in a 50 mL Erlenmeyer flask.

The solution slowly darkened to brown upon warming to room temperature. The solution was stirred overnight whereupon the solvent was removed and toluene added. The solution was filtered thru Celite and the solvent removed to yield an orange/brown residue. Trituration of the residue with hexane yielded an orange solid which was recrystallized from toluene. Yield = 383 mg, 79%.

**5.3:**  $^1\text{H NMR (C}_6\text{D}_6\text{)}$ : 2.45 (s, 6H, -ArCH<sub>3</sub>), 3.22 (s, 12H, -NCH<sub>3</sub>), 3.53 (m, 4H, -NCH<sub>2</sub>), 3.68 (s, 6H, -NCH<sub>3</sub>), 4.15 (m, 4H, -NCH<sub>2</sub>), 6.00 (s, 2H, -imidH), 7.11 (d, J = 8Hz, 4H, -ArH), 7.27 (d, J = 8Hz, 4H, -ArH).

$^{13}\text{C}\{^1\text{H}\}$  NMR (C<sub>6</sub>D<sub>6</sub>): 18.7 (-CH<sub>3</sub>), 45.4 (-NCH<sub>3</sub>), 47.0 (-NCH<sub>3</sub>), 48.0 (-NCH<sub>2</sub>), 50.7 (-NCH<sub>2</sub>), 117.3 (-ArC), 118.3 (-ArC), 124.4 (-imidC), 126.6 (-ArC), 152.6 (-ArC), 186.7 (-NCN).

Anal. Calcd. for C<sub>27</sub>H<sub>42</sub>N<sub>7</sub>Ta: C, 50.23; H, 6.56; N, 15.19; Found: C, 50.10; H, 6.35; N, 15.05.

**5.4:**  $^1\text{H NMR (C}_6\text{D}_6\text{)}$ : 2.26 (s, 6H, -ArCH<sub>3</sub>), 3.26 (s, 6H, -NCH<sub>3</sub>), 3.36 (m, 2H, -NCHH), 3.60 (m, 2H, -NCHH), 3.80 (s, 6H, -NCH<sub>3</sub>), 3.88 (m, 2H, -NCHH), 4.35 (m, 2H, -NCHH), 5.96 (s, 2H, -imidH), 7.10 (d, J = 8 Hz, 4H, -ArH), 7.36 7.10 (d, J = 8 Hz, 4H, -ArH).

$^{13}\text{C}\{^1\text{H}\}$  NMR (C<sub>6</sub>D<sub>6</sub>): 19.5 (-CH<sub>3</sub>), 45.6 (-NCH<sub>3</sub>), 46.5 (-NCH<sub>3</sub>), 47.5 (-NCH<sub>2</sub>), 48.9 (-NCH<sub>2</sub>), 116.8 (-ArC), 119.1 (-ArC), 123.9 (-imidC), 127.5 (-ArC), 149.9 (-ArC), 187.1 (-NCN).

Anal. Calcd. for C<sub>25</sub>H<sub>36</sub>ClN<sub>6</sub>Ta: C, 47.14; H, 5.70; N, 13.19; Found: C, 47.09; H, 5.52; N, 12.95.

**Minor isomer (5.5):**  $^1\text{H NMR (C}_6\text{D}_6\text{)}$ : 0.60 (t, J = 9 Hz, 6H, -N(CH<sub>2</sub>CH<sub>3</sub>)<sub>2</sub>), 2.28 (s, 6H, -ArCH<sub>3</sub>), 3.25 (m, 2H, -NCHH), 3.52 (m, 2H, -NCHH), 3.56 (q, J = 9 Hz, 4H, -N(CH<sub>2</sub>CH<sub>3</sub>)<sub>2</sub>), 3.98 (m, 2H, -NCHH), 4.70 (m, 2H, -NCHH), 6.10 (s, 2H, -imidH), 7.17 (d, J = 8 Hz, 4H, -ArH), 7.61 (d, J = 8 Hz, 4H, -ArH).

$^{13}\text{C}\{^1\text{H}\}$  NMR (C<sub>6</sub>D<sub>6</sub>): 15.0 (-NCH<sub>2</sub>CH<sub>3</sub>), 22.5 (-CH<sub>3</sub>), 45.4 (-NCH<sub>2</sub>CH<sub>3</sub>), 48.0 (-NCH<sub>2</sub>), 50.7 (-NCH<sub>2</sub>), 119.5 (-ArC), 120.5 (-ArC), 125.6 (-imidC), 131.5 (-ArC), 151.6 (-ArC), 189.5 (-NCN).

**Major isomer (5.6):  $^1\text{H}$  NMR ( $\text{C}_6\text{D}_6$ ):** 0.81 (t,  $J = 9$  Hz, 6H,  $-\text{N}(\text{CH}_2\text{CH}_3)_2$ ), 2.21 (s, 6H,  $-\text{ArCH}_3$ ), 3.30 (m, 4H,  $-\text{NCH}_2$ ), 3.74 (q,  $J = 9$  Hz, 4H,  $-\text{N}(\text{CH}_2\text{CH}_3)_2$ ), 4.52 (m, 4H,  $-\text{NCH}_2$ ), 5.78 (s, 2H,  $-\text{imidH}$ ), 7.02 (d,  $J = 8$  Hz, 4H,  $-\text{ArH}$ ), 7.49 (d,  $J = 8$  Hz, 4H,  $-\text{ArH}$ ).

**$^{13}\text{C}\{^1\text{H}\}$  NMR ( $\text{C}_6\text{D}_6$ ):** 15.2 ( $-\text{NCH}_2\text{CH}_3$ ), 23.4 ( $-\text{CH}_3$ ), 45.9 ( $-\text{NCH}_2\text{CH}_3$ ), 48.6 ( $-\text{NCH}_2$ ), 51.6 ( $-\text{NCH}_2$ ), 117.6 ( $-\text{ArC}$ ), 120.9 ( $-\text{ArC}$ ), 126.8 ( $-\text{imidC}$ ), 132.6 ( $-\text{ArC}$ ), 153.9 ( $-\text{ArC}$ ), 185.6 ( $-\text{NCN}$ ).

Anal. Calcd. for  $\text{C}_{25}\text{H}_{34}\text{Cl}_2\text{N}_5\text{Ta}$ : C, 45.74; H, 5.22; N, 10.67; Found: C, 45.45; H, 5.01; N, 10.52. Ratio of minor isomer **5.5**: major isomer **5.6** = 1:1.3.

**Synthesis of  $^{\text{Mes}}[\text{NCCN}]\text{Ta}(\text{CH}_2^t\text{Bu})_2$  (5.7)  $^{\text{Mes}}[\text{NCCN}]\text{TaMe}_2$  (5.8)**  
 **$^{\text{Mes}}[\text{NCCN}]\text{Ta}(\text{CH}_2\text{Ph})_2$  (5.9)  $^{\text{Mes}}[\text{NCCN}]\text{Ta}(\text{CD}_2\text{Ph})_2$  ( $d_3$ -5.9)**

The following procedure is representative of the synthesis of **5.7-5.9**. To a cooled ( $-30^\circ\text{C}$ ) THF solution (5 mL) of  $\text{Cl}_2\text{Ta}(\text{CH}_2^t\text{Bu})_3$  (360 mg, 0.77 mmol) in a 50 mL Erlenmeyer flask was added a chilled ( $-30^\circ\text{C}$ ) THF solution (5 mL) of **3.11** (270 mg, 0.77 mmol). The dark brown solution was slowly warmed to room temperature. The solution was stirred overnight whereupon the solvent was removed and toluene added. The solution was filtered thru Celite and the solvent removed to yield a dark orange solid. Yield = 356 mg, 68%. Yellow crystals were obtained from recrystallization in hexane.

**5.7:  $^1\text{H}$  NMR ( $\text{C}_6\text{D}_6$ ):** 0.80 (d,  $J = 8$  Hz, 1H,  $-\text{TaCHH}$ ), 0.92 (s, 9H,  $-\text{C}(\text{CH}_3)_3$ ), 1.10 (d,  $J = 8$  Hz, 1H,  $-\text{TaCHH}$ ), 1.18 (d,  $J = 8$  Hz, 1H,  $-\text{TaCHH}$ ), 1.29 (d,  $J = 8$  Hz, 1H,  $-\text{TaCHH}$ ), 1.30 (s, 9H,  $-\text{C}(\text{CH}_3)_3$ ), 2.18 (s, 3H,  $-\text{ArCH}_3$ ), 2.25 (s, 3H,  $-\text{ArCH}_3$ ), 2.28 (s, 3H,  $-\text{ArCH}_3$ ), 2.67 (m, 1H,  $-\text{NCHH}$ ), 2.86 (s, 3H,  $-\text{ArCH}_3$ ), 3.60 (m, 1H,  $-\text{NCHH}$ ), 3.67 (m, 1H,  $-\text{NCHH}$ ), 3.84 (m, 2H,  $-\text{NCHH}$ ), 4.34 (m, 1H,  $-\text{NCHH}$ ), 4.48 (m, 1H,  $-\text{NCHH}$ ), 5.82 (d,  $J = 2$  Hz, 1H,  $-\text{imidH}$ ), 5.88 (d,  $J = 2$  Hz, 1H,  $-\text{imidH}$ ), 6.80 (br s, 2H,  $-\text{ArH}$ ), 7.05 (s, 1H,  $-\text{ArH}$ ), 7.14 (s, 1H,  $-\text{ArH}$ ).

**$^{13}\text{C}\{^1\text{H}\}$  NMR ( $\text{C}_6\text{D}_6$ ):** 18.8 ( $-\text{CH}_3$ ), 19.2 ( $-\text{CH}_3$ ), 20.5 ( $-\text{CH}_3$ ), 21.9 ( $-\text{CH}_3$ ), 22.9 ( $-\text{CH}_3$ ), 35.1 ( $-\text{C}(\text{CH}_3)_3$ ), 36.0 ( $-\text{C}(\text{CH}_3)_3$ ), 51.2 ( $-\text{NCH}_2$ ), 55.9 ( $-\text{NCH}_2$ ), 56.3 ( $-\text{NCH}_2$ ), 68.1 ( $-\text{TaC}$ ), 72.1 ( $-\text{TaC}$ ), 85.6 ( $-\text{TaC}$ ), 117.5 ( $-\text{ArC}$ ), 119.5 ( $-\text{ArC}$ ), 120.5 ( $-\text{imidC}$ ), 121.6 ( $-\text{imidC}$ ), 129.6 ( $-\text{ArC}$ ), 130.9 ( $-\text{ArC}$ ), 132.1 ( $-\text{ArC}$ ), 133.9 ( $-\text{ArC}$ ), 148.6 ( $-\text{ArC}$ ), 149.9 ( $-\text{ArC}$ ), 197.5 ( $-\text{NCN}$ ).

Anal. Calcd. for  $C_{33}H_{47}N_4Ta$ : C, 59.14; H, 7.52; N, 7.88; Found: C, 58.95; H, 7.26; N, 7.59.

**5.8:**  $^1H$  NMR ( $C_6D_6$ ): 0.46 (s, 3H, -TaCH<sub>3</sub>), 0.62 (s, 3H, -TaCH<sub>3</sub>), 1.89 (s, 3H, -ArCH<sub>3</sub>), 2.21 (s, 3H, -ArCH<sub>3</sub>), 2.27 (s, 3H, -ArCH<sub>3</sub>), 2.70 (s, 3H, -ArCH<sub>3</sub>), 2.72 (m, 1H, -NCHH), 3.31 (m, 1H, -NCHH), 3.49 (m, 1H, -NCHH), 3.71 (m, 1H, -NCHH), 3.86 (m, 1H, -NCHH), 4.19 (m, 1H, -NCHH), 4.37 (m, 1H, -NCHH), 5.91 (d, J=2 Hz, 1H, -imidH), 5.94 (d, J=2 Hz, 1H, -imidH), 6.84 (br s, 2H, -ArH), 7.02 (s, 1H, -ArH), 7.09 (s, 1H, -ArH).

A satisfactory  $^{13}C$  NMR spectrum and elemental analysis could not be obtained due to the sensitivity of the product.

**5.9:**  $^1H$  NMR ( $C_6D_6$ ): 1.67 (d, J = 7 Hz, -TaCHH), 2.27 (s, 3H, -ArCH<sub>3</sub>), 2.29 (s, 3H, -ArCH<sub>3</sub>), 2.32 (s, 3H, -ArCH<sub>3</sub>), 2.45 (d, J = 7 Hz, -TaCHH), 2.61 (d, J = 7 Hz, -TaCHH), 2.76 (s, 3H, -ArCH<sub>3</sub>), 2.82 (d, J = 7 Hz, -TaCHH), 3.28 (m, 1H, -TaCHH), 3.45 (m, 1H, -TaCHH), 3.55 (m, 1H, -TaCHH), 3.88 (m, 1H, -TaCHH), 4.12 (m, 1H, -TaCHH), 4.55 (m, 1H, -TaCHH), 5.90 (d, J=2 Hz, 1H, -imidH), 5.92 (d, J=2 Hz, 1H, -imidH), 6.64-6.71 (m, 3H, -ArH), 6.81-6.93 (m, 6H, -ArH), 6.99-7.17 (m, 7H, -ArH).

$^{13}C\{^1H\}$  NMR ( $C_6D_6$ ): 17.6 (-CH<sub>3</sub>), 18.9 (-CH<sub>3</sub>), 19.6 (-CH<sub>3</sub>), 20.5 (-CH<sub>3</sub>), 50.1 (-NCH<sub>2</sub>), 54.6 (-NCH<sub>2</sub>), 55.4 (-NCH<sub>2</sub>), 79.2 (-TaC), 81.6 (-TaC), 90.1 (-TaC), 119.2 (-ArC), 120.2 (-imidC), 121.9 (-ArC), 122.3 (-imidC), 124.6 (-ArC), 124.9 (-ArC), 129.6 (-ArC), 130.6 (-ArC), 131.5 (-ArC), 135.6 (-ArC), 145.6 (-ArC), 148.6 (-ArC), 149.6 (-ArC), 151.2 (-ArC), 196.2 (-NCN). Some aryl resonances obscured by solvent signals.

Anal. Calcd. for  $C_{43}H_{41}N_4Ta$ : C, 62.39; H, 6.04; N, 7.46; Found: C, 61.98; H, 5.89; N, 7.19.

***d*<sub>3</sub>-5.9:**  $^1H$  NMR ( $C_6D_6$ ): NMR is identical to **5.9** with the absence of the peaks at ppm and the presence  $\delta$  2.70 (t, J=11 Hz, 1H, -TaCHD).

### Synthesis of $^{Mes}[NCCN]Ta(CH_2^tBu)Cl$ (**5.10**)

To a cooled (-30°C) THF solution (5 mL) of  $Cl_3Ta=CH^tBu(THF)_2$  (311 mg, 0.62 mmol) in a 50 mL Erlenmeyer flask was added a chilled (-30°C) THF solution (5 mL) of **3.11** (249 mg, 0.62 mmol). The dark brown solution was slowly warmed to room temperature. The solution was stirred overnight whereupon the solvent was removed and

toluene added. The solution was filtered thru Celite and the solvent removed to yield a dark orange solid. Yield = 344 mg, 84%. Yellow crystals were obtained from recrystallization in hexane.

**<sup>1</sup>H NMR (C<sub>6</sub>D<sub>6</sub>):** 1.26 (s, 9H, -C(CH<sub>3</sub>)<sub>3</sub>), 1.93 (d, J = 12 Hz, 1H, -TaCHH), 2.10 (s, 3H, -ArCH<sub>3</sub>), 2.12 (s, 3H, -ArCH<sub>3</sub>), 2.21 (d, J = 12 Hz, 1H, -TaCHH), 2.24 (s, 3H, -ArCH<sub>3</sub>), 2.73 (s, 3H, -ArCH<sub>3</sub>), 2.91 (m, 1H, -NCHH), 3.13 (m, 1H, -NCHH), 3.60 (m, 1H, -NCHH), 3.83 (m, 2H, -NCHH), 3.96 (m, 1H, -NCHH), 4.42 (m, 1H, -NCHH), 5.82 (br s, 1H, -imidH), 5.85 (br s, 1H, -imidH), 6.60 (s, 1H, -ArH), 6.87 (s, 2H, -ArH), 7.01 (s, 1H, -ArH).

**<sup>13</sup>C{<sup>1</sup>H} NMR (C<sub>6</sub>D<sub>6</sub>):** 19.1 (-CH<sub>3</sub>), 20.1 (-CH<sub>3</sub>), 21.1 (-CH<sub>3</sub>), 21.9 (-CH<sub>3</sub>), 36.1 (-C(CH<sub>3</sub>)), 52.0 (-NCH<sub>2</sub>), 54.6 (-NCH<sub>2</sub>), 57.2 (-NCH<sub>2</sub>), 75.2 (-TaC), 83.3 (-TaC), 116.9 (-ArC), 121.5 (-imidC), 122.8 (-imidC), 132.0 (-ArC), 134.2 (-ArC), 136.2 (-ArC), 138.6 (-ArC), 150.6 (-ArC), 150.8 (-ArC), 196.3 (-NCN).

Anal. Calcd. for C<sub>29</sub>H<sub>39</sub>ClN<sub>4</sub>Ta: C, 53.37; H, 6.27; Cl, 5.25; N, 8.30; Found: 53.05; H, 6.02; N, 8.22.

#### 5.9.4. Theoretical Calculations

All calculations were performed using the Gaussian 03 suite of programs.<sup>33</sup> Optimized gas-phase geometries were obtained using the Becke3 exchange functional,<sup>34</sup> in combination the Lee, Yang, and Parr correlation functional,<sup>35</sup> *i.e.* the B3LYP method, as implemented in Gaussian 03. The basis set (BS1) used for geometry optimizations and energy calculations was implemented as follows: for tantalum, the valence double- $\zeta$  LANL2DZ<sup>36-38</sup> basis set was supplemented with a set of 6p functions for transition metals developed by Couty and Hall,<sup>39</sup> while for all hydrogen, carbon, and nitrogen atoms, the 6-31G(d',p') basis sets<sup>40-45</sup> were used. All structures were calculated in singlet spin states using the restricted B3LYP method. Calculating the harmonic vibrational frequencies and noting the number of imaginary frequencies confirmed the nature of all intermediates (NImag = 0) and transition state structures (NImag = 1). All gas-phase relative free energies are reported in kcal mol<sup>-1</sup>, with the energy of <sup>H</sup>[NCN]TaMe<sub>3</sub> (<sup>H</sup>[NCN] = (HNCH<sub>2</sub>CH<sub>2</sub>)<sub>2</sub>N<sub>2</sub>C<sub>3</sub>H<sub>2</sub>) set to 0.0 kcal mol<sup>-1</sup>. Relative electronic energies, zero-point

corrected energies, and enthalpies are provided in the supplemental information. For the computational investigation,  $^{\text{H}}[\text{NCN}]$  was used in place of the experimental ligand (*p*-Me-C<sub>6</sub>H<sub>4</sub>NCH<sub>2</sub>CH<sub>2</sub>)<sub>2</sub>N<sub>2</sub>C<sub>3</sub>H<sub>2</sub> ( $^{\text{ToI}}[\text{NCN}]$ ) in order to reduce the computational demands, while still providing two amide donors and one *N*-heterocyclic carbene donor to the tantalum centre.

### 5.10. References

- (1) Herrmann, W. A. O., Karl; Elison, Martina; Kuehn, Fritz E.; Roesky, Peter W. J. *Organomet. Chem.* **1994**, *480*, C7.
- (2) Rietveld, M. H. P.; Klumpers, E. G.; Jastrzebski, J. T. B. H.; Grove, D. M.; Veldman, N.; Spek, A. L.; van Koten, G. *Organometallics* **1997**, *16*, 4260.
- (3) Rietveld, M. H. P.; Lohner, P.; Nijkamp, M. G.; Grove, D. M.; Veldman, N.; Spek, A. L.; Pfeffer, M.; Van Koten, G. *Chem. Eur. J.* **1997**, *3*, 817.
- (4) Abbenhuis, H. C. L.; Rietveld, M. H. P.; Haarman, H. F.; Hogerheide, M. P.; Spek, A. L.; van Koten, G. *Organometallics* **1994**, *13*, 3259.
- (5) Abbenhuis, H. C. L.; Feiken, N.; Haarman, H. F.; Grove, D. M.; Horn, E.; Spek, A. L.; Pfeffer, M.; van Koten, G. *Organometallics* **1993**, *12*, 2227.
- (6) Abbenhuis, H. C. L.; Feiken, N.; Grove, D. M.; Jastrzebski, J. T. B. H.; Kooijman, H.; Van der Sluis, P.; Smeets, W. J. J.; Spek, A. L.; Van Koten, G. *J. Am. Chem. Soc.* **1992**, *114*, 9773.
- (7) Abbenhuis, H. C. L.; Feiken, N.; Haarman, H. F.; Grove, D. M.; Horn, E.; Kooijman, H.; Spek, A. L.; Van Koten, G. *Angew. Chem., Int. Ed.* **1991**, *103*, 1046.
- (8) Abbenhuis, H. C. L.; Grove, D. M.; Van der Sluis, P.; Spek, A. L.; Van Koten, G. *Recl. Trav. Chim. Pays-Bas* **1990**, *109*, 446.
- (9) Tanski, J. M.; Parkin, G. *Inorg. Chem.* **2003**, *42*, 264.
- (10) Tin, M. K. T.; Yap, G. P. A.; Richeson, D. S. *Inorg. Chem.* **1998**, *37*, 6728.
- (11) Tin, M. K. T.; Yap, G. P. A.; Richeson, D. S. *Inorg. Chem.* **1999**, *38*, 998.
- (12) Guzei, I. A.; Yap, G. P. A.; Winter, C. H. *Inorg. Chem.* **1997**, *36*, 1738.
- (13) Chisholm, M. H.; Huffman, J. C.; Tan, L.-S. *Inorg. Chem.* **1981**, *20*, 1859.
- (14) Schrock, R. R. *Chem. Rev.* **2002**, *102*, 145.
- (15) Arnold, P. L.; Mungur, S. A.; Blake, A. J.; Wilson, C. *Angew. Chem. Int. Ed.* **2003**, *42*, 5981.
- (16) Messerle, L. W.; Jennische, P.; Schrock, R. R.; Stucky, G. *J. Am. Chem. Soc.* **1980**, *102*, 6744.

- (17) Fryzuk, M. D.; Johnson, S. A.; Patrick, B. O.; Albinati, A.; Mason, S. A.; Koetzle, T. F. *J. Am. Chem. Soc.* **2001**, *123*, 3960.
- (18) Bazinet, P.; Yap, G. P. A.; Richeson, D. S. *Organometallics* **2001**, *20*, 4129.
- (19) Groysman, S.; Goldberg, I.; Kol, M.; Genizi, E.; Goldschmidt, Z. *Organometallics* **2004**, *23*, 1880.
- (20) Chamberlain, L. R.; Kerschner, J. L.; Rothwell, A. P.; Rothwell, I. P.; Huffman, J. C. *J. Am. Chem. Soc.* **1987**, *109*, 6471.
- (21) Chamberlain, L. R.; Rothwell, I. P.; Huffman, J. C. *J. Am. Chem. Soc.* **1986**, *108*, 1502.
- (22) Freundlich, J. S.; Schrock, R. R.; Davis, W. M. *Organometallics* **1996**, *15*, 2777.
- (23) Freundlich, J. S.; Schrock, R. R.; Davis, W. M. *J. Am. Chem. Soc.* **1996**, *118*, 3643.
- (24) Abbenhuis, H. C. L.; Van Belzen, R.; Grove, D. M.; Klomp, A. J. A.; Van Mier, G. P. M.; Spek, A. L.; Van Koten, G. *Organometallics* **1993**, *12*, 210.
- (25) de Castro, I.; Galakhov, M. V.; Gomez, M.; Gomez-Sal, P.; Royo, P. *Organometallics* **1996**, *15*, 1362.
- (26) Manson, J.; Webster, C. E.; Hall, M. B. In *JIMP Development Version 0.1.v117 (built for Windows PC and Redhat Linux 7.3)* Department of Chemistry, Texas A&M University, College Station, TX 77842, 2006.
- (27) Groysman, S.; Goldberg, I.; Kol, M.; Goldschmidt, Z. *Organometallics* **2003**, *22*, 3793.
- (28) Chao, Y. W.; Polson, S.; Wigley, D. E. *Polyhedron* **1990**, *9*, 2709.
- (29) Schrock, R. R.; Sharp, P. R. *J. Am. Chem. Soc.* **1978**, *100*, 2389.
- (30) Schrock, R. R. *J. Organomet. Chem.* **1976**, *122*, 209.
- (31) Li, L.; Diminnie, J. B.; Liu, X.; Pollitte, J. L.; Xue, Z. *Organometallics* **1996**, *15*, 3520.
- (32) Boncella, J. M.; Cajigal, M. L.; Abboud, K. A. *Organometallics* **1996**, *15*, 1905.
- (33) Frisch, M. J.; Trucks, G. W.; Schlegel, H. B.; Scuseria, G. E.; Robb, M. A.; Cheeseman, J. R.; Montgomery, J. A. J.; Vreven, T.; Kudin, K. N.; Burant, J. C.; Millam, J. M.; Iyengar, S. S.; Tomasi, J.; Barone, V.; Mennucci, B.; Cossi, M.; Scalmani, G.; Rega, N.; Petersson, G. A.; Nakatsuji, H.; Hada, M.; Ehara, M.;

Toyota, K.; Fukuda, R.; Hasegawa, J.; Ishida, M.; Nakajima, T.; Honda, Y.; Kitao, O.; Nakai, H.; Klene, M.; Li, X.; Knox, J. E.; Hratchian, H. P.; Cross, J. B.; Adamo, C.; Jaramillo, J.; Gomperts, R.; Stratmann, R. E.; Yazyev, O.; Austin, A. J.; Cammi, R.; Pomelli, C.; Ochterski, J. W.; Ayala, P. Y.; Morokuma, K.; Voth, G. A.; Salvador, P.; Dannenberg, J. J.; Zakrzewski, V. G.; Dapprich, S.; Daniels, A. D.; Strain, M. C.; Farkas, O.; Malick, D. K.; Rabuck, A. D.; Raghavachari, K.; Foresman, J. B.; Ortiz, J. V.; Cui, Q.; Baboul, A. G.; Clifford, S.; Cioslowski, J.; Stefanov, B. B.; Liu, G.; Liashenko, A.; Piskorz, P.; Komaromi, I.; Martin, R. L.; Fox, D. J.; Keith, T.; Al-Laham, M. A.; Peng, C. Y.; Nanayakkara, A.; Challacombe, M.; Gill, P. M. W.; Johnson, B.; Chen, W.; Wong, M. W.; Gonzalez, C.; Pople, J. A. *Gaussian 03, Revision B.4; Gaussian, Inc.: Pittsburgh, PA, 2003.*

- (34) Becke, A. D. *J. Chem. Phys.* **1993**, *98*, 5648.
- (35) Lee, C.; Yang, W.; Parr, R. G. *Phys. Rev. B: Condens. Matter* **1988**, *37*, 785.
- (36) Hay, P. J.; Wadt, W. R. *J. Chem. Phys.* **1985**, *82*, 270.
- (37) Wadt, W. R.; Hay, P. J. *J. Chem. Phys.* **1985**, *82*, 284.
- (38) Hay, P. J.; Wadt, W. R. *J. Chem. Phys.* **1985**, *82*, 299.
- (39) Couty, M.; Hall, M. B. *J. Comput. Chem.* **1996**, *17*, 1359.
- (40) Ditchfield, R.; Hehre, W. J.; Pople, J. A. *J. Chem. Phys.* **1971**, *54*, 724.
- (41) Hehre, W. J.; Ditchfield, R.; Pople, J. A. *J. Chem. Phys.* **1972**, *56*, 2257.
- (42) Hariharan, P. C.; Pople, J. A. *Theor. Chim. Acta* **1973**, *28*, 213.
- (43) Petersson, G. A.; Al-Laham, M. A. *J. Chem. Phys.* **1991**, *94*, 6081.
- (44) Petersson, G. A.; Bennett, A.; Tensfeldt, T. G.; Al-Laham, M. A.; Shirley, W. A.; Mantzaris, J. *J. Chem. Phys.* **1988**, *89*, 2193.
- (45) Foresman, J. B.; Frisch, A. E. *Exploring Chemistry with Electronic Structure Methods, 2nd Ed. (Gaussian, Inc, Pittsburgh, PA), p. 110. The 6-31G(d',p') basis set has the d polarization functions for C, N, O, and F taken from the 6-311G(d) basis set, instead of the original arbitrarily assigned value of 0.8 used in the 6-31G(d) basis set.*

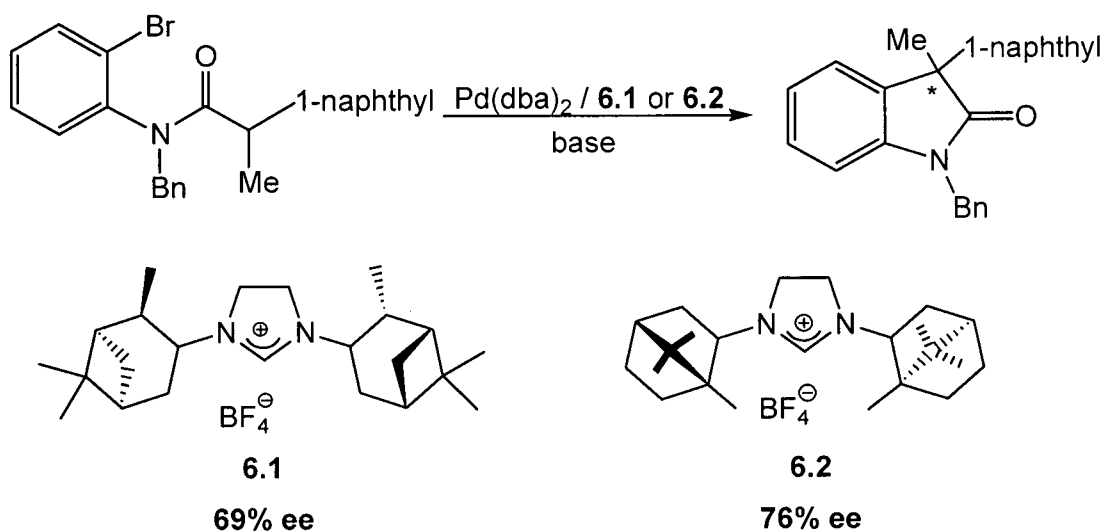
## **Chapter Six**

### **Thesis Extensions: Chiral Group 4 [NCN] Complexes**

#### **6.1. Introduction**

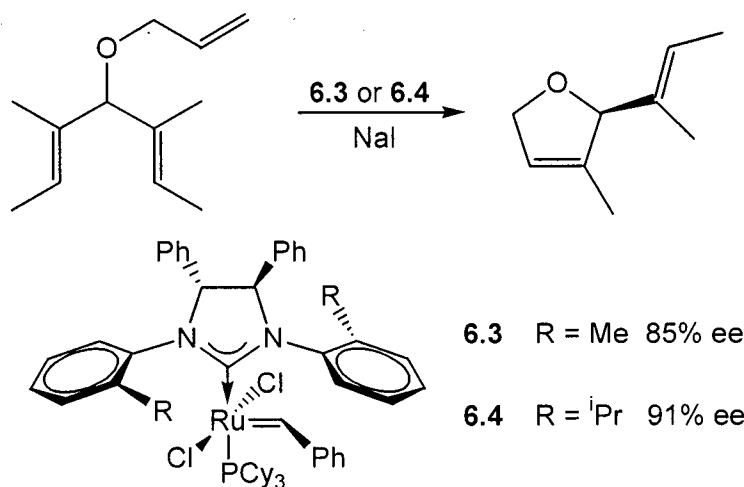
Several of the preceding chapters have explored the synthesis of a diamido-N-heterocyclic carbene ligand set and the coordination to group 4 and 5 transition metals. A logical extension of this research is to introduce chirality into the [NCN] architecture to produce chiral transition metal complexes that could facilitate enantioselective catalysis. The development of efficient and practical chiral ligands and derived catalysts is believed to be “one of the most critical research objectives in modern organic synthesis”.<sup>1</sup> Because of the incredible success enjoyed by the application of chiral phosphine ligands in asymmetric catalysis,<sup>2,3</sup> interest in introducing chirality into NHCs, so-called phosphine analogs, has dramatically increased. To date, several distinct classes of chiral NHC ligands have emerged, which can be characterized by the position of the chiral unit in relation to the NHC donor. Furthermore, each of these classes can be broadly subdivided into (i) monodentate and (ii) bidentate NHC ligands, the former being further divided into substitution of chiral groups on either the carbon backbone or the nitrogen atoms of the NHC ring, and the latter into chirality on either the spacer group or substituent on the donor atom.

In the case of monodentate ligands, chiral information can be provided by the incorporation of chiral units at different positions of the five-membered heterocyclic ring.<sup>4-14</sup> For example, introduction of chiral substituents on the nitrogen atoms as shown in the use of chiral imidazolium precursors **6.1** and **6.2** was examined in the palladium-catalyzed asymmetric oxindole reaction (Scheme 6.1).<sup>13</sup> Moderate enantioselectivities were obtained using **6.1** and **6.2** as ligand precursors in the cyclization of  $\alpha$ -naphthyl- $\alpha$ -methyl amides.



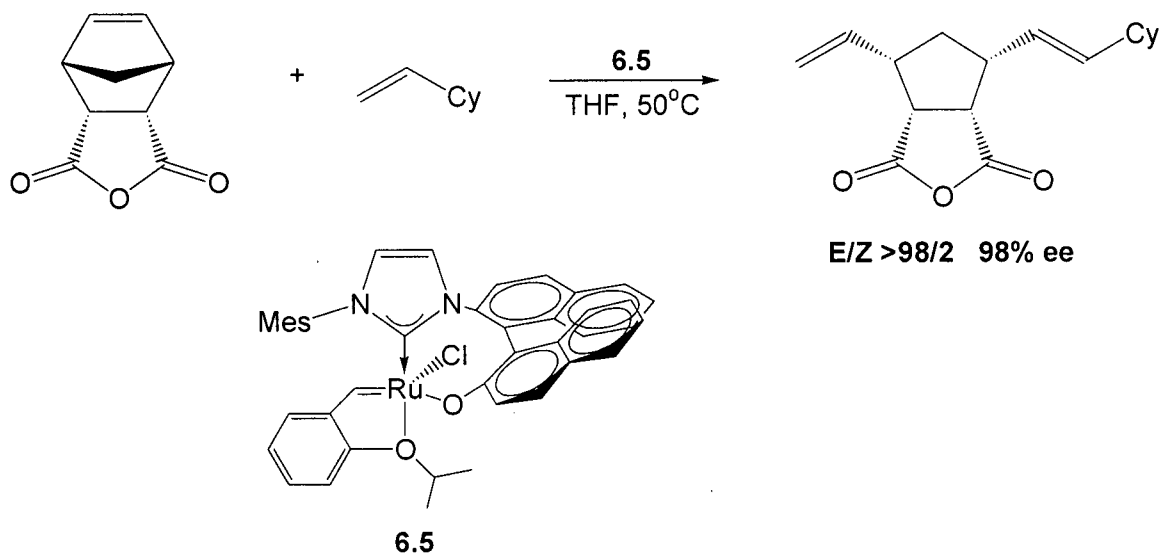
Scheme 6.1.

Substitution on the carbon backbone of the five-membered NHC ring has also been exploited.<sup>15-22</sup> Chiral ruthenium complexes **6.3** and **6.4** were examined in the desymmetrization of triolefins and found to give the ring-closed metathesis products with high enantioselectivities (Scheme 6.2).<sup>19</sup> In this example, steric repulsion between the chiral backbone phenyl groups and the *ortho*-aryl substituents stabilizes a mutual *anti* configuration that permits efficient transmission of chiral information at the active site of the catalyst.



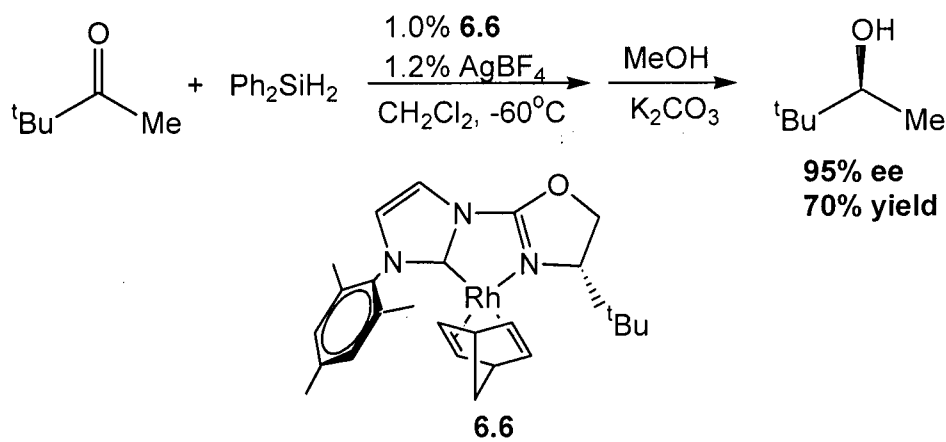
**Scheme 6.2.**

Chiral multidentate NHC ligands have also been exploited in asymmetric catalysis. In contrast to monodentate ligands, this class has the benefit that chiral substituents can be introduced at unique positions on the chelating ligand. For example, the introduction of chiral spacer units between the NHC and a pendant donor atom has been reported.<sup>23-27</sup> A ruthenium complex employing an anionic bidentate ligand with a chiral 1,1-binaphthyl spacer (**6.5**) has been investigated in the asymmetric ring opening cross-metathesis (AROM-CM) of olefins (Scheme 6.3).<sup>26</sup> Examination of this catalyst in the AROM-CM of tricyclic norbornenes with a terminal monoalkene revealed excellent stereoselective control on the product formed.



Scheme 6.3.

Transition metal complexes incorporating chiral oxazoline-NHC ligands have also emerged as promising asymmetric catalyst precursors.<sup>28-33</sup> The design of this ligand was inspired by chiral bidentate phosphine-oxazoline complexes, which are highly selective in the enantioselective hydrogenation of alkenes.<sup>34</sup> In both the phosphine and NHC examples, the chiral information is provided by a stereodirecting substituent located adjacent to the N-donor on the oxazoline heterocyclic ring. This substituent is positioned in close proximity to the metal centre and can control the space available for substrate coordination. For example, the rhodium complex **6.6** has been shown to be a highly selective catalyst for the asymmetric hydrosilylation of ketones (Scheme 6.4).<sup>30</sup>



Scheme 6.4.

The use of chiral NHC derivatives in asymmetric catalysis continues to expand. However, research in this area has been focused on late transition-metal-mediated catalysis. In this chapter, the synthesis of chiral group 4 transition metal [NCN] complexes will be investigated. Several complexes will be examined for their potential to promote asymmetric hydroamination catalysis.

## 6.2. Synthesis of Group 4 [NCN] Complexes

The construction of a chiral [NCN] ligand introduces the possibility to incorporate chiral substituents at discrete positions in the [NCN] framework. Chiral groups could be substituted at: 1) the amide-N-donor; 2) along the ethylene spacer; or 3) at the 4- and 5-positions on the NHC ring. The latter two possibilities introduce stereocentres remote from the metal centre, options that may not effectively transfer stereochemical information during the catalytic process. Given this possibility, a ligand design incorporating chiral amine groups was investigated, which would introduce chiral information in close proximity to the metal centre.

In chapter 3, aryl amido substituted imidazolium precursors were synthesized utilizing a substituted chloroethylamine precursor. Given this result, a similar approach was investigated for the preparation of a chiral [NCN] ligand. A well-known procedure for the synthesis of these derivatives is the reaction of a substituted aminoethanol derivative with  $\text{SOCl}_2$ .<sup>35</sup> (1*R*,2'*S*,4*R*)-2-(1,7,7-Trimethylbicyclo[2.2.1]-hept-2-ylideneamino)ethanol **6.7** offers the desired chiral amine component and has been previously prepared.<sup>36</sup> Treatment of optically pure **6.7** with  $\text{SOCl}_2$  in  $\text{CHCl}_3$  yields **6.8** in near quantitative yield as an air-stable white solid (Equation 6.1). The  $^1\text{H}$  NMR spectrum of **6.8** is shown in Figure 6.1 and features three distinct methyl resonances, several complicated cyclohexyl methylene resonances, and methylene resonances attributable to a  $-\text{NCH}_2\text{CH}_2\text{Cl}$  moiety. Two broad diastereotopic  $-\text{NH}$  resonances are also observed at 8.31 and 9.45 ppm.

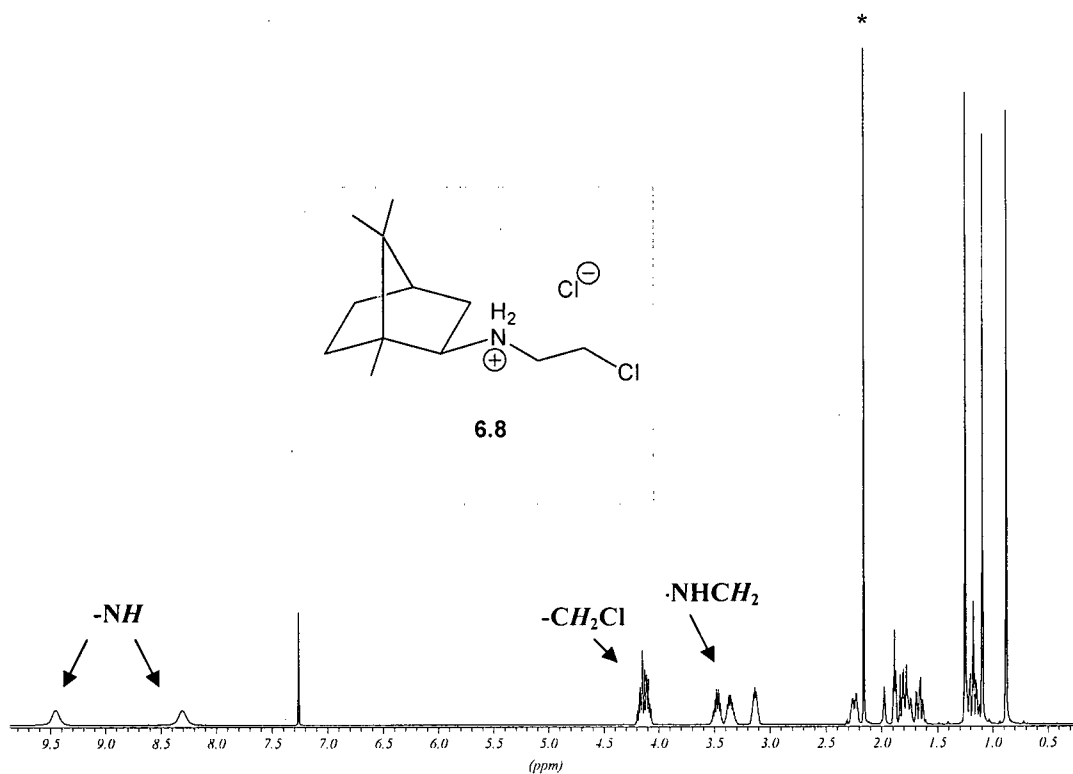
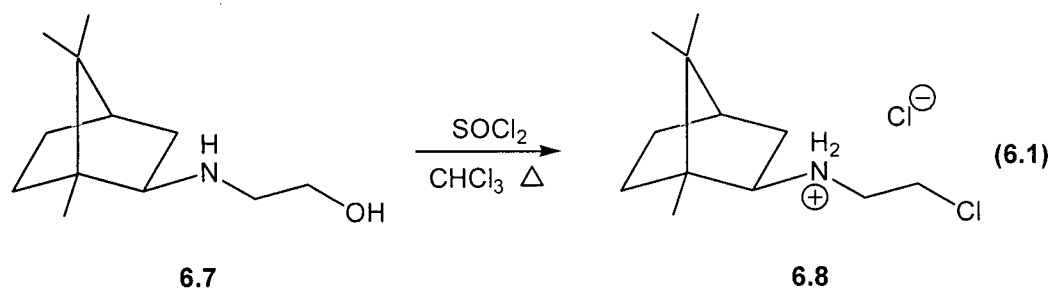


**Figure 6.1.**  $^1\text{H}$  NMR spectrum of (1*R*,2'*S*,4*R*)-2-(1,7,7-trimethylbicyclo[2.2.1]hept-2-ylamino)ethyl ammonium chloride (**6.8**) in  $\text{CDCl}_3$ . (\* denotes  $\frac{1}{2}$  equivalent of  $\text{CH}_3\text{C}(\text{O})\text{CH}_3$ ).

X-ray quality crystals of **6.8** were grown from a saturated solution of methanol and the molecular solid state structure was determined by an X-ray diffraction study. Selected bond lengths and angles are given in Table 6.1 and crystallographic details are presented in Appendix A. The orientation of the stereocentre on the cyclohexyl ring

shows there has been no change in configuration as a result of the reaction of **6.7** with  $\text{SOCl}_2$ . Furthermore, the presence of a chloride counterion infers that an ammonium moiety is present. Unfortunately, the data collected from X-ray diffraction is quite poor and the results presented here are used to establish the connectivity and orientation of the atoms in the molecule.

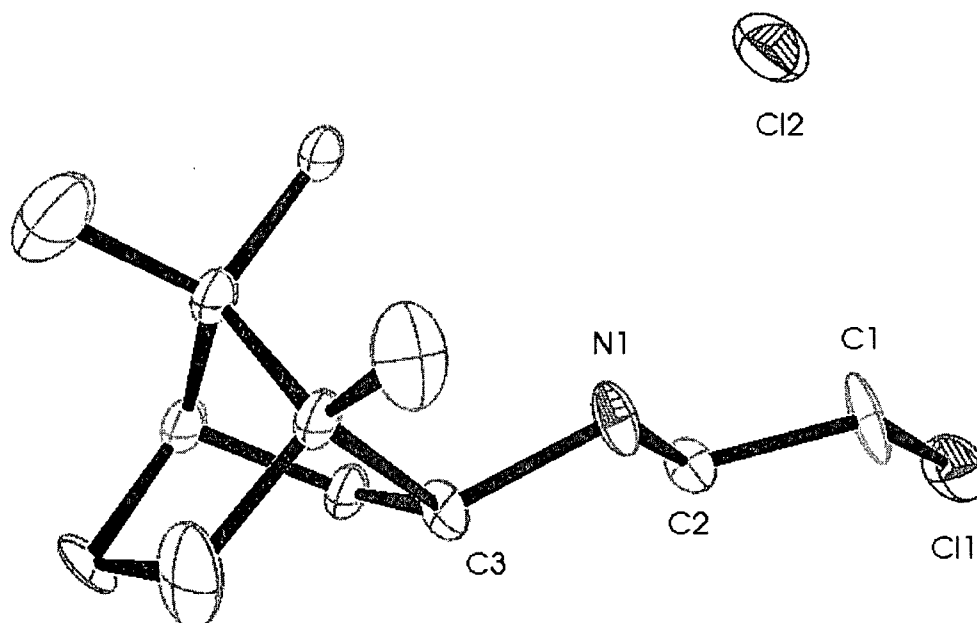


**Figure 6.2.** ORTEP view of (-)-(1*R*,2'*S*,4*R*)-2-(1,7,7-trimethylbicyclo[2.2.1]hept-2-ylamino)ethyl ammonium chloride (**6.8**) depicted with 50% thermal ellipsoids; all hydrogen atoms have been omitted for clarity.

**Table 6.1.** Selected Bond Distances (Å) and Bond Angles (°) for (-)-(1*R*,2'*S*,4*R*)-2-(1,7,7-trimethylbicyclo[2.2.1]hept-2-ylamino)ethyl ammonium chloride, (**6.8**).

Bond Lengths		Bond Angles	
N1-C2	1.453(13)	Cl1-C1-C2	107.6(10)
N1-C3	1.571(13)	C3-N1-C2	110.1(10)
Cl1-C1	1.771(19)		

Conversion of the ammonium salt **6.8** to the corresponding amine was achieved by the reaction of **6.8** with an excess of  $\text{K}_2\text{CO}_3$  (Equation 6.2). This reaction provides the free amine **6.9** in quantitative yield as a colorless oil. The  $^1\text{H}$  NMR spectrum of **6.9**, shown in Figure 6.3, reveals the absence of the ammonium resonances at 8.31 and 9.45

ppm that were observed in **6.8**, in addition to ethylene spacer units at 2.88 and 3.63 ppm. The  $-NH$  resonance was not located in the  $^1H$  NMR spectrum.

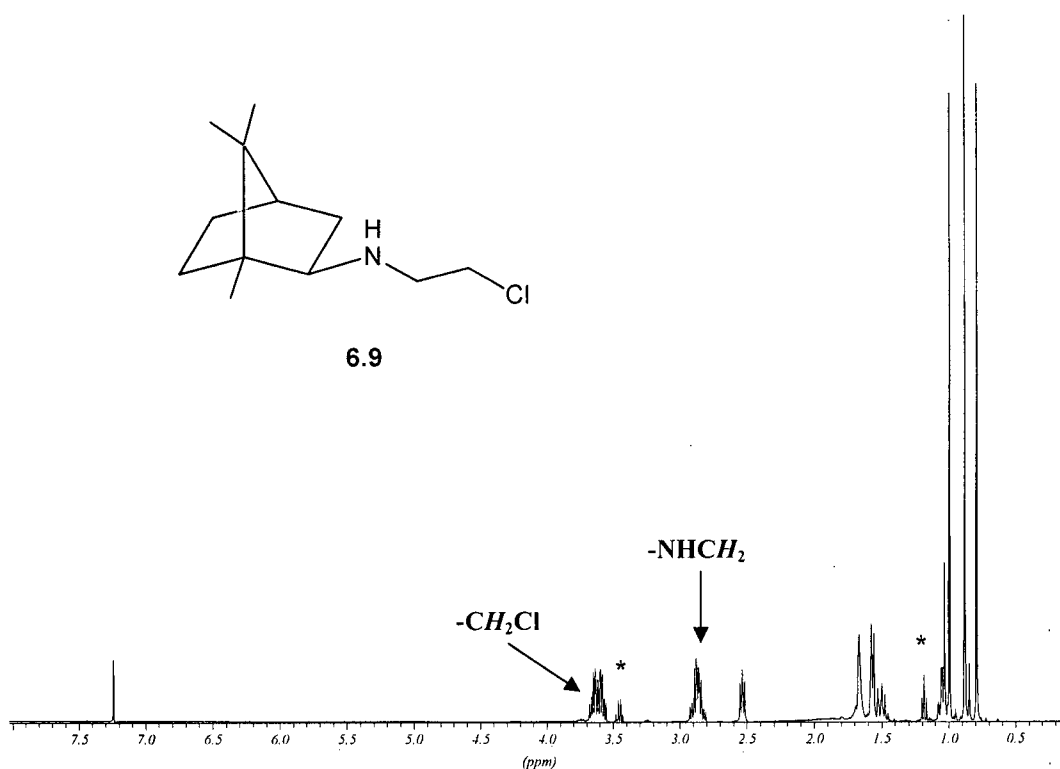
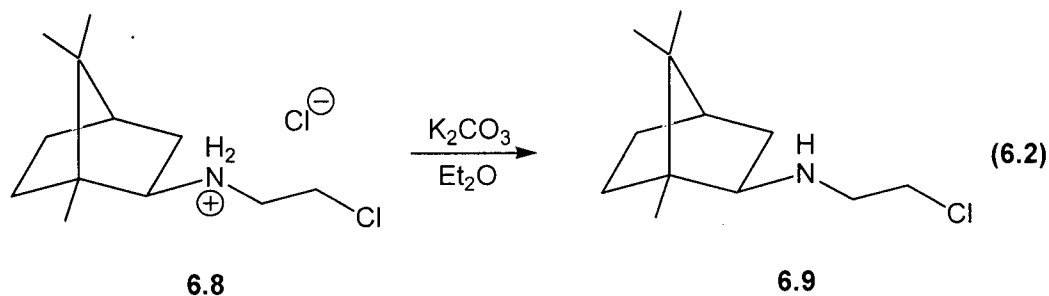


**Figure 6.3.**  $^1H$  NMR spectrum of (1*R*,2'*S*,4*R*)-2-(1,7,7-trimethylbicyclo[2.2.1]hept-2-ylamino)ethyl chloride (**6.9**) in  $CDCl_3$ . (\* denotes  $Et_2O$  impurity).

The first approach to the synthesis of a chiral [NCN] imidazolium species was the reaction of two equivalents of **6.9** with imidazole in the presence of  $NEt_3$  (Equation 6.3). This reaction produced a  $CH_2Cl_2$  insoluble solid in low yield that was identified as **6.10** by  $^1H$  and  $^{13}C\{^1H\}$  NMR spectroscopy. The formation of **6.10** was confirmed by the

presence of an iminium resonance at 9.05 ppm, along with anticipated ethylene spacer, imidazole and cyclohexylamine resonances. The resonances in the  $^1\text{H}$  NMR spectrum are broad, possibly a result of a fluxional process in the molecule or fast exchange with  $d_4\text{-CD}_3\text{OD}$  (Figure 6.4).

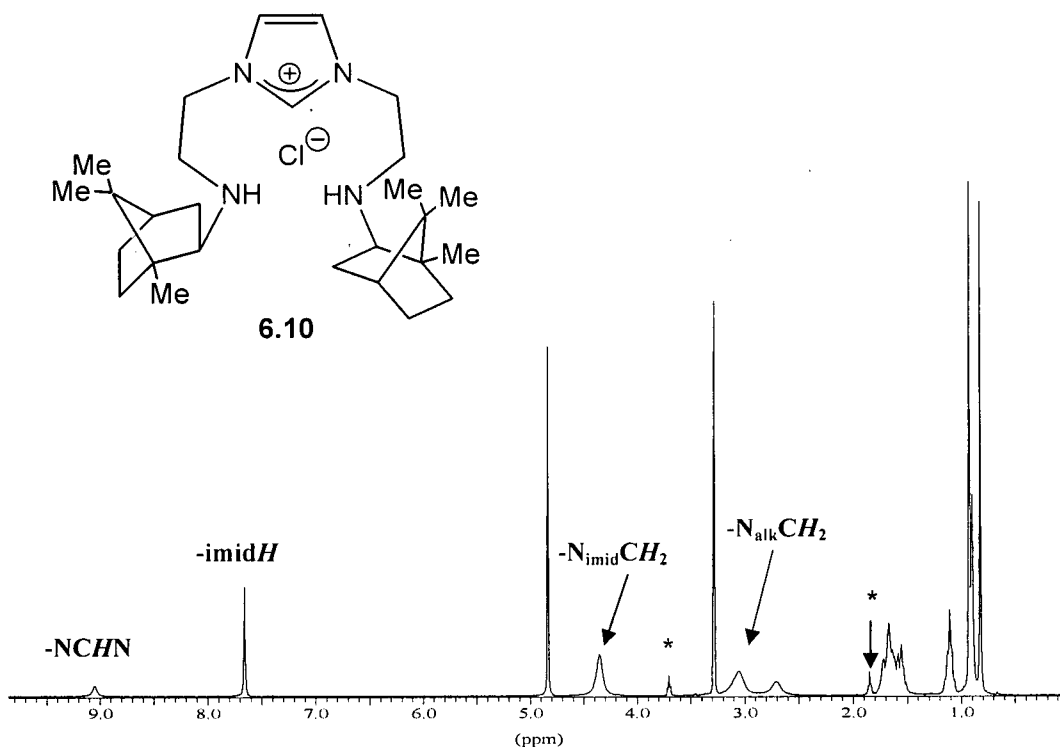
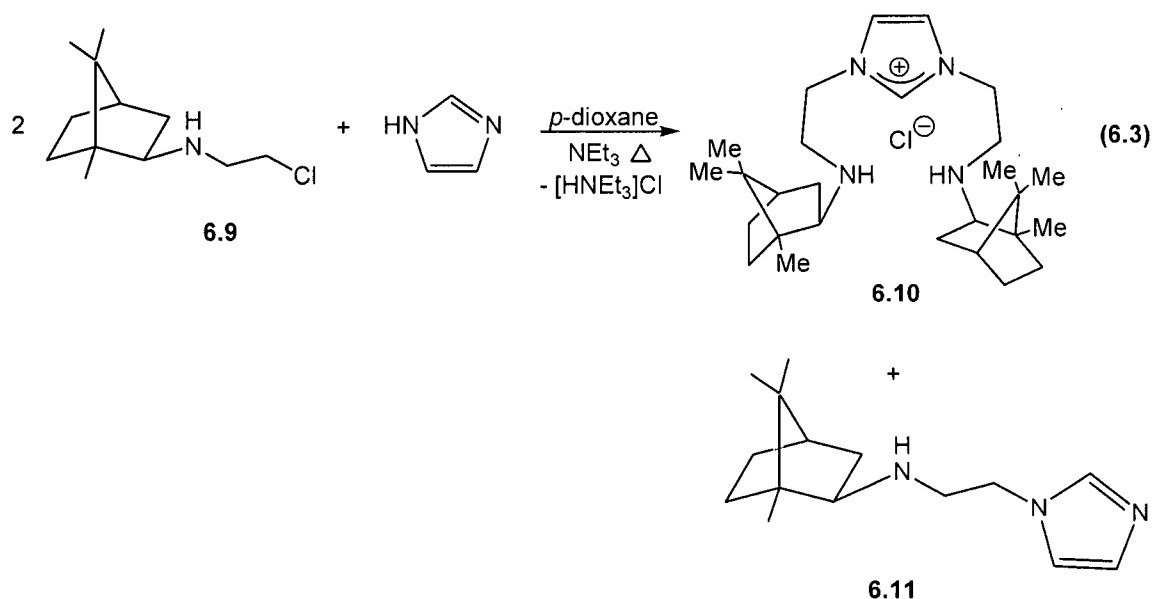


**Figure 6.4.**  $^1\text{H}$  NMR spectrum of  $[\text{scam}][\text{NCHN}]\text{H}_2\text{Cl}$  (**6.10**) in  $d_4\text{-CD}_3\text{OD}$  ( $*$  denotes THF impurity).

Intrigued by the low yield of **6.10** in this reaction, the  $\text{CH}_2\text{Cl}_2$  soluble fraction was examined to ascertain the formation of other products. The  $^1\text{H}$  NMR spectrum of the crude product suggested the synthesis of the neutral chiral 2-aminoethyl imidazole compound **6.11** (Equation 6.3), with imidazole resonances at 7.00, 7.08, and 7.69 ppm. Although the synthesis or purification of this compound was not optimized, the crude  $\text{CH}_2\text{Cl}_2$ -soluble fraction could be used as a precursor for the synthesis of **6.10**. Treatment of the crude chiral 2-aminoethyl imidazole **6.11** with the chiral 2-chloroethylamine **6.9** at  $160^\circ\text{C}$  provided the imidazolium chloride **6.10** in excellent yields.



Deprotonation of **6.10** with one equivalent of  $\text{KN}(\text{SiMe}_3)_2$  at  $-30^\circ\text{C}$  resulted in the isolation of a highly soluble yellow oil. The disappearance of the iminium resonance at 9.05 ppm in the  $^1\text{H}$  NMR spectrum supports the presence of an NHC, however, other unidentifiable resonances were present. Over an extended period of time (ca. 2 days), the resonances attributed to the NHC disappear, which suggests decomposition of the NHC ligand. As a result, the synthesis of the NHC ligand was performed *in situ* and used immediately in further reactions.

Given the success with aminolysis reactions in the synthesis of group 4 [NCN] complexes described in chapter 3, a similar approach was investigated for the synthesis of chiral group 4 [NCN] complexes. The reaction of **6.10** with  $\text{Ti}(\text{NMe}_2)_4$  in the presence of one equivalent of  $\text{KN}(\text{SiMe}_3)_2$  at  $-30^\circ\text{C}$  yielded **6.12** as a highly soluble orange solid (Equation 6.4). The  $^1\text{H}$  NMR spectrum of **6.12** is shown in Figure 6.5 and shows equivalent ethylene spacer, imidazole, and  $\text{N}(\text{CH}_3)_2$  groups. The  $^{13}\text{C}\{^1\text{H}\}$  NMR spectrum features a weak resonance at 190.5 ppm indicative of a  $\text{Ti}-\text{C}_{\text{carbene}}$  bond. Single crystals suitable for an X-ray structure determination have yet to be obtained due to the high solubility of **6.12** in organic solvents.

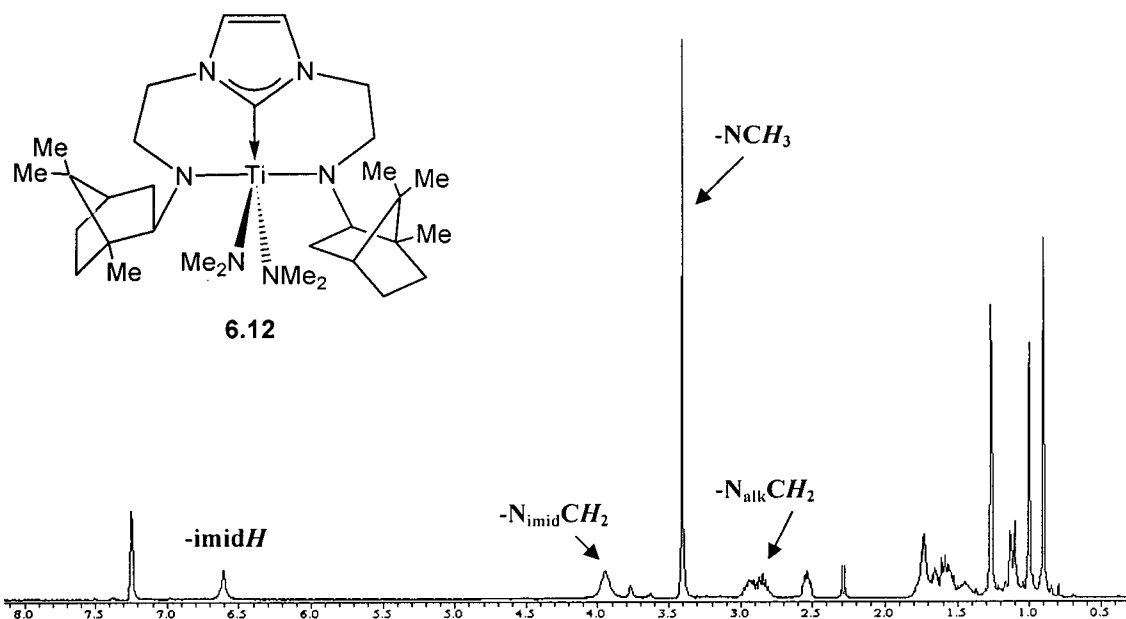
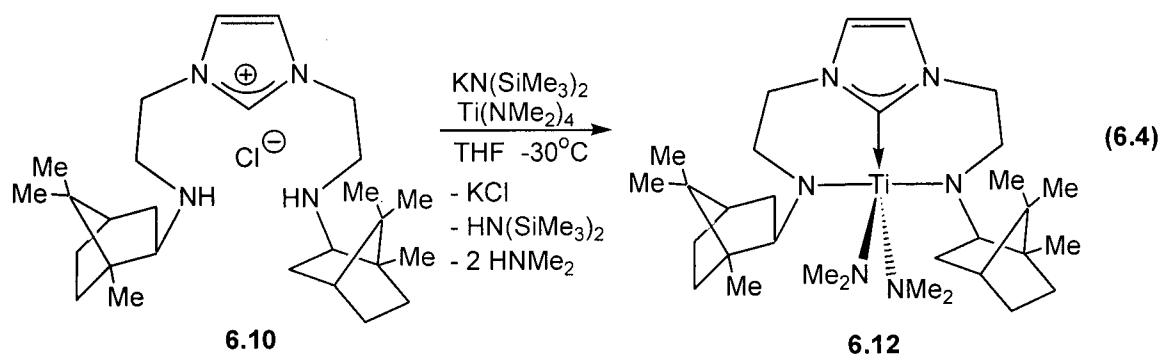
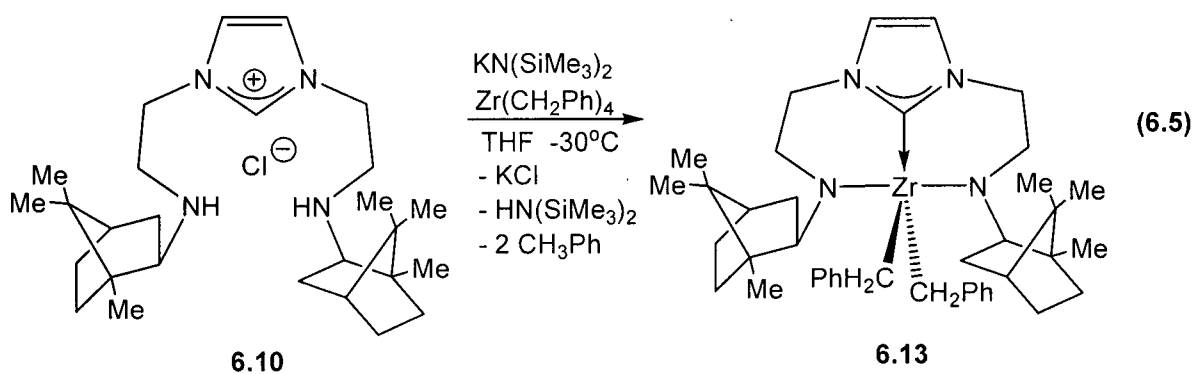


**Figure 6.5.**  $^1\text{H}$  NMR spectrum of  $^{\text{scam}}[\text{NCN}]\text{Ti}(\text{NMe}_2)_2$  (**6.12**) in  $\text{C}_6\text{D}_6$ .

Alkyl elimination reactions were also successful for the synthesis of chiral group 4 [NCN] complexes. The addition of a solution of **6.10** to  $\text{Zr}(\text{CH}_2\text{Ph})_4$  in the presence of one equivalent of  $\text{KN}(\text{SiMe}_3)_2$  at  $-30^\circ\text{C}$  yielded **6.12** as a highly soluble yellow solid (Equation 6.5). The  $^1\text{H}$  NMR spectrum of **6.12** shows a  $C_2$  symmetric species in solution with equivalent ethylene spacer and imidazole resonances. The  $\text{ZrCH}_2$  groups are observed as a diastereomeric set of doublets and are obscured by the resonances of an ethylene spacer group. A  $\text{ZrCH}_2$  resonance is also observed at 77.2 ppm in the  $^{13}\text{C}\{^1\text{H}\}$  NMR spectrum. Unfortunately, crystals of **6.13** suitable for X-ray diffraction have yet to be obtained.



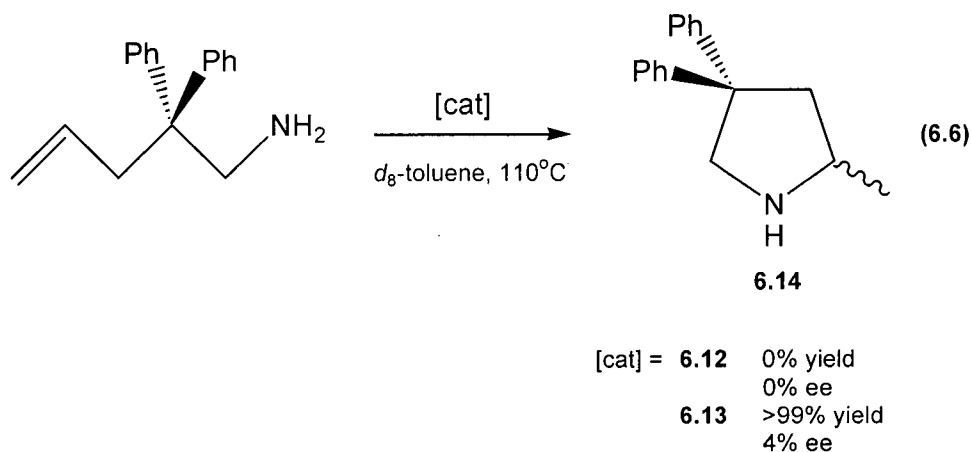
### 6.3. Asymmetric Intramolecular Hydroamination Studies

The catalytic formation of organic nitrogen containing molecules is of great academic and industrial interest. One method that has shown success is the hydroamination reaction, in which an amine is added to an olefin in either an intermolecular or intramolecular fashion.<sup>37,38</sup> Transition metal complexes have been extensively examined as catalysts for this process with examples reported for many transition metals.<sup>39,40</sup> One common goal for the design of these catalysts has been to gain control over the diastereoselectivity and regiochemistry of the hydroamination product.

The enantioselective addition of amines to olefins is a logical extension of this chemistry and remains a challenging task. With respect to early transition metals and lanthanides, several examples that display moderate to high enantioselectivities are known. Chiral yttrium binaphtholate complexes and cationic zirconium aminophenolate complexes are known to accomplish this with high enantioselectivity values.<sup>41,42</sup> Chiral lanthanide complexes with salicylaldimine<sup>43</sup> and binaphthyl diamine<sup>44</sup> ligands have also been reported to catalyze intramolecular hydroamination with moderate enantiomeric excess values.

Preliminary experiments in our laboratory with the titanium and zirconium species, **6.12** and **6.13**, focused on the intramolecular hydroamination of 2,2-diphenyl-4-pentenylamine (Equation 6.6). The catalytic reaction was initially performed at 110°C in *d*<sub>8</sub>-toluene with a 10 mol % precatalyst loading. <sup>1</sup>H NMR spectroscopy was used to monitor the disappearance of the olefinic signals in the amine substrate and the presence of diagnostic signals for the pyrrolidine product. A heated *d*<sub>8</sub>-toluene solution of

diphenyl-4-pentenylamine and the titanium precursor **6.12** was monitored by  $^1\text{H}$  NMR spectroscopy and revealed no conversion to the corresponding heterocycle after 24 hours.



It has been shown that the activities of hydroamination catalysts increase with the increasing ionic radius of the metal centre.<sup>39</sup> With this in mind, the zirconium precursor **6.13** was examined under the same conditions used for **6.12** (110°C,  $d_8$ -toluene). The reaction was followed by  $^1\text{H}$  NMR spectroscopy, which revealed complete conversion to 2-methyl-4,4-diphenylpyrrolidine **6.14** after heating for 1 hour (Equation 6.6). The enantiomeric excess of each of the two pyrrolidine products was determined by derivatizing the heterocycle **6.14** with (-)-Mosher's acid chloride.<sup>42</sup>  $^1\text{H}$  NMR spectroscopic analysis of the diastereomers formed showed that a nominal enantiomeric excess (4%) was achieved during the catalytic process.

While catalytic formation of the N-heterocycle **6.14** is encouraging, there are several possible explanations for the low enantioselectivity obtained with the zirconium precatalyst **6.13**. This low value may be a result of the ineffective transmission of chiral information by the camphor chiral unit. Alternatively, the presence of the dialkylamido donors in the chiral [NCN] ligand set presents the potential for aminolysis of the Zr-N bond by the amine precursor. Although it is anticipated that the hydroamination reaction with the aminoalkene and **6.14** would proceed to eliminate toluene (Path 1, Figure 6.6), the presence of an excess amount of aminoalkene at high temperatures could react to form a metal derivative with a new M-N amido bond and an amido-amino substituted

$^{scam}$ [NCNH] ligand array (Path 2, Figure 6.6). As a result of this protonolysis, the transfer of chiral information during the catalytic process may be disrupted.

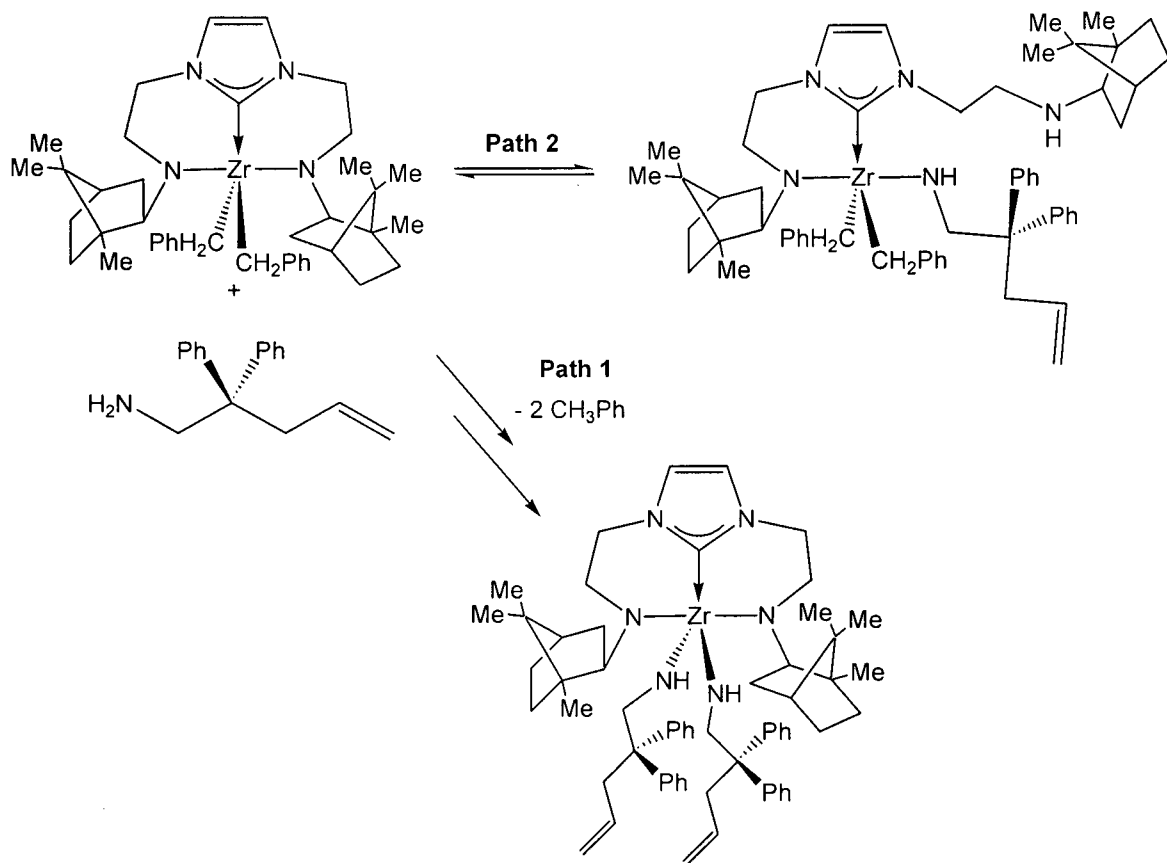


**Figure 6.6.** Aminolysis of a Zr-N bond in  $^{scam}$ [NCN]Zr(CH<sub>2</sub>Ph)<sub>2</sub>.

#### 6.4. Conclusions and Future Work

In this chapter, the synthesis of a chiral camphor-based [NCN] ligand set was investigated. Coordination of this ligand to titanium and zirconium was accomplished by aminolysis and alkyl elimination reactions, respectively. The complexes **6.12** and **6.13** were investigated in the asymmetric intramolecular hydroamination of an aminoalkene in an attempt to promote selectivity in the N-heterocycle synthesized. While the titanium complex **6.12** showed no activity, the zirconium complex **6.13** was an efficient catalyst

for the intramolecular formation of a substituted pyrrolidine. Examination of the stereoselectivity in the N-heterocyclic product revealed nominal enantioselective excess.

Chiral group 4 metallocene complexes have attracted a great deal of attention as precursors for stereoregular  $\alpha$ -olefin polymerization. It is well established that the tacticities of synthesized polyolefins are highly dependent on the structure of the precatalyst. When activated, achiral complexes such as  $\text{Cp}_2\text{ZrCl}_2$  produce atactic polymers, whereas  $C_2$ -symmetric and  $C_s$ -symmetric chiral complexes produce isotactic and syndiotactic polymers, respectively.<sup>45</sup> Given the potential  $C_2$  symmetry of **6.13**, the ability of activated **6.13** to form isotactic polypropylene would be of interest.

This chapter has demonstrated that the chiral dianionic, tridentate [NCN] ligand is well-suited for the stabilization of titanium and zirconium complexes. An analogous bidentate chiral amido-NHC ligand would be of great interest, in particular for late transition-metal-mediated asymmetric catalysis. The synthesis of a chiral amino-imidazolium chloride precursor has been investigated. Thermolysis of 1-mesitylimidazole and **6.9** at 160°C for 1 hour produces the desired imidazolium compound **6.15** in near quantitative yield (Equation 6.7). The  $^1\text{H}$  NMR spectrum (Figure 6.7) shows an iminium resonance at 9.48 ppm in addition to signals for the cyclohexylamine, aryl, and ethylene spacer groups.

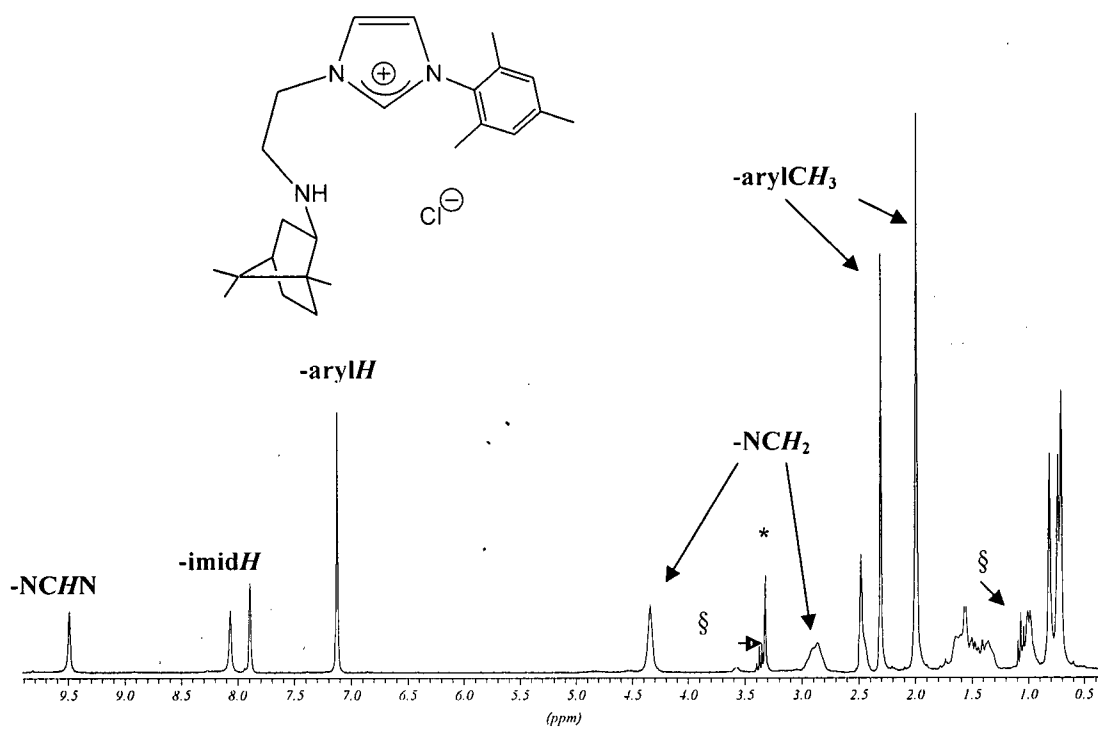
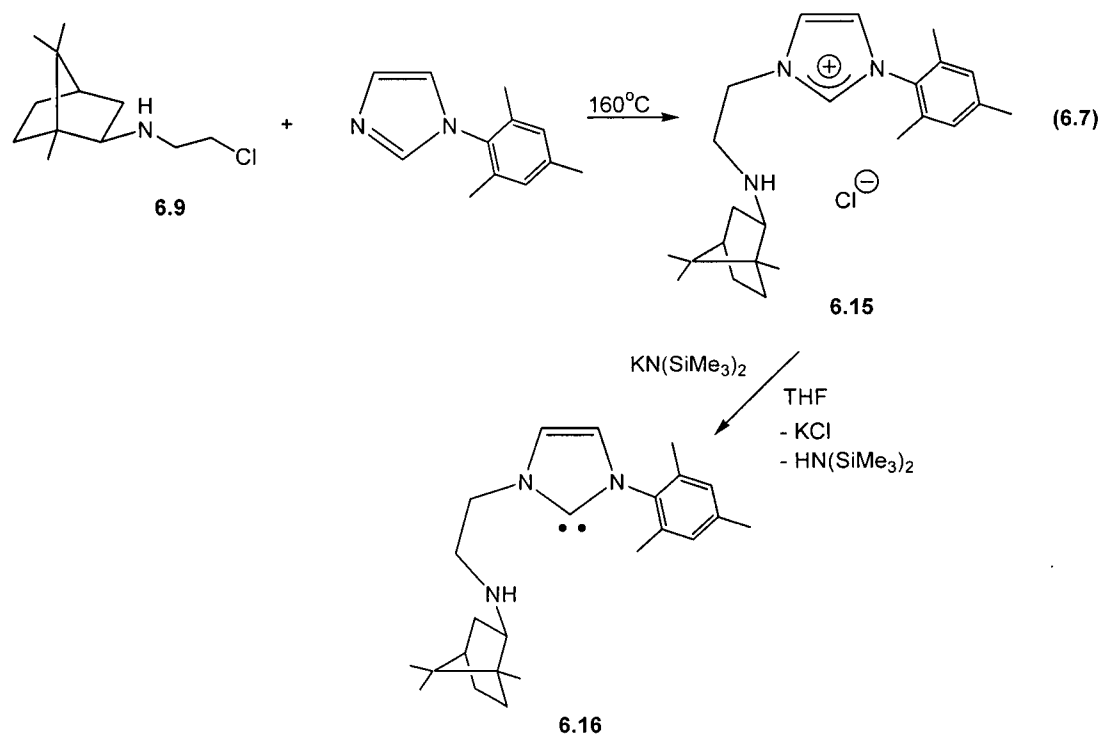
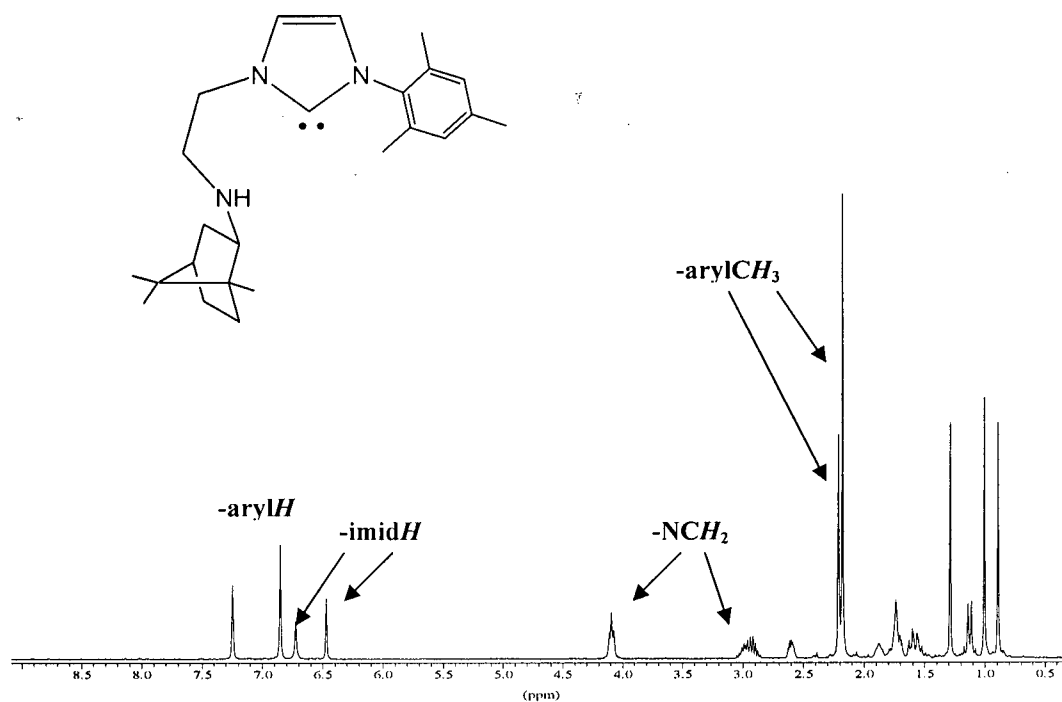


Figure 6.7.  $^1\text{H}$  NMR spectrum of  $^{\text{scam}}[\text{NCH}]\text{H}\cdot\text{Cl}$  (6.15) in  $d_6$ -DMSO (\* denotes contamination with  $\text{H}_2\text{O}$  and § denotes a trace amount of  $\text{Et}_2\text{O}$ ).

Deprotonation of **6.14** with one equivalent of  $\text{KN}(\text{SiMe}_3)_2$  proceeds immediately at room temperature to give the chiral NHC **6.16** in near quantitative yield (Equation 6.7). The  $^1\text{H}$  NMR spectrum shown in Figure 6.8 features a loss of the iminium resonance at 9.50 ppm, which is diagnostic for NHC formation. Unfortunately, the  $^{13}\text{C}$  resonance expected for the divalent carbon atom of the NHC ligand was not observed in the  $^{13}\text{C}\{^1\text{H}\}$  NMR spectrum.



**Figure 6.8.**  $^1\text{H}$  NMR spectrum of  $^{\text{scam}}[\text{NC}]\text{H}$  (**6.16**) in  $\text{C}_6\text{D}_6$ .

The coordination of the chiral bidentate NHC **6.16** remains unexplored and could yield a number of potentially chiral metal complexes. Enantioselective catalysis involving these ligands, in particular with late transition metals, offers a vast potential, which will be explored in the near future.

## 6.5. Experimental Section

### 6.5.1. General Considerations

Unless otherwise stated, general procedures were performed as described in Section 2.5.1.

### 6.5.2. Materials and Reagents

All chemicals were purchased from a chemical supplier and used as received. (-)-(1*R*,2'*S*,4*R*)-2-(1,7,7-trimethylbicyclo[2.2.1]-hept-2-ylideneamino)ethanol (**6.7**) was prepared by a literature method.<sup>36</sup>

### 6.5.3. Synthesis and Characterization of Complexes **6.8 - 6.13**, **6.14 - 6.15**

#### Synthesis of (-)-(1*R*,2'*S*,4*R*)-2-(1,7,7-trimethylbicyclo[2.2.1]-hept-2-ylideneamino)-ethyl ammonium chloride (**6.8**)

To a stirred solution of **6.7** (3.25 g, 16.5 mmol) in 50 mL CHCl<sub>3</sub> in a 100 mL Schlenk flask was added SOCl<sub>2</sub> (5.89 g, 49.5 mmol) dropwise. The orange solution was carefully heated at 80°C for 4 hours, cooled to room temperature, and the solvent removed *in vacuo* to yield a brown powder. This solid was triturated with acetone to yield a white crystalline solid that was recovered by filtration and recrystallized from MeOH. Yield = 3.87 g, 93%.

<sup>1</sup>H NMR (CDCl<sub>3</sub>): δ 0.88 (s, 3H, -CH<sub>3</sub>), 1.09 (s, 3H, -CH<sub>3</sub>), 1.15 (m, 2H, -camphorCH<sub>2</sub>), 1.25 (s, 3H, -CH<sub>3</sub>), 1.63-1.97 (m, 4H, -camphorCH<sub>2</sub>), 2.22 (m, 1H, - camphorCH), 3.13 (m, 1H, - camphorCH), 3.42 (m, 2H, -NHCH<sub>2</sub>), 4.12 (m, 2H, -CH<sub>2</sub>Cl), 8.31 (br s, 1H, -NHH), 9.45 (br s, 1H, -NHH).

<sup>13</sup>C{<sup>1</sup>H} NMR (CDCl<sub>3</sub>): δ 12.8 (-CH<sub>3</sub>), 20.0 (-CH<sub>3</sub>), 20.8 (-CH<sub>3</sub>), 26.7 (-CH<sub>2</sub>), 34.9 (-CH<sub>2</sub>), 36.7 (-CH<sub>2</sub>), 38.8 (-CH), 44.8 (-CH<sub>2</sub>Cl), 47.5 (-CHCH<sub>3</sub>), 49.1 (-C(CH<sub>3</sub>)<sub>2</sub>), 49.5 (-CH<sub>2</sub>N), 67.2 (-CHN).

[α]<sub>D</sub> = -67.0° (c 0.01; MeOH).

Anal Calcd. for C<sub>12</sub>H<sub>23</sub>Cl<sub>2</sub>N: C, 57.14; H, 9.19; N, 5.55. Found: C, 57.52; H, 9.06; N, 5.32.

**Synthesis of (1*R*,2'*S*,4*R*)-2-(1,7,7-trimethylbicyclo[2.2.1]-hept-2-ylideneamino)-ethyl chloride (6.9)**

A 250 mL Schlenk flask was charged with **6.8** (3.85 g, 14.2 mmol), 100 mL distilled H<sub>2</sub>O, and 100 mL Et<sub>2</sub>O. An aqueous solution (10 mL) of K<sub>2</sub>CO<sub>3</sub> (2.16 g, 15.6 mmol) was slowly added and the biphasic solution stirred for 1 hour. The Et<sub>2</sub>O layer was removed and the aqueous layer washed with 2 portions of Et<sub>2</sub>O (50 mL). The ethereal solutions were combined, dried with MgSO<sub>4</sub>, and filtered. Upon removal of the solid *in vacuo* a colourless oil was recovered. Yield = 3.06 g, 100%.

<sup>1</sup>H NMR (CDCl<sub>3</sub>): δ 0.81 (s, 3H, -CH<sub>3</sub>), 0.92 (s, 3H, -CH<sub>3</sub>), 1.03 (s, 3H, -CH<sub>3</sub>), 1.17 (m, 2H, -camphorCH<sub>2</sub>), 1.48-1.71 (m, 5H, -camphorCH<sub>2</sub> and -camphorCH), 2.54 (m, 1H, -camphorCH), 2.91 (m, 2H, -NHCH<sub>2</sub>), 3.63 (m, 2H, -CH<sub>2</sub>Cl).

<sup>13</sup>C{<sup>1</sup>H} NMR (CDCl<sub>3</sub>): δ 12.3 (-CH<sub>3</sub>), 20.6 (-CH<sub>3</sub>), 20.7 (-CH<sub>3</sub>), 27.4 (-CH<sub>2</sub>), 37.0 (-CH<sub>2</sub>), 38.7 (-CH<sub>2</sub>), 44.9 (-CH<sub>2</sub>Cl), 45.3 (-CH), 46.9 (-CHCH<sub>3</sub>), 48.7 (-C(CH<sub>3</sub>)<sub>2</sub>), 49.8 (-CH<sub>2</sub>N), 66.2 (-CHN).

**Synthesis of (-)-<sup>scam</sup>[NCHN]H<sub>2</sub>·Cl (6.10) (scam = (1*R*,2'*S*,4*R*)-2-(1,7,7-trimethylbicyclo[2.2.1]-hept-2-ylideneamino)**

A 500 mL Schlenk flask was charged with **6.9** (1.12 g, 5.2 mmol), imidazole (177 mg, 2.6 mmol), NEt<sub>3</sub> (0.37 mL, 5.3 mmol), and 250 mL of *p*-dioxane. The slurry was heated to 120°C and stirred overnight. Upon cooling to room temperature, the solvent was removed *in vacuo* and 50 mL CH<sub>2</sub>Cl<sub>2</sub> added. Filtration of this solution yielded a white solid, which was washed several times with CH<sub>2</sub>Cl<sub>2</sub>. The solid was dried *in vacuo* overnight as it is mildly hygroscopic. Yield = 252 mg, 21%.

<sup>1</sup>H NMR (CD<sub>3</sub>OD): δ 0.83 (s, 6H, -CH<sub>3</sub>), 0.90 (s, 6H, -CH<sub>3</sub>), 0.93 (s, 6H, -CH<sub>3</sub>), 1.11 (m, 4H, -camphorCH<sub>2</sub>), 1.56-1.72 (m, 10H, -camphorCH<sub>2</sub> and -camphorCH), 2.71 (br m, 2H, -camphorCH), 3.06 (br m, 4H, -NCH<sub>2</sub>), 4.35 (br m, 4H, -NCH<sub>2</sub>), 7.68 (s, 2H, -imidH), 9.05 (br s, 1H, -NCHN).

$^{13}\text{C}\{^1\text{H}\}$  NMR ( $\text{CD}_3\text{OD}$ ):  $\delta$  14.7 (- $\text{CH}_3$ ), 21.2 (- $\text{CH}_3$ ), 21.9 (- $\text{CH}_3$ ), 29.1 (- $\text{CH}_2$ ), 38.3 (- $\text{CH}_2$ ), 38.9 (- $\text{CH}_2$ ), 46.2 (- $\text{CH}$ ), 47.7 (- $\text{CH}$ ), 48.3 (- $\text{CH}_2\text{N}$ ), 49.0 (- $\text{CHCH}_3$ ), 51.3 (- $\text{CH}_2\text{N}$ ), 67.9 (- $\text{C}(\text{CH}_3)_2$ ), 126.4 (-imidC), 138.6 (-NCHN).

$[\alpha]_{\text{D}} = -83.5^\circ$  ( $c$  0.01; MeOH).

Anal Calcd. for  $\text{C}_{27}\text{H}_{46}\text{ClN}_4$ : C, 70.17; H, 10.03; N, 12.12. Found: C, 70.02; H, 9.68; N, 12.35.

### Synthesis of (1*R*,2'*S*,4*R*)-2-(1,7,7-trimethylbicyclo[2.2.1]-hept-2-ylideneamino)ethyl imidazole (6.11)

The  $\text{CH}_2\text{Cl}_2$  filtrate that was obtained in the synthesis of **6.10** was recovered and the solvent removed *in vacuo* to yield a dark oil.  $^1\text{H}$  analysis of this residue revealed the formation of **6.11** in about ~85% purity.

$^1\text{H}$  NMR ( $\text{CDCl}_3$ ):  $\delta$  0.73 (s, 3H, - $\text{CH}_3$ ), 0.86 (s, 3H, - $\text{CH}_3$ ), 0.94 (s, 3H, - $\text{CH}_3$ ), 1.05 (m, 2H, -camphor $\text{CH}_2$ ), 1.48-1.74 (m, 5H, -camphor $\text{CH}_2$  and -camphor $\text{CH}$ ), 2.52 (m, 1H, -camphor $\text{CH}$ ), 2.95 (m, 1H, -camphor $\text{CH}$ ), 2.54 (m, 2H, - $\text{N}_{\text{cam}}\text{CH}_2$ ), 4.14 (m, 2H, - $\text{N}_{\text{imid}}\text{CH}_2$ ), 7.00 (s, 1H, -imid $\text{H}$ ), 7.08 (s, 1H, -imid $\text{H}$ ), 7.69 (s, 1H, -NCHN).

### Alternative synthesis of (-)- $^{\text{scam}}[\text{NCHN}]\text{H}_2\cdot\text{Cl}$ (6.10)

A 25 mL Schlenk flask was charged with **6.9** (262 mg, 1.2 mmol) and crude **6.11** (300 mg, 1.2 mmol) and slowly heated to  $160^\circ\text{C}$  for 1 hour. The reaction mixture was cooled to room temperature and THF added to give a white solid (**6.10**) which was collected by filtration and washed with several portions of THF. Yield = 505 mg, 91%.

### Synthesis of $^{\text{scam}}[\text{NCN}]\text{Ti}(\text{NMe}_2)_2$ (6.12)

A suspension of **6.10** (296 mg, 0.64 mmol) in THF (5 mL) was cooled to  $-30^\circ\text{C}$  in a 50 mL Erlenmeyer flask and a THF (5 mL) solution of  $\text{KN}(\text{SiMe}_3)_2$  (127 mg, 0.64 mmol) was slowly added dropwise. The solution was left to stand at  $-30^\circ\text{C}$  for 15 minutes without stirring. A THF (5 mL) solution of  $\text{Ti}(\text{NMe}_2)_4$  (143 mg, 0.64 mmol) was slowly added dropwise and the entire mixture slowly warmed to room temperature and stirred overnight. The solvent was removed and the yellow residue extracted with hexane

(2 x10 mL). The solvent was removed in vacuo and HMDSO added to yield a bright orange powder. Yield = 143 mg, 40%.

$^1\text{H NMR (C}_6\text{D}_6)$ :  $\delta$  0.82 (s, 6H,  $-\text{CH}_3$ ), 0.92 (s, 6H,  $-\text{CH}_3$ ), 1.03 (m, 4H,  $-\text{camphorCH}_2$ ), 1.18 (s, 6H,  $-\text{CH}_3$ ), 1.41-1.70 (m, 10H,  $-\text{camphorCH}$  and  $\text{camphorCH}_2$ ), 2.45 (m, 2H,  $-\text{camphorCH}$ ), 2.70-2.91 (m, 4H,  $-\text{NCH}_2$ ), 3.32 (s, 12H,  $-\text{N(CH}_3)_2$ ), 3.85 (m, 4H,  $-\text{NCH}_2$ ), 6.52 (s, 2H,  $-\text{imidH}$ )

$^{13}\text{C}\{^1\text{H}\}$  NMR ( $\text{C}_6\text{D}_6$ ):  $\delta$  13.2 ( $-\text{CH}_3$ ), 20.6 ( $-\text{CH}_3$ ), 21.7 ( $-\text{CH}_3$ ), 28.5 ( $-\text{CH}_2$ ), 36.9 ( $-\text{CH}_2$ ), 37.3 ( $-\text{CH}_2$ ), 45.1 ( $-\text{CH}$ ), 45.9 ( $-\text{NCH}_3$ ), 47.8 ( $-\text{CH}$ ), 47.9 ( $-\text{CHCH}_3$ ), 48.2 ( $-\text{NCH}_2$ ), 51.0 ( $-\text{NCH}_2$ ), 66.8 ( $-\text{C(CH}_3)_2$ ), 120.4 ( $-\text{imidC}$ ), 190.5 ( $-\text{TiC}_{\text{carbene}}$ ).

Satisfactory elemental analysis has yet to be obtained.

### Synthesis of $^{\text{scam}}[\text{NCN}]\text{Zr}(\text{CH}_2\text{Ph})_2$ (6.13)

A suspension of **6.10** (286 mg, 0.62 mmol) in THF (5 mL) was cooled to  $-30^\circ\text{C}$  in a 50 mL Erlenmeyer flask and a THF (5 mL) solution of  $\text{KN}(\text{SiMe}_3)_2$  (136 mg, 0.62 mmol) was slowly added dropwise. The solution was left to stand at  $-30^\circ\text{C}$  for 15 minutes without stirring. A THF (5 mL) solution of  $\text{Zr}(\text{CH}_2\text{Ph})_4$  (282 mg, 0.62 mmol) was slowly added dropwise and the entire mixture slowly warmed to room temperature and stirred overnight. The solvent was removed and the yellow residue extracted with hexane (2 x10 mL). The solvent was removed in vacuo and HMDSO added to yield a bright yellow powder. Yield = 295 mg, 68%.

$^1\text{H NMR (C}_6\text{D}_6)$ :  $\delta$  0.86 (s, 6H,  $-\text{CH}_3$ ), 0.96 (s, 6H,  $-\text{CH}_3$ ), 1.11 (m, 4H,  $-\text{camphorCH}_2$ ), 1.16 (s, 6H,  $-\text{CH}_3$ ), 1.50-1.71 (m, 8H,  $-\text{camphorCH}$  and  $\text{camphorCH}_2$ ), 2.20 (m, 2H,  $-\text{camphorCH}$ ), 2.26-2.51 (m, 10H,  $-\text{camphorCH}$ ,  $\text{ZrCH}_2$ , and  $\text{NCH}_2$ ), 3.11 (m, 4H,  $-\text{NCH}_2$ ), 6.90 (s, 2H,  $-\text{imidH}$ ), 6.95-7.01 (m, 6H,  $-\text{ArH}$ ), 7.19 (t,  $J = 8$  Hz, 4H,  $-\text{ArH}$ )

$^{13}\text{C}\{^1\text{H}\}$  NMR ( $\text{C}_6\text{D}_6$ ):  $\delta$  15.2 ( $-\text{CH}_3$ ), 20.0 ( $-\text{CH}_3$ ), 20.9 ( $-\text{CH}_3$ ), 27.7 ( $-\text{CH}_2$ ), 37.4 ( $-\text{CH}_2$ ), 38.2 ( $-\text{CH}_2$ ), 44.9 ( $-\text{CH}$ ), 45.1 ( $-\text{CH}$ ), 46.3 ( $-\text{CHCH}_3$ ), 49.3 ( $-\text{NCH}_2$ ), 51.8 ( $-\text{NCH}_2$ ), 66.2 ( $-\text{C(CH}_3)_2$ ), 77.3 ( $-\text{ZrCH}_2$ ), 118.5 ( $-\text{ArC}$ ), 119.7 ( $-\text{imidC}$ ), 128.6 ( $-\text{ArC}$ ), 130.1 ( $-\text{ArC}$ ), 148.2 ( $-\text{ArC}$ ), 193.0 ( $-\text{ZrC}_{\text{carbene}}$ ).

Anal Calcd. for  $\text{C}_{41}\text{H}_{58}\text{N}_4\text{Zr}$ : C, 70.53; H, 8.37; N, 8.03. Found: C, 70.22; H, 8.56; N, 8.16.

### Synthesis of (-)-<sup>scam</sup>[NCH]H·Cl (6.15)

A 25 mL Schlenk flask was charged with **6.9** (1.05 g, 4.9 mmol) and 1-mesitylimidazole (0.906 mg, 4.9 mmol) then slowly heated to 160°C for 1 hour. The reaction mixture was cooled to room temperature and THF added to give a white solid (**6.15**) which was collected by filtration and washed with several portions of THF. Yield = 1.87 g, 95%.

<sup>1</sup>H NMR (*d*<sub>6</sub>-DMSO): δ 0.72 (s, 6H, -CH<sub>3</sub>), 0.75 (s, 6H, -CH<sub>3</sub>), 0.82 (s, 6H, -CH<sub>3</sub>), 0.99 (m, 4H, -camphorCH), 1.30-1.68 (m, 4H, -camphorCH and camphorCH<sub>2</sub>), 2.00 (s, 3H, -*o*-ArCH<sub>3</sub>), 2.32 (s, 3H, -*p*-ArCH<sub>3</sub>), 2.48 (m, 1H, - camphorCH), 2.87 (m, 2H, -NCH<sub>2</sub>), 4.35 (m, 2H, -NCH<sub>2</sub>), 7.13 (s, 2H, -ArH), 7.90 (br s, 1H, -imidH), 8.07 (br s, 1H, -imidH), 9.50.

<sup>13</sup>C{<sup>1</sup>H} NMR (*d*<sub>6</sub>-DMSO): δ 13.0 (-CH<sub>3</sub>), 18.6 (-CH<sub>3</sub>), 22.6 (-CH<sub>3</sub>), 28.2 (-CH<sub>2</sub>), 35.6 (-CH<sub>2</sub>), 38.3 (-CH<sub>2</sub>), 45.1 (-CH), 47.0 (-CH), 48.1 (-CHCH<sub>3</sub>), 48.9 (-NCH<sub>2</sub>), 51.9 (-NCH<sub>2</sub>), 67.1 (-C(CH<sub>3</sub>)<sub>2</sub>), 118.0 (-imidC), 119.1 (-imidC), 127.8 (-ArC), 130.2 (-ArC), 131.2 (-ArC), 139.4 (-ArC), 142.1 (-NCHN).

[α]<sub>D</sub> = -41.3° (*c* 0.01; MeOH).

Satisfactory elemental analysis has yet to be obtained.

### Synthesis of <sup>scam</sup>[NC]H (6.16)

A THF solution (5 mL) of KN(SiMe<sub>3</sub>)<sub>2</sub> (390 mg, 2.0 mmol) was slowly added dropwise to **6.15** (786 mg, 2.0 mmol) dissolved in 5 mL THF, creating a slightly yellow suspension. The suspension was stirred for ½ hr and the solvent removed in vacuo. The pale yellow residue was extracted with toluene (20 mL) and the solution filtered through celite. Removal of the solvent yielded a white solid which was washed several times with hexane and dried in vacuo. Yield = 702 mg, 96%.

<sup>1</sup>H NMR (C<sub>6</sub>D<sub>6</sub>): δ 0.89 (s, 6H, -CH<sub>3</sub>), 1.00 (s, 6H, -CH<sub>3</sub>), 1.12 (m, 2H, -camphorCH<sub>2</sub>), 1.29 (s, 6H, -CH<sub>3</sub>), 1.49-1.92 (m, 4H, -camphorCH and camphorCH<sub>2</sub>), 2.18 (s, 6H, -*o*-ArCH<sub>3</sub>), 2.21 (s, 3H, -*p*-ArCH<sub>3</sub>), 2.60 (m, 1H, - camphorCH), 2.91 (m, 2H, -NCH<sub>2</sub>), 4.09 (m, 2H, -NCH<sub>2</sub>), 6.46 (br s, 1H, -imidH), 6.72 (br s, 1H, -imidH), 6.85 (s, 2H, -ArH).

<sup>13</sup>C{<sup>1</sup>H} NMR (C<sub>6</sub>D<sub>6</sub>): δ 12.2 (-CH<sub>3</sub>), 17.9 (-CH<sub>3</sub>), 20.7 (-CH<sub>3</sub>), 27.6 (-CH<sub>2</sub>), 36.9 (-CH<sub>2</sub>), 38.8 (-CH<sub>2</sub>), 45.5 (-CH), 46.7 (-CH), 48.4 (-CHCH<sub>3</sub>), 49.6 (-NCH<sub>2</sub>), 51.0 (-NCH<sub>2</sub>),

66.7 (-C(CH<sub>3</sub>)<sub>2</sub>), 119.3 (-imidC), 120.0 (-imidC), 128.8 (-ArC), 135.1 (-ArC), 136.9 (-ArC), 138.9 (-ArC).

Satisfactory elemental analysis has yet to be obtained.

### Procedure for Intramolecular Hydroamination

A J. Young's tube was charged with a ferrocene internal standard sealed in a glass capillary tube, catalyst (0.025 mmol), and the amino alkene (0.5 mmol) and dissolved in *d*<sub>8</sub>-toluene (~ 1 ml). The NMR tube was heated to 110°C and the progress of the reaction was monitored by <sup>1</sup>H NMR spectroscopy at regular intervals. The NMR yields were determined by comparing the integration of the internal standard with a well-resolved signal for the heterocyclic product. The <sup>1</sup>H NMR spectrum of 2-methyl-4,4-diphenylpyrrolidine recovered during **6.13**-mediated hydroamination is identical to reported values.<sup>47</sup>

### Enantioselective Excess Determination<sup>42</sup>

The NMR solution was transferred to a 50 mL Erlenmeyer flask and the tube rinsed with several portions of CHCl<sub>3</sub>. To this solution was added (-)-Mosher chloride and ~ 1 mL triethylamine. The solution was stirred for 15 minutes and solvent removed in vacuo. The residue was dissolved in CDCl<sub>3</sub> and the enantiomeric excess was determined by <sup>1</sup>H NMR spectroscopy.

## 6.7. References

- (1) Jacobsen, E. N.; Pfaltz, A.; Yamamoto, H.; Editors *Comprehensive Asymmetric Catalysis I-III, Volume I*; Springer: Berlin, Germany, 1999.
- (2) Cesar, V.; Bellemin-Lapponnaz, S.; Gade, L. H. *Chem. Soc. Rev.* **2004**, *33*, 619.
- (3) Roland, S.; Mangeney, P. *Top. Organomet. Chem.* **2005**, *15*, 191.
- (4) Herrmann, W. A.; Goossen, L. J.; Koecher, C.; Artus, G. R. J. *Angew. Chem., Int. Ed. Engl.* **1997**, *35*, 2805.
- (5) Enders, D.; Gielen, H. *J. Organomet. Chem.* **2001**, *617-618*, 70.
- (6) Enders, D.; Gielen, H.; Breuer, K. *Tetrahedron: Asymmetry* **1997**, *8*, 3571.
- (7) Enders, D.; Breuer, K.; Runsink, J.; Teles, J. H. *Helv. Chim. Acta* **1996**, *79*, 1899.
- (8) Enders, D.; Breuer, K.; Teles, J. H. *Helv. Chim. Acta* **1996**, *79*, 1217.
- (9) Knight, R. L.; Leeper, F. J. *J. Chem. Soc., Perkin Trans. 1* **1998**, 1891.
- (10) Kerr, M. S.; Rovis, T. *Synlett* **2003**, 1934.
- (11) Kerr, M. S.; Read de Alaniz, J.; Rovis, T. *J. Am. Chem. Soc.* **2002**, *124*, 10298.
- (12) Culkin, D. A.; Hartwig, J. F. *Acc. Chem. Res.* **2003**, *36*, 234.
- (13) Lee, S.; Hartwig, J. F. *J. Org. Chem.* **2001**, *66*, 3402.
- (14) Seo, H.; Kim, B. Y.; Lee, J. H.; Park, H.-J.; Son, S. U.; Chung, Y. K. *Organometallics* **2003**, *22*, 4783.
- (15) Fraser, P. K.; Woodward, S. *Tetrahedron Lett.* **2001**, *42*, 2747.
- (16) Alexakis, A.; Benhaim, C.; Rosset, S.; Humam, M. *J. Am. Chem. Soc.* **2002**, *124*, 5262.
- (17) Feringa, B. L. *Acc. Chem. Res.* **2000**, *33*, 346.
- (18) Masamune, S.; Choy, W.; Petersen, J. S.; Sita, L. R. *Angew. Chem., Int. Ed.* **1985**, *97*, 1.
- (19) Seiders, T. J.; Ward, D. W.; Grubbs, R. H. *Org. Lett.* **2001**, *3*, 3225.
- (20) Jensen, D. R.; Sigman, M. S. *Org. Lett.* **2003**, *5*, 63.
- (21) Bappert, E.; Helmchen, G. *Synlett* **2004**, 1789.
- (22) Chianese, A. R.; Li, X.; Janzen, M. C.; Faller, J. W.; Crabtree, R. H. *Organometallics* **2003**, *22*, 1663.

- (23) Clyne, D. S.; Jin, J.; Genest, E.; Gallucci, J. C.; RajanBabu, T. V. *Org. Lett.* **2000**, 2, 1125.
- (24) Albrecht, M.; Crabtree, R. H.; Mata, J.; Peris, E. *Chem. Commun.* **2002**, 32.
- (25) Van Veldhuizen, J. J.; Gillingham, D. G.; Garber, S. B.; Kataoka, O.; Hoveyda, A. H. *J. Am. Chem. Soc.* **2003**, 125, 12502.
- (26) Van Veldhuizen, J. J.; Garber, S. B.; Kingsbury, J. S.; Hoveyda, A. H. *J. Am. Chem. Soc.* **2002**, 124, 4954.
- (27) Garber, S. B.; Kingsbury, J. S.; Gray, B. L.; Hoveyda, A. H. *J. Am. Chem. Soc.* **2000**, 122, 8168.
- (28) Perry, M. C.; Cui, X.; Powell, M. T.; Hou, D.-R.; Reibenspies, J. H.; Burgess, K. *J. Am. Chem. Soc.* **2003**, 125, 113.
- (29) Powell, M. T.; Hou, D.-R.; Perry, M. C.; Cui, X.; Burgess, K. *J. Am. Chem. Soc.* **2001**, 123, 8878.
- (30) Gade, L. H.; Cesar, V.; Bellemin-Laponnaz, S. *Angew. Chem. Int. Ed.* **2004**, 43, 1014.
- (31) Glorius, F.; Altenhoff, G.; Goddard, R.; Lehmann, C. *Chem. Commun.* **2002**, 2704.
- (32) Bolm, C.; Focken, T.; Raabe, G. *Tetrahedron: Asymmetry* **2003**, 14, 1733.
- (33) Enders, D.; Kallfass, U. *Angew. Chem. Int. Ed.* **2002**, 41, 1743.
- (34) Pfaltz, A.; Blankenstein, J.; Hilgraf, R.; Hormann, E.; McIntyre, S.; Menges, F.; Schonleber, M.; Smidt, S. P.; Wustenberg, B.; Zimmermann, N. *Adv. Synth. Catal.* **2003**, 345, 33.
- (35) Foster, P.; Chien, J. C. W.; Rausch, M. D. *J. Organomet. Chem.* **1997**, 545-546, 35.
- (36) Squire, M. D.; Burwell, A.; Ferrence, G. M.; Hitchcock, S. R. *Tetrahedron: Asymmetry* **2002**, 13, 1849.
- (37) Pohlki, F.; Doye, S. *Chem. Soc. Rev.* **2003**, 32, 104.
- (38) Mueller, T. E.; Beller, M. *Chem. Rev.* **1998**, 98, 675.
- (39) Roesky, P. W.; Mueller, T. E. *Angew. Chem. Int. Ed.* **2003**, 42, 2708.
- (40) Hultsch, K. C. *Adv. Synth. Catal.* **2005**, 347, 367.
- (41) Gribkov, D. V.; Hultsch, K. C. *Chem. Commun.* **2004**, 730.

- (42) Knight, P. D.; Munslow, I.; O'Shaughnessy, P. N.; Scott, P. *Chem. Commun.* **2004**, 894.
- (43) O'Shaughnessy, P. N.; Knight, P. D.; Morton, C.; Gillespie, K. M.; Scott, P. *Chem. Commun.* **2003**, 1770.
- (44) Collin, J.; Daran, J.-C.; Schulz, E.; Trifonov, A. *Chem. Commun.* **2003**, 3048.
- (45) Nakayama, Y.; Shiono, T. *Molecules* **2005**, *10*, 620.
- (46) Danopoulos, A. A.; Wright, J. A.; Motherwell, W. B. *Chem. Commun.* **2005**, 784.
- (47) Bexrud, J. A.; Beard, J. D.; Leitch, D. C.; Schafer, L. L. *Org. Lett.* **2005**, *7*, 1959.

## Chapter Seven

### Thesis Summary and Future Work

This thesis has investigated the chemistry of two different ligand sets on early transition metals. In chapter 2, the reactivity of a tantalum [NPN] dinitrogen complex with several transition metal hydrides was investigated. The addition of Schwartz's reagent,  $([\text{Cp}_2\text{Zr}(\text{Cl})\text{H}]_x)$ , led to the unanticipated reduction of the N-N unit without Zr-H addition. Examination of the product revealed the formation of a phosphinimide derivative with insertion of a "Cp<sub>2</sub>Zr" fragment into the N-N bond. A series of experiments determined that the origin of the "Cp<sub>2</sub>Zr" was from the reductive elimination of H<sub>2</sub> from  $[\text{Cp}_2\text{ZrH}_2]_2$ . An independent reaction with a "Cp<sub>2</sub>Zr" source verified that this species induced N-N bond cleavage. This type of dinitrogen reduction was extended to include the insertion of a "Cp<sub>2</sub>Ti" fragment into the N-N bond and represents a new approach in dinitrogen chemistry to cleave an N<sub>2</sub> ligand.

Early transition metal chemistry with a unique diamido-N-heterocyclic carbene ligand set was pursued in chapter 3. Ligands with an ethylene spacer between the N-heterocyclic ring and the amido donor were successfully synthesized. Aminolysis and alkyl elimination reactions with group 4 transition metal precursors afforded a successful way to synthesize group 4 [NCN] complexes. The central position of the NHC in this tridentate architecture renders the carbene stable to dissociation from the metal centre in strongly coordinating solvents.

The application and reactivity of group 4 [NCN] complexes was the focus of chapter 4. Fundamental processes such as olefin polymerization, migratory insertion, and dinitrogen activation were examined and revealed the NHC moiety remains coordinated to the metal centre and does not participate in a manner that would alter the NHC donor. Activation of a zirconium-dimethyl derivative with  $[\text{Ph}_3\text{C}][\text{B}(\text{C}_6\text{F}_5)_4]$  in the presence of ethylene yielded a moderately active polymerization catalyst. Migratory insertion of simple organic molecules, such as isocyanides, carbon monoxide and cumulenes, into the hafnium- $\text{sp}^3$ -carbon bond of several hafnium-alkyl derivatives yielded the expected insertion products. In some examples, further C-C bond coupling was observed to generate new enamidolate and enediolate metallacycles. Despite many attempts, no early transition metal dinitrogen complexes were recovered utilizing the [NCN] ligand set.

In chapter 5, the coordination of the [NCN] ligand set to tantalum(V) was examined in anticipation that a dinitrogen complex could be synthesized. While tantalum-amide and -halide complexes were isolated with an intact [NCN] architecture, reduction of these complexes in the presence of dinitrogen resulted in a complicated mixture of products. Attempts to synthesize tantalum alkyl complexes resulted in the isolation of compounds where the ligand has undergone C-H bond activation at one of the backbone positions. Density functional calculations and isotopic labeling studies examined the mechanism of this C-H bond activation process and suggested the intermediacy of an alkylidene species.

The research described in this thesis has provided insight into the use of two different ligand sets in different areas of early transition metal chemistry. Future research with [NPN] chemistry will be aimed at the addition of other reduced transition metal and main group complexes to **2.5**, in an attempt to extend the functionalization of coordinated nitrogen atoms with other elements. In light of the inability to obtain an ETM dinitrogen complex stabilized by a [NCN] ancillary ligand, other transition metals may assist in accomplishing this elusive goal. Further research utilizing the chiral tridentate [NCN] and bidentate [NC] ligands may also yield a highly active and selective ETM or LTM catalyst. In conclusion, the research presented herein has provided solid groundwork for future research in both [NPN] and [NCN] chemistry.

## **Appendix A**

### **X-ray Crystal Structure Data**

#### ***A.1. General Considerations***

In all cases, suitable crystals were selected and mounted on a glass fibre using Paratone-N oil and frozen to  $-100^{\circ}\text{C}$ . Measurements for structures **2.10**, **3.5**, **3.17**, **3.22**, **3.24**· $\text{C}_5\text{H}_5\text{N}$ , **3.30**, **4.22**, **5.1** and **5.2** were made on a Rigaku/ADSC CCD area detector with graphite monochromated Mo-K $\alpha$  radiation by either Dr. Brian O. Patrick or Dr. Christopher Carmichael. Data was processed using the d\*TREK<sup>1</sup> module, part of the CrystalClear software package, version 1.3.6 SP0,<sup>2</sup> and corrected for Lorentz and polarization effects and absorption. Neutral atom scattering factors for all non-hydrogen atoms were taken from Cromer and Waber.<sup>3</sup> Anomalous dispersion effects were included in  $F_{\text{calc}}$ .<sup>4</sup>

Measurements for structure **6.8** were made on a Bruker X8 area detector with graphite monochromated Mo-K $\alpha$  radiation by Howard Jong. Data was determined to be a two component twin using the Twinsolve module of the CrystalClear software package, version 1.3.6 SP0.<sup>2</sup> Measurements for structures **3.8**, **3.38**, **4.7**, **4.8**, **4.11**, **4.16**, **4.17**, **4.18**, **4.23**, **5.3**, **5.7**, and **5.10** were made on a Bruker X8 area detector with graphite monochromated Mo-K $\alpha$  radiation by either Brian O. Patrick or Howard Jong. Data was

processed and integrated using the Bruker SAINT software package<sup>5</sup> and corrected for absorption effects using the multi-scan technique (SADABS).<sup>6</sup> Neutral atom scattering factors for all non-hydrogen atoms were taken from Cromer and Waber.<sup>3</sup> Anomalous dispersion effects were included in  $F_{\text{calc}}$ ;<sup>4</sup> the values for  $\Delta f''$  and  $\Delta f'''$  were those of Creagh and McAuley.<sup>7</sup> The values for the mass attenuation coefficients are those of Creagh and Hubbell.<sup>8</sup>

All structures were solved by direct methods using the program SIR97.<sup>9</sup> All non-hydrogen atoms were refined anisotropically by least square procedures on  $F^2$  using SHELXL-97.<sup>10</sup> Hydrogen atoms were included but not refined; their positional parameters were calculated with fixed C-H bond distances of 0.99 Å for  $sp^2$  C, 0.98 Å for  $sp^3$  C, and 0.95 Å for aromatic  $sp$  C, with  $U_{\text{iso}}$  set to 1.2 times the  $U_{\text{eq}}$  of the attached  $sp$  or  $sp^2$  C and 1.5 times the  $U_{\text{eq}}$  values of the attached  $sp^3$  C atom. Methyl hydrogen torsion angles were determined by electron density. Structure solution and refinements were conducted using the WinGX software package, version 1.64.05.<sup>11</sup> Structural illustrations were created using ORTEP-III for Windows.<sup>12</sup>

**A.2. References**

- 1) Pflugrath, J. W. *Acta Cryst.* **1999**, D55, 1718.
- 2) CrystalClear: An Integrated Program for the Collection and Processing of Area Detector Data, Rigaku Corporation, 2002.
- 3) Cromer, D. T.; Waber, J. T. *International Tables for X-ray Crystallography*; Kynoch Press, 1974; Vol. IV.
- 4) Ibers, J. A.; Hamilton, W. C. *Acta Cryst.* **1964**, 17, 781.
- 5) *SAINTE Software User Guide*, Version 7.03A, Bruker Analytical X-ray Systems, Inc., Madison, WI, 1997.
- 6) Sheldrick, G. M. SADABS, Version 2.05, Bruker Analytical X-ray Systems, Inc., Madison, WI, 2003.
- 7) Creagh, D. C.; McAuley, W. J. In *International Tables for Crystallography*; Wilson, A. J. C., Ed.; Kluwer Academic Publishers; Boston, 1992; Vol. C, pp 219-222.
- 8) Creagh, D. C.; Hubbell, J. H. In *International Tables for Crystallography*; Wilson, A. J. C., Ed.; Kluwer Academic Publishers; Boston, 1992; Vol. C, pp 200-206.
- 9) Altomare, A.; Burla, M. C.; Cammali, G.; Cascarano, M.; Giacovazzo, C.; Guagliardi, A.; Moliterni, A. G. G.; Polidori, G.; Spagna, A. *J. Appl. Crystallogr.* **1999**, 32, 115.
- 10) Sheldrick, G. M. *SHELXL-97: Programs for Crystal Structure Analysis (Release 97-2)*, University of Gottingen, Gottingen, Germany, 1998.
- 11) Farrugia, L. J. *J. Appl. Crystallogr.* **1999**, 32, 837.
- 12) Farrugia, L. J. *J. Appl. Crystallogr.* **1997**, 30, 565.

## A.3. Tables of Crystallographic Data

**Table A.1.** Crystallographic and structure refinement for  $[\text{N}(\mu\text{-P}=\text{N})\text{N}]\text{Ta}(\mu\text{-H})_2(\mu\text{-N})(\text{Ta}[\text{NPN}])$  ( $\text{ZrCp}_2$ ) (2.10),  $^{\text{Mes}}(\text{NCHN})\text{H}_2\text{-Cl}$  (3.5), and  $^{\text{Mes}}(\text{NCN})\text{H}_2$  (3.8).

	$[\text{NP}(\text{N})\text{N}]\text{Ta}(\mu\text{-H})_2(\mu\text{-N})(\text{Ta}[\text{NPN}])$ ( $\text{ZrCp}_2$ ) (2.10)	$^{\text{Mes}}(\text{NCHN})\text{H}_2\text{-Cl}$ (3.5)	$^{\text{Mes}}(\text{NCN})\text{H}_2$ (3.8)
Formula	$\text{C}_{58}\text{H}_{74}\text{N}_6\text{P}_2\text{Si}_4$ $\text{Ta}_2\text{Zr}$	$\text{C}_{25}\text{H}_{35}\text{ClN}_4$	$\text{C}_{25}\text{H}_{34}\text{N}_4$
Formula weight	1482.65	427.02	390.56
Colour, Habit	Purple, plate	Colourless, plate	Colourless, prism
Crystal size, mm	0.4 x 0.2 x 0.1	0.25 x 0.15 x 0.05	0.40 x 0.40 x 0.20
Crystal system	Orthorhombic	Monoclinic	Orthorhombic
Space group	<i>Pccn</i>	<i>P2<sub>1</sub>/c</i>	<i>P22<sub>1</sub>2<sub>1</sub></i>
a, Å	13.4310(10)	7.5827(13)	8.8133(2) A
b, Å	38.984(3)	25.577(4)	9.2024(2)
c, Å	28.4871(19)	12.453(2)	14.0787(3)
α, deg	90	90	90
β, deg	90	91.802(10)	90
γ, deg	90	90	90
V, Å <sup>3</sup>	14915.6(18)	2414.0(7)	1141.83(4)
Z	8	4	2
ρ <sub>calc</sub> , g cm <sup>-3</sup>	1.320	1.175	1.136
F <sub>000</sub>	5888	920	424
μ, (MoKα), cm <sup>-1</sup>	3.205	0.177	0.068
transmission factors	0.7238-1.0000	0.7870-1.0000	0.8403-1.0000
2θ <sub>max</sub> , deg	55.76	54.98	55.72
total no. of reflns	93218	19828	13829
no. of unique reflns	17760	9450	4303
R <sub>int</sub>	0.563	0.0820	0.0306
no. of variables	666	289	139
R <sub>1</sub> (F <sup>2</sup> , I > 2σ(I))	0.0766	0.0510	0.0370
R <sub>w</sub> (F <sup>2</sup> , all data)	0.0889	0.1056	0.0463
Gof	1.221	0.979	0.969

$$R_1 = \sum ||F_o| - |F_c|| / \sum |F_o|; R_w = (\sum w(|F_o|^2 - |F_c|^2)^2 / \sum w|F_o|^2)^{1/2}$$

**Table A.2.** Crystallographic and structure refinement for  $^{tol}[\text{NCN}]\text{Zr}(\text{NEt}_2)_2$  (**3.17**),  $^{Mes}[\text{NCNH}]\text{Ti}(\text{NMe}_2)_3$  (**3.22**), and  $^{tol}[\text{NCN}]\text{ZrCl}_2(\text{py})$  (**3.30**).

	$^{tol}[\text{NCN}]\text{Zr}(\text{NEt}_2)_2$ ( <b>3.17</b> )	$^{Mes}[\text{NCNH}]\text{Ti}(\text{NMe}_2)_3$ ( <b>3.22</b> )	$^{tol}[\text{NCN}]\text{ZrCl}_2(\text{py})$ ( <b>3.30</b> )
Formula	$\text{C}_{29}\text{H}_{44}\text{N}_6\text{Zr}$	$\text{C}_{31}\text{H}_{51}\text{N}_7\text{Ti}$	$\text{C}_{29}\text{H}_{29}\text{Cl}_2\text{N}_5\text{Zr}$
Formula weight	567.92	569.69	609.69
Colour, Habit	Colourless, platelet	Red, prism	Red, prism
Crystal size, mm	0.40 x 0.20 x 0.05	0.40 x 0.40 x 0.20	0.05 x 0.04 x 0.03
Crystal system	Monoclinic	Monoclinic	Monoclinic
Space group	$P2_1/n$	$P2_1/c$	$P2_1/n$
a, Å	9.8762(14)	13.1845(12)	8.2213(8)
b, Å	12.3743(19)	18.7121(17)	31.764(3)
c, Å	24.325(4)	13.2384(11)	10.8884(11)
$\alpha$ , deg	90	90	90
$\beta$ , deg	93.812(9)	98.130(4)	91.757(3)
$\gamma$ , deg	90	90	90
V, Å <sup>3</sup>	2963(37)	3233.2(5)	2842.0(5)
Z	4	4	4
$\rho_{\text{calc}}$ , g cm <sup>-3</sup>	1.273	1.170	1.425
F <sub>000</sub>	1200	1232	1248
$\mu$ , (MoK $\alpha$ ), cm <sup>-1</sup>	0.398	0.295	0.602
transmission factors	0.8765-1.0000	0.8516-1.0000	0.8419-1.0000
2 $\theta_{\text{max}}$ , deg	55.00	55.12	55.76
total no. of reflns	24721	26981	25486
no. of unique reflns	6345	9771	6283
R <sub>int</sub>	0.0871	0.0826	0.0793
no. of variables	151	368	336
R <sub>1</sub> (F <sup>2</sup> , I > 2 $\sigma$ (I))	0.0743	0.0384	0.0751
R <sub>w</sub> (F <sup>2</sup> , all data)	0.1168	0.0584	0.1036
Gof	1.034	0.958	1.088

$$R_1 = \sum ||F_o| - |F_c|| / \sum |F_o|; R_w = (\sum w(|F_o|^2 - |F_c|^2)^2 / \sum w|F_o|^2)^{1/2}$$

**Table A.3.** Crystallographic and structure refinement for  $^{tol}[\text{NCN}]\text{Zr}(\text{CH}_2\text{SiMe}_3)_2$  (**3.30**),  $^{Mes}[\text{NCN}]\text{Hf}^t\text{Bu}_2$  (**3.38**), and  $^{Mes}[\text{NCN}]\text{Hf}(\eta^2\text{-XyNCCH}_3)(\text{CH}_3)$  (**4.7**).

	$^{tol}[\text{NCN}]\text{Zr}(\text{CH}_2\text{SiMe}_3)_2$ ( <b>3.30</b> )	$^{Mes}[\text{NCN}]\text{Hf}^t\text{Bu}_2$ ( <b>3.38</b> )	$^{Mes}[\text{NCN}]\text{Hf}(\eta^2\text{-XyNCCH}_3)(\text{CH}_3)$ ( <b>4.7</b> )
Formula	$\text{C}_{29}\text{H}_{46}\text{N}_4\text{Si}_2\text{Zr}$	$\text{C}_{33}\text{H}_{50}\text{HfN}_4\text{-}1/2\text{C}_4\text{H}_8\text{O}$	$\text{C}_{36}\text{H}_{47}\text{HfN}_5\text{-C}_4\text{H}_8\text{O}$
Formula weight	598.10	726.33	800.39
Colour, Habit	Yellow, block	colourless, plate	colourless, plate
Crystal size, mm	$0.25 \times 0.25 \times 0.2$	$0.15 \times 0.15 \times 0.15$	$0.40 \times 0.30 \times 0.10$
Crystal system	Monoclinic	Monoclinic	Monoclinic
Space group	$P2_1/c$	$C2/c$	$C2/c$
a, Å	13.105(3)	19.9312(3)	32.883(5)
b, Å	12.676(3)	13.7149(3)	11.614(5)
c, Å	19.448(4)	28.0013(6)	23.793(5)
$\alpha$ , deg	90	90	90
$\beta$ , deg	99.398(2)	113.0590(10)	112.217(5)
$\gamma$ , deg	90	90	90
V, Å <sup>3</sup>	3198.6(6)	7042.7(2)	8412(4)
Z	4	4	4
$\rho_{\text{calc}}$ , g cm <sup>-3</sup>	1.242	1.355	1.378
F <sub>000</sub>	1264	2952	3600
$\mu$ , (MoK $\alpha$ ), cm <sup>-1</sup>	0.442	2.991	2.521
transmission factors	0.7550-1.0000	0.8448-1.0000	0.7118-1.0000
2 $\theta_{\text{max}}$ , deg	53.24	56.30	55.24
total no. of reflns	27267	97131	115842
no. of unique reflns	7173	8473	9958
R <sub>int</sub>	0.0374	0.0396	0.0388
no. of variables	333	377	479
R <sub>1</sub> (F <sup>2</sup> , I > 2 $\sigma$ (I))	0.0301	0.0217	0.0285
R <sub>w</sub> (F <sup>2</sup> , all data)	0.0629	0.0576	0.0454
Gof	0.821	1.066	1.021
$R_1 = \sum   F_o  -  F_c   / \sum  F_o $ ; $R_w = (\sum w( F_o ^2 -  F_c ^2)^2 / \sum w F_o ^2)^{1/2}$			

**Table A.4.** Crystallographic and structure refinement for  $^{\text{Mes}}[\text{NCN}]\text{Hf}(\eta^2\text{-XyNCCH}_3)_2$  (**4.8**),  $^{\text{Mes}}[\text{NCN}]\text{Hf}(\text{OC}(\text{CH}_3)=\text{C}(\text{CH}_3)\text{NXy})$  (**4.11**), and  $^{\text{Mes}}[\text{NCN}]\text{Hf}_2(\mu\text{-OC}(\text{tBu})=\text{C}(\text{tBu})\text{O})_2$  (**4.16**).

	$^{\text{Mes}}[\text{NCN}]\text{Hf}(\eta^2\text{-XyNCCH}_3)_2$ ( <b>4.8</b> )	$^{\text{Mes}}[\text{NCN}]\text{Hf}(\text{OC}(\text{CH}_3)=\text{C}(\text{CH}_3)\text{NXy})$ ( <b>4.11</b> )	$^{\text{Mes}}[\text{NCN}]\text{Hf}_2(\mu\text{-OC}(\text{tBu})=\text{C}(\text{tBu})\text{O})_2$ ( <b>4.16</b> )
Formula	$\text{C}_{90}\text{H}_{112}\text{Hf}_2\text{N}_{12}\text{-CH}_2\text{Cl}_2$	$\text{C}_{37}\text{H}_{47}\text{HfN}_5\text{O-C}_2\text{H}_5\text{O}$	$\text{C}_{70}\text{H}_{100}\text{Hf}_2\text{N}_8\text{O}_4\text{-4C}_6\text{H}_6$
Formula weight	1803.82	801.35	1786.99
Colour, Habit	Colourless, irregular	Yellow, irregular	Colourless, tablet
Crystal size, mm	0.20 x 0.07 x 0.04	0.10 x 0.05 x 0.03	0.15 x 0.07 x 0.04
Crystal system	Triclinic	Monoclinic	Triclinic
Space group	<i>P</i> -1	<i>P</i> 2 <sub>1</sub> / <i>c</i>	<i>P</i> -1
a, Å	15.6616(8)	10.9435(6)	12.377(5)
b, Å	16.3972(7)	20.0210(11)	18.530(5)
c, Å	21.5514(10)	17.3179(8)	21.408(5)
α, deg	70.757(2)	90	107.656(5)
β, deg	73.887(2)	92.451(2)	103.930(5)
γ, deg	68.167(2)	90	100.104(5)
V, Å <sup>3</sup>	4774.1(4)	3790.9(3)	4374(2)
Z	2	4	2
ρ <sub>calc</sub> , g cm <sup>-3</sup>	1.255	1.404	1.357
F <sub>000</sub>	1844	1636	1840
μ, (MoKα), cm <sup>-1</sup>	2.275	2.790	2.425
transmission factors	0.8093-1.0000	0.7300-1.0000	0.6694-1.0000
2θ <sub>max</sub> , deg	48.10	41.20	46.92
total no. of reflns	108780	25826	44117
no. of unique reflns	19273	6703	11428
R <sub>int</sub>	0.0649	0.1030	0.1051
no. of variables	988	420	993
R <sub>1</sub> (F <sup>2</sup> , I > 2σ(I))	0.0656	0.0479	0.0473
R <sub>w</sub> (F <sup>2</sup> , all data)	0.0963	0.1058	0.1106
Gof	1.281	0.999	0.982

$$R_1 = \sum ||F_o| - |F_c|| / \sum |F_o|; R_w = (\sum w(|F_o|^2 - |F_c|^2)^2 / \sum w|F_o|^2)^{1/2}$$

**Table A.5.** Crystallographic and structure refinement for  $\text{Mes}[\text{NCN}]\text{Hf}(\text{Me})(\eta^3\text{-}^t\text{BuNC}(\text{Me})\text{O})$  (**4.17**),  $\text{Mes}[\text{NCN}]\text{Hf}(\text{Me})(\eta^3\text{-}^i\text{PrNC}(\text{Me})\text{N}^i\text{Pr})$  (**4.18**), and  $\text{Mes}[\text{NCN}]\text{Zr}(\text{Cl})(\text{OBu})$  (**4.22**).

	$\text{Mes}[\text{NCN}]\text{Hf}(\text{Me})(\eta^3\text{-}^t\text{BuNC}(\text{Me})\text{O})$ ( <b>4.17</b> )	$\text{Mes}[\text{NCN}]\text{Hf}(\text{Me})(\eta^3\text{-}^i\text{PrNC}(\text{Me})\text{N}^i\text{Pr})$ ( <b>4.18</b> )	$\text{Mes}[\text{NCN}]\text{Zr}(\text{Cl})(\text{OBu})$ ( <b>4.22</b> )
Formula	$\text{C}_{32}\text{H}_{47}\text{HfN}_5\text{O}$	$\text{C}_{34}\text{H}_{52}\text{HfN}_6$	$\text{C}_{29}\text{H}_{41}\text{Cl N}_4\text{OZr}$
Formula weight	696.24	723.31	588.33
Colour, Habit	Colourless, prism	Colourless, plate	Yellow, irregular
Crystal size, mm	0.3 x 0.2 x 0.15	0.35 x 0.25 x 0.1	0.4 x 0.4 x 0.35
Crystal system	Orthorhombic	Triclinic	Triclinic
Space group	<i>Pbca</i>	<i>P</i> -1	<i>P</i> -1
a, Å	10.1327(2)	10.4245(2)	10.367(5)
b, Å	21.6299(4)	19.3938(4)	10.894(5)
c, Å	28.8509(6)	19.9828(4)	13.550(5)
$\alpha$ , deg	90	113.8580(10)	80.965(5)
$\beta$ , deg	90	104.8770(10)	81.615(5)
$\gamma$ , deg	90	96.0180(10)	80.095(5)
V, Å <sup>3</sup>	6323.2(2)	3469.92(12)	1477.7(11)
Z	8	4	2
$\rho_{\text{calc}}$ , g cm <sup>-3</sup>	1.463	1.385	1.322
F <sub>000</sub>	2832	1480	616
$\mu$ , (MoK $\alpha$ ), cm <sup>-1</sup>	3.331	3.037	0.490
transmission factors	0.7831-1.0000	0.6466-1.0000	0.7971-1.0000
2 $\theta_{\text{max}}$ , deg	55.68	55.88	55.74
total no. of reflns	58871	94064	13213
no. of unique reflns	7501	16394	6026
R <sub>int</sub>	0.0448	0.0378	0.0331
no. of variables	363	763	332
R <sub>1</sub> (F <sup>2</sup> , I > 2 $\sigma$ (I))	0.0227	0.0237	0.0488
R <sub>w</sub> (F <sup>2</sup> , all data)	0.0379	0.0407	0.0561
Gof	1.028	1.028	1.090

$$R_1 = \sum ||F_o| - |F_c|| / \sum |F_o|; R_w = (\sum w(|F_o|^2 - |F_c|^2)^2 / \sum w|F_o|^2)^{1/2}$$

**Table A.6.** Crystallographic and structure refinement for  $^{\text{Mes}}[\text{NCN}]\text{Hf}(\text{Me})(\eta^2\text{-NNMe}_2)$  (**4.23**),  $^{\text{tol}}[\text{NCNH}]\text{Ta}(\text{NMe}_2)_4$  (**5.1**), and  $^{\text{Mes}}[\text{NCNH}]\text{Ta}(\text{CHPh})(\text{CH}_2\text{Ph})_2$  (**5.2**).

	$^{\text{Mes}}[\text{NCN}]\text{Hf}(\text{Me})(\eta^2\text{-NNMe}_2)$ ( <b>4.23</b> )	$^{\text{tol}}[\text{NCNH}]\text{Ta}(\text{NMe}_2)_4$ ( <b>5.1</b> )	$^{\text{Mes}}[\text{NCNH}]\text{Ta}(\text{CHPh})(\text{CH}_2\text{Ph})_2$ ( <b>5.2</b> )
Formula	$\text{C}_{28}\text{H}_{42}\text{HfN}_6$	$\text{C}_{36}\text{H}_{57}\text{N}_8\text{Ta}$	$\text{C}_{46}\text{H}_{50}\text{N}_4\text{Ta}$ ,
Formula weight	641.17	782.85	839.85
Colour, Habit	Colourless, prism	Yellow, fiber	Orange, prism
Crystal size, mm	0.25 x 0.2 x 0.05	0.4 x 0.25 x 0.15	0.2 x 0.1 x 0.05
Crystal system	Monoclinic	Monoclinic	Monoclinic
Space group	$P2_1/m$	$P2_1/c$	$P2_1/c$
a, Å	8.1361(4)	12.669(5)	11.0925(10)
b, Å	22.1536(10)	11.681(5)	27.769(3)
c, Å	8.5276(4)	25.201(5)	13.3194(14)
$\alpha$ , deg	90	90	90
$\beta$ , deg	113.3560(10)	87.021(5)	96.253(4)
$\gamma$ , deg	90	90	90
V, Å <sup>3</sup>	1411.10(12)	3724(2)	4078.3(7)
Z	2	4	4
$\rho_{\text{calc}}$ , g cm <sup>-3</sup>	1.509	1.396	1.368
F <sub>000</sub>	648	1608	1708
$\mu$ , (MoK $\alpha$ ), cm <sup>-1</sup>	3.723	2.986	2.730
transmission factors	0.7458-1.0000	0.6390-1.0000	0.8017-1.0000
2 $\theta_{\text{max}}$ , deg	55.82	55.00	55.66
total no. of reflns	19552	13436	105524
no. of unique reflns	3452	7557	9567
R <sub>int</sub>	0.0400	0.0245	0.0619
no. of variables	174	421	474
R <sub>1</sub> (F <sup>2</sup> , I > 2 $\sigma$ (I))	0.0257	0.0294	0.0255
R <sub>w</sub> (F <sup>2</sup> , all data)	0.0312	0.0438	0.0463
Gof	1.087	1.044	1.011

$$R_1 = \sum ||F_o| - |F_c|| / \sum |F_o|; R_w = (\sum w(|F_o|^2 - |F_c|^2)^2 / \sum w|F_o|^2)^{1/2}$$

**Table A.7.** Crystallographic and structure refinement for  $^{tol}[\text{NCN}]\text{Ta}(\text{NMe}_2)_3$  (**5.3**),  $^{Mes}[\text{NCCN}]\text{Ta}(\text{CH}_2^t\text{Bu})_2$  (**5.7**), and  $^{Mes}[\text{NCCN}]\text{Ta}(\text{Cl})(\text{CH}_2^t\text{Bu})$  (**5.10**).

	$^{tol}[\text{NCN}]\text{Ta}(\text{NMe}_2)_3$ ( <b>5.3</b> )	$^{Mes}[\text{NCCN}]\text{Ta}(\text{CH}_2^t\text{Bu})_2$ ( <b>5.7</b> )	$^{Mes}[\text{NCCN}]\text{Ta}(\text{Cl})(\text{CH}_2^t\text{Bu})$ ( <b>5.10</b> )
Formula	$\text{C}_{31}\text{H}_{42}\text{N}_7\text{Ta}$	$\text{C}_{35}\text{H}_{53}\text{N}_4\text{Ta}$	$\text{C}_{30}\text{H}_{42}\text{ClN}_4$
Formula weight	693.67	710.76	675.08
Colour, Habit	Orange, irregular	Yellow, irregular	Yellow, irregular
Crystal size, mm	0.25 x 0.18 x 0.12	0.35 x 0.2 x 0.1	0.12 x 0.05 x 0.05
Crystal system	Monoclinic	Monoclinic	Triclinic
Space group	$C2/c$	$P2_1/n$	$P-1$
a, Å	15.668(5)	9.67930(10)	9.3783(8)
b, Å	11.495(5)	22.4522(3)	11.5711(10)
c, Å	19.926(5)	16.0990(2)	14.6775(11)
$\alpha$ , deg	90	90	109.568(3)
$\beta$ , deg	102.002(5)	104.6490(10)	90.206(3)
$\gamma$ , deg	90	90	94.935(3)
V, Å <sup>3</sup>	3510(2)	3384.93(7)	1494.3(2)
Z	4	4	2
$\rho_{\text{calc}}$ , g cm <sup>-3</sup>	1.313	1.395	1.500
F <sub>000</sub>	1400	680	1456
$\mu$ , (MoK $\alpha$ ), cm <sup>-1</sup>	3.159	3.275	3.791
transmission factors	0.8542-1.000	0.7666-1.0000	0.8698-1.0000
2 $\theta_{\text{max}}$ , deg	55.46	55.92	55.84
total no. of rflns	39215	31089	49582
no. of unique rflns	4086	7008	8005
R <sub>int</sub>	0.0315	0.0678	0.0316
no. of variables	182	334	373
R <sub>1</sub> (F <sup>2</sup> , I > 2 $\sigma$ (I))	0.0285	0.0357	0.0181
R <sub>w</sub> (F <sup>2</sup> , all data)	0.0307	0.0518	0.0271
Gof	1.122	1.056	1.072

$$R_1 = \sum ||F_o| - |F_c|| / \sum |F_o|; R_w = (\sum w(|F_o|^2 - |F_c|^2)^2 / \sum w|F_o|^2)^{1/2}$$

**Table A.8.** Crystallographic and structure refinement for (-)-(1*R*,2'*S*,4*R*)-2-(1,7,7-trimethylbicyclo[2.2.1]hept-2-ylamino)ethyl ammonium chloride (**6.8**).

	(-)-(1 <i>R</i> ,2' <i>S</i> ,4 <i>R</i> )-2-(1,7,7-trimethylbicyclo[2.2.1]hept-2-ylamino)ethyl ammonium chloride ( <b>6.8</b> )
Formula	C <sub>12</sub> H <sub>24</sub> Cl <sub>2</sub> N
Formula weight	253.22
Colour, Habit	Colourless, prism
Crystal size, mm	0.40 x 0.20 x 0.10
Crystal system	Triclinic
Space group	P1
a, Å	10.661(2)
b, Å	10.659(2)
c, Å	14.141(3)
α, deg	108.308(7)
β, deg	114.205(7)
γ, deg	92.053(8)
V, Å <sup>3</sup>	1366.0(8)
Z	4
ρ <sub>calc</sub> , g cm <sup>-3</sup>	1.231
F <sub>000</sub>	548
μ, (MoKα), cm <sup>-1</sup>	0.448
transmission factors	0.5679-1.0000
2θ <sub>max</sub> , deg	51.50
total no. of reflns	34817
no. of unique reflns	18462
R <sub>int</sub>	0.0802
no. of variables	559
R <sub>1</sub> (F <sup>2</sup> , I > 2σ(I))	0.1523
R <sub>w</sub> (F <sup>2</sup> , all data)	0.1873
Gof	1.659
$R_1 = \sum   F_o  -  F_c   / \sum  F_o $ ; $R_w = (\sum w( F_o ^2 -  F_c ^2)^2 / \sum w F_o ^2)^{1/2}$	

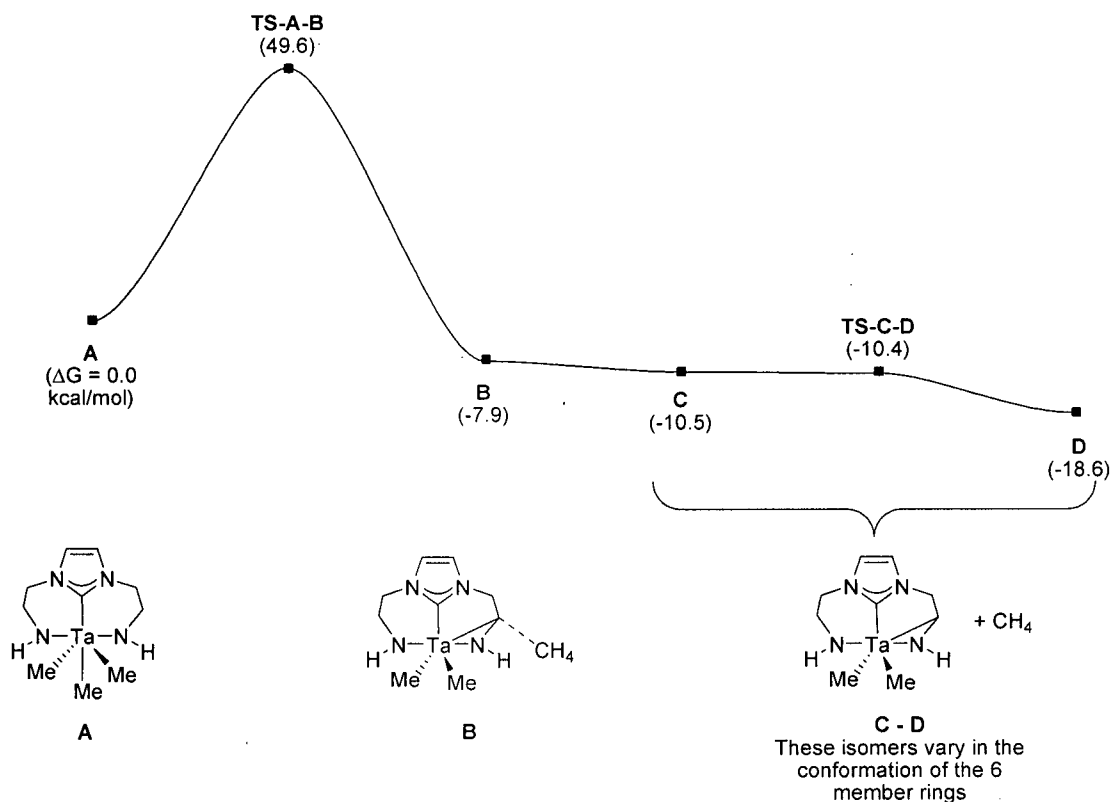
## **Appendix B**

### **Evaluating the Formation of a Tantalum Metallaaziridine Complex by Density Functional Calculations**

#### ***B.1. Evaluation of a $\sigma$ -Bond Metathesis Mechanism***

In the calculated  $\sigma$ -bond metathesis pathway (Figure B.1), the lowest energy trimethyl complex (**A**, 0.0 kcal/mol, Table B.1) is converted to a methane adduct of the ligand activated metallaziridine dimethyl complex, (**B**, -7.9 kcal/mol), via the  $\sigma$ -bond metathesis transition state (**TS-A-B**, 49.6 kcal/mol). The calculated structures of **A**, **TS-A-B**, and **B** are provided in Figure B.2. In the transition state **TS-A-B**, the breaking Ta-C bond distance is 2.96 Å, while the forming and breaking C-H bond distances are 1.36 and 1.47 Å, respectively. The Ta-H distance in **TS-A-B** is 2.79 Å, which indicates that there is very little interaction between the migrating hydrogen and the tantalum centre in this transition state. Separating methane from the methane adduct complex **B** generates the metallaaziridine complex **C** and free methane (-10.5 kcal/mol). The metallaaziridine complex **C** is able to change conformations to the most stable metallaaziridine complex **D** via the low barrier isomerization transition state (**TS-C-D**, -10.4 kcal/mol). Overall the reaction is exergonic, with the free energy of the metallaziridine **D** and CH<sub>4</sub> products being 18.6 kcal/mol lower in energy than the starting trimethyl complex **A**. However, the

high energy point on this pathway, the transition state **TS-A-B**, is 49.6 kcal/mol higher in energy than the starting trimethyl complex **A**, which is too large of an energy difference between the starting complex and the transition state for this transformation to readily occur without heating the solution, which indicates that this pathway may not be operating under the experimental conditions employed in this study.



<sup>a</sup> Gas-phase relative free energies at the B3LYP/BS1 level of theory based on the energy of separated **1** set to 0.0 kcal/mol are provided in parentheses in kcal/mol. Electronic energies, corrected zero-point energies, enthalpies, and free energies are provided in Table B.1.

**Figure B.1.** Relative energies of the intermediates and transition states in a potential  $\sigma$ -bond metathesis mechanism.

**Table B.1.** Gas-phase relative energies (kcal/mol) of the intermediates and transition states in a  $\sigma$ -bond metathesis mechanism.

Structure	$\Delta E_e^{(a)}$	$\Delta E_0^{(b)}$	$\Delta H^{(c)}$	$\Delta G^{(d)}$
<b>A</b>	0.00	0.0	0.0	0.0
<b>TS-A-B</b>	55.33	49.7	49.9	49.6
<b>B</b>	1.99	-1.3	0.6	-7.9
<b>C + CH<sub>4</sub></b>	2.36	-1.1	-0.2	-10.5
<b>TS-C-D + CH<sub>4</sub></b>	2.89	-1.0	-0.4	-10.4
<b>D + CH<sub>4</sub></b>	-5.85	-9.3	-8.4	-18.6

(a) based on the gas-phase relative electronic energy of **A** set to 0.00 kcal/mol

(b) based on the gas-phase relative zero point corrected energy of **A** set to 0.0 kcal/mol

(c) based on the gas-phase relative enthalpy of **A** set to 0.0 kcal/mol

(d) based on the gas-phase relative free energy of **A** set to 0.0 kcal/mol

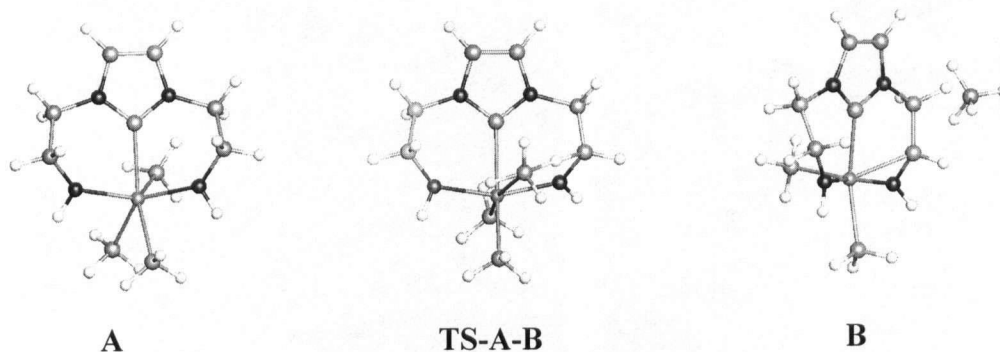
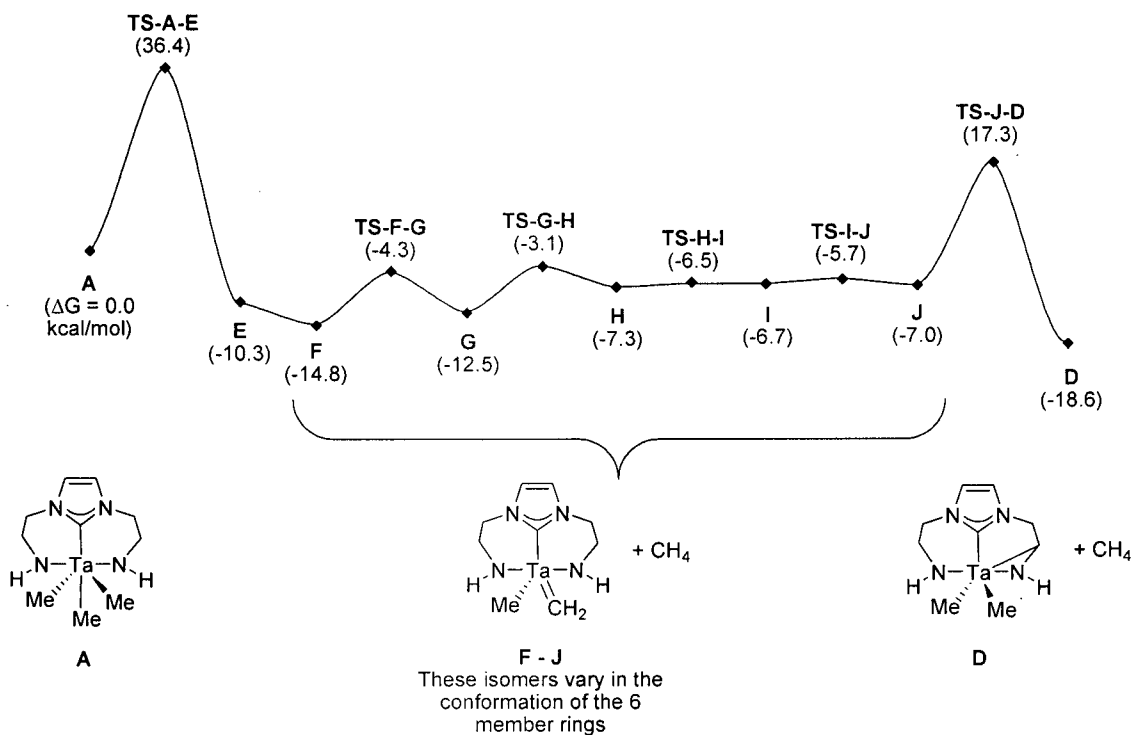


**Figure B.2.** JIMP<sup>1</sup> Pictures of the one-step  $\sigma$ -bond metathesis pathway.

### B.2. Investigation of an Alkylidene Intermediate Followed by C-H Bond Activation

In the calculated two-step pathway for metallaaziridine formation (Figure B.3), in which  $\alpha$ -H abstraction is followed by alkylidene mediated C-H activation, the starting trimethyl complex (**A**, 0.0 kcal/mol, Table B.2) is initially converted to the methane-adduct methylidene-methyl complex (**E**, -10.3 kcal/mol) via the  $\alpha$ -H abstraction transition state (**TS-A-E**, 36.4 kcal/mol) (Figure B.4). Separating methane from the adduct-complex yields the methylidene-methyl complex and free methane (**F** + CH<sub>4</sub>, -14.8 kcal/mol). The  $\alpha$ -H abstraction sequence (**A**  $\rightarrow$  **TS-A-E**  $\rightarrow$  **E**  $\rightarrow$  **F** + CH<sub>4</sub>) is exergonic by -14.8 kcal/mol, thus indicating that this step is an energetically favorable process. The  $\alpha$ -H abstraction transition state (**TS-A-E**) is 36.4 kcal/mol higher in energy

than the starting trimethyl complex **A**, which shows  $\alpha$ -H abstraction is energetically favored over  $\sigma$ -bond metathesis for the trimethyl complex **A** by 13.5 kcal/mol.



<sup>a</sup> Gas-phase relative free energies at the B3LYP/BS1 level of theory based on the energy of separated **1** set to 0.0 kcal/mol are provided in parentheses in kcal/mol. Electronic energies, corrected zero-point energies, enthalpies, and free energies are provided in Table 1.

**Figure B.3.** Relative energies of the intermediates and transition states in a potential two-step  $\alpha$ -H abstraction/alkylidene mediated C-H activation mechanism.

**Table B.2.** Gas-phase relative energies (kcal/mol) of the intermediates and transition states in a mechanism involving  $\alpha$ -H abstraction followed by alkylidene mediated C-H bond activation.

Structure	$\Delta E_e^{(a)}$	$\Delta E_0^{(b)}$	$\Delta H^{o(c)}$	$\Delta G^{o(d)}$
<b>A</b>	0.00	0.0	0.0	0.0
<b>TS-A-E</b> + CH <sub>4</sub>	38.30	36.0	35.6	36.4
<b>E</b> + CH <sub>4</sub>	-1.90	-4.7	-2.8	-10.3
<b>F</b> + CH <sub>4</sub>	-1.56	-4.8	-3.6	-14.8
<b>TS-F-G</b> + CH <sub>4</sub>	8.09	4.8	5.4	-4.3
<b>G</b> + CH <sub>4</sub>	-0.01	-3.0	-2.1	-12.5
<b>TS-G-H</b> + CH <sub>4</sub>	9.69	6.3	7.0	-3.1
<b>H</b> + CH <sub>4</sub>	5.67	2.7	3.7	-7.3
<b>TS-H-I</b> + CH <sub>4</sub>	6.35	2.9	3.6	-6.5
<b>I</b> + CH <sub>4</sub>	6.20	3.0	4.0	-6.7
<b>TS-I-J</b> + CH <sub>4</sub>	7.65	3.7	4.6	-5.7
<b>J</b> + CH <sub>4</sub>	7.63	3.8	5.2	-7.0
<b>TS-J-D</b> + CH <sub>4</sub>	31.43	25.8	26.2	17.3
<b>D</b> + CH <sub>4</sub>	-5.85	-9.3	-8.4	-18.6

(a) based on the gas-phase relative electronic energy of **A** set to 0.00 kcal/mol

(b) based on the gas-phase relative zero point corrected energy of **A** set to 0.0 kcal/mol

(c) based on the gas-phase relative enthalpy of **A** set to 0.0 kcal/mol

(d) based on the gas-phase relative free energy of **A** set to 0.0 kcal/mol

A series of low energy rearrangements (**F**  $\rightarrow$  **TS-F-G**  $\rightarrow$  **G**  $\rightarrow$  **TS-G-H**  $\rightarrow$  **H**  $\rightarrow$  **TS-H-I**  $\rightarrow$  **I**  $\rightarrow$  **TS-I-J**  $\rightarrow$  **J**) positions the CH<sub>2</sub>CH<sub>2</sub> carbene-amido linker in the proper position for alkylidene mediated C-H activation of the ligand backbone. In the ligand C-H bond activation process, the methylidene unit of the rearranged methylidene-methyl complex (**J**, -7.0 kcal/mol, Figures B.3 and B.4) abstracts a proton from the ligand backbone via the alkylidene mediated C-H activation transition state (**TS-J-D**, 17.3 kcal/mol) to yield the ligand activated metallaziridine product **D** (Figures B.3 and B.4). Overall, the final products **D** and CH<sub>4</sub> are lower in energy than all of the methylidene-methyl complexes (**F-J**), thus indicating that the metallaaziridine complex and CH<sub>4</sub> are the favored products for methane elimination from the trimethyl complex **A** in agreement with the experimental observations. In addition, the energy difference between the lowest energy methylidene-methyl complex (**F**) and the alkylidene mediated C-H activation transition state (**TS-H-D**) is 32.1 kcal/mol, which indicates that the alkylidene mediated C-H bond activation occurs more readily than the initial  $\alpha$ -H abstraction step. It should also be noted that the barrier for the reaction to proceed in the reverse direction

from lowest energy methylidene-methyl complex (**F**), for example the energy difference between **F** and  $\text{CH}_4$  and the  $\alpha$ -H abstraction transition state (**TS-A-E**), is 51.2 kcal/mol, which implies that endocyclic C-H activation of the ligand backbone is highly favored over C-H activation of alkanes in solution.

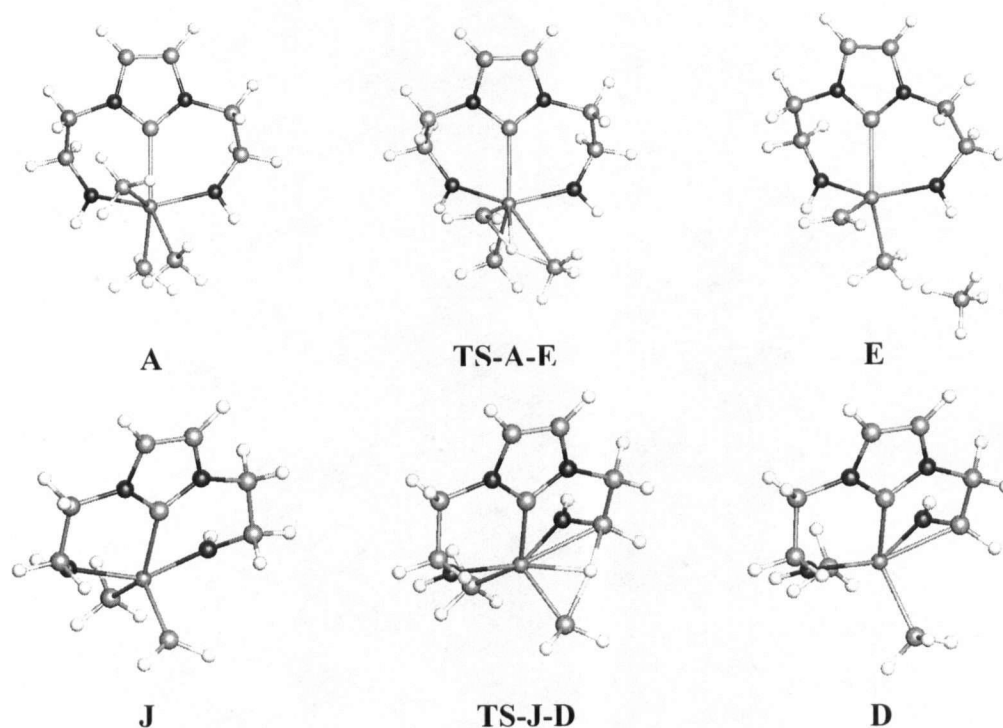


**Figure B.4.** JIMP<sup>1</sup> Pictures of  $\alpha$ -H abstraction by a methyl group to generate a  $[\text{NCCN}]\text{Ta}(=\text{CHR}')\text{R}$  alkylidene intermediate.

### B.3. Thermodynamic Considerations for the Formation of Metallated Ta $[\text{NCCN}]$ Derivatives

In addition to studying the mechanism of the ligand activation, part of the motivation for the DFT investigation was to address the question, why are the ligand activated metallazaaziridine products formed instead of the trialkyl derivatives? For our model complexes, the metallazaaziridine product **D** and separated  $\text{CH}_4$  are favored relative to the trimethyl complex **A** both in terms of both enthalpy and entropy (Table B.1). Although we expected that formation of two molecules (**D** +  $\text{CH}_4$ ) instead of one molecule (**A**) would be entropically favored, it was not obvious why the metallazaaziridine

product **D** and CH<sub>4</sub> were enthalpically favored over the trimethyl complex **A**, especially because **D** contains a three-membered ring, which is a potential source of ring strain.

An examination of the bond lengths and angles in the trimethyl complex **A** (Figure B.5) and the metallaaziridine product **D** (Figure B.6) revealed several features that contribute to **D** and CH<sub>4</sub> being enthalpically favored relative to **A**: (1) The Ta-carbene bond is much shorter in **D** (2.248 Å) than in **A** (2.381 Å), indicative of a much stronger bond; (2) The Ta-CH<sub>3</sub> bonds in **D** (2.173 and 2.219 Å) are shorter than the Ta-CH<sub>3</sub> bonds in **A** (2.238, 2.248, and 2.252 Å); and (3) The Ta-N bonds in **D** (1.982 and 2.065 Å) are, on average, shorter than the Ta-N bonds in **A** (2.020 and 2.053 Å). Furthermore, the ring strain due to the metallaaziridine fragment in complex **D** is reduced relative to the strain in organic three-membered rings because **D** can be viewed as a six-coordinate *d*<sup>0</sup> Ta complex in which Ta-L σ-bonding occurs through ligand orbital interactions with Ta *sd*<sup>5</sup> hybrids. In six coordinate, *d*<sup>0</sup> early transition metal complexes such as WH<sub>6</sub>, formation of localized, electron pair bonds draws from all *s* and *d* orbitals to form six *sd*<sup>5</sup> hybrids, which have energy minimas at angles of 63° and 117°.<sup>2,3</sup> The calculated C4-Ta1-N2 angle in the metallaaziridine ring of **D** is 38.2°, which represents less than a 25° distortion from the smaller angle energy minima.

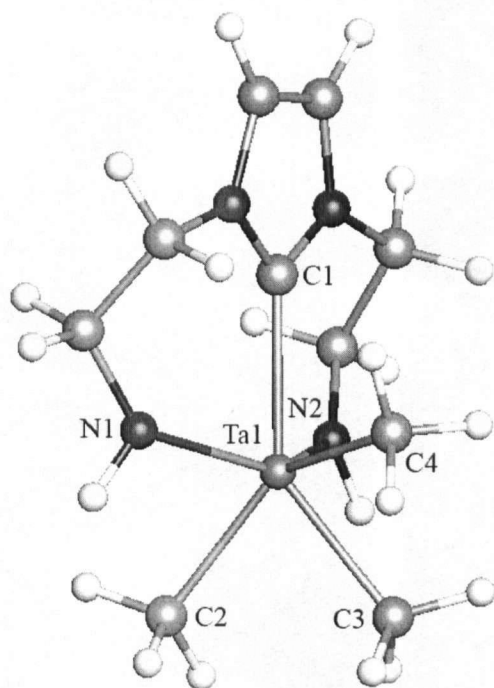


**Figure B.5.** JIMP<sup>1</sup> view of A. Selected bond distances (Å) and angles (deg): Ta1-C1 2.381, Ta1-C2 2.252, Ta1-C3 2.248, Ta1-C4 2.238, Ta1-N1 2.053, Ta1-N2 2.020, C1-Ta1-C2 139.6, C1-Ta1-C3 142.0, C2-Ta1-C3 76.4.

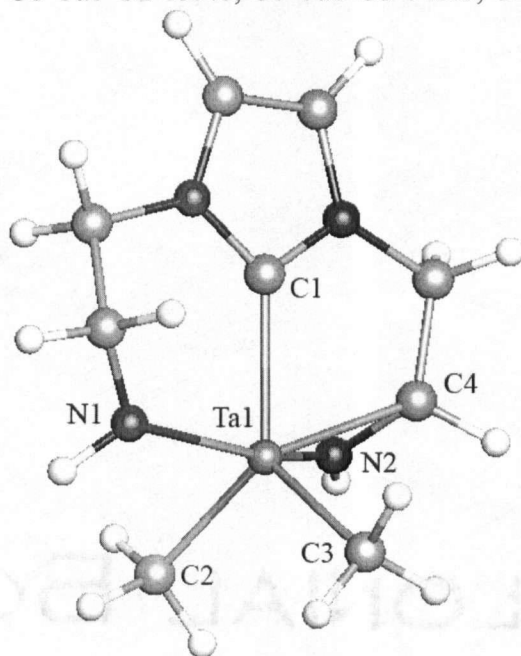


**Figure B.6.** JIMP<sup>1</sup> view of D. Selected bond distances (Å) and angles (deg): Ta1-C1 2.248, Ta1-C2 2.219, Ta1-C3 2.173, Ta1-C4 2.257, Ta1-N1 2.065, Ta1-N2 1.982, C1-Ta1-C2 130.5, C1-Ta1-C3 122.7, C2-Ta1-C3 106.1, C4-Ta1-N2 38.2.

In addition, formation of the metallaaziridine ring in **D** facilitates the close proximity of two Ta substituents, which provides more space around the Ta centre for the remaining substituents to adopt more favorable bonding positions. Natural Bond Orbital<sup>4</sup> (NBO) analyses of the trimethyl complex **A**, and the metallaaziridine product **D**, indicate that shortening of the Ta-carbene and Ta-Me bonds in **D** relative to **A** results from changes in the occupancy of the  $\sigma$ -bonding and  $\sigma^*$ -anti-bonding orbitals. The occupancies of the Ta-carbene and Ta-Me<sub>3</sub>  $\sigma$ -bonding orbitals in **D** are higher than the occupancies of the corresponding  $\sigma$ -bonding orbitals in **A**, while the occupancies of the Ta-carbene and Ta-Me<sub>3</sub>  $\sigma^*$ -anti-bonding orbitals in **D** are lower than the occupancies of the corresponding  $\sigma$ -bonding orbitals in **A** (Table B.3).

**Table B.3.** NBO Occupancies of bonding and anti-bonding orbitals in the trimethyl complex **A** and the metallaaziridine complex **D**.

	<b>A</b>	<b>D</b>
Ta1-C1 $\sigma$	1.853	1.933
Ta1-C2 $\sigma$	1.833	1.946
Ta1-C3 $\sigma$	1.795	1.892
Ta1-C1 $\sigma^*$	0.168	0.091
Ta1-C2 $\sigma^*$	0.126	0.094
Ta1-C3 $\sigma^*$	0.129	0.103

Examination of the second order perturbation theory analysis of the NBO orbitals of **A** reveals the origin of the differences in the orbital occupancies between **A** and **D** (Table B.4). Strong donation from the  $\sigma$ -bonding orbitals to the trans Ta-C  $\sigma^*$  orbitals (Table B.4, Figure B.7) is shown by the large interaction terms for **A**. It should be noted that in **D**, the corresponding donation from the Ta-C  $\sigma$ -bonding orbitals the Ta-C  $\sigma^*$  orbitals is significantly reduced (Table B.4, Figure B.8) because the more favorable C1-Ta-Me bond angles of **D** can avoid the mixing of bonding and anti-bonding orbitals observed in **A**. Thus, it appears that formation of the metallaaziridine ring is a key

component that allows the remaining methyl and carbene substituents in **D** to adopt preferable bonding positions.

**Table B.4.** Important second order perturbation theory analysis NBO donor – acceptor interactions  $\Delta E_{ij}$  (kcal/mol) that contribute to shorter Ta-carbene and Ta-Me bonds in the metallaaziridine product **D** relative to the trimethyl complex **A**.

NBO Donor orbital	NBO Acceptor orbital	$\Delta E_{ij}$ (kcal/mol)	
		<b>A</b>	<b>D</b>
Ta1-C1 $\sigma$	Ta1-C2 $\sigma^*$	26.13	1.02
Ta1-C1 $\sigma$	Ta1-C3 $\sigma^*$	31.50	2.64
Ta1-C2 $\sigma$	Ta1-C1 $\sigma^*$	38.32	1.81
Ta1-C3 $\sigma$	Ta1-C1 $\sigma^*$	54.62	3.02

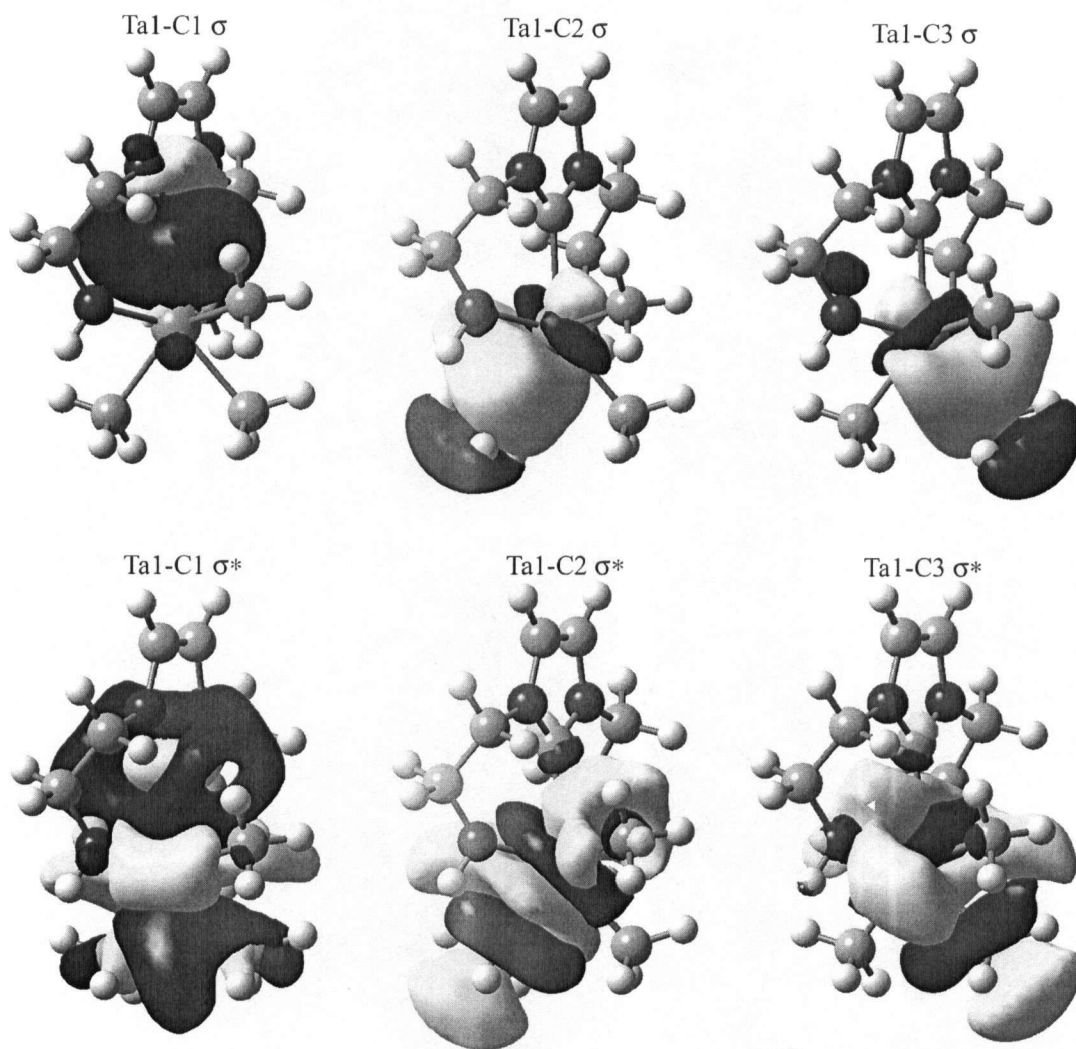


**Figure B.7.** Gaussview representations of selected NBO bonding and antibonding orbitals in the trimethyl complex A.

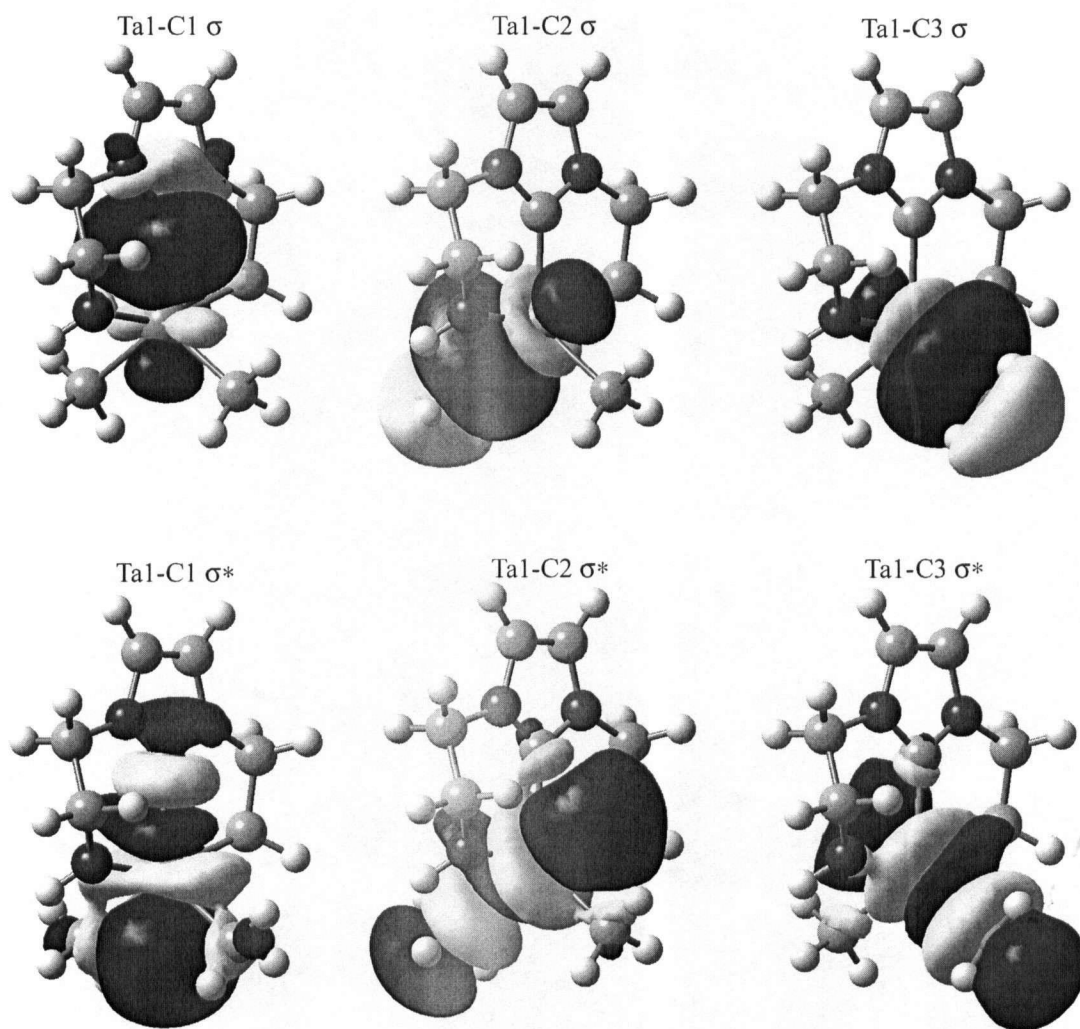


**Figure B.8.** Gaussview representations of selected NBO bonding and antibonding orbitals in the trimethyl complex **D**.

The other factor that causes the Ta-carbene distance to be shorter in the metallaziridine complex **D** than in the trimethyl complex **A** is the formation of the five-membered ring. To gauge how much of the shortening of the Ta-carbene bond in **D** relative to **A** is a result of the five-membered ring pulling the carbene toward the Ta-centre, calculations were conducted on model complexes in which atoms linking the

carbene unit to the amido donors were removed. In the first calculation, both  $\text{CH}_2\text{CH}_2$  linkages in **A** were removed and replaced with H atoms to generate  $(\text{H}_4\text{N}_2\text{C}_3)\text{Ta}(\text{NH}_2)_2(\text{Me})_3$ , **A'** (Figure B.9). Optimization of **A'** resulted in a Ta-carbene bond length of 2.378 Å, which is only 0.003 Å shorter than for **A**, and indicates that the two six-membered rings do not significantly influence the Ta-carbene distance. In the second calculation, the  $\text{CH}_2\text{CH}_2$  linkage between the carbene and amido units, and the  $\text{CH}_2$  linkage between the carbene and the metallazaaziridine ring were removed to generate  $(\text{H}_4\text{N}_2\text{C}_3)\text{Ta}(\text{NH}_2)(\text{NHCH}_2)(\text{Me})_2$ , **D'** (Figure B.9). The optimized Ta-carbene distance in **D'** is 2.275 Å, which is 0.027 Å longer than is observed in **D**. Thus, the calculations suggest that approximately 20% of the Ta-carbene bond shortening observed in **D** can be attributed to the five-membered ring pulling the carbene toward the Ta-centre, while the remaining shortening can be attributed to electronic effects brought upon by the formation of the metallazaaziridine ring (*vide ante*).

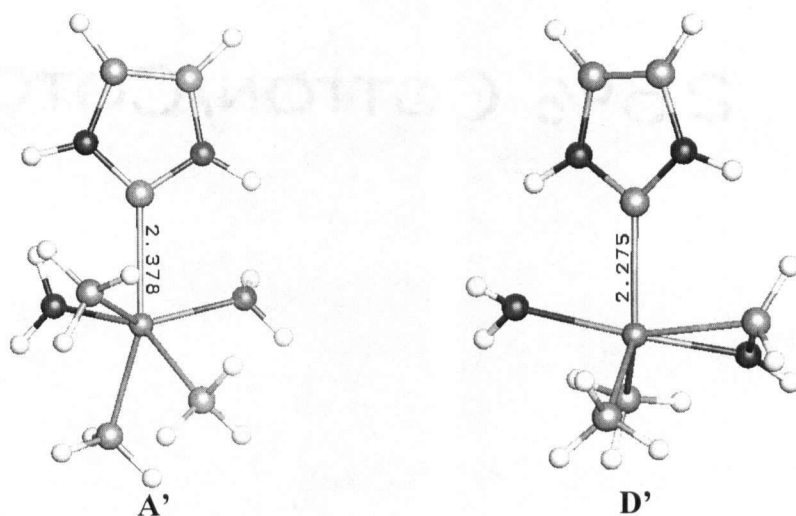


Figure B.9. JIMP<sup>1</sup> Pictures of **A'** and **D'**.

#### B.4. General Considerations

All calculations were performed using the Gaussian 03 suite of programs.<sup>5</sup> Optimized gas-phase geometries were obtained using the Becke3 exchange functional,<sup>6</sup> in combination the Lee, Yang, and Parr correlation functional,<sup>7</sup> *i.e.* the B3LYP method, as implemented in Gaussian 03. The basis set (BS1) used for geometry optimizations and energy calculations was implemented as follows: for tantalum, the valence double- $\zeta$  LANL2DZ<sup>8-10</sup> basis set was supplemented with a set of 6p functions for transition metals developed by Couty and Hall,<sup>11</sup> while for all hydrogen, carbon, and nitrogen atoms, the 6-31G(d',p') basis sets<sup>12-17</sup> were used. All structures were calculated in singlet spin states using the restricted B3LYP method. Calculating the harmonic vibrational frequencies and noting the number of imaginary frequencies confirmed the nature of all intermediates (NImag = 0) and transition state structures (NImag = 1). All gas-phase relative free energies are reported in kcal mol<sup>-1</sup>, with the energy of <sup>H</sup>[NCN]TaMe<sub>3</sub> (<sup>H</sup>[NCN] = (HNCH<sub>2</sub>CH<sub>2</sub>)<sub>2</sub>N<sub>2</sub>C<sub>3</sub>H<sub>2</sub>) set to 0.0 kcal mol<sup>-1</sup>. Relative electronic energies, zero-point corrected energies, and enthalpies are provided in the supplemental information. For the computational investigation, <sup>H</sup>[NCN] was used in place of the experimental ligand (*p*-Me-C<sub>6</sub>H<sub>4</sub>NCH<sub>2</sub>CH<sub>2</sub>)<sub>2</sub>N<sub>2</sub>C<sub>3</sub>H<sub>2</sub> (<sup>Tol</sup>[NCN]) in order to reduce the computational demands, while still providing two amide donors and one *N*-heterocyclic carbene donor to the tantalum centre. Natural Bond Orbitals (NBO) calculations were conducted with Gaussian NBO Version 3.1.<sup>4,18-21</sup>

### B.5. References

- (1) Manson, J.; Webster, C. E.; Hall, M. B. In *JIMP Development Version 0.1.v117 (built for Windows PC and Redhat Linux 7.3)* Department of Chemistry, Texas A&M University, College Station, TX 77842, 2006.
- (2) Landis, C. R.; Cleveland, T.; Firman, T. K. *J. Am. Chem. Soc.* **1995**, *117*, 1859.
- (3) Bayse, C. A.; Hall, M. B. *J. Am. Chem. Soc.* **1999**, *121*, 1348.
- (4) Reed, A. E.; Curtiss, L. A.; Weinhold, F. *Chem. Rev.* **1988**, *88*, 899.
- (5) Frisch, M. J.; Trucks, G. W.; Schlegel, H. B.; Scuseria, G. E.; Robb, M. A.; Cheeseman, J. R.; Montgomery, J. A. J.; Vreven, T.; Kudin, K. N.; Burant, J. C.; Millam, J. M.; Iyengar, S. S.; Tomasi, J.; Barone, V.; Mennucci, B.; Cossi, M.; Scalmani, G.; Rega, N.; Petersson, G. A.; Nakatsuji, H.; Hada, M.; Ehara, M.; Toyota, K.; Fukuda, R.; Hasegawa, J.; Ishida, M.; Nakajima, T.; Honda, Y.; Kitao, O.; Nakai, H.; Klene, M.; Li, X.; Knox, J. E.; Hratchian, H. P.; Cross, J. B.; Adamo, C.; Jaramillo, J.; Gomperts, R.; Stratmann, R. E.; Yazyev, O.; Austin, A. J.; Cammi, R.; Pomelli, C.; Ochterski, J. W.; Ayala, P. Y.; Morokuma, K.; Voth, G. A.; Salvador, P.; Dannenberg, J. J.; Zakrzewski, V. G.; Dapprich, S.; Daniels, A. D.; Strain, M. C.; Farkas, O.; Malick, D. K.; Rabuck, A. D.; Raghavachari, K.; Foresman, J. B.; Ortiz, J. V.; Cui, Q.; Baboul, A. G.; Clifford, S.; Cioslowski, J.; Stefanov, B. B.; Liu, G.; Liashenko, A.; Piskorz, P.; Komaromi, I.; Martin, R. L.; Fox, D. J.; Keith, T.; Al-Laham, M. A.; Peng, C. Y.; Nanayakkara, A.; Challacombe, M.; Gill, P. M. W.; Johnson, B.; Chen, W.; Wong, M. W.; Gonzalez, C.; Pople, J. A. *Gaussian 03, Revision B.4; Gaussian, Inc.: Pittsburgh, PA, 2003*.
- (6) Becke, A. D. *J. Chem. Phys.* **1993**, *98*, 5648.
- (7) Lee, C.; Yang, W.; Parr, R. G. *Phys. Rev. B: Condens. Matter* **1988**, *37*, 785.
- (8) Hay, P. J.; Wadt, W. R. *J. Chem. Phys.* **1985**, *82*, 270.
- (9) Wadt, W. R.; Hay, P. J. *J. Chem. Phys.* **1985**, *82*, 284.
- (10) Hay, P. J.; Wadt, W. R. *J. Chem. Phys.* **1985**, *82*, 299.
- (11) Couty, M.; Hall, M. B. *J. Comput. Chem.* **1996**, *17*, 1359.
- (12) Ditchfield, R.; Hehre, W. J.; Pople, J. A. *J. Chem. Phys.* **1971**, *54*, 724.

- (13) Hehre, W. J.; Ditchfield, R.; Pople, J. A. *J. Chem. Phys.* **1972**, *56*, 2257.
- (14) Hariharan, P. C.; Pople, J. A. *Theor. Chim. Acta* **1973**, *28*, 213.
- (15) Petersson, G. A.; Al-Laham, M. A. *J. Chem. Phys.* **1991**, *94*, 6081.
- (16) Petersson, G. A.; Bennett, A.; Tensfeldt, T. G.; Al-Laham, M. A.; Shirley, W. A.; Mantzaris, J. *J. Chem. Phys.* **1988**, *89*, 2193.
- (17) Foresman, J. B.; Frisch, A. *Exploring Chemistry with Electronic Structure Methods, 2nd Ed.* (Gaussian, Inc, Pittsburgh, PA), p. 110. The 6-31G(d',p') basis set has the d polarization functions for C, N, O, and F taken from the 6-311G(d) basis set, instead of the original arbitrarily assigned value of 0.8 used in the 6-31G(d) basis set.
- (18) Foster, J. P.; Weinhold, F. *J. Am. Chem. Soc.* **1980**, *102*, 7211.
- (19) Reed, A. E.; Weinstock, R. B.; Weinhold, F. *J. Chem. Phys.* **1985**, *83*, 735.
- (20) Reed, A. E.; Weinhold, F. *J. Chem. Phys.* **1985**, *83*, 1736.
- (21) Carpenter, J. E.; Weinhold, F. *Theochem* **1988**, *46*, 41.